CHARLES UNIVERSITY

Faculty of Science

Study program: Organic chemistry

Mgr. Iveta Chena Tichá

Synthesis of cyclodextrin derivatives for organocatalysis

Syntéza cyklodextrinových derivátů pro organokatalýzu

Doctoral thesis

Supervisor: doc. RNDr. Jindřich Jindřich, CSc.
Consultant: RNDr. Ivan Barvík, Ph.D.

Prague 2019

PROHLÁŠENÍ

Prohlašuji, že jsem tuto práci vypracovala samostatně pod vedením školitele doc. RNDr. Jindřicha Jindřicha, CSc., a řádně ocitovala všechny použité prameny. Jsem si vědoma, že použití výsledků této práce mimo Univerzitu Karlovu je možné pouze po předchozím souhlasu univerzity. Dále prohlašuji, že jsem tuto práci ani její část nepředložila k získání stejného nebo jiného akademického titulu.

V Praze dne 15. března 2019 …..……

Iveta Chena Tichá

STATEMENT

I declare that I worked up this doctoral thesis individually, under the supervision of doc. RNDr. Jindřich Jindřich, CSc., and that all literature sources have been cited properly. I am aware that the potential use of the results published in this work, outside of the Charles University, is possible only with the official permission of this university. Neither this work, nor any of its sections have been used for acquiring another academic degree.

In Prague, 15th March 2019 ……..

Iveta Chena Tichá

ACKNOWLEDGEMENTS

First and foremost, I would like to thank my supervisor doc. RNDr. Jindřich Jindřich, CSc., very much for his research ideas and advice and for time he dedicated to my PhD studies. Second, I would like to thank RNDr. Ivan Barvík, Ph.D., from Institute of Physics, Faculty of Mathematics and Physics, Charles University for his astonishing help with all computational studies and for his tutoring on cyclodextrin simulations.

In addition, I would like to thank the Group of Asymmetric Synthesis, particularly to doc. RNDr. Jan Veselý, Ph.D., for the initial idea of organocatalysts based on cyclodextrin and to Mgr. Vojtěch Dočekal for the idea about the application of my cyclodextrin derivatives in enantioselective catalysis.

Many thanks also to RNDr. Simona Hybelbauerová, Ph.D., for her great help with 2D NMR interpretation and NMR elucidation of my cyclodextrin derivatives and NMR measurements. Similarly, thanks also to my laboratory colleague Mgr. Petr Kasal for all his advice, discussions and for the almost 5 years we spent together in Supramolecular chemistry group.

I sincerely thank Dr. Milo Malanga, Ph.D., and Ing. Gábor Benkovics, Ph.D., for their collaboration and for my traineeship in CycloLab, Cyclodextrin Research and Development Company, Ltd., Budapest, Hungary.

I would like to thank Ing. Adam Málek for measurement of IR spectra and to Mgr. Bohunka Šperlichová for the measurement of optical rotations. This thesis would not been written in this form without the help of Dr. Carlos V. Melo, Ph.D., who edited my PhD texts and also my research articles.

All my colleagues and friends from Department of Organic Chemistry deserve my sincere acknowledgement, namely Mgr. Bedřich Formánek, Mgr. Michal Urban, Mgr. Eva Bednářová, Ph.D., Mgr. Markéta Bláhová, Bc. Ema Kouřilová, Bc. Attila Palágyi, Lucie Josefa Lamačová and Mgr. Martin Kamlar, Ph.D. for all their support and time we spent together.

I would like to thank the Grant Agency of Charles University for funding this project and to the Erasmus Program for funding my traineeship in CycloLab, Hungary.

Lastly, I would like to thank my friends and family, especially to my grandfather, grandmother and to my husband, for their inspiration, motivation, help and support during my studies at university. Without them, I could not have written this thesis.

ABSTRACT

Synthesis of cyclodextrin derivatives for organocatalysis

This doctoral thesis examines the preparation of new cyclodextrin (CD) derivatives suitable for organocatalysis. The aim of this work is to prepare monosubstituted and disubstituted CD derivatives as organocatalysts for different types of enantioselective reactions potentially performed in water. In addition, disubstituted CD derivatives require considering the potential mixture of regioisomers and pseudoenantiomers. Thus, this thesis is divided into several sections – preparation of CD precursors and derivatives for organocatalysis, preparation of pure regioisomers and pseudoenantiomers of disubstituted CDs and final application of CD derivatives in enantioselective reactions. Furthermore, this thesis also focuses on the molecular modeling of the prepared CD derivatives and on their catalytic activity *in silico*.

The first section covers the preparation of new disubstituted CD precursors as pure regioisomers for organocatalysts, specifically to develop a new method for the preparation of heterodisubstituted AC regioisomers on the primary rim of α-CD. This section also includes the determination of the regioisomer ratios of common α-CD intermediates disubstituted on the primary rim to evaluate their potential as precursors in organocatalysis.

The second section of this thesis focuses on the preparation of new monosubstituted and disubstituted CD derivatives (of native and permethylated CDs) with Cinchona alkaloids (cinchonine, cinchonidine, quinine and quinidine), their application as organocatalysts in enantioselective reactions and the evaluation of their catalytic activity also in water.

The third section includes the molecular modeling of Cinchona alkaloids and CDs. The inclusion complex of quinine and native β-CD in water was investigated as a model system. Moreover, all monosubstituted Cinchona-CD derivatives were geometric-optimized and equilibrated, and their spatial arrangement with substrates in enantioselective reactions was predicted based on these calculations.

Keywords: Cyclodextrins, catalysis, Cinchona alkaloids, regioisomers, molecular modeling

ABSTRAKT

Syntéza cyklodextrinových derivátů pro organokatalýzu

Tato disertační práce se zabývá přípravou nových cyklodextrinových (CD) derivátů vhodných pro organokatalýzu. Cílem této práce je připravit monosubstituované a disubstituované CD prekurzory a deriváty jako organokatalyzátory, které by bylo možné použít v různých enantioselektivních reakcích, provedených potenciálně ve vodě. V případě disubstituovaných CD derivátů bylo též nezbytné uvažovat o případných regioisomerech a pseudoenantiomerech těchto derivátů. Práce je tedy rozdělena do několika částí – příprava CD prekurzorů a derivátů pro organokatalýzu, příprava a separace regioisomerů a pseudoenantiomerů disubstituovaných CD derivátů a finální aplikace CD derivátů v různých enantioselektivních reakcích. Navíc je tato práce doplněna o molekulové modelování připravených CD derivátů a jejich katalytické aktivity *in silico*.

První část práce se zabývá přípravou nových disubstituovaných CD prekurzorů jako čistých regioisomerů pro organokatalýzu, zejména se zabývá vývojem metody pro přípravu heterodisubstituovaného AC regioisomeru na primární straně α-CD. Tato část také zahrnuje stanovení poměru jednotlivých regioisomerů běžně používaných disubstituovaných α-CD intermediátů s ohledem na jejich možné využití jako prekurzorů v organokatalýze.

Druhá část se zabývá přípravou nových monosubstituovaných a disubstituovaných CD derivátů (od nativních a permethylovaných CD) s chinolinovými (Cinchona) alkaloidy, jejich aplikací jako organokatalyzátorů v enantioselektivních reakcích a zhodnocením jejich katalytické aktivity v těchto reakcích proveditelných ve vodě.

Třetí část zahrnuje molekulové modelování chinolinových alkaloidů a CD. Nejdříve byl zkoumán vznik inkluzního komplexu chininu a nativního β-CD ve vodě pro ověření podmínek použitých v molekulárně-dynamických simulacích. Dále byly CD deriváty monosubstituované chinolinovými alkaloidy optimalizovány metodami molekulové dynamiky a na základě těchto výpočtů bylo zkoumáno jejich prostorové uspořádání se substráty v enantioselektivních reakcích.

Klíčová slova: Cyklodextriny, katalýza, chinolinové alkaloidy, regioisomery, molekulové modelování

TABLE OF CONTENTS

LIST OF ABBREVIATIONS

AAA	asymmetric allylic amination
ACN	acetonitrile
AMBER	Assisted Model Building with Energy Refinement
CD	cyclodextrin
CHARMM	Chemistry at Harvard Macromolecular Mechanics
COSY	correlation spectroscopy
CSA	10-camphorsulfonic acid
CuAAC	copper-catalyzed azide-alkyne cycloaddition
DABCO	1,4-diazabicyclo[2.2.2]octane
DEPT	Distortionless Enhancement by Polarization Transfer
DFT	Density Functional Theory
$(DHQD)_2AQN$	hydroquinidine(antraquinone-1,4-diyl)diether
DIBAL-H	diisobutylaluminium hydride
DIMEB	heptakis(2,6-di-*O*-methyl)-β-CD
DMF	*N*,*N*-dimethylformamide
DMSO	dimethylsulfoxide
DTA	differential thermal analysis
ee	enantiomeric excess
IR	infrared spectroscopy
ITC	isothermal titration calorimetry
IUPAC	International Union of Pure and Applied Chemistry
GPU	Graphical Processor Units
HMBC	Heteronuclear Multiple Bond Coherence
HPBCD	2-hydroxypropyl-β-cyclodextrin
HPLC	high performance liquid chromatography
HRMS	high resolution mass spectrometry
HSQC	Heteronuclear Single Quantum Coherence
MBH	Morita-Baylis-Hillman
MD	molecular dynamics
MTBE	methyl(*tert*-butyl)ether
MS	mass spectrometry
NAMD	Nanoscale Molecular Dynamics
NBS	*N*-bromosuccinimide
NMR	nuclear magnetic resonance
PME	particle-mesh Ewald summation

RAMEB	randomly methylated β-CD
R_F	retardation factor
ROESY	rotating frame Overhauser effect spectroscopy
TLC	thin layer chromatography
TRIMEB	heptakis(2,3,6-tri-*O*-methyl)-β-CD
Ts	*p*-toluenesulfonyl, tosyl
VMD	Visual Molecular Dynamics
wt%	weight percentage

1. INTRODUCTION

Cyclodextrins[1] (CDs), synthetic compounds known for more than 120 years, have become key compounds in the industry and in research in recent decades. These non-toxic molecules prepared from starch have a hydrophobic cavity which determines their applications in the pharmaceutical and food industries. Accordingly, considerable research effort has been put into synthesizing new CD derivatives with enhanced properties and into applying them in different fields (pharmacy, food, agriculture and toiletry, among others), in addition to catalysis.

As catalysts, CDs show promising properties by enabling (new) organic reactions in water, they are quite easily removed and recovered from reaction mixtures and enhance the stereoselectivity and enantioselectivity of products.[2] In comparison, asymmetric organocatalysis[3] has become important research field in organic synthesis thanks to the preparation of various enantiomer-enriched compounds. Creating new efficient catalytic systems (non-toxic, without metal) has made it possible to prepare a wide range of new chiral compounds for the pharmaceutical and other industries.

However, systems combining organocatalytic groups and CDs for asymmetric synthesis are still scarce. Furthermore, only a limited number of organic reactions have been catalyzed with CDs with a good enantiomer excess thus far. Furthermore, research has also focused on developing water-soluble new CD derivatives for different purposes, which is the key step in green chemistry.[4]

CD derivatization is crucial step to improve the properties of CDs (solubility, catalytic groups) and thus, to widen the applications of CDs in research and in the industry. Derivatizations of the CD skeleton can be performed either randomly or selectively. For some applications, only randomly substituted CD derivatives can be used, requiring no method for the selective modification of CD skeleton. One of these examples is randomly-methylated β-CD (RAMEB). Although the methyl groups are not selectively attached to CD anchor in this derivative, its preparation is highly reproducible.[5] These randomly substituted CDs are directly used as mixtures of derivatives in some applications, but the preparation of selectively modified CD derivatives is often required in other applications. Nevertheless, a range of different selectively modified CD derivatives has been already prepared, but the similar reactivity of hydroxyl groups of the CD skeleton remains a problem; thus preparation of selectively substituted CD derivatives is a leading challenge for synthetic chemists.

Concurrently, molecular modeling and simulation studies have helped experimental synthetic chemists to visualize molecules easily without any experimental background and to predict chemical phenomena. Moreover, using relatively inexpensive computational equipment, the arrangement of the molecules and thus, the catalytic activity of (not only) CD derivatives can be predicted in order to confirm or disprove hypotheses of synthetic chemists. Based on the above, computational simulation accelerates chemical research and helps us propose and design better and more efficient catalysts.

2. OBJECTIVES

The main goal of this thesis was to prepare new CD precursors and derivatives for asymmetric organocatalysis and to evaluate them in enantioselective reactions.

This general goal encompasses the following partial goals:

a) to prepare different regioisomers on the primary rim of disubstituted CD derivatives as precursors for heterodisubstituted CD organocatalysts for enantioselective reactions
b) to investigate the regioisomer ratio of commonly used primary-rim disubstituted CD precursors for their future use as pure regioisomers and pseudoenantiomers
c) to develop a method for attaching the CD skeleton to catalytic groups commonly used in asymmetric synthesis - Cinchona alkaloids
d) to prepare a series monosubstituted Cinchona alkaloid-CD derivatives (non-methylated and permethylated) using the method developed in c)
e) to evaluate the prepared CD derivatives in various asymmetric reactions investigating the possible use of water as a solvent
f) to simulate the catalytic behavior of Cinchona-CD derivatives with various substrates *in silico*

3. STATE OF THE ART

3.1. Cyclodextrins

Cyclodextrins (CDs) are cyclic oligosaccharides consisting of a $^4C_1$ chair conformation of α-(1→4)-D-glucopyranoside units. The most common CDs are α-, β- and γ-CDs with 6, 7 and 8 glucose units (Figure 1). The cyclic arrangement of glucose units creates the cone shape of these molecules. Because of this truncated cone, the inner space termed cavity is mainly hydrophobic (mainly C-H bonds and glycosidic oxygens), whereas the outer part of the CD with hydroxyl groups is hydrophilic.[1]

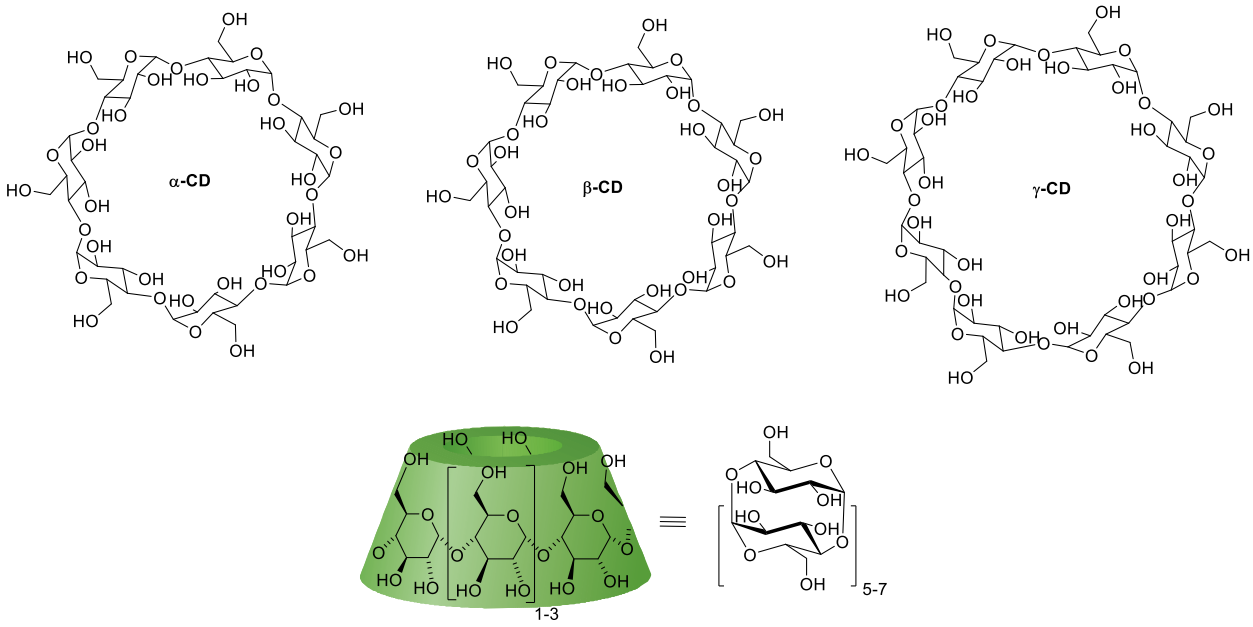

Figure 1. Graphical representations of the most common α-, β-, γ-CDs used in this work

CDs were discovered in 1891 by French scientist Antoine Villiers (1854 – 1932), who identified new compounds after heating starch with *Bacillus amylobacter*. Nearly a century later, CDs entered their renaissance in the 1980s when researchers found breakthrough applications and new approaches for the mass production of these compounds. The pioneer of this period was József Szejtli (1933 – 2004), who reviewed the knowledge on CDs in a seminal paper of this field[5] and also founded a private company focused on CDs – Cyclodextrin Research and Development Laboratory (CycloLab) in Budapest, Hungary. Moreover, numerous research groups worldwide focus on CDs and on their applications in different research and industrial fields, and international (European and global) conferences on CDs are held every year.[1,5]

Currently, CDs are produced as white crystalline powders by enzymatic degradation of starch (amylose, respectively) using *Bacillus macerans*. This degradation results in a mixture of linear and

cyclic dextrins, which are usually separated by complexation with suitable agents (toluene, 1-decanol, cyclohexadecenol). With the fast development of this technique, the yield of β-CD has become virtually quantitative and thus, the price and availability of this compound is appropriate for their mass use in the industry.[6,7]

Due to the cyclic shape of CDs and to the $^4C_1$ conformation of glucose units, all secondary hydroxyl groups are situated on one (wider) edge, whereas all primary hydroxyl groups are situated on another (narrow) edge, as previously shown in Figure 1. Thus, the CD skeleton contains hydroxyl groups on primary (narrow) and secondary (wide) rims. Furthermore, hydrogen bonds between hydroxyl groups of C-2 and C-3 on the secondary rim of the CD skeleton create a "belt" which most likely explains the low solubility of β-CD in water. Conversely, one glucose unit of α-CD is distorted, and γ-CD is larger and more flexible molecule than β-CD, and thus, these properties could not allow creating a rigid belt, as outlined in Table 1.[5]

Table 1. Characteristic parameters (solubility, cavity diameters) of α-, β- and γ-CDs.[5]

	α-CD	β-CD	γ-CD
Number of units	6	7	8
Cavity diameter (Å)	4.7-5.3	6.0-6.5	7.5-8.3
Height of torus (Å)	7.9	7.9	7.9
Specific optical rotation ($[\alpha]^{25}_D$)	150.0	162.5	177.4
Aqueous solubility (g/100 mL) at 25 °C	14.5	1.85	23.2
Crystal water (wt, %)	10.2	13.2-14.5	8.1-17.7
Diameter of outer periphery (Å)	14.6	15.4	17.5

Thanks to their hydrophobic cavity and hydrophilic outer shell, CDs are crucial for better solubility of organic molecules (drugs, respectively) in water. For example, some groundbreaking CD derivatives, such as 2-hydroxypropyl-β-CD (HPBCD), have been used in the pharmaceutical industry by improving the properties of drugs through encapsulation.[8] Encapsulating molecules (not only organic) into CD cavity causes the formation of "inclusion complexes" and thus, the solubilization of otherwise insoluble molecules or slow releasing of molecules from CD cavity.[9] Since then, numerous CD-based drug systems have also been tested and launched in the market.[10] Moreover, CDs are not used only as drug carriers or solubilizers; for example, sugammadex[11] is widely used as a neuromuscular reversal drug, reversely binding the muscle relaxants rocuronium and vecuronium to prevent the side effects of these relaxants during anesthesia.

3.1.1. Inclusion complexes of CDs

The ability to form inclusion complexes is a key property of CD molecules. Generally, the cavity of CD is filled with water molecules in aqueous solution, which is an unstable system (polar water molecules - slightly apolar CD cavity). However, the addition of non-polar (organic) molecules (guests) to the solution causes their inclusion into CD (host) cavity, thereby expelling the water molecules from the cavity (Figure 2).[5]

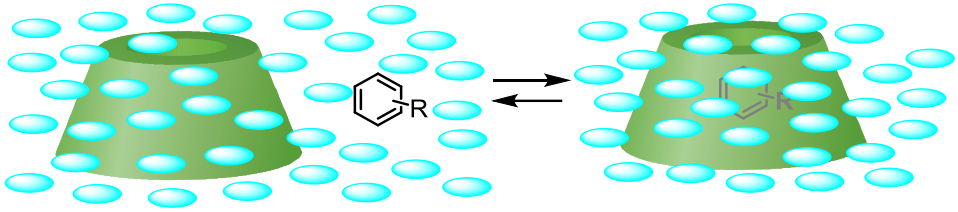

Figure 2. Graphical representation of an inclusion complex of host (CD) and guest (G)

This host-guest interaction represented in Figure 2 can be expressed using the following equations (eq. 1, 2)

$$CD + G \leftrightarrows CD \cdots G \qquad \text{(eq. 1)}$$

$$K = \frac{[CD \cdots G]}{[CD][G]} \qquad \text{(eq. 2)}$$

wherein CD is cyclodextrin (host), G is the guest and K is the complex stability constant. The host-guest ratio is usually 1:1, but 2:1, 1:2 or 2:2 inclusion complexes have also been prepared. Usually, guest inclusion into the cavity can be confirmed by NMR measurements[5,12], by ITC analysis[13] or by X-ray analysis[14].

3.2. Synthesis of CD derivatives

Although native CDs (α-, β- and γ-) have outstanding properties as mentioned above, the preparation of CD derivatives is necessary for several reasons; to increase the solubility of CDs in water and in other solvents, to improve their complexation properties and to prepare target CD derivatives by attaching various functional or catalytic groups to CD, among others.[15]

The methods for the derivatization of CD skeletons can be divided into two groups: random and selective substitution. A specific method is chosen depending on the final purpose of the derivative. In some applications, only randomly substituted derivatives can be used and the methods applied for their preparation are highly reproducible, although these randomly substituted derivatives contain a mixture of isomers, for example, RAMEB or HPBCD, which are important in the pharmaceutical industry, specifically enhancing the membrane permeability of poorly soluble drugs and properties of anesthetics, respectively.[16,10] In other applications, new methods for the preparation

of selectively substituted CD derivatives must be developed based on the desired properties of the target CD derivatives.

Currently, several research groups are trying to develop new methods for the selective substitution of CD anchors. Although all hydroxyl groups of CDs have similar reactivities which generally leads to mixtures of products and positional isomers, small differences in reactivity were observed depending on the positions of hydroxyl groups in the CD molecule (Figure 3).[17]

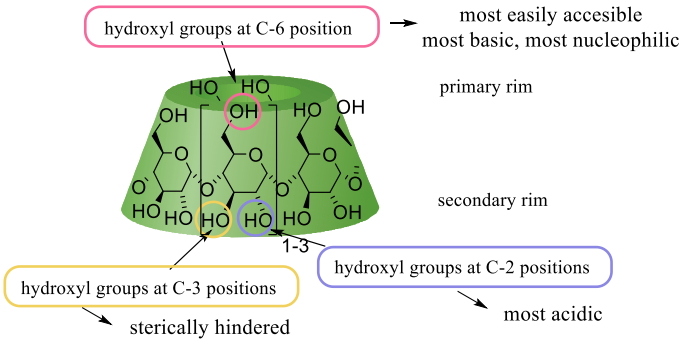

Figure 3. General differences in the reactivity of hydroxyl groups of CD skeleton[17]

As shown in Figure 3, the hydroxyl groups at position 6 (OH-6) are the most sterically accessible, the most basic and the most nucleophilic. In contrast, the hydroxyl groups at position 3 (OH-3) are the most sterically hindered and the most difficult to access; however, the advantage of CD inclusion complexes with suitable agents is the introduction of selectivity at this position, similarly to the monocinnamylation of β-CD.[18] The hydroxyl groups at position 2 (OH-2) are the most acidic, and some approaches have resulted in preparation of these selectively substituted CD derivatives, albeit with very low yields.[17]

These differences in reactivity have enabled the preparation of selectively mono-, di- and persubstituted CD derivatives on positions C-2, C-3 or C-6.[17] Considering the purpose and scope of this thesis, only selective monosubstitution and disubstitution on the primary rim of CD skeletons (C-6 atoms) will be discussed herein.

3.2.1. Monosubstituted CD derivatives

Monosubstitution of a CD skeleton is one of the most common types of derivatization which is commonly used to prepare a wide range of derivatives for different purposes, as previously reviewed.[15,17] Generally, monosubstitution can occur on three different positions of the CD skeleton (Figure 3), thus allowing the preparation of mono-2-, mono-3-, mono-6-CD derivatives.

However, among CD precursors monosubstituted on the primary rim for further use, 6-*O*-tosyl-CDs are the most common precursors of several types of C-6 monosubstituted derivatives.[17] The widely used tosylation method[19] is based on the fact that OH-6 atoms on the primary rim are the most

nucleophilic and the most accessible. Furthermore, pyridine, both as a solvent and as a base, can be included into the CD cavity, therein activating the primary rim hydroxyl groups. Importantly, full conversion into monotosylated CDs has not been achieved because the formation of overtosylated products could not be avoided due to the presence of hydroxyl groups of similar reactivity. Accordingly, the yields[20] of this reaction range from 10 to 25%. Nevertheless, other important precursors are usually prepared from 6^{I}-*O*-tosyl-CDs (**I**) such as 6^{I}-azido-6^{I}-deoxy-CDs (**II**) which are the most commonly used derivatives in CuAAC click reactions[21,22] (Figure 4).

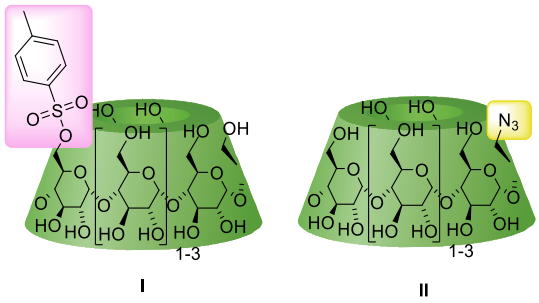

Figure 4. 6^{I}-Monotosyl-CDs (**I**) and 6^{I}-monoazido-CDs (**II**)

Other monosubstituted precursors should be mentioned, such as 6^{I}-bromo-6^{I}-deoxy-CDs, which are also used to prepare different kind of CD derivatives by nucleophilic substitution, for example the previously mentioned 6^{I}-azido-6^{I}-deoxy-CDs (**II**).[23]

3.2.2. Disubstituted CD derivatives

In comparison with the selective monosubstitution of CDs, disubstitution methods are less direct, and no general precursor of disubstituted CDs can be easily prepared by direct disubstitution because products usually consist of a mixture of regioisomers. Accordingly, disubstitution is not used for CD derivatization as much as monosubstitution since these mixtures of regioisomers require sophisticated, time-consuming chromatographic separations. Notwithstanding, both direct (A, B) and indirect (C) approaches (Scheme 1) for the preparation of selectively disubstituted CDs have been already proposed.[24,17] This problem of mixtures of regioisomers and pseudoenantiomers will be discussed in more detail in the section 3.2.3.

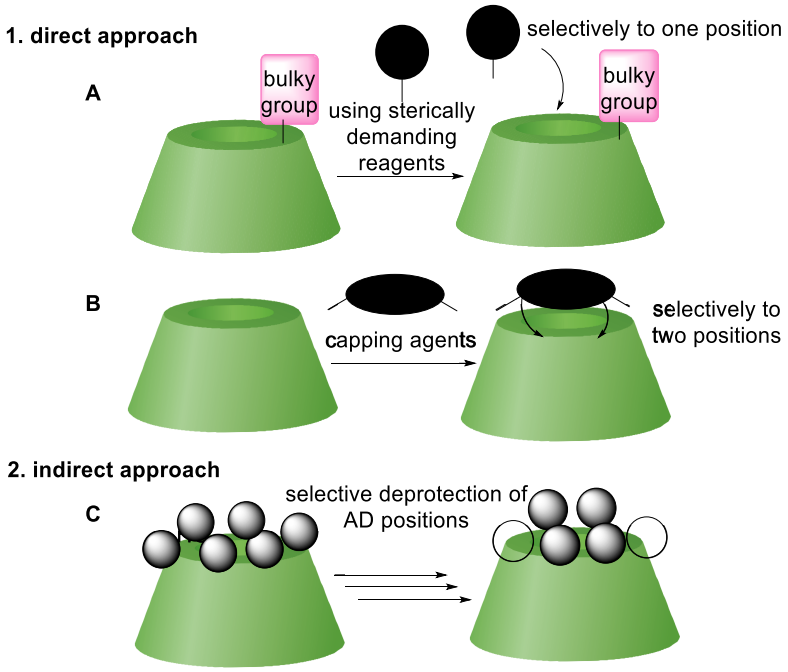

Scheme 1. General approaches for CDs disubstituted on the primary rim[25]

3.2.2.1. Direct approach for the preparation of disubstituted CDs

The first – direct – approach consists of using (sterically demanding or capping) agents to modify the preferential position on the CD skeleton (Scheme 1).[25,26] On the one hand, sterically demanding agents, blocked by bulky functional groups already attached on CD (reaction A), can modify only an accessible glucose unit; on the other hand, capping agents (usually a single organic molecule with two reactive functional groups) are preferentially attached to two glucose units on CD skeleton (reaction B).[27]

Tabushi and Fujita pioneered capping methods testing a wide range of capping agents, and observed preferentially capped positions in some cases. Their reaction with *m*-benzenedisulfonyl chloride reached 97% selectivity for the AB position (**III**) on β-CD (Scheme 2).[28] A different regioisomer ratio was observed with benzophenone-3,3´-disulfonyl chloride (61% selectivity for AC regioisomer **IV**) and with 4,4´-biphenyldisulfonyl chloride (84% selectivity for AD regioisomer **V**).[29] Although these methods became milestones in the preparation of disubstituted CDs as particular regioisomers, they still have some limitations. The main issue is that the selectivity is lower than 100%; thus, most of these products consist of impurities, which could hinder subsequent chromatographic separations. Subsequently, most of the regioisomer ratios were identified *via* enzymatic degradation[28], which is no longer the most convenient method due to improvements in HPLC and NMR techniques. Lastly, capped-CDs are very easily hydrolyzed which may also complicate their further conversion into single isomer CD derivatives. Thus, they could be immediately transformed into more stable CD derivatives, such as diazido-CD derivatives.

Nevertheless, these one-step methods for the preparation of AB-, AC- and AD-regioisomers on β-CD have already been applied to prepare several CD derivatives.[30,31]

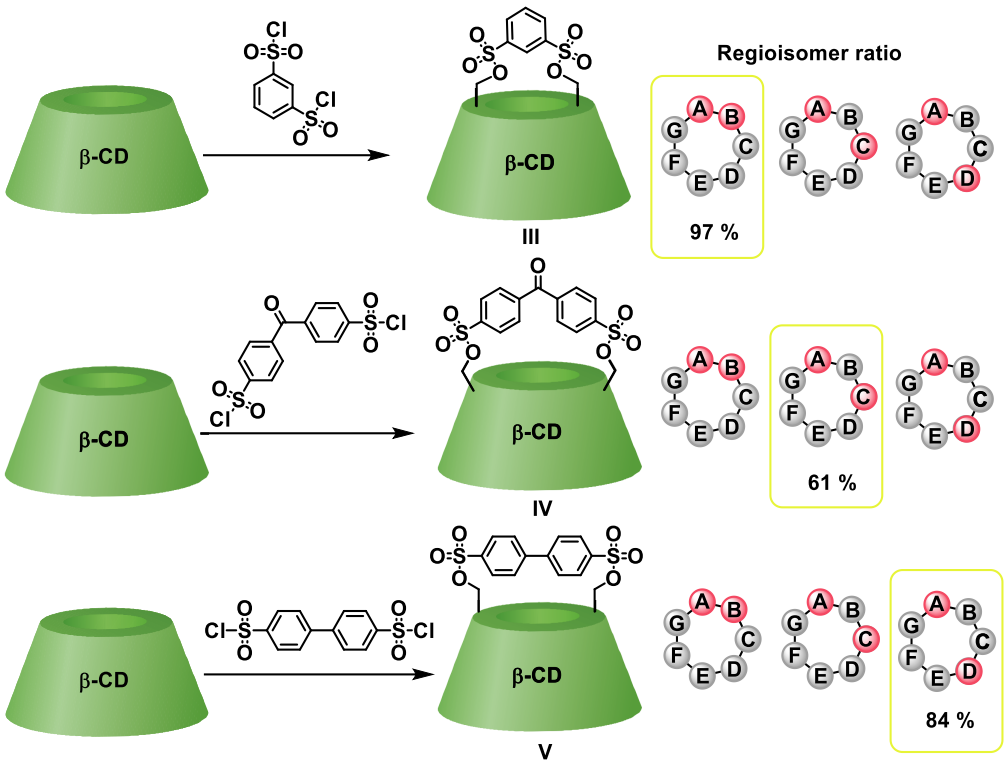

Scheme 2. Regioisomer ratio of capped-β-CDs[28,29]

However, the preparation of regioisomers of α-CD using capping agents (Scheme 3) is less thoroughly studied than the synthesis of capped-β-CDs. More specifically, the reaction between native α-CD with *m*-benzenedisulfonyl chloride resulted in the preferential capping of A and B positions, but the regioisomer ratio was unclear (**VI**).[32] Moreover, the capped-α-CDs prepared with the capping agent *m*-benzenedisulfonyl chloride hydrolyzed very quickly. Thus, this capping agent was replaced with dimethoxy-*m*-benzenedisulfonyl chloride which resulted in a more stable, but still easily hydrolyzed capped-α-CDs. Similarly, the regioisomer ratio of this preferred AB regioisomer was not investigated because compound **VI** with methoxy groups**,** still easily hydrolyzed, was immediately transformed into a more stable diiodo-α-CD.[33] Conversely, dibenzofuran-2,8-disulfonyl chloride as a special capping agent was used to form AC regioisomer **VII**, nevertheless the regioisomer ratio was not published and the most abundant regioisomer was indirectly confirmed.[34] Lastly, the use of methyl-4,4´-biphenyldisulfonyl chloride resulted in a mixture of AC and AD isomers (**VIII**).[35] Similarly to β-CD skeleton, capping of the α-CD skeleton continued in the problem of the selectivity which is not 100%. Overall, this α-CD capping results in mixtures of regioisomers, and the products of these reactions are much more labile to hydrolysis than capped-β-CD.[33]

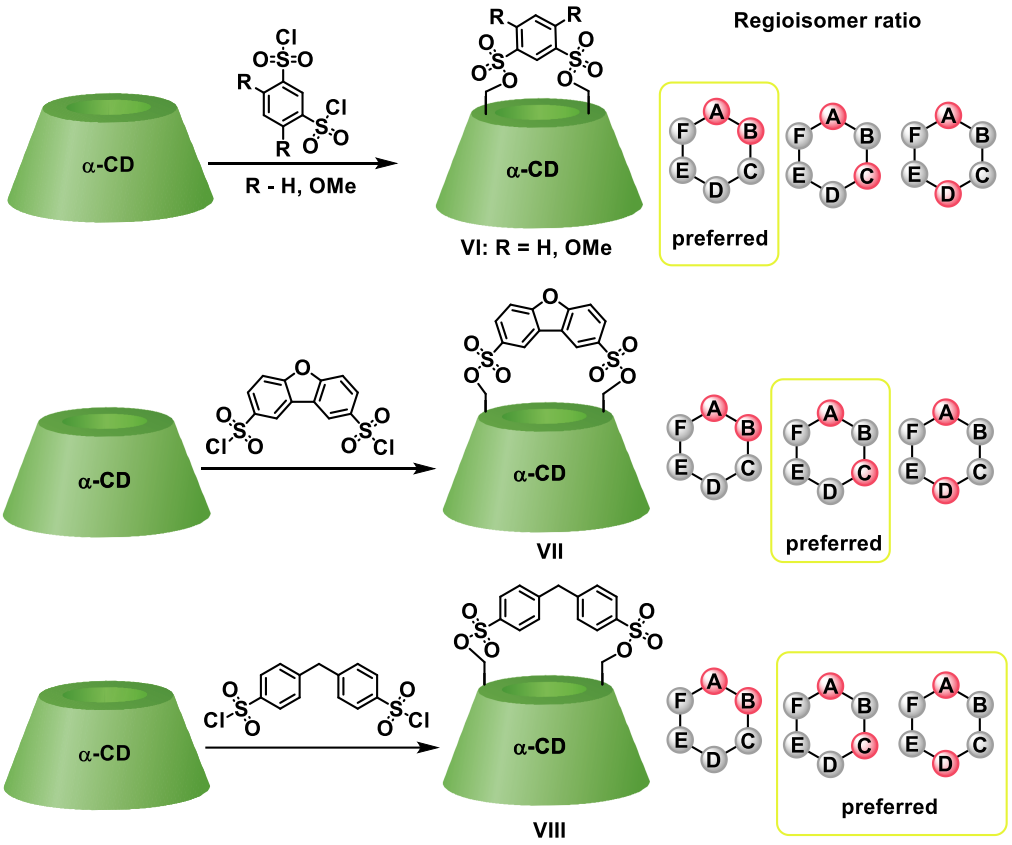

Scheme 3. Regioisomer ratio of capped-α-CDs[33–35]

AD regioisomer precursors on α-CD were later developed by Armspach and Matt,[36] who used the supertrityl group to selectively substitute the AD position on the primary rim of α-CD (Scheme 4). The main advantage of this strategy is the separation of regioisomers **IX** in gram scale, and not only in HPLC scale. However, the product required permethylation before the separation of regioisomers. In parallel, Armspach also investigated different unsymmetrically capped CDs for their potential use in asymmetric synthesis.[37]

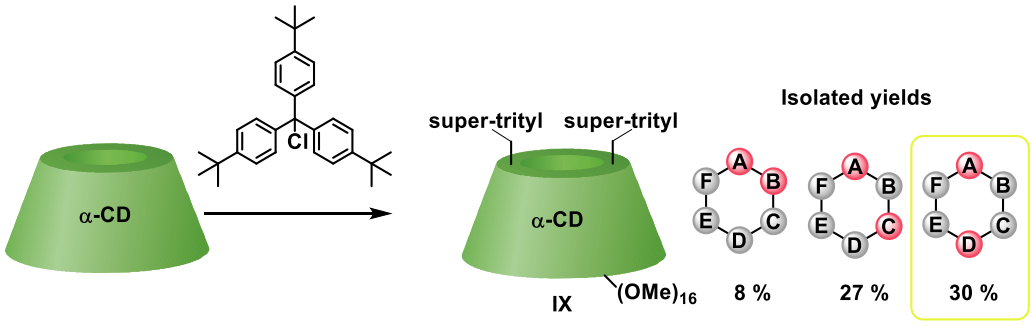

Scheme 4. Direct approach for the preparation of AD-regioisomer on α-CD[36]

3.2.2.2. Indirect approach for disubstituted CDs

A second – indirect – approach for the preparation of disubstituted CDs was extensively studied in the group of Sinaÿ,[38] and the highly selective deprotection of perbenzylated CDs produced deprotected products as 100% for one regioisomer (**X**, Scheme 5). This method was a milestone in the preparation of selectively 1,4-disubstituted α- and β-CDs without any capping agents. However, this deprotective method also has limitations – primarily, this is a time-consuming, four-step-synthesis. Another disadvantage is that this reaction is very sensitive to the concentration of diisobutylaluminium hydride (DIBAL-H) in the reaction mixture and to the reaction temperature.

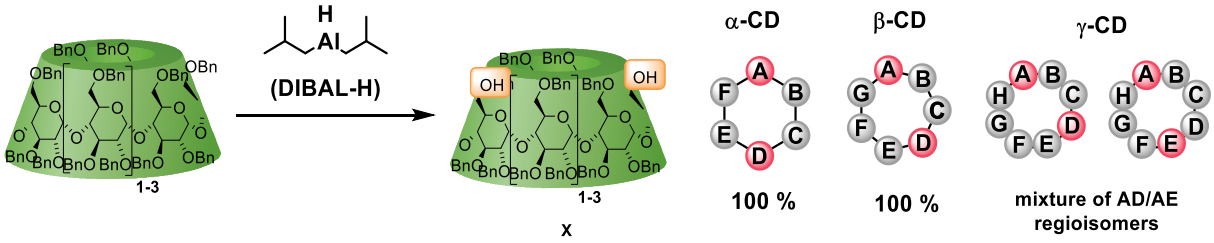

Scheme 5. Preparation of disubstituted CDs *via* debenzylation[38]

Considering the excellent regioselectivity of this DIBAL-H deprotection, Sinaÿ and Sollogoub´s group continued using this method for the preparation of various other CD derivatives[39–46], including CDs used in medical treatments[47]. Starting from total deprotection of benzyl groups of dimesyl-perbenzylated α-CD[48] (**XI**), this group also prepared AD-diazido-α-CD **XII** (a key CD derivative for click reactions[21,49]). Furthermore, this ongoing research culminated with the preparation of hetero-hexasubstituted derivative **XIII** on the primary rim of α-CD (Scheme 6).[50]

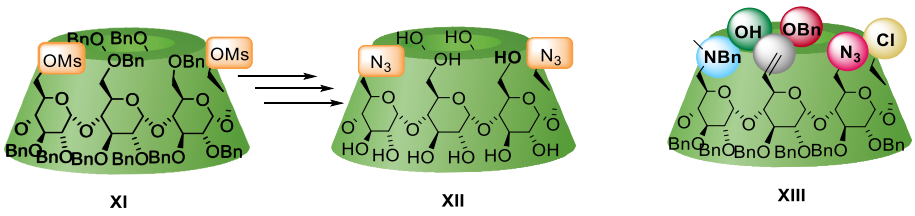

Scheme 6. α-CD derivatives (**XI-XII**) prepared *via* DIBAL-H deprotection[50,48]

As mentioned above, the DIBAL-H debenzylation procedure is quite sensitive to experimental conditions – concentrations of DIBAL-H and starting material in the reaction mixture and reaction temperature and time. Unsurprisingly, other research groups repeated and improved the original procedure described by Sinaÿ[38]. For example, Ling *et al.*[51,52] investigated the reaction for the preparation of diol **X** with DIBAL-H in a hexane solution.

Furthermore, Kraus *et al.*[23,53–56] developed complementary procedures towards total debenzylation by deprotection of the bisbrominated perbenzylated α-CD **XIV** using a Pd/C catalyst,

thereby producing CD intermediate for the preparation of the dimer **XVI** connected *via* disulfide bonds (Scheme 7).

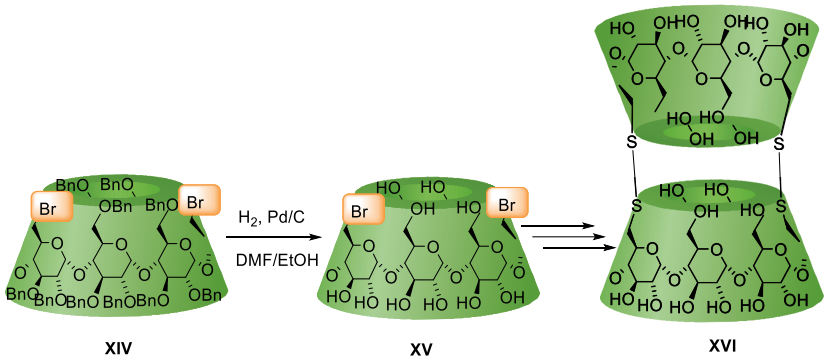

Scheme 7. Dimer **XVI** prepared *via* debenzylated intermediate **XV**[23]

In turn, Bols and his research team[57,58] successfully used Sinaÿ diol on α-CD (**X**, Scheme 8) for the preparation of heterobifunctionalized CD derivatives, such as amino-hydroxyl-perbenzylated-α-CD (**XVII**) towards the total deprotected α-CD with amino and carboxylic functional groups (**XVIII**).

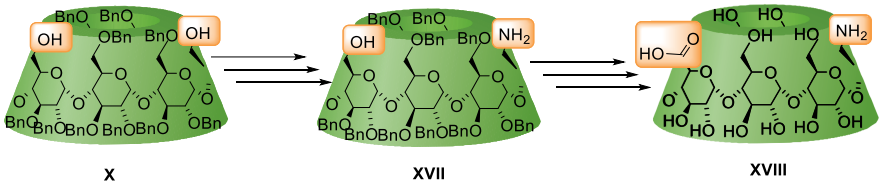

Scheme 8. Heterodisubstituted α-CD derivatives **XVII** and **XVIII** prepared by Bols *et al.*[57,58]

3.2.3. Regioisomers of disubstituted CD derivatives

As explained in the previous chapter, the problem of regioisomers and pseudoenantiomers is one of the main obstacles in the preparation of disubstituted CD derivatives. However, our ultimate goal was to prepare organocatalysts on a CD skeleton as a pure regioisomer. Therefore, we only focused on α- and β-CD skeletons because the number of possibilities for regioisomers and pseudoenantiomers on their primary rims is rather limited.[17]

The chiral nature of the CD skeleton makes it possible to differentiate the clockwise (**CW**) from the counterclockwise (**CC**) orientations of the CD skeleton, as viewed from the secondary rim (for example α-CD, Figure 5). The alphabetic numbering of α-CD glucose units with A - F letters was originally started in the study by Tabushi and Fujita[28], and this numbering is easier to understand in di- and higher substituted glucose units than the IUPAC numbering using Greek numbers[59].

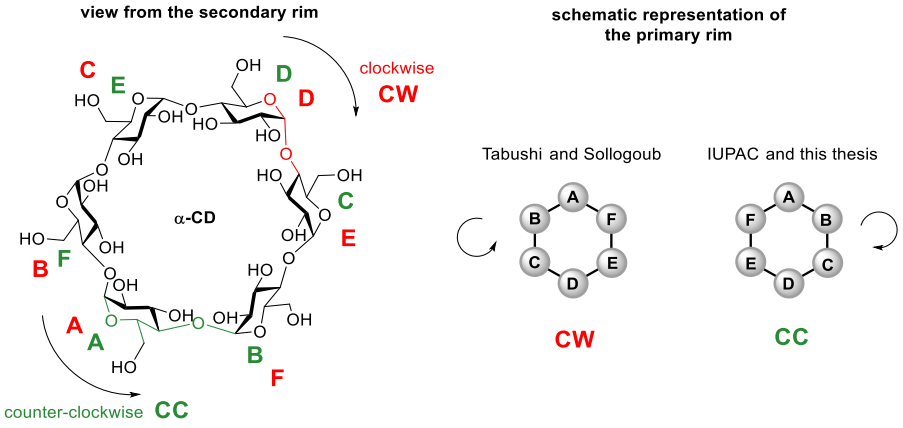

Figure 5. Clockwise and counter-clockwise alphabetical numberings of α-CD glucose units

Accordingly, Tabushi and Fujita used this alphabetical **CW** numbering (red bonds) for schematic representation of the primary rim. Moreover, Sinaÿ and Sollogoub continued using this **CW** numbering.[39,60] However, according to IUPAC reccommendations[61], the glucose units of oligosaccharides should be numbered from the anomeric carbon (C-1) *via* the longest part of a glucose unit first and only then *via* the 1,4-linkage, subsequently continuing in the following glucose units (**CC** numbering, green bonds in Figure 5). Therefore, the **CC** numbering, which does not depend on the substitution of glucose units, is used in this thesis (and in Tichá et al., *Beilstein J. Org. Chem.* 2018[62]).

Furthermore, this inherent chirality of CD skeletons results in an existence of pseudoenantiomer pairs of di- and more substituted CD derivatives.[28] To better illustrate this problem, Figure 6 shows possible regioisomers and pseudoenantiomers of the primary-rim disubstituted α- and β-CD skeletons. However, the problem of different pseudoenantiomers has been rarely addressed thus far, except for Sollogoub *et al.*[63,60], who discussed the equality of AD/DA disubstituted perbenzylated α-CDs.

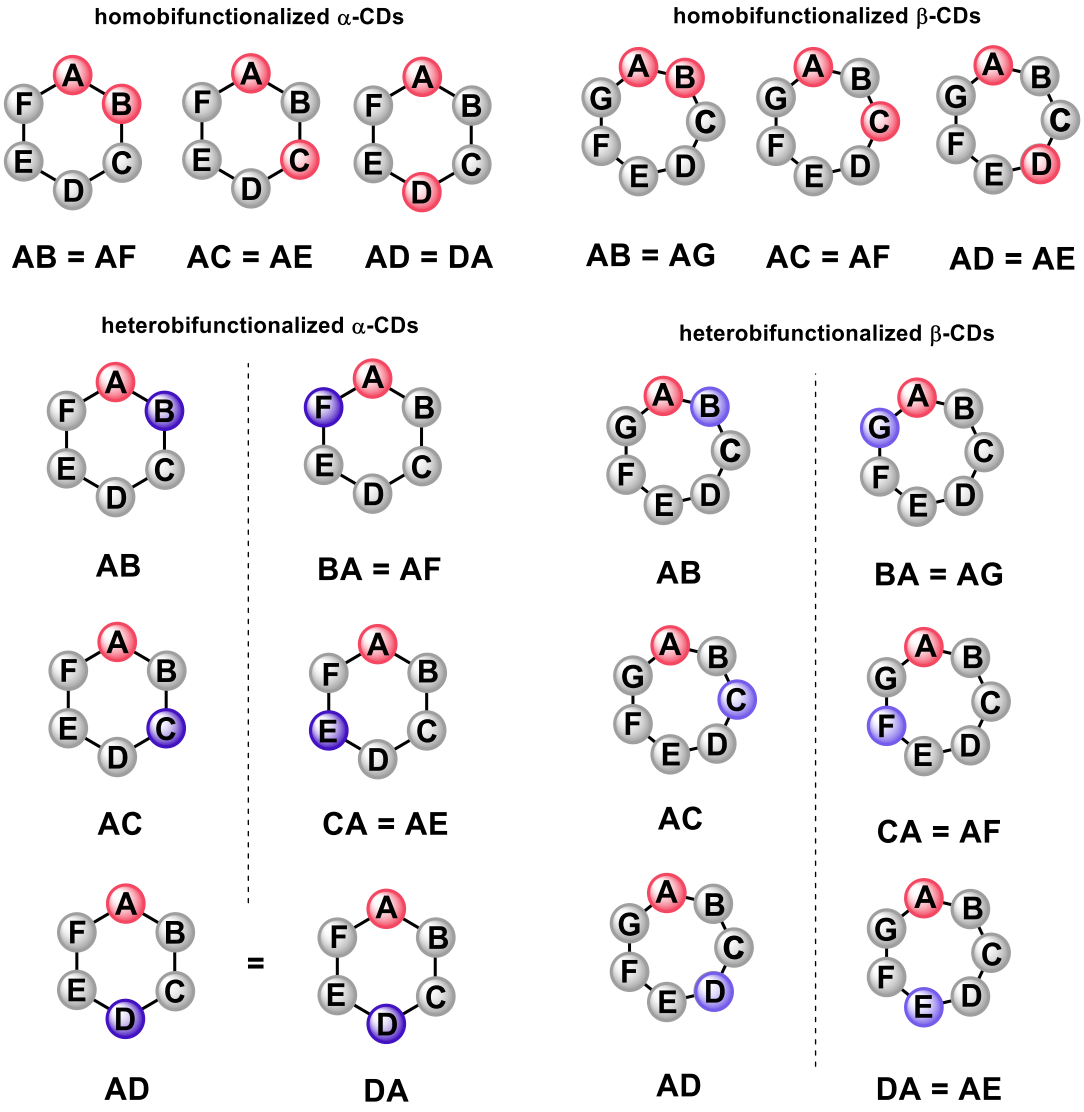

Figure 6. Schematic representation of regioisomers and pseudoenantiomers of α- and β-CD derivatives viewed from the primary rim[28,60]

Several research groups have aimed to differentiate regioisomers and to determine the regioisomer ratio of disubstituted CDs. In pioneering studies, Tabushi and Fujita[28] were able to determine the regioisomer ratio *via* enzymatic degradation using Taka-amylase[64] hydrolysis and $NaBH_4$, reduction, thereby opening the CD ring and detecting the products of these degradations by MS methods. However, these methods were time-consuming; some of these degradations took 12 days. Thus, Fujita *et al.*[65,66] started new, more convenient HPLC separations of CD regioisomers. Currently, HPLC separation of regioisomers is a powerful tool for determining the regioisomer ratio, albeit requiring standards for the unambiguous characterization of regioisomers. Among others, Yamamoto *et al.*[67] investigated the regioisomers of di- and trisubstituted α-CD derivatives with trityl groups on the primary rim.

3.3. Organocatalysts based on CDs

As non-toxic and water-soluble molecules, CDs are key compounds for dissolving organic molecules in water. More specifically, CDs can serve as "microvessels" to perform organic reactions *via* covalently bonded intermediates or to mediate such a reaction *via* non-covalent bonding in the CD cavity.[68] Regardless, both covalent and non-covalent binding approaches play a key role in catalysis.

CDs have been applied in catalysis, since the initial research on the CD skeleton. CDs have been used as catalysts in biomimetic reactions to mimic the activity of enzymes (literally "to describe chemistry inspired by biological processes"). Breslow pioneered this research, successfully applying bifunctionalized CDs **XIX** (different regioisomers) for enolization purposes (Figure 7)[69] or for mimicking enzymes such as cytochrome P-450 (**XX**)[70,71], among other applications. In addition, he also summarized the state of the art in this field two decades ago.[72,73]

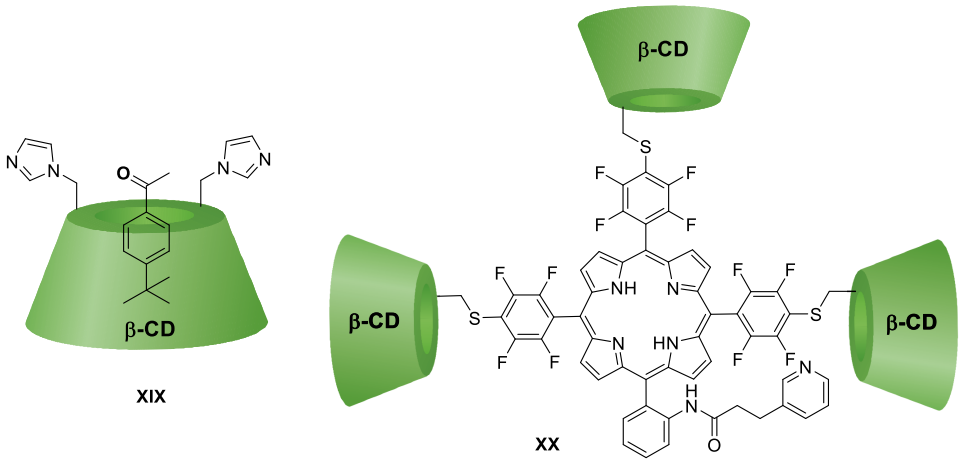

Figure 7. Imidazole-derived CDs **XIX** and porphyrin-derived CDs **XX** successfully mimic enzymes.[69,70]

Following Breslow, Levine *et al.*[74] summarized the current applications of CDs in biomimetic catalysis. The important part of this research field focuses on the performing organic reaction in water. Monflier's group is interested in the preparation CD catalysts for various purposes, for the preparation of pyrrole rings in water using RAMEB.[75] Not only organocatalysts but also metal-CD catalytic systems were extensively studied. For example, Gao's group successfully used Pd-β-CD complex for Suzuki-Miyaura coupling in water.[76] Other research group used native β-CD as catalysts for the preparation of pyrazoles in aqueous solution.[77]

Concomitantly, Bols conducted key research on CD-based organocatalysts,[78] primarily focusing on the preparation of disubstituted α-CD catalysts with an acetone bridge (**XXI**) for epoxidation reactions (Scheme 9).[79] Moreover, the Bols group prepared other CD catalysts with different types of acetone bridges on β-CD (for example **XXII**) and with similar activity in epoxidation,[80] in addition to synthesizing CD derivatives (for example **XXIII**) as artificial enzymes for

amine and benzyl alcohol oxidation[81,82]. Furthermore, the authors investigated the chiral version of their epoxidation reactions, albeit with almost no enantiomeric excess.

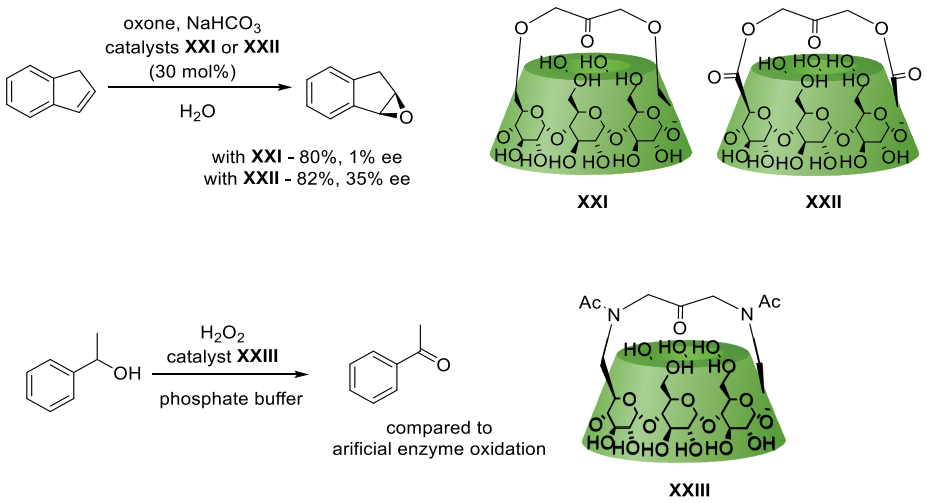

Scheme 9. CD catalysts (**XXI–XXIII**) successful in epoxidation and oxidation[79,80]

Wong *et al.*[83] were also interested in epoxidation reactions catalyzed by the CD derivative monosubstituted with ketoester **XXIV** with 40% ee (Scheme 10). Despite the low enantiomeric excess, CD derivates have been used in enantioselective catalysis based on these preliminary findings and have since shown promising results (Section 3.3.1).

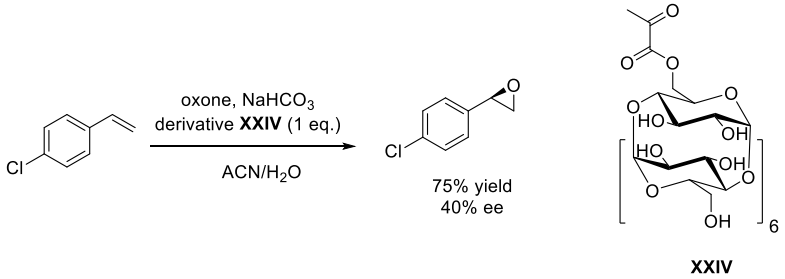

Scheme 10. CD derivative substituted with ketoester (**XXIV)** for asymmetric epoxidation[83]

3.3.1. Enantioselective reactions promoted and catalyzed by CD derivatives

The separation of enantiomers using native CD chiral skeletons has become the crucial area of analytical chemistry. Furthermore, CD skeleton derivatization can enhance the separation of the previously inseparable mixture of enantiomers of several compounds.[84]

CD-based organocatalysts could also be successfully used in enantioselective catalysis as outlined in the previous chapter. Macaev *et al.*[85] and Wang *et al.*[86] have previously reviewed this application of CD derivatives in enantioselective reactions. More specifically, proline derivatives have already been used in combination with CDs to assess the high efficiency of these organocatalysts. For

example, a proline derivative immobilized in the β-CD cavity (**XXV**), successfully catalyzed an aldol reaction with 84% ee (Scheme 11).[87]

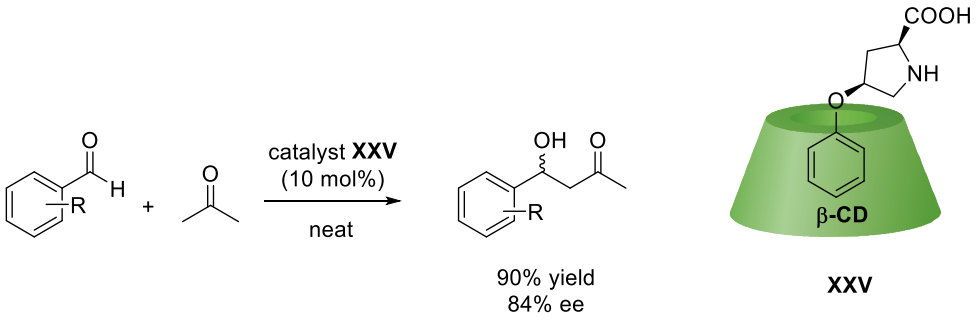

Scheme 11. Proline derivative immobilized in the β-CD cavity (**XXV**) catalyzed an aldol reaction.[87]

In addition, proline covalently bonded *via* urea linker to β-CD derivative (**XXVI**) has also been prepared and applied in a direct aldol reaction in water with excellent enantiomeric excess (Scheme 12).[88]

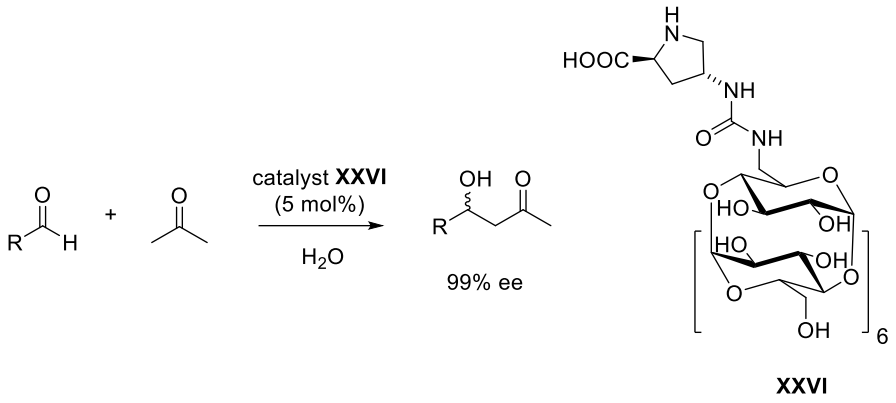

Scheme 12. Proline attached to β-CD derivative *via* a urea linker (**XXVI**) catalyzed a direct aldol reaction[88]

In a third application of a proline-CD derivative to enantioselective catalysis, the nature of the linker between proline and CD affected the enantiomeric excess of the product of a direct aldol reaction[89]. Moreover, the authors of this study also investigated permethylated CD derivatives with a proline moiety (**XXVII**), albeit with only 54% ee (Scheme 13).

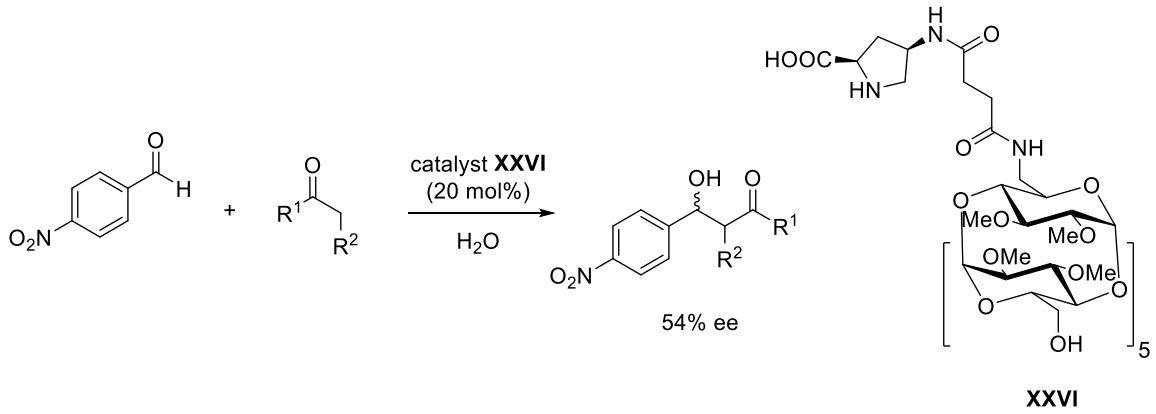

Scheme 13. Proline-derived CDs (**XXVI**) catalyzed a direct aldol reaction.[89]

Not only aldol reactions, but also enantioselective Henry reactions were performed by Pitchumani *et al.*[90] who used per-6-amino-β-CD (**XXVII**) (Scheme 14) and achieved an excellent 99% ee in ACN/H_2O.

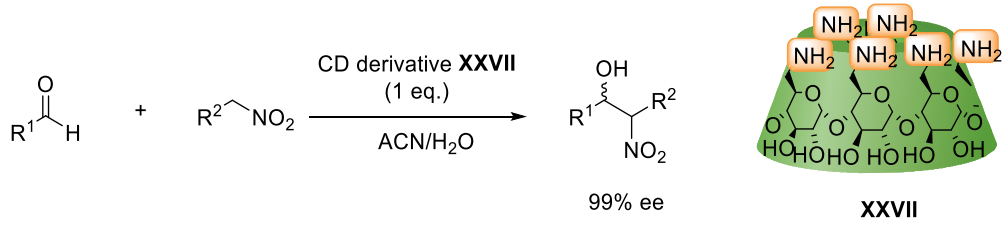

Scheme 14. Per-amino-β-CD derivative (**XXVII**) promoted the Henry reaction.[90]

Kraus *et al.*[91–93] used β-CD catalysts attached to flavin moieties (**XXVIII**) in enantioselective sulfoxidations with 91% ee (Scheme 15).

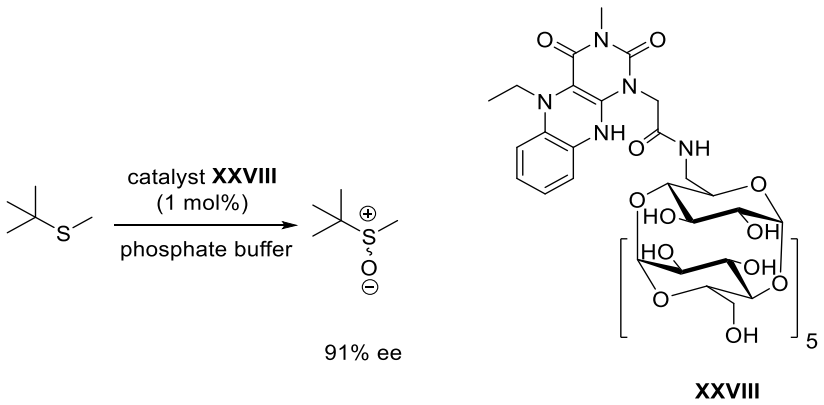

Scheme 15. Flavin-derived CDs (**XXVIII**) used for enantioselective sulfoxidations[93]

In addition, native CDs have also been shown to promote transition-metal enantioselective catalysis. For example, allylation of benzaldehyde using Zn and native β-CD as chiral promoter resulted in 93% ee.[94] Moreover, γ-CD was used as a "chiral cage" for the photochemical rearrangement of Morita-Baylis-Hillman (MBH) products, albeit with a lower enantiomeric excess (Scheme 16). [95]

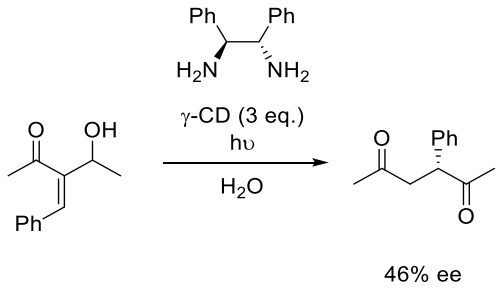

Scheme 16. Photochemical rearrangement of MBH products promoted by γ-CD

Lastly, the diamine-based CD derivative (**XXIX**) was used in a direct aldol reaction with an excellent 99% ee in acetate buffer (Scheme 17).[96]

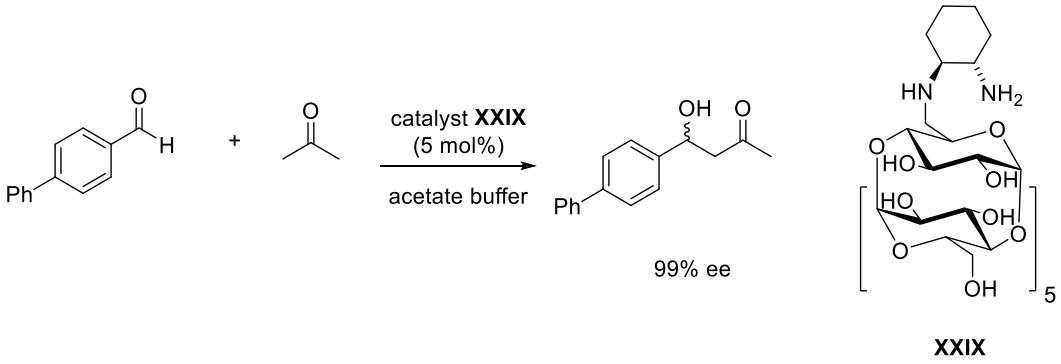

Scheme 17. Diamine-β-CD (**XXIX**) catalyzed a direct aldol reaction.

3.4. Cinchona alkaloids and CDs

Among other groups used in asymmetric organocatalysis, Cinchona alkaloids stand out for their efficiency and wide use in various asymmetric reactions with an excellent enantiomeric excess. Originally used as anti-malarial drugs, these natural compounds are now also widely used in various biology and chemistry areas. Ongoing research on Cinchona alkaloids, including their chemical modifications, continues in preparation of new derivatives, particularly used as cytotoxic compounds. The four main derivatives of Cinchona alkaloids group, containing quinoline and quinuclidine parts, are cinchonine, cinchonidine, quinine and quinidine (Figure 8).[97]

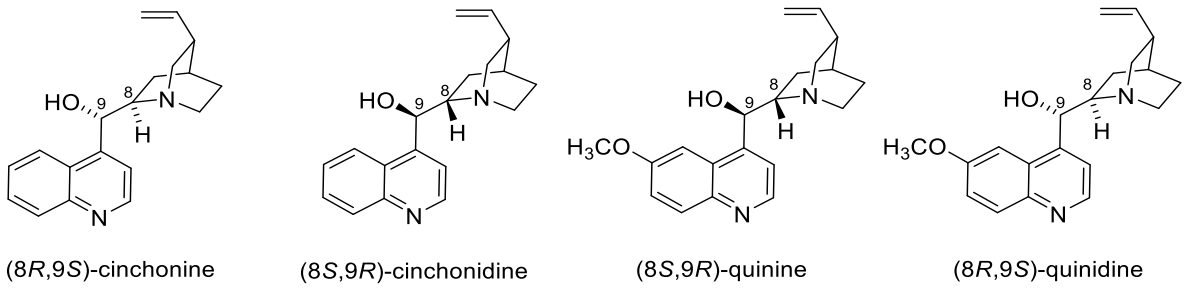

Figure 8. Most common Cinchona alkaloids (cinchonidine, cinchonine, quinine, quinidine)

Cinchona alkaloids are a privileged class of chiral catalysts. Several enantioselective reactions are catalyzed by these alkaloids and their analogs with excellent enantiomeric excess.[98] For example, salts of Cinchona alkaloids which are easily removed and reused from the reaction mixture, achieved 91% ee in Michael addition.[99]

Despite the wide use of Cinchona alkaloids in many industry and research fields, the combination of CD skeletons with Cinchona alkaloids has been scarcely investigated. Initially, inclusion complexes of CDs or a dimer of β-CD and Cinchona alkaloids were prepared (Figure 9).[100] Their binding constants were experimentally measured by fluorometric titrations which was later used to develop a pH-responsive system for drug delivery.[101]

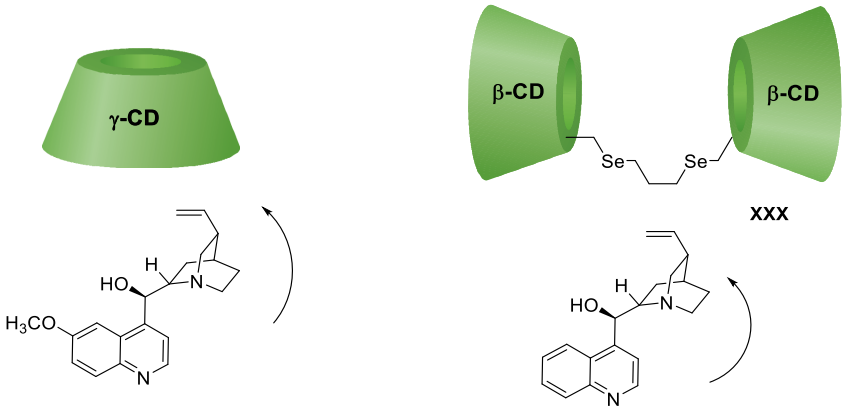

Figure 9. Inclusion complexes of CD and Cinchona alkaloids[100]

This study revealed that the complexes between γ-CD with quinine and between the bridged CD dimer (**XXX**) and cinchonidine are the most stable inclusion complexes, as shown in Figure 9. In addition, while investigating the direction of encapsulation of Cinchona alkaloids in the CD cavity, the authors of this study revealed that Cinchona alkaloids are most likely included through the narrow (secondary) rim; regardless of the part included (quinoline or quinuclidine moieties).

Other research group has tested CDs as stereodiscriminants for the separation of quinine and quinidine potentially used in drug development.[102] Furthermore, the inclusion complexes of quinuclidine and α-CD were also investigated *via* NMR measurements confirming the 1:1 inclusion complex of α-CD and quinuclidine.[103]

A study published earlier this year has further confirmed the importance of research based on the combination of Cinchona alkaloids and CDs.[104] In this study, the hydroquinine moiety was connected to the per-Me-β-CD through thiourea and squaramide linkers (Scheme 18) and these Cinchona-CD derivatives (**XXXI** and **XXXII**) catalyzed a Michael addition with excellent enantiomeric excess, applied in flow reactors.

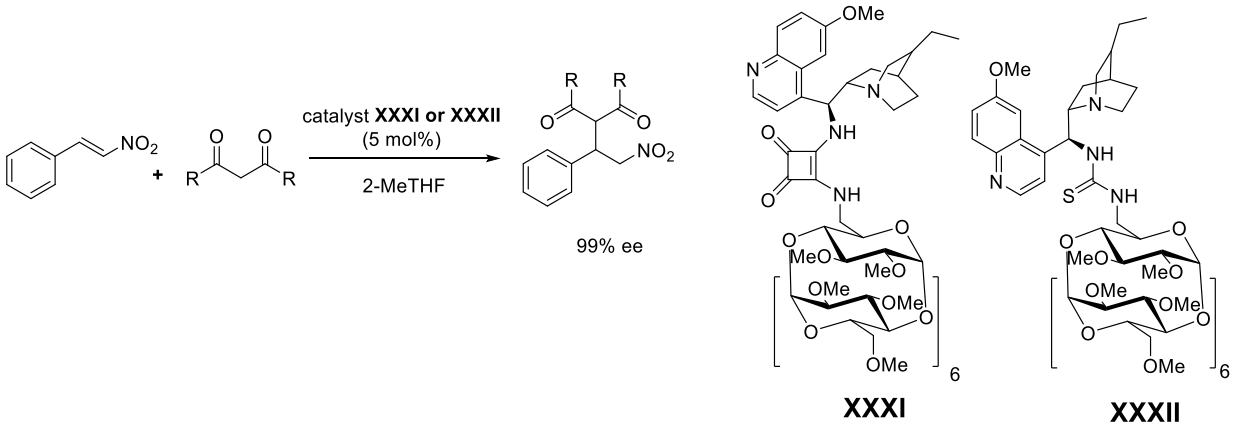

Scheme 18. Cinchona-β-CD catalysts (**XXXI** and **XXXII**) used in flow chemistry[104]

As shown above, the importance of Cinchona alkaloids either creating inclusion complexes with CDs or attaching *via* covalent bonds to CD skeletons have been unequivocally confirmed. However, this promising research of Cinchona-CD derivatives for enantioselective organocatalysis is still in progress and other studies will likely follow.

3.5. *In silico* molecular modeling

Molecular modeling, theoretical calculations and computer simulations have been increasingly attracting considerable research interest in many fields, including synthetic chemistry, because theoretical findings greatly complement experimental results. Thanks to the development of sophisticated and user-friendly software tools, computer simulations are now often used to study experimentally feasible but extremely expensive or even completely unfeasible phenomena.[105]

Concurrently, the spatial arrangement of molecules and molecular complexes can be visualized, thus enhancing our understanding of various chemical processes. In the most advanced studies of large macromolecules (including ribosomes), computers help us understand substrate binding to the active sites of enzymes[106] and even decipher the mechanisms of chemical reactions catalyzed by these enzymes, thereby bringing new insights into protein function.[107]

Several *in silico* methods are used to study molecular host-guest complexes. In the molecular docking[108], host molecules are usually treated as rather rigid entities. Numerous possible orientations and conformations of guest molecules are generated, and their binding affinities are estimated using simple empirical scoring functions.[108] However, this often leads to many false-positive and false-negative findings.

In contrast, in molecular dynamics[109] (MD) simulations of host-guest complexes surrounded by various solvents, the time evolution of whole-simulated systems can be studied in atomic detail.[110] Indeed, relative binding free energies determined by MD quantitatively match the experimental

values.[111] Accordingly, MD simulations are commonly used to study inclusion complex dynamics, more specifically to study dynamics of the inclusion complexes between CDs and various guests.[112,113]

Moreover, in recent decades, MD simulations have become widely accessible thanks to low-cost hardware resources such as large Linux clusters and many-core Graphical Processor Units (GPUs).[105] Furthermore, several software packages with user-friendly tools are now available and can be used as black-boxes.[105] One of the most commonly used software packages is NAnoscale Molecular Dynamics (NAMD)[109], which enables MD simulations of large biomolecular systems such as ribosomes or viral particles.[114] NAMD is deeply connected with the molecular graphics program Visual Molecular Dynamics (VMD)[115], which creates an user-friendly environment for the preparation of simulated systems and in-depth analysis of MD trajectories (conformational preferences and free-energy changes, among other parameters).[116,117]

Molecular dynamics simulations

In the MD simulations, atoms are supposed to move according to one of the classical Newton laws of motion

$$\vec{a}_i = \vec{F}/m_i \qquad \text{(eq. 3)}$$

where $\vec{a}_i$ is the acceleration of an atom, m_i is the atom mass and $\vec{F}$ is the net force applied.[109] This force is usually expressed as a partial derivative of the total potential energy U_{tot} of the simulated system, which leads to

$$m_i\vec{r}_i = -\frac{\partial}{\partial r_i} U_{tot}\,(\vec{r}_1, \vec{r}_2, \ldots \vec{r}_N)\;\; i = 1, 2, \ldots N, \qquad \text{(eq. 4)}$$

where $\vec{r}_i$ is the position of the atom i and N is the number of atoms in the simulated system.[109]

Numerical integration – Verlet algoritm

In MD simulations of molecular systems, Newton equations of motion are usually numerically solved by the Verlet algorithm. The positions and velocities at the next step (n+1) are obtained from the current step (n), resulting in the force expression as

$$v_{n+1/2} = v_n + M^{-1} F_n \bullet \Delta t/2\,, \qquad \text{(eq. 12)}$$

$$r_{n+1} = r_n + v_{n+1/2}\,\Delta t\,, \qquad \text{(eq. 13)}$$

$$F_{n+1} = F(r_{n+1})\,, \qquad \text{(eq. 14)}$$

$$v_{n+1} = v_{n+1/2} + M^{-1} F_{n+1} \bullet \Delta t/2 \qquad \text{(eq. 15)}$$

where v_{n+1} is the velocity at the next step, r_{n+1} is the position at the next step, M^{-1} is the mass.[109]

MD simulations of large molecular systems usually require at least hundreds of millions of time steps (1-5 fs) leading to ns-ms trajectories. The goal of these MD simulations is not to accurately determine the trajectories of atoms and molecules but to correctly sample their phase space.[109]

Numerically solving equations of motion lead to the preservation of total energy in microcanonical *NVE* ensembles with a constant number of particles, volume and energy. Temperature can be controlled in MD, for example, by Langevin dynamics (*NVT*), whereas pressure can be controlled by Hoover dynamics (*NPT*).[109] Nevertheless, many other thermostats and barostats are implemented in software packages like NAMD[109] and Assisted Model Building with Energy Refinement[118] (AMBER). In MD simulations, higher temperatures may enhance the ability of molecules to overcome energetic barriers, which was also used in this thesis (section Results and Discussion).

Force field

The total potential energy U_{tot} of simulated system usually consists of the following partial energy contributions

$$U_{tot} = U_{bond} + U_{angle} + U_{dihedral} + U_{vdW} + U_{Coulomb} \quad \text{(eq. 5)}$$

where U_{bond} is the potential energy of covalent bonds, U_{angle} represents the potential energy of angles between each pair of the covalently bonded atoms and $U_{dihedral}$ consists of the potential energy of the torsion angles of three covalent bonds between four atoms. In addition, U_{vdW} and $U_{Coulomb}$ expressed the potential energy of interactions between pairs of non-bonded atoms, that are van der Waals and electrostatic interactions. These contributions can be calculated using following equations (eq. 6-10)

$$U_{bond} = \sum_{bond\ i} k_i^{bond} (r_i - r_{0i})^2, \quad \text{(eq. 6)}$$

$$U_{angle} = \sum_{angles\ i} k_i^{angle} (\theta_i - \theta_{0i})^2, \quad \text{(eq. 7)}$$

$$U_{dihedral} = \sum_{dihedral\ i} \begin{cases} k_i^{dihe} [1 + \cos(n_i \phi_i - \gamma_i)], & n_i \neq 0 \\ k_i^{dihe} (0_i - \gamma_i)^2, & n = 0 \end{cases} \quad \text{(eq. 8)}$$

$$U_{vdW} = \sum_i \sum_{j>i} 4\varepsilon_{ij} \left[\left(\frac{\sigma_{ij}}{r_{ij}} \right)^{12} - \left(\frac{\sigma_{ij}}{r_{ij}} \right)^{6} \right], \quad \text{(eq. 9)}$$

$$U_{Coulomb} = \sum_i \sum_{j>i} \frac{q_i q_j}{4\pi\varepsilon_0 r_{ij}}. \quad \text{(eq. 10)}$$

where k_i^{bond}, k_i^{angle}, k_i^{dihe} are constants for i-bond, i-angle and i-dihedral angle, respectively, whereas the r_i is the position of *i*-particle, r_{i0} and θ_{0i} is their values in equilibrium. Then, constant n_i indicates periodicity, the γ_i is the dihedral angle, σ_{ij} is the distance for Lennard-Jones potential, q_i and q_j are the charges of i-particle and j-particle, e_{ij} is the depth of the potential well, r_{ij} is the distance between atoms *i* and *j*, ε_0 is the vacuum permittivity, θ_i is the angle between each pair of bonds and ϕ_i is torsion angle.[109]

Energy contributions described above can be visualized using solid balls are connected by spring. This model represents atoms connected *via* the covalent bonds and involved in no chemical reactions or electron transfer.[109] The parameter *r* represents the bond stretching, σ represents the bond angle, θ represents the dihedral angle and α represents the small-out-plane angle (Figure 10).[109]

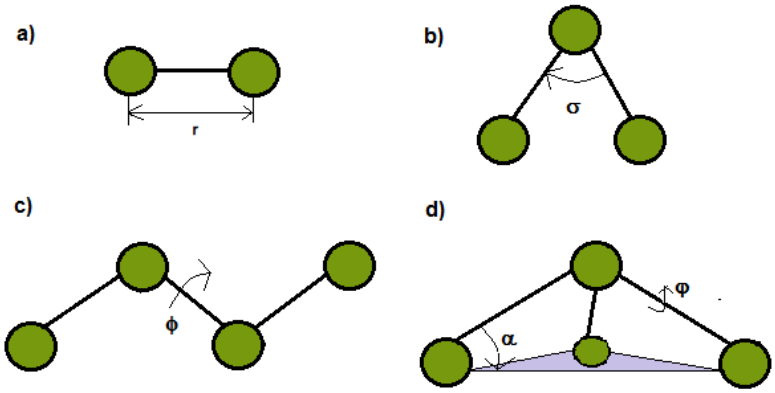

Figure 10. The interactions between atoms in MD simulations (modified from literature [109])

Periodic boundary conditions

Periodic boundary conditions are commonly used in MD simulations to prevent surface effects at boundaries. In other words, particles are enclosed in the cell, which is infinitely replicated by periodic translations. If a particle leaves the simulated system through one side of the boundary, another identical particle immediately replaces it on the opposite side. Importantly, every cell is the identical copy of all other cells. Therefore, only one cell suffices to represent a simulated system.[109]

Second approximation used in MD algorithm is the truncation of van der Waals interactions of non-bonded atoms in the system at the user-specified cutoff distance. These two approximations (i) periodic boundary conditions and (ii) the truncation of long-distance Waals interactions also apply in calculations of electrostatic interactions using the Ewald summation method.[109]

Ewald summation

The Ewald method is often used for the summation of long-range electrostatic interactions between atoms, not only inside the original cell but also with virtual replicas of atoms due to periodic boundary conditions. The Ewald sum involves the following terms

$$E_{Ewald} = E_{dir} + E_{rec} + E_{self} + E_{surface} \quad \text{(eq. 11)}$$

where E_{Ewald} is Ewald sum of energy, E_{dir} is the direct sum, E_{rec} is the reciprocal sum computed *via* fast Fourier transform, E_{self} is the self-energy which is constant, and $E_{surface}$ is the surface energy, which is usually neglected due to the high dielectric constant of water as a solvent.[109]

NAMD and AMBER software packages use the particle-mesh Ewald (PME) method[119], which distributes the charges of atoms to the nodes of a uniform grid. Furthermore, the electrostatic potentials of molecules can be computed and visualized in VMD using the "PME Electrostatics" plugin.[109]

Binding free energy of host-guest complex

Differences in binding free energies ΔF are often computed in MD simulations to predict the dynamics of host-guest inclusion complexes, in this case complexes between CDs and numerous guest (ligand) molecules.[113] These theoretical values can be compared with the experimentally determined stability constant K_s, thereby enabling the development of more potent drug carriers (for example, CD drug carriers), among others.

More specifically for CD, a ligand 1 could be very slowly detached from CDs by external forces (route A in Figure 11). The needed energy (work) could be used to estimate relative binding free energies of ligands (ligand 1). However, this geometrical approach is extremely time-consuming because the simulated system would have to remain close to thermodynamic equilibrium.[109]

A much more practical way of calculating relative binding free energies is based on "computer alchemy"[109], represented by thermodynamic cycle in route B in Figure 11. This alchemical approach consists of small, gradual, and neither physically nor chemically meaningful, conversions of one ligand (ligand 1) into another intermediate (ligand 2), performed outside (B_o) or inside (B_i) the CD cavity. Thus, determined free energy differences ΔG are subtracted.[109]

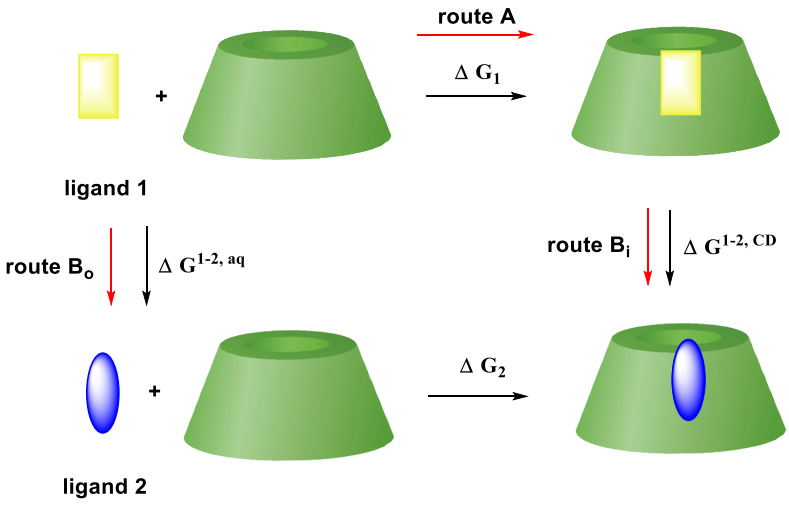

Figure 11. Thermodynamic cycle, calculation of the binding free energies ΔF using either geometrical or alchemical transformations

More accurately, the difference in free energy between state *a* and *b* of the simulated system is expressed as

$$\Delta F_{a\to b} = -\frac{1}{\beta} ln \int_0^\infty Q\ (N,V,T) e^{-\beta pV} dV \qquad \text{(eq. 16)}$$

where $\Delta F_{a\to b}$ is difference between free energy in basic state *a* and target state *b*, β is $\frac{1}{kT}$ and $Q\ (N,V,T)$ is the partition function. The relative binding free energy of ligands (guests) is then calculated using equation

$$\Delta G_1 - \Delta G_2 = \Delta G^{1\to 2,aq} - \Delta G^{1\to 2,CD} = \Delta G_{rel} = \Delta F_{a\to b} \qquad \text{(eq.17)}$$

where ΔG_1 is the binding free energy of ligand 1, ΔG_2 is the binding free energy of ligand 2, $\Delta G^{1\to 2,aq}$ is the free energy needed for the alchemist transformation of ligand 1 into ligand 2 in aqueous box, $\Delta G^{1\to 2,CD}$ is the free energy needed for the alchemist transformation of ligand 1 into ligand 2 in the CD cavity. These alchemist calculations were successfully applied to study CD complexes with isoflavones[120], fullerenes[121] and some drugs[122].

4. RESULTS AND DISCUSSION

4.1. Preparation of CD starting materials

4.1.1. Preparation of monosubstituted CD precursors

The ultimate goal of this thesis was to prepare organocatalysts based on a CD skeleton for enantioselective reactions. Thus, the first approach consisted of preparing monosubstituted CD precursors. Monosubstitution of the CD skeleton is an initial and easier method for the preparation and preliminary testing of CD derivatives as organocatalysts than disubstitution. Accordingly, 6^A-*O*-tosyl-α-CD (**1a**) and 6^A-*O*-tosyl-β-CD (**1b**) as common monosubstituted precursors were prepared according to previously published procedures (Scheme 19).[19,20]

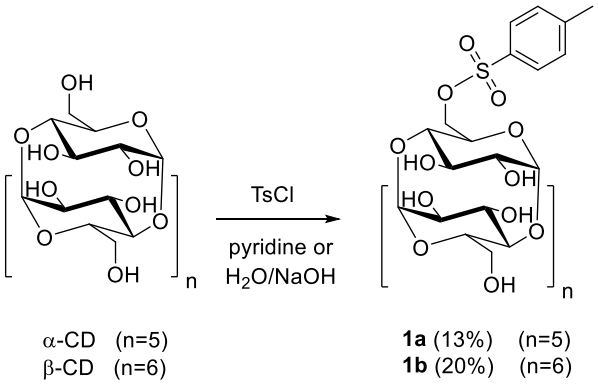

Scheme 19. Preparation of 6^A-*O*-tosyl-α-CD (**1a**) and 6^A-*O*-tosyl-β-CD (**1b**)

Subsequently, 6^A-azido-6^A-deoxy-α-CD (**2a**) and 6^A-azido-6^A-deoxy-β-CD (**2b**) were prepared from these 6^A-*O*-tosyl-CDs (**1a** and **1b**) under classical azidation conditions (Scheme 20).[19] In this thesis, we followed the commonly used (but less accurate) nomenclature of the CDs with functional groups replacing oxygen atoms, for example, 6^A-azido- instead of longer 6^A-azido-6^A-deoxy-, for simplification purposes.

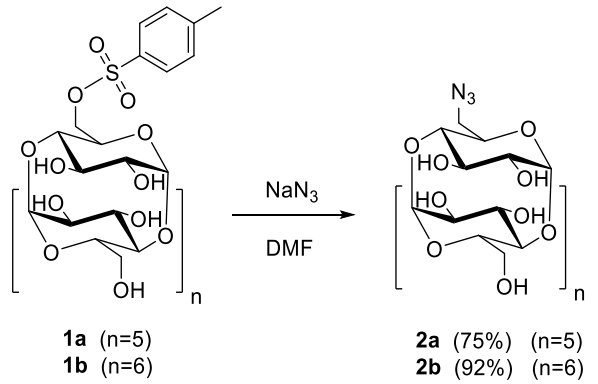

Scheme 20. Preparation of 6^A-azido-α-CD (**2a**) and 6^A-azido-β-CD (**2b**)

4.1.2. Preparation of disubstituted α-CD precursors

After preparing monosubstituted precursors for α-CD and β-CD, we focused on synthesis of disubstituted CD precursors. However, the α-CD skeleton was chosen for the simplicity because disubstitution on its primary rim results in fewer possible mixtures of regioisomers and pseudoenantiomers than the disubstitution on β-CD, as discussed in section 3.2.3. Furthermore, the smaller cavity of α-CD can prevent a high number of conformational changes of substrates during the reaction, which could strongly affect the enantioselectivity. For these reasons, the disubstituted precursors containing two azido moieties or two bromo moieties on α-CD were chosen for synthesis according to previously published procedures (Scheme 21).[23,48]

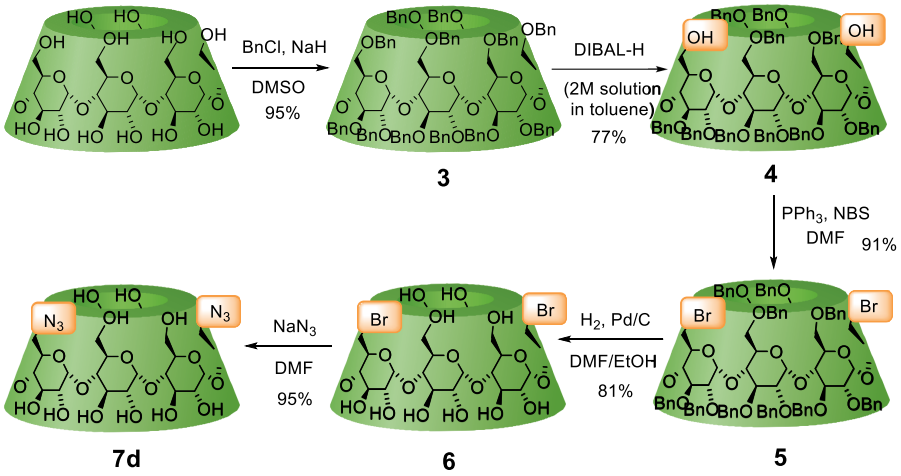

Scheme 21. Preparation of $6^{A,D}$-diazido-α-CD (**7d**)

This 5-step synthesis (*via* total perbenzylated α-CD **3**, partially debenzylated derivative **4**, dibromo perbenzylated α-CD **5** and deprotected dibromo-α-CD (**6**) with 52% overall yield resulted in a pure AD regioisomer. Moreover, the CD derivative **7d** was prepared in gram scale (from 20 g of native α-CD), and no chromatographic purifications are needed after optimizing each step thanks to full conversion into all intermediates (**3, 4, 5, 6**) and final product (**7d**).

The most problematic step in this sequence is partial deprotection with DIBAL-H to prepare CD derivative **4**. The presence of monodebenzylated byproduct **8** complicated the purification and resulted in very low yield of diol **4** (Scheme 22).

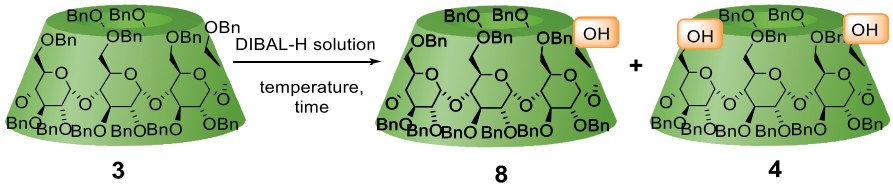

Scheme 22. Preparation of the partial deprotected CD derivatives (**8** and **4**)

Several conditions were examined to solve this problem of partial debenzylation; different equivalents of the DIBAL-H solution (Table 2, Entries 1 and 2), reaction times (Entries 3, 4 and 5) and reaction temperatures (Entries 6 and 7) were tested to optimize this deprotection. In addition, the DIBAL-H solution (commercially available as 1.0 M in toluene) had to be concentrated twice (to 2.0 M in toluene), as indicated in Kraus procedure[54]; otherwise, the concentration of DIBAL-H would not be high enough to deprotect both benzyl group. If the DIBAL-H concentration in solution is approximately 2.0 M, the reaction takes 16 hours (Entry 7).

Table 2. Optimization of DIBAL-H deprotection

Entry	DIBAL-H (eq.)	Time (h)	Temperature (°C)	Yields (%) of **8**/**4**
1	120	2	50	44/0
2	30	1.5	rt	13/0
3	30	1.5	60	36/4
4	30	48	75	10/2
5	30	144	rt	44/0
6	50	24	75	30/8
7[a]	30	16	rt	0/77

[a] the DIBAL-H solution is concentrated twice.

The reaction is also sensitive to temperature variations when adding DIBAL-H; the optimal temperature for partial deprotection of benzyl groups, determined during DIBAL-H addition, is 50 °C.

Furthermore, we benefited from the byproduct of the optimization process monodebenzylated derivative **8**, which was used to prepare the heterodisubstituted α-CD, as previously published.[44] In this sequence of reactions (depicted in Scheme 23), the monomesylated per-Bn-α-CD derivative (**9**) is converted into monoazidated per-Bn-α-CD derivative (**10**), which is then put to the tandem reduction/deprotection with DIBAL-H solution towards heterodisubstituted α-CD derivative (**11**).

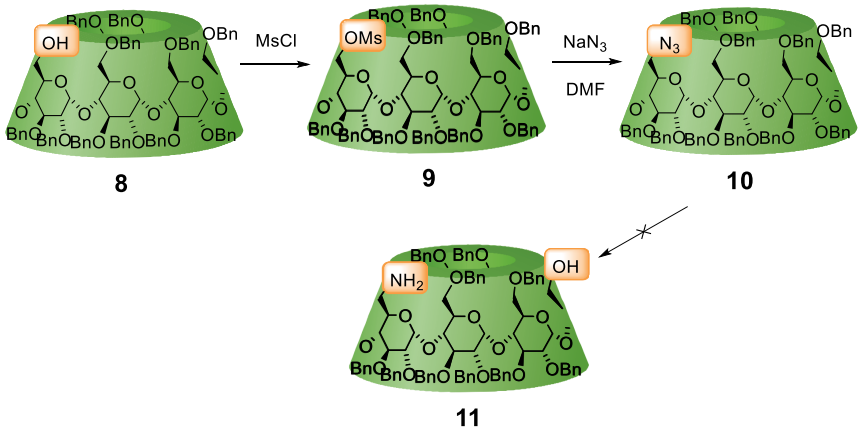

Scheme 23. Unsuccessful preparation of the heterodisubstituted perbenzylated α-CD derivative (**11**)

However, the preparation of this precursor **11** was unsuccessful, because the reaction mixture contained products with azido group and partly deprotected benzyl groups (azido with one hydroxyl group, azido with two hydroxyl groups or azido with three hydroxyl groups, among others). Moreover, derivative **11** was not prepared even when optimizing this reaction (under reaction conditions using a concentrated DIBAL-H solution, similarly to Scheme 22). Thus, different approach for the preparation of heterodisubstituted α-CD derivatives was investigated as discussed in next section.

4.2. Regioisomer ratio of CD derivatives

One of the goals of this thesis was to prepare catalysts as AC regioisomers on the primary rim of α-CDs in order to compare their catalytic activity with those catalysts prepared from AD precursors. Accordingly, a synthetic/analytical approach in which AC regioisomer can be prepared in a mixture of regioisomers (AB, AC and AD) and from which these regioisomers were subsequently separated by column chromatography was investigated. First, standards of each regioisomer had to be prepared for the unequivocal identification of regioisomers in our mixture. This strategy was previously used in another work by Fujita *et al.*[123]

From the special capping agents previously used on α-CD, we selected the most common, relatively inexpensive and commercially available *m*-benzenedisulfonyl chloride (Method 1, Scheme 24) and biphenyl-4,4´-disulfonyl chloride (Method 2, Scheme 24).

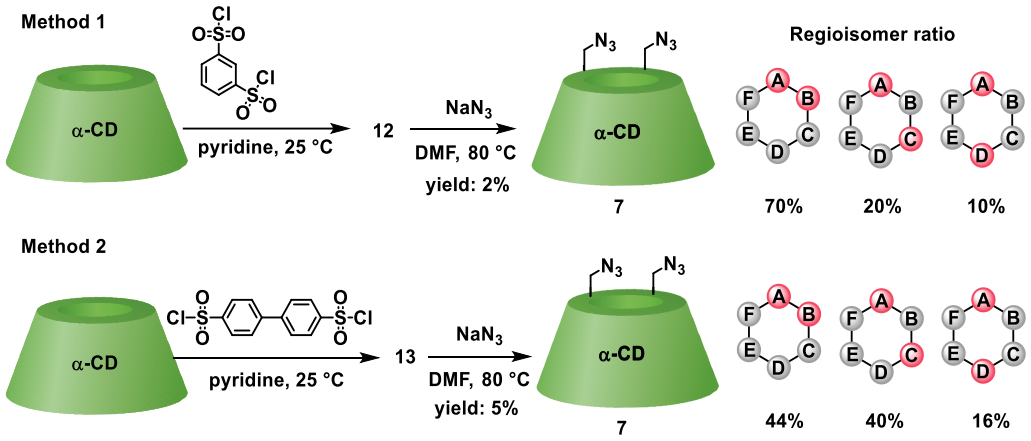

Scheme 24. Regioisomer ratio of the capping reactions on α-CD

The regioisomer ratio is given as the percentage areas of HPLC peaks (100% corresponds to the total area of AB, AC and AD peaks). These capped CDs **12** and **13** (Scheme 24) due to labile sulfonyl bridges can be easily hydrolyzed which could not be completely suppressed. Accordingly, the yields of these capped CDs were not optimal and thus, these intermediates were immediately transformed into more stable $6^{A,X}$-diazido-α-CDs (**7**). Moreover, the presence of either intramolecular or intermolecular disulfonyl bridges resulted in an interesting regioisomer ratio with biphenyl-4,4´-disulfonyl-α-CD (**13**, 44% for AB regioisomer). However, these bridges cannot be investigated in

detail due to their high hydrolysis rates. Furthermore, the formation of these intra- or intermolecular disulfonyl bridges of capped CD derivatives is not even discussed in the original papers of Tabushi and Fujita.[29]

Second, the standard for the AD regioisomer was also synthesized *via* an indirect, 5-step synthesis sequence (Method 4, Scheme 25), as discussed in section 4.1. Moreover, this reaction sequence was compared with the direct bromination of α-CD under Vilsmeier/Haack conditions (Method 3, Scheme 25). Again, both $6^{A,X}$-dibromo-α-CD derivatives (**14** and **6**) were transformed into corresponding $6^{A,X}$-diazido-α-CDs (**7**) to compare the regioisomer ratios. Furthermore, the hydrolysis of $6^{A,X}$-dibromo-α-CD (**14**) was slower than that of capped-disulfonyl-α-CDs (**12** and **13**).

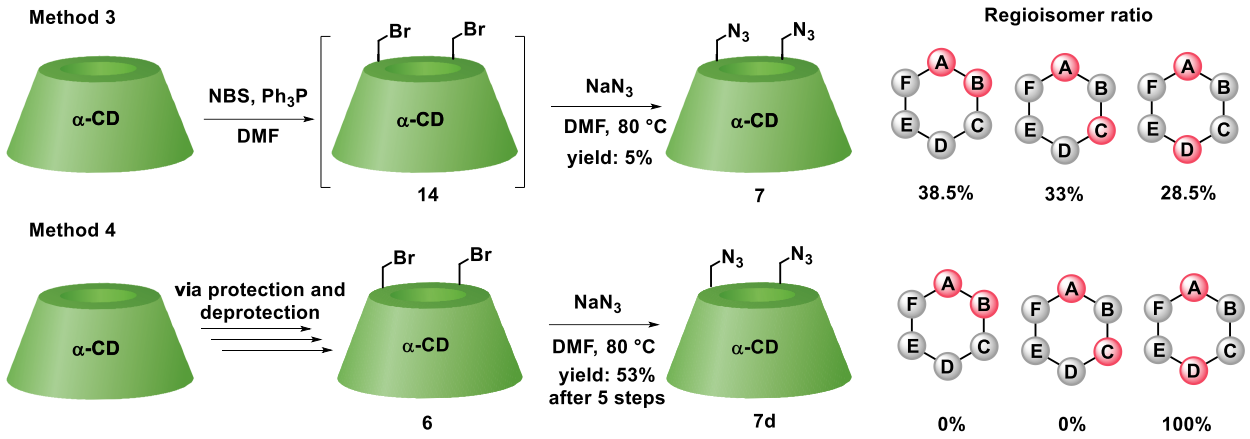

Scheme 25. Regioisomer ratio of direct (**7**) and indirect bromination (**7d**) on α-CD

The regioisomer ratio (0% vs. 0% vs. 100%) of indirect bromination (Method 4, Scheme 25) was confirmed, thus supporting the need for this time-consuming synthesis because the regioisomer ratio of direct bromination was 39% vs. 33% vs. 29%.

Lastly, to fully compare the regioisomer ratios of common disubstituted α-CDs, the most common CD intermediate $6^{A,X}$-*O*-ditosyl-α-CD (**15**) was synthesized and converted into the $6^{A,X}$-diazido-α-CD (Method 5, Scheme 26). However, almost no preference for the substituted position was observed (38% vs. 34% vs. 28%) in this ditosylation of α-CD.

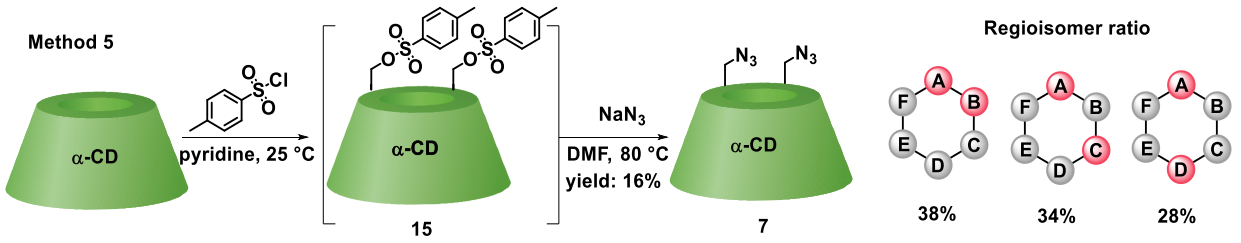

Scheme 26. Regioisomer ratio of ditosylation of α-CD

The prepared $6^{A,X}$-diazido-α-CDs (**7**) were separated by HPLC into single AB, AC and AD regioisomers (Figure 12). Concomitantly, the reaction towards capped-α-CDs (Method 1, Scheme 24) confirmed that the preferential position is AB, hence and it was used as standard for further elucidation of regioisomer ratios. The reaction of indirect bromination (Method 4, Scheme 25) confirmed the exclusive formation of the AD regioisomer, which was also used as a second standard. In addition, all other reactions resulted in mixtures of regioisomers.

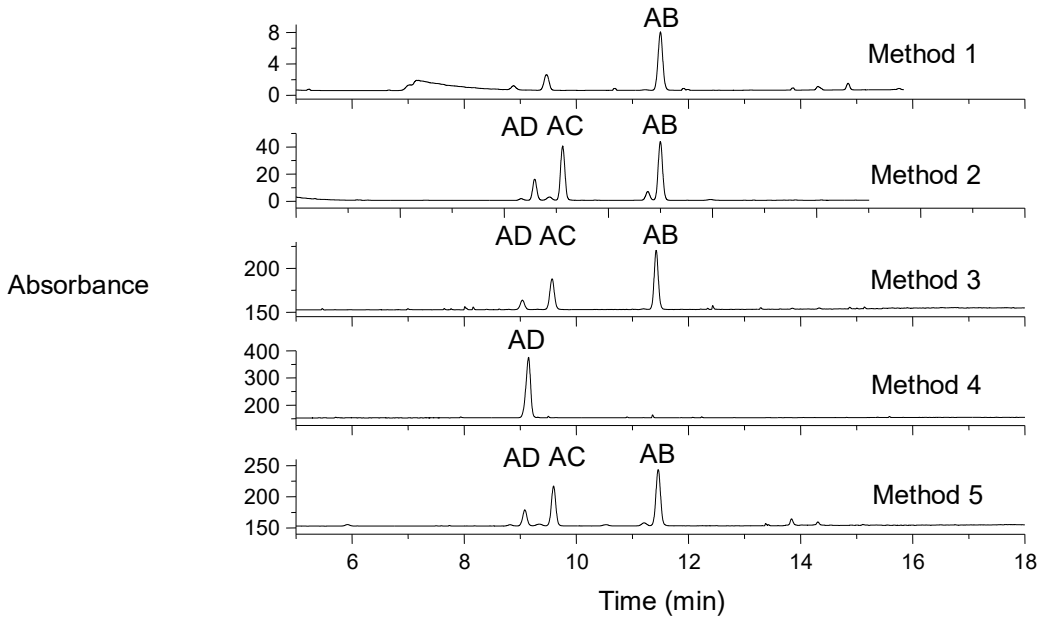

Figure 12. HPLC chromatograms of 6^{A},6^{X}-diazido-α-CDs (**7**)

Regioisomer ratios from above mentioned reactions (capping, bromination and tosylation) provided crucial data for the unambiguous determination of the regioisomer pattern of 6^{A},6^{X}-diazido-α-CD, and moreover, this comparative analysis revealed the regioisomer ratios of the most commonly used CD intermediates. Furthermore, the observed regioisomer pattern (first AD regioisomer, second AC regioisomer and third AB regioisomer) could also be supported by the fact that the mixture of 6^{A},6^{X}-ditritylates on the primary rim on α-CD showed the same order of elution of regioisomers in HPLC.[67]

4.3. Synthesis of pure regioisomer heterodisubstituted α-CD derivatives

After determining of the regioisomer ratio of common disubstituted CDs and identifying the AB and AD regioisomers as standards, target heterodisubstituted α-CD derivative with azido and mesitylene moieties was synthesized. Based on the previous research in which 6^{A}-azido-6^{C}-mesitylenesulfonyl-β-CD as an AC regioisomer was prepared as the predominant species on β-CD,[124] the mesitylenesulfonyl group was chosen as a good leaving group of the precursor **16** (Scheme 27)

because regioisomers of similar CD derivatives (with tosyl moiety, for example) can be separated by reversed-phase column chromatography.[65,125] More importantly, the mesitylenesulfonyl moiety was chosen because this group is hydrolyzed more slowly than the tosyl group.[124] Thus, the starting material 6^A-azido-α-CD was prepared from 6^A-bromo-α-CD, prepared as a byproduct of direct bromination of α-CD (Scheme 25), and the reaction of 6^A-azido-α-CD with mesitylenesulfonyl chloride resulted in the target product (**16**). Furthermore, after the reaction work-up, the crude mixture was partly converted into $6^A,6^X$-diazido-α-CD (**7**, Scheme 27) for comparison with the standards (Figure 12) in order to elucidate the regioisomer pattern of this diazido-α-CD prepared from heterodisubstituted α-CD derivatives.

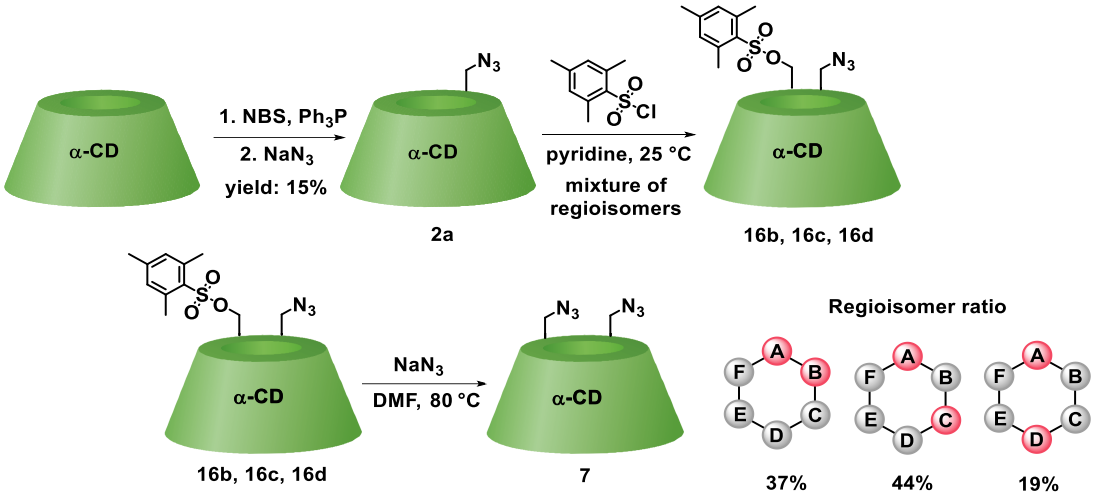

Scheme 27. Preparation of 6^A-azido-6^X-mesitylenesulfonyl-α-CD (**16**) and conversion into $6^A,6^X$-diazido-α-CD (**7**)

The observed regioisomer ratio AB:AC:AD = 37:44:19 (Scheme 27) supported the small preferences for AB and AC regioisomers; however, the AD derivative was slightly suppressed. These HPLC measurements were performed with a crude reaction mixture consisting of the starting material (**2a**), $6^A,6^X$-diazido-α-CD regioisomers (**7**) and oversubstituted $6^A,6^X,6^Y$-triazido-α-CDs. As shown in Figure 13, the HPLC signals of all components were nicely separated; thus, the regioisomer pattern could be achieved in a single step with no need to separate the starting material first and $6^A,6^X$-diazido-α-CD regioisomers afterwards.

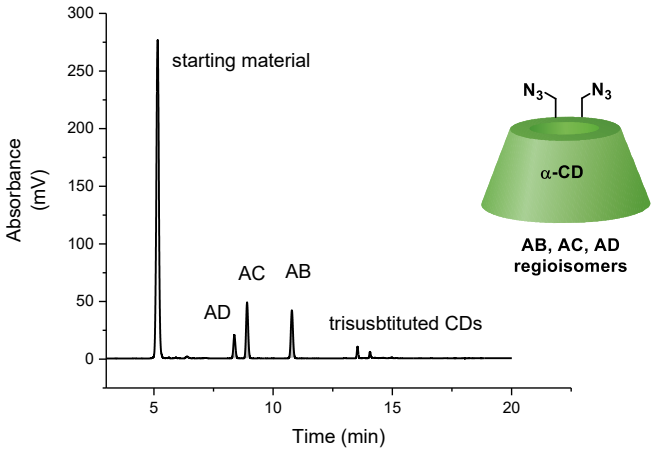

Figure 13. HPLC chromatograms of reaction mixture (Scheme 27) with separated 6^A-azido-α-CD (**2a**) as starting material and regioisomers of $6^A,6^X$-diazido-α-CD (**7**).

After identifying the regioisomer pattern (Figure 13), separation methods for 6^A-azido-6^X-mesitylenesulfonyl-α-CD (**16b**, **16c**, **16d**) were investigated. First, an analytical method was developed using UV-Vis detection with an ACN/H_2O gradient elution (Figure 14a). Consequently, the regioisomer ratio AB:AC:AD = 32:44:24 was observed. As shown in Figure 14a, the starting material 6^A-azido-α-CD (**2a**), each 6^A-azido-6^X-mesitylenesulfonyl-α-CD regioisomer (**16b**, **16c**, **16d**) and more substituted 6^A-azido-$6^X,6^Y$-dimesitylenesulfonyl-α-CD products were separated in a single and reproducible separation step. This method (analytical-scale) also confirmed that the mesitylenesulfonyl group is not hydrolyzed during the separation; thus, this functional group could be used to separate CD derivatives in gram-scale quantities by reversed-phase column chromatography (Figure 14b). However, the formation of more substituted derivatives (6^A-azido-$6^X,6^Y$-dimesitylenesulfonyl-α-CD) cannot be avoided as confirmed in Figures 14a and 14b which show incomplete conversion into the corresponding AB, AC and AD heterodisubstituted products. Therefore, the starting material 6^A-azido-α-CD remains the main component of the reaction mixture and can be recovered. Furthermore, the peak splitting of the AC regioisomer (Figure 14a) could be caused by the presence of pseudoenantiomers (AC/CA). This hypothesis was further investigated (in the section Identification of pseudoenantiomers).

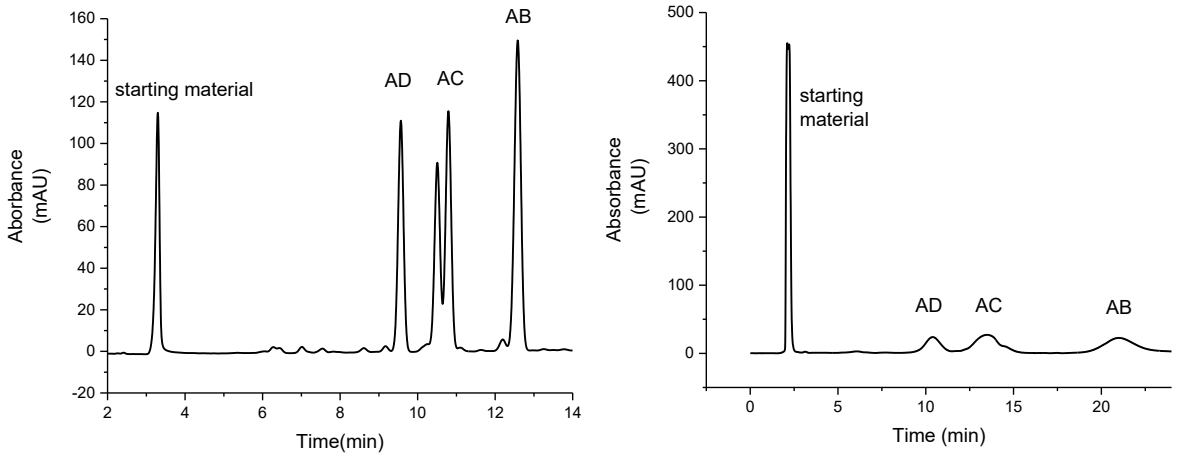

Figure 14. HPLC chromatograms of 6^{A}-azido-6^{X}-mesitylenesulfonyl-α-CD (**16**): a) analytical and b) preparative scale at 25 °C.

AB, AC and AD regioisomers were isolated by reversed-phase column chromatography with ACN/H_2O gradient elution. The AB (**16b**) and AC (**16c**) regioisomers were separated in similar yields (approximately 4%), whereas AD regioisomer (**16d**) was isolated in 3% yield. These isolated yields matched the HPLC regioisomer ratio observed in Figure 14a.

NMR characterization of heterodisubstituted α-CD derivatives

Each regioisomer of 6^{A}-azido-6^{X}-mesitylenesulfonyl-α-CD was dissolved in deuterated water (D_2O) to simplify NMR peak assignment (assignment in DMSO-d_6 included OH groups). Overall, the ^{1}H NMR spectra of all three regioisomers match the disubstituted α-CD derivative patterns. The separated AC regioisomer (**16c**) was chosen as a representative example (measurements were performed with the mixture of pseudoenantiomers). Specifically, three basic sets of signals were observed (Figure 15). The first (Mes-1) corresponded to the mesitylene aromatic peak (7.15 ppm), the second to the α-CD region (5.24-3.41 ppm) and the third (Mes-2) to methyl groups on the mesitylene skeleton (2.60-2.30 ppm). In the CD region, three areas are clearly distinguished – peaks about 5.07 ppm (CD H-1) belong to H-1 protons of four unsubstituted glucose units, whereas H-1 protons of glucoses with the azido moiety and the mesitylenesulfonyl group are shifted upfield (4.98-4.95 ppm). The separated part of the CD region is also H-6 protons (CD H-6 Mes) attached to the mesitylenesulfonyl group (~ 4.40 ppm).

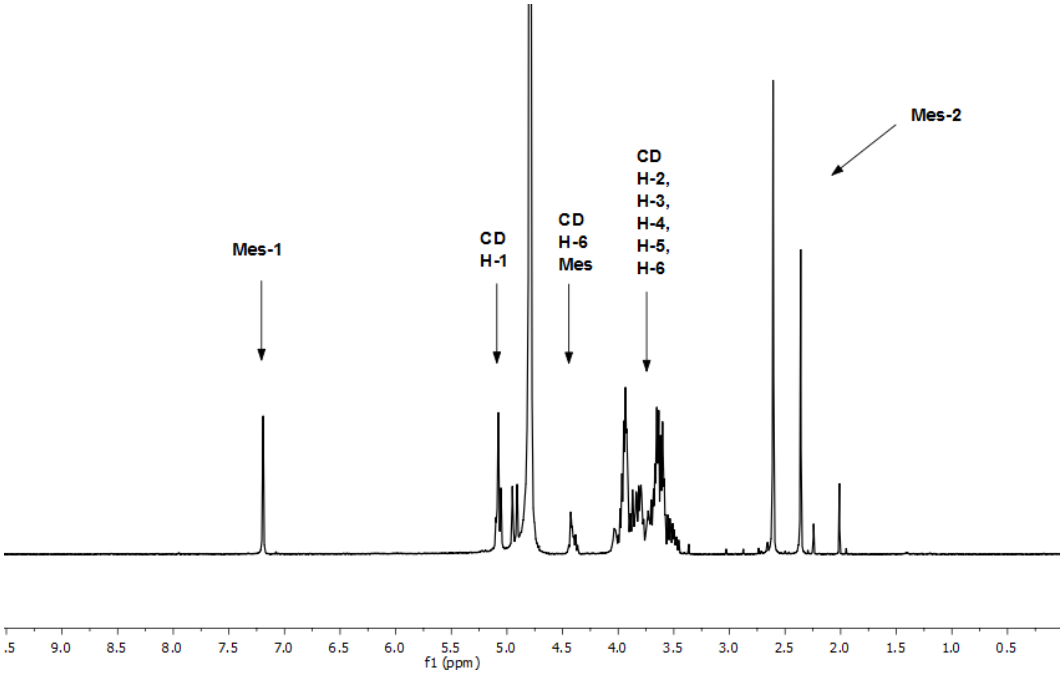

Figure 15. ^{1}H NMR spectrum of the AC regioisomer (**16c**) as a mixture of pseudoenantiomers (D_2O)

In Figure 16, the ^{13}C NMR spectrum also showed the substituted C-6 carbons at 51 ppm for azido and at 68 ppm for mesitylenesulfonyl moieties. Both substituents on the α-CD primary rim were also confirmed by separating the anomeric region into three parts in HSQC. However, the crucial splitting of six C-1 anomeric doublets for the characterization of each glucose unit was not achieved.

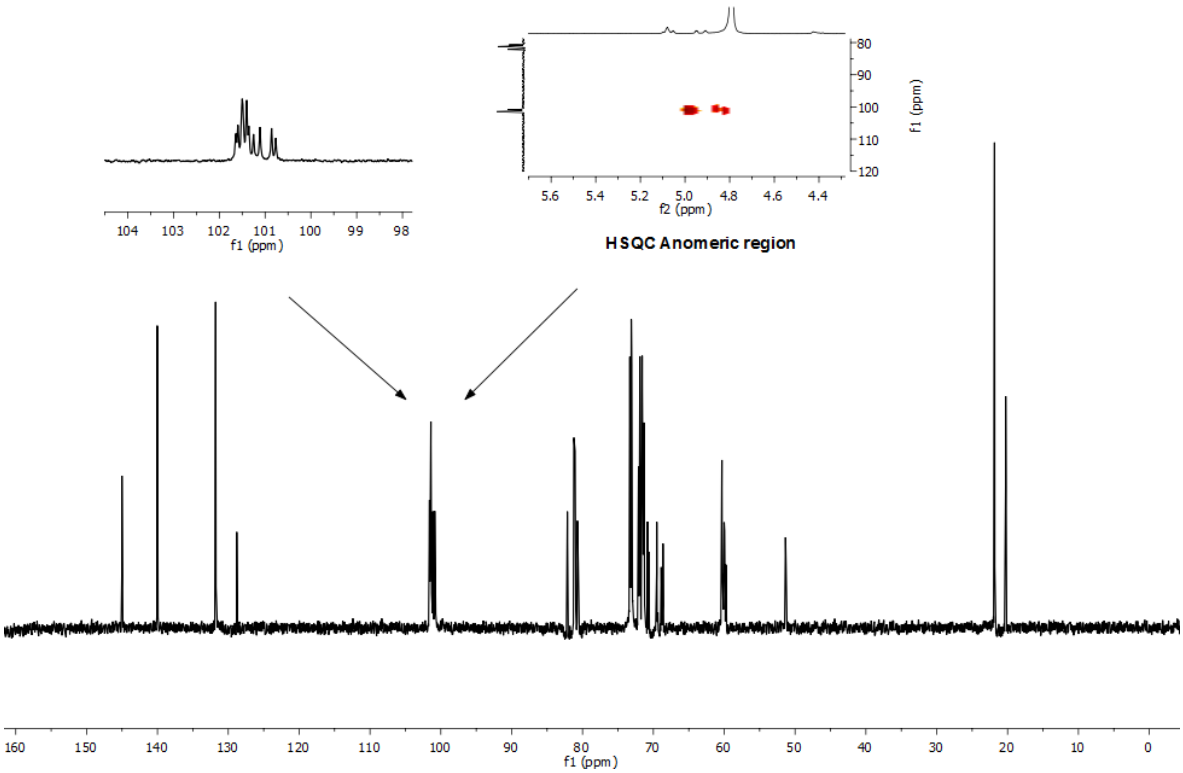

Figure 16. ^{13}C NMR spectrum of the AC regioisomer (**16c**) as a mixture of pseudoenantiomers (D_2O)

Overall, two different substituents (mesitylenesulfonyl and azido) were attached to the primary rim of α-CD, but the incomplete splitting of anomeric doublets prevented us from fully identifying different regioisomer peaks by NMR measurements.

4.3.1. Identification of pseudoenantiomers of heterodisubstituted α-CDs by HPLC-MS

As mentioned above, a peak splitting of the AC regioisomer was observed (Figure 14a) at 25 °C attributing to the possible mixture of pseudoenantiomers AC/CA (or AC/AE). Further HPLC-MS investigation explained this splitting. Peak splitting was also observed in the case of the AB regioisomer (**16b**) at 10 °C (Figure 17). Conversely, this splitting was not observed in the spectra of the AD regioisomer (**16d**) which supports the hypothesis of possible pseudoenantiomers on the primary rim of α-CD, as discussed in the section 3.2.3. This symmetrically heterodisubstituted regioisomer does not contain the pair of pseudoenantiomers (AD/DA). These results are also in accordance with Sollogoub *et al.*[60], who did not observe this peak-splitting caused by the presence of pseudoenantiomers of AD regioisomer of heterodisubstituted perbenzylated α-CDs.

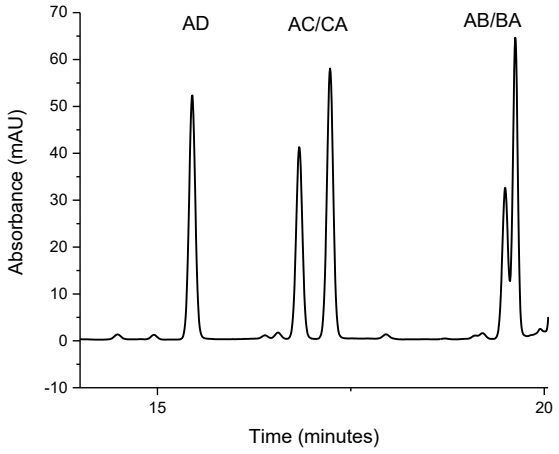

Figure 17. HPLC-MS chromatogram with the separated pseudoenantiomers of 6^{A}-azido-6^{B}-mesitylenesulfonyl-α-CD (**16b**) and 6^{A}-azido-6^{C}-mesitylenesulfonyl-α-CD (**16c**) at 10 °C

In conclusion, these heterodisubstituted AB-, AC- and AD-regioisomers of CD derivatives were not further studied or used in this project to develop new CD-based organocatalysts because the AB- and AC-regioisomer consist of the pseudoenantiomer pairs AB/BA and AC/CA, thereby preventing their application in enantioselective catalysis, and AD-regioisomer was separated as a minor product. Nevertheless, the synthesis of these heterodisubstituted α-CD precursors introduced a new approach for the preparation of preferential AC regioisomers on the primary rim of α-CD with suitable functional groups for further derivatization. Based on the above, our subsequent studies only

focused on the preparation of monosubstituted and AD-disubstituted CD derivatives as pure regioisomers, enabling their large-scale preparation, and not only as a mixture of regioisomers requiring time-consuming chromatographic separations.

4.4. Synthesis of Cinchona-CD derivatives

After confirming the existence of pseudoenantiomers of heterodisubstituted AB and AC regioisomers on the primary rim of α-CD, the method for the preparation of monosubstituted CDs was developed in order to apply it for the synthesis of the disubstituted AD regioisomer of α-CD. Four Cinchona alkaloids (cinchonine, cinchonidine, quinine and quinidine) were chosen as organocatalytic moieties for attachment to the CD skeleton.

The first method for attaching Cinchona alkaloids to the CD skeleton consisted of nucleophilic substitution of 6^A-*O*-tosyl-α-CD (**1a**) and 9-amino derivatives of Cinchona alkaloids, cinchonidine and quinidine (**17a**, **17b**, Scheme 28). 9-Amino-derivatives of cinchonidine (**17a**) and quinidine (**17b**) were prepared according to previously published procedures[126] through mesyl[127] and azido[128] intermediates inverting the configuration on C-9. This nucleophilic substitution approach was chosen because of our laboratory´s experience in substitution on 6^A-*O*-tosyl-CDs with various (alkyl)amines.[129] Thus, we performed the reaction with an excess of 9-amino-(9-deoxy)-Cinchona alkaloids (**17a** and **17b**) in DMSO under different conditions (140 °C, 2,6-lutidine, *N*-methylmorpholine, among other bases). Unfortunately, all attempts to synthesize these products failed.

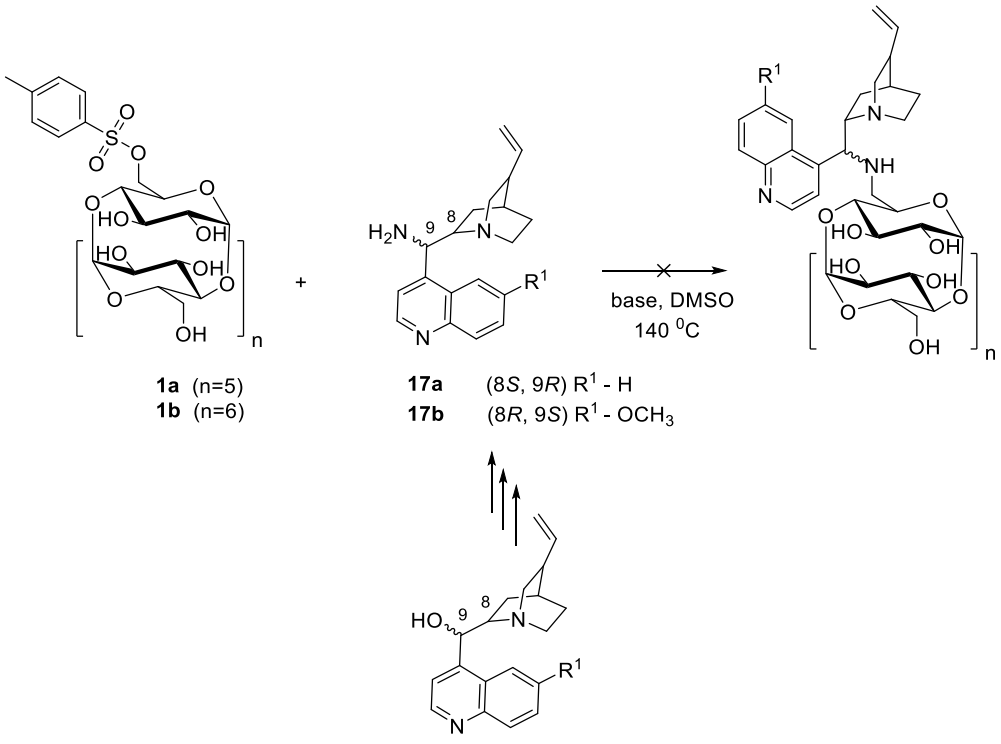

Scheme 28. Unsuccessful preparation of Cinchona-CD derivatives *via* substitution

In addition to the failed nucleophilic substitution of Cinchona alkaloids, the starting material (**1a**) was decomposed into α-CD and 3,6-anhydro-α-CD after a prolonged time. Moreover, several aromatic amines were also tested in this substitution e.g. ethyl(naphthyl)amine (similar in sterical demand with Cinchona alkaloids), but the results were similarly unsuccessful. Most likely, this reaction failed to proceed due to the high sterical demand of the Cinchona alkaloid and of the leaving tosyl moiety in nucleophilic substitution.

After the first unsuccessful approach, a different synthetic approach *via* a CuAAC click reaction[22] was started. Accordingly, 6^A-azido-α-CD (**2a**, Scheme 29) reacted with 9-*O*-propargylated Cinchona alkaloids (**18a-18d**) resulting in the preparation of α-CD products (**19a-19d**). Thus, the CuAAC click reaction was also applied for 6^A-azido-β-CD (**2b**) with 9-*O*-propargylated Cinchona alkaloids, thereby preparing a series of Cinchona-CD derivatives (**19a-19d**, **20a-20d**) linked by a triazole moiety.

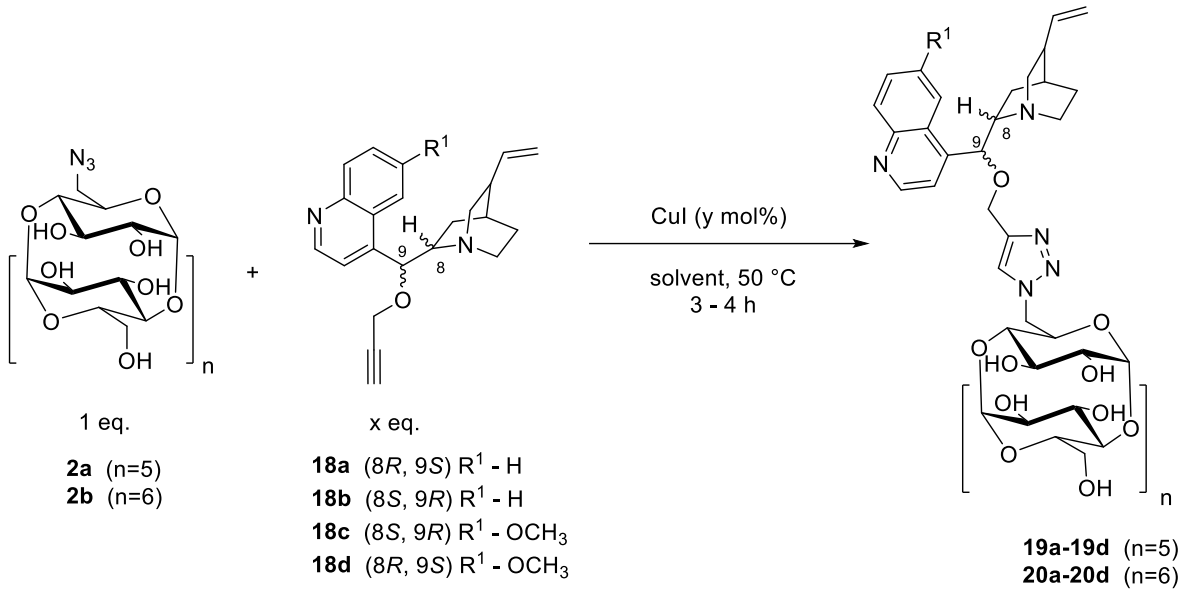

Scheme 29. Preparation of Cinchona-CD derivatives *via* a CuAAC click reaction

The preparation of Cinchona-CD derivatives *via* a CuAAC reaction was optimized (Table 3). First, the α-CD product was formed in a THF/H_2O mixture with 1.5 eq. of 9-*O*-propargylated cinchonine (**18a**) and 50 mol % CuI (Entry 1). The same yield of the product (Entry 2) was obtained when using fewer equivalents of the propargylated cinchonine (**18a**, 1.3 eq.), with a lower amount of Cu salts (20 mol %). Conversely, conversion into the product was lower (Entry 3) when using less amount (1.05 eq.) of propargylated cinchonine (**18a**). Thus, reactions with other Cinchona alkaloids (**18b–8d**) were performed in a mixture of THF/H_2O with 20 mol% Cu and with 1.3 eq. of Cinchona alkaloid. Overall, the α-CD derivatives (**19a–19d**) were isolated in high yields (up to 86% yield, Entries 2 and 4–6). However, the solvent mixture THF/H_2O was not appropriate for full conversion into the product on the β-CD skeleton (**2b**, Table 3), not even after 48 hours (Entry 7). Conversely, when changing the solvent to DMF, full conversion was achieved after 2 hours with excellent yields

(up to 95%, **20a–20d**, Entries 8–11). Moreover, the yield of the product decreased when using DMF for a CuAAC reaction on an α-CD skeleton (only 38% of **19a** after 48 hours, Entry 12).

Table 3. Optimized conditions for the CuAAC from Scheme 29.

Entry	CD	Alkaloid	R^1	x (eq.)	y (mol %)	Solvent	Yield[a] in %
1	**2a**	**18a** (8*R*, 9*S*)	H	1.5	50	THF/H_2O (1:1)	78 (**19a**)
2	**2a**	**18a** (8*R*, 9*S*)	H	1.3	20	THF/H_2O (1:1)	77 (**19a**)
3	**2a**	**18a** (8*R*, 9*S*)	H	1.05	20	THF/H_2O (1:1)	56 (**19a**)
4	**2a**	**18b** (8*S*, 9*R*)	H	1.3	20	THF/H_2O (1:1)	86 (**19b**)
5	**2a**	**18c** (8*S*, 9*R*)	OCH_3	1.3	20	THF/H_2O (1:1)	72 (**19c**)
6	**2a**	**18d** (8*R*, 9*S*)	OCH_3	1.3	20	THF/H_2O (1:1)	74 (**19d**)
7[b]	**2b**	**18a** (8*R*, 9*S*)	H	1.3	20	THF/H_2O (1:1)	20 (**20a**)
8	**2b**	**18a** (8*R*, 9*S*)	H	1.3	20	DMF	89 (**20a**)
9	**2b**	**18b** (8*S*, 9*R*)	H	1.3	20	DMF	70 (**20b**)
10	**2b**	**18c** (8*S*, 9*R*)	OCH_3	1.3	20	DMF	80 (**20c**)
11	**2b**	**18d** (8*R*, 9*S*)	OCH_3	1.3	20	DMF	95 (**20d**)
12[b]	**2a**	**18a** (8*R*, 9*S*)	H	1.3	20	DMF	38 (**19a**)

[a] Isolated yield. [b] After 48 hours.

NMR elucidation of Cinchona-non-methylated CD derivatives

Structures of non-methylated CD derivatives (**19a–19d, 20a–20d**) were unambiguously confirmed in NMR measurements (numbering of CD skeletons is depicted in section 6.1). As a representative example of these CD derivatives, we chose an α-CD derivative with quinidine (**19d**). The ^{1}H NMR spectrum of this non-methylated CD derivative (in DMSO-d_6) is in accordance with monosubstituted derivatives at position 6 on the primary rim (Figure 18). Generally, four different regions with typical signals were observed: the first, a well-resolved aromatic region belongs to the quinoline part of Cinchona alkaloids (9.00–7.55 ppm) and to the hydrogen signal of triazole (8.21 ppm), thus confirming the attachment of Cinchona alkaloids to the CD skeleton in CuAAC click reactions. The second part of the ^{1}H NMR spectrum is the resolved signal of the double bond on the quinuclidine skeleton of the Cinchona alkaloid (5.93 ppm). The third part of the spectrum consisted of the CD region (5.50-3.20 ppm) with H-1 atoms of nonsubstituted glucose units (4.80 ppm) and H-1 (5.03 ppm) of the substituted glucose. Accordingly, signals of H-2, H-3, H-4 and H-6 atoms of nonsubstituted units were found around 4.00–3.00 ppm, whereas the H-6 signal of the substituted glucose unit is visible around 4.75 ppm (especially in HSQC and ^{1}H-^{1}H COSY spectra). This part also includes primary (4.49-4.34 ppm) and secondary (5.91-5.53 ppm) rim OH groups. The last part of this

^{1}H NMR spectrum corresponds to the signals of the quinuclidine skeleton of the Cinchona alkaloid, which are identified around 2.00–1.20 ppm.

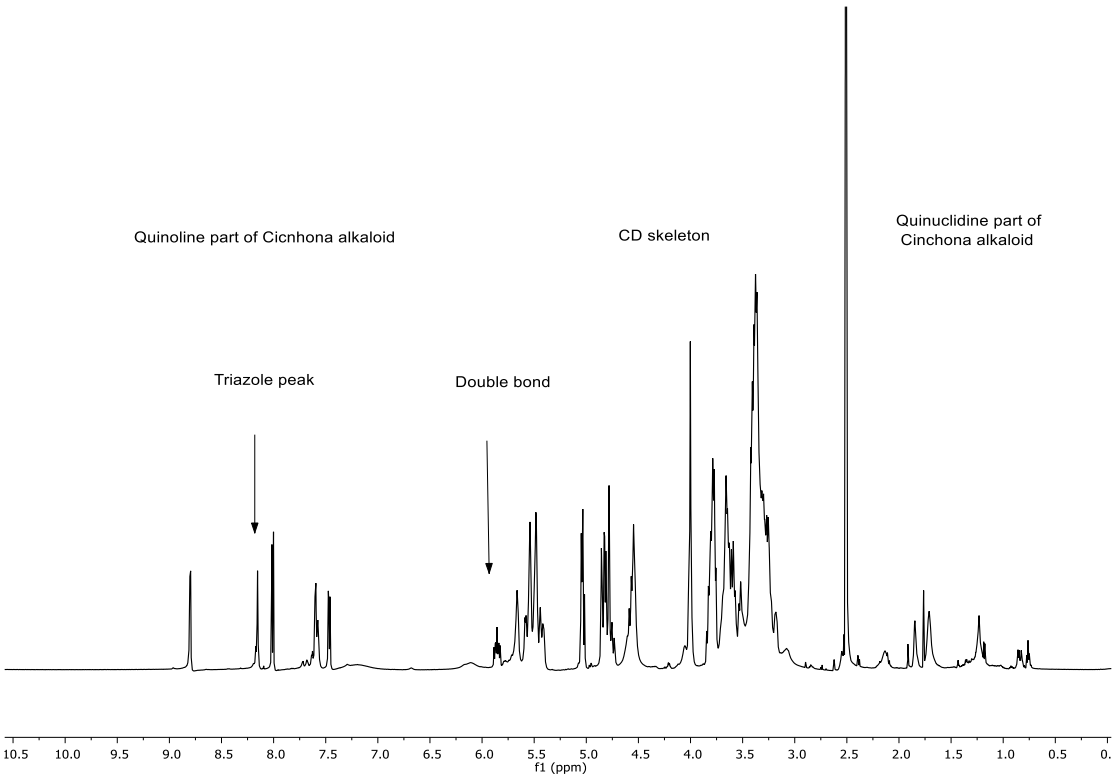

Figure 18. ^{1}H NMR spectrum of the non-methylated quinidine-α-CD derivative (**19d**, DMSO-d6)

Subsequently, ^{13}C NMR, DEPT-edited HSQC and HMBC spectra also confirmed substitution on the primary rim of CD skeleton (Figure 19). The C-6 atom from the substituted glucose unit is correlated with the hydrogen signal of the triazole (50.41 ppm of C-6^{I} to 8.16 ppm of H-14´of triazole) and the peak at 126.13 ppm of C-14´ triazole is correlated with the signal at 4.57 ppm of the quinidine part.

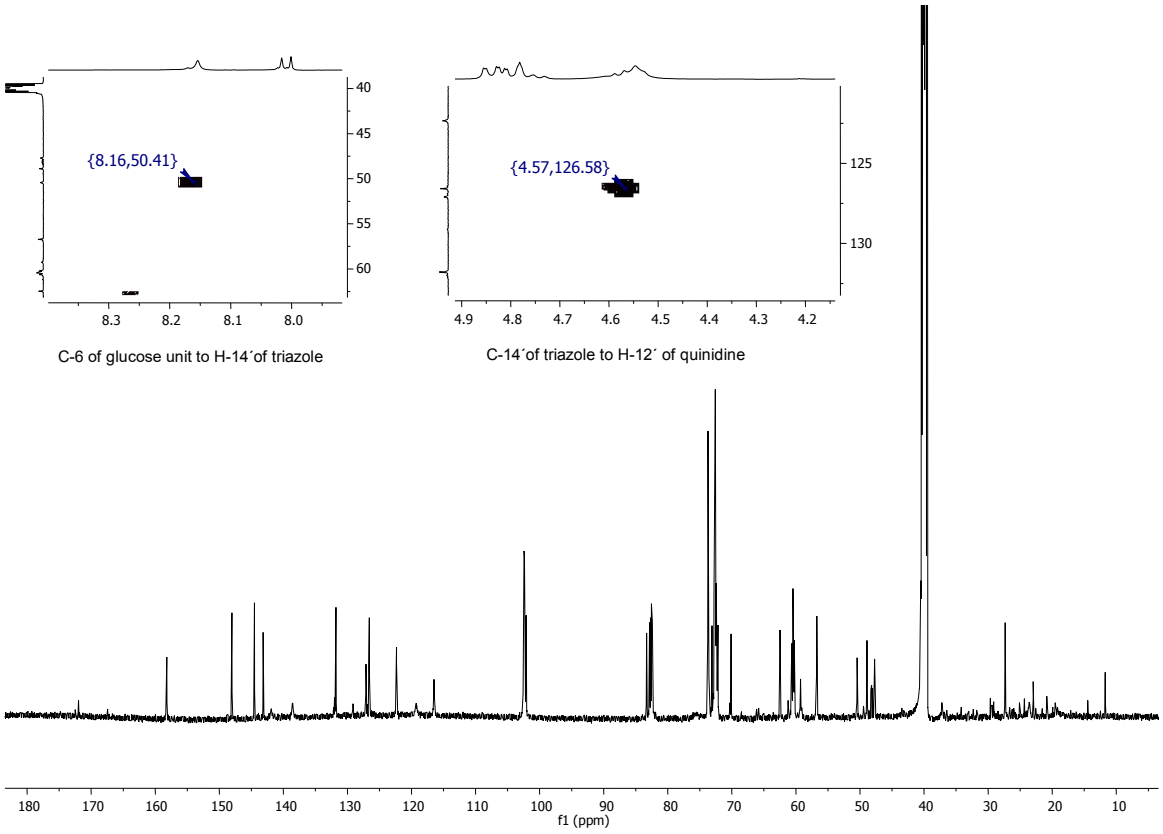

Figure 19. ^{13}C NMR spectrum and parts of HMBC spectra of the non-methylated quinidine-α-CD derivative (**19d**, DMSO-d6).

Moreover, the supramolecular properties of these Cinchona-CD derivatives were also investigated in order to study the possible inclusion of the Cinchona alkaloid moiety into CD cavity. Thus, cinchonine-β-CD (**20a**) and quinine-β-CD (**20c**) were measured in D_2O; the additional 2D ROESY spectrum showed crosspeaks between substituent (hydrogen atoms of double bond on the quinuclidine skeleton) and the inner H-3 atoms of β-CD cavity (Figure 20). Nevertheless, low solubility of these non-methylated Cinchona-β-CDs in H_2O (approximately 1 mg/1 mL) did not allow us to further investigate the nature of the inclusion, e.g., with a concentration dependence. Overall, these observed crosspeaks in ROESY can be caused by intermolecular interactions (inclusion of the cinchonine moiety to the second CD cavity) or intramolecular interactions (as discussed by Hapiot and Monflier[130]). This phenomenon was further studied by MD and discussed in section 4.9.2.

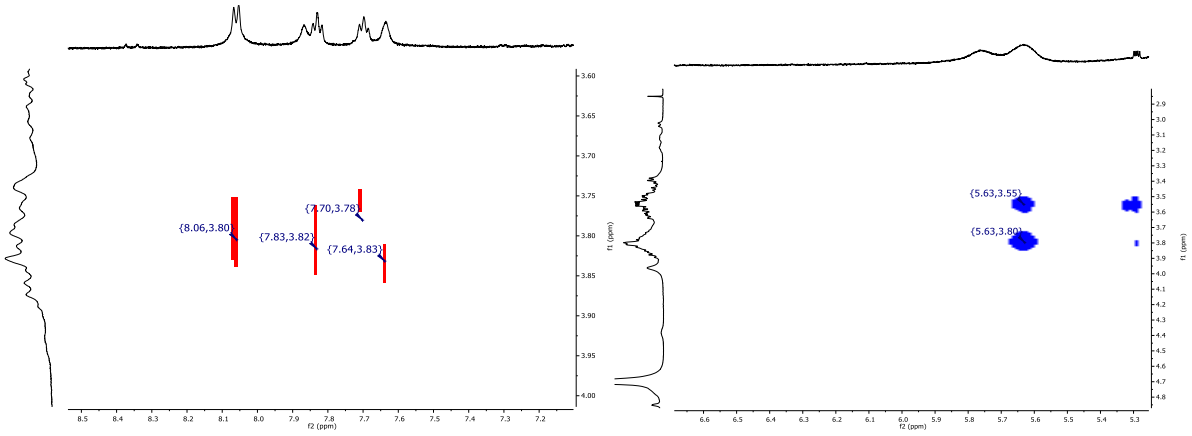

Figure 20. 2D ROESY spectra of non-methylated Cinchona-β-CD derivatives **20a** (red) and **20c** (blue) in D_2O showing crosspeaks between double bond of the Cinchona alkaloid and inner protons (H-3) of β-CD cavity.

In conclusion, we unambiguously confirmed Cinchona alkaloid attachment to the CD skeleton through triazole using 2D NMR measurements. This thorough investigation revealed no triple bond and a new triazole hydrogen signal, simultaneously correlating C6 atom on the substituted glucose unit with triazole. Therefore, the prepared CD derivatives are substituted on the primary side.

4.5. Synthesis of Cinchona-permethylated CD derivatives

After developing the approach for attaching Cinchona alkaloids to non-methylated CDs, permethylated CD derivatives were also prepared for their better solubility in water and in organic solvents. First, the starting CD compounds per-Me-N_3-α-CD (**21**) and per-Me-N_3-β-CD (**22**) were prepared according to published procedures[131,132] and they were used under previously optimized conditions for CuAAC click reactions (non-methylated CDs with propargylated Cinchona alkaloids **18a–18d** as outlined in Table 3). Cinchona-permethylated CD derivatives (**23a–23d, 24a–24d**) were isolated in high yields (up to 69%, Scheme 30).

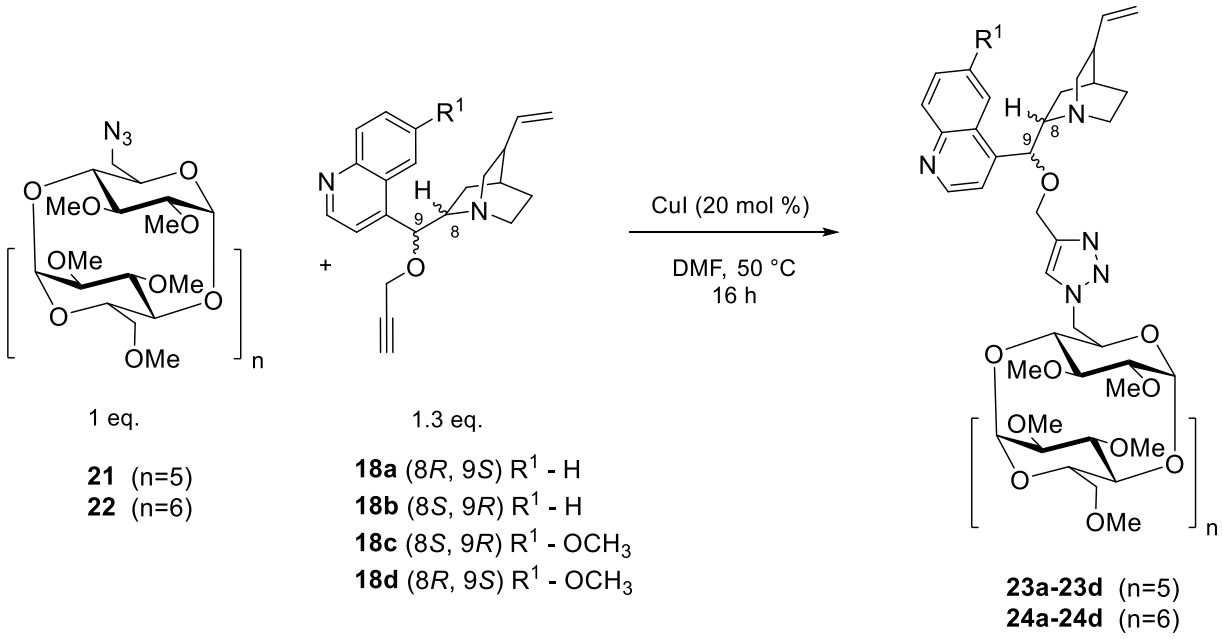

Scheme 30. Preparation of Cinchona-permethylated CD derivatives (**23a**-**23d**, **24a**-**24d**)

As mentioned above, the conditions assessed using non-methylated CDs were applied to prepare their analogs on per-Me-α-CD (**21**); the propargylated Cinchona alkaloid (**18a**) was added in 1.3 molar equivalents, with 20 mol% CuI in DMF (Table 4, Entry 1). Thus, a series of permethylated Cinchona α-CD derivatives (**23a–23d**) was prepared with good yields (59-42% yield, Entries 1–4). In the case of per-Me-β-CD (**22**), the products (**24a–24d**) were also isolated with good to high yields (up to 69% yield, Entries 6–9). Furthermore, the mixture of solvents THF/H_2O was investigated (Entry 5), but the reaction in DMF showed a higher isolated yield (Entry 3).

Table 4. Optimized conditions for the CuAAC reaction from the Scheme 30

Entry	CD	Alkaloid	R^1	Yield[a] in % (Product)
1	**21**	**18a** (8*R*, 9*S*)	H	59 (**23a**)
2	**21**	**18b** (8*S*, 9*R*)	H	48 (**23b**)
3	**21**	**18c** (8*S*, 9*R*)	OCH_3	49 (**23c**)
4	**21**	**18d** (8*R*, 9*S*)	OCH_3	42 (**23d**)
5[b]	**21**	**18c** (8*S*, 9*R*)	OCH_3	34 (**23c**)
6	**22**	**18a** (8*R*, 9*S*)	H	64 (**24a**)
7	**22**	**18b** (8*S*, 9*R*)	H	69 (**24b**)
8	**22**	**18c** (8*S*, 9*R*)	OCH_3	48 (**24c**)
9	**22**	**18d** (8*R*, 9*S*)	OCH_3	63 (**24d**)

[a] Isolated yield. [b] THF/H_2O mixture.

NMR elucidation of permethylated CD derivatives

NMR spectra of permethylated derivatives were assessed in CD_3OD. A representative example, per-Me-β-CD derivative with quinidine (**24d**) was chosen to compare the spectra with those of the non-methylated CD derivatives. The ^1H NMR spectrum of this derivative **24d** is also divided into several parts; the aromatic region was similar to the region of non-methylated CD analogs (8.75 – 7.15 ppm), and the CD region (5.45 – 2.55 ppm) included methyl groups instead of hydroxyl groups (Figure 21). The quinuclidine skeleton was also observed around 1.2 ppm.

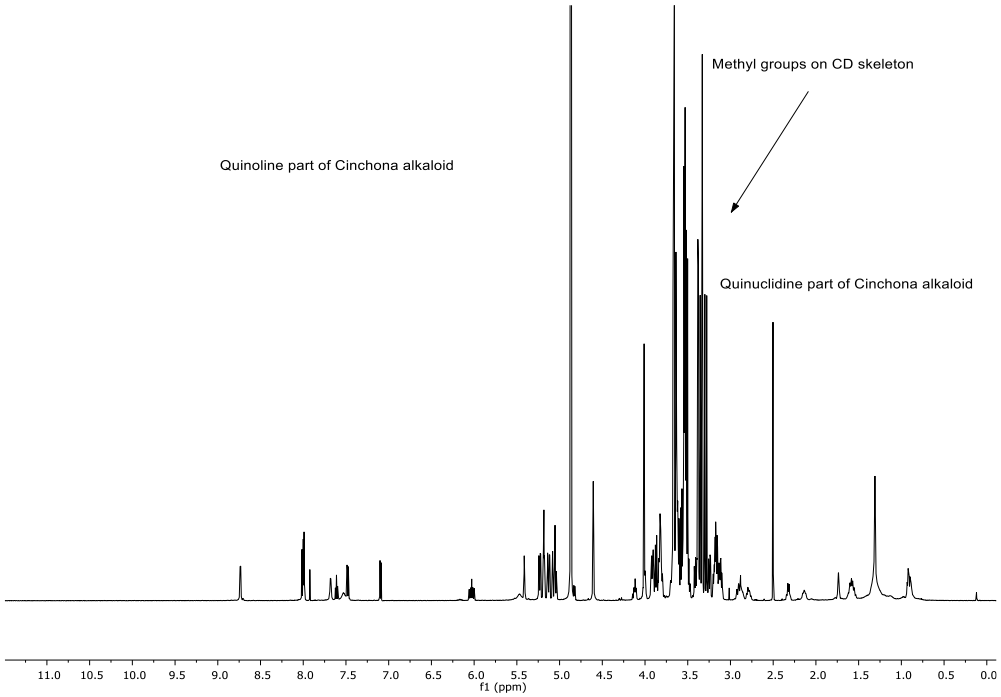

Figure 21. ^1H NMR spectrum of the per-Me-quinidine-β-CD derivative (**24d**) in CD_3OD

Similarly to non-methylated CD derivatives, ^{13}C NMR, DEPT-edited HSQC and HMBC spectra also confirmed substitution on the primary rim of permethylated CD skeleton (Figure 22). The C-6 atom from the substituted glucose unit is correlated with the hydrogen signal of the triazole moiety (50.93 ppm of C-6^I to 7.99 ppm of H-14´of triazole).

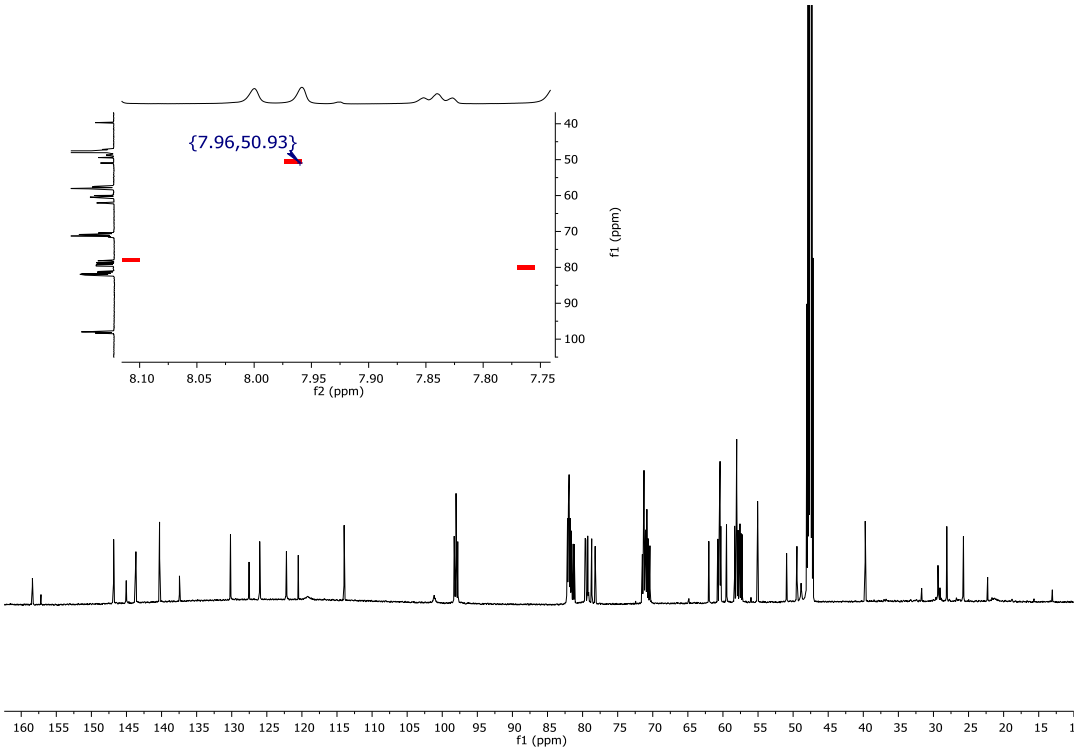

Figure 22. ^{13}C NMR spectrum and a part of HMBC spectra of the per-Me-quinidine-β-CD derivative (**24d**) in CD_3OD

In conclusion, Cinchona alkaloid attachment to the CD skeleton through triazole linker was confirmed by 2D NMR spectra. These results revealed no triple bond and a new triazole hydrogen signal. Moreover, C6 atom on the substituted glucose unit correlated with the triazole. Therefore, the prepared permethylated CD derivatives are substituted on the primary side.

4.6. Solubility of prepared Cinchona-CD derivatives and gram-scale preparation

Before assessing the catalytic activity of Cinchona-CD derivatives, their solubility in water was examined. As expected,[133] permethylated CD derivatives were more soluble in water than non-methylated CDs (Figure 23).

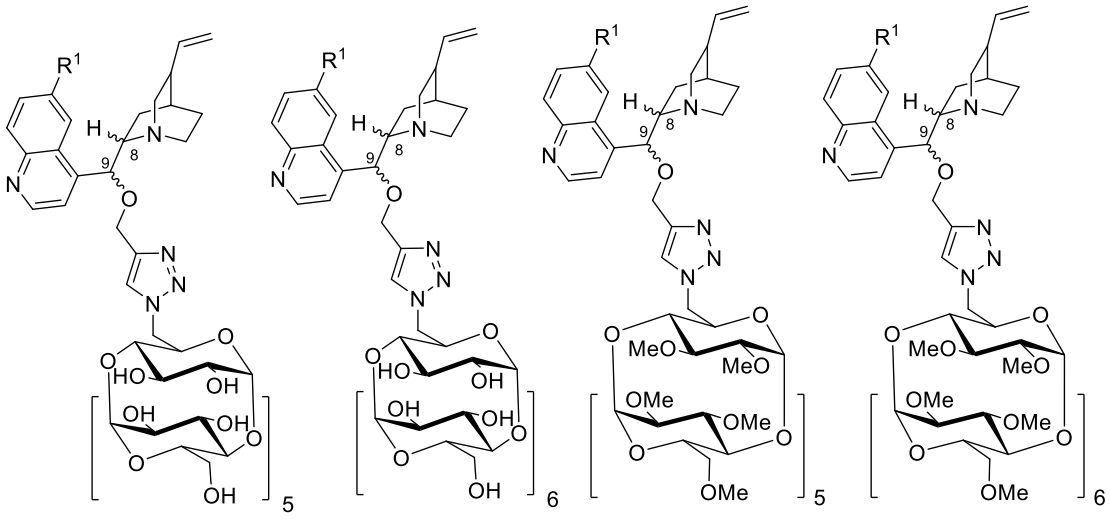

Figure 23. Solubility of Cinchona-CD derivatives in water

Moreover, the cinchonidine-β-CD (**20b**) was prepared in gram-scale for further tests in enantioselective reactions. This CuAAC reaction proceeded in 0.95 g of product (53% isolated yield); in addition, an excess amount of 9-*O*-propargyl-cinchonidine (2.5 eq.) and the catalyst CuI (40 mol %) were needed for the conversion into the product, which occurred after 16 hours of reaction (Scheme 31). This derivative is currently being tested in enantioselective hydroformylation reactions in collaboration with Professor Éric Monflier's group, Université de d´Artois, Lens, France.

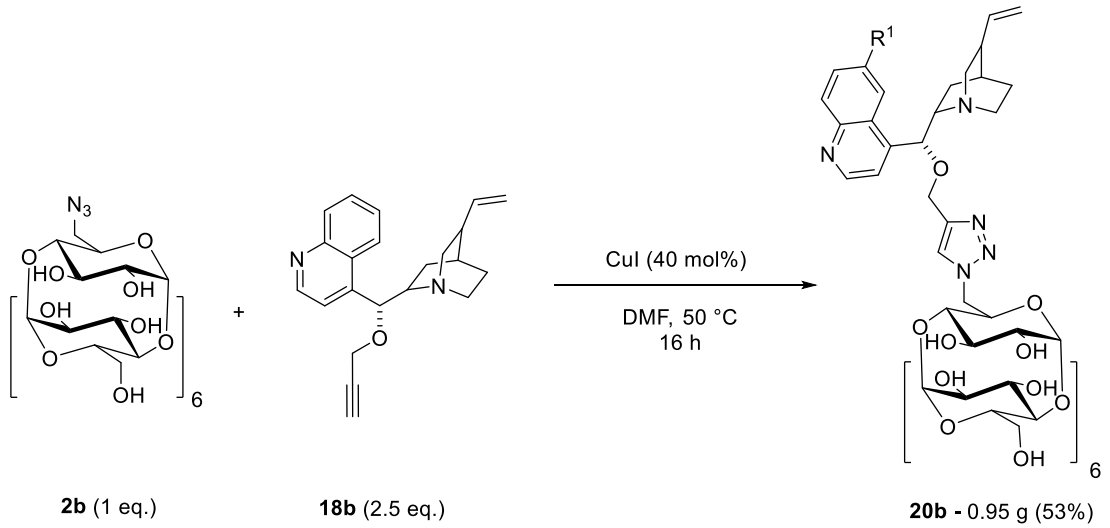

Scheme 31. Gram-scale preparation of cinchonidine-non-methylated-β-CD (**20b**)

4.7. Preparation of AD disubstituted α-CD derivatives

After developing the method for attaching Cinchona alkaloid to CD skeletons, the preparation of AD disubstituted α-CD derivatives was investigated. Although nucleophilic substitution failed when attempting to attach Cinchona alkaloids to monosubstituted CD skeletons (section 4.4), two leaving groups (bromo groups instead of tosyl moiety) of the precursors may differently influence the nucleophilic substitution. Thus, $6^A,6^D$-dibromo-α-CD (**6**) was tested in this reaction with an excess of 9-amino-(9-deoxy)-cinchonidine (**17a**) in DMSO under harsh conditions (140 °C, 2,6-lutidine, N-methylmorpholine, among other bases, Scheme 32). Similarly to the nucleophilic substitution on the monosubstituted CD derivatives, the reaction did not proceed at all, similarly due to sterical demand of the bulky Cinchona alkaloid.

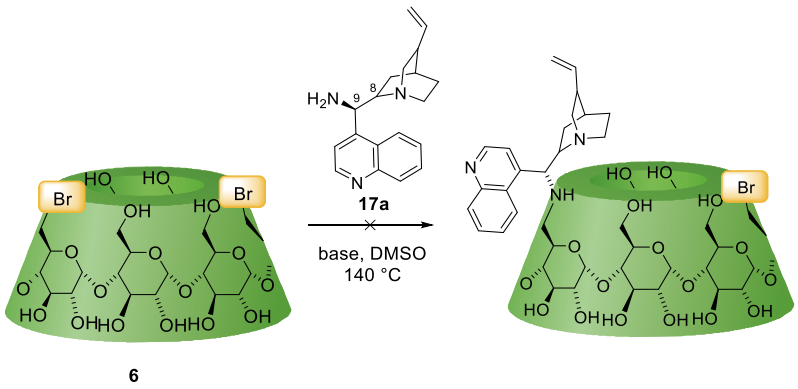

Scheme 32. Unsuccessful substitution on the $6^A,6^D$-dibromo-α-CD derivative (**6**).

However, the approach of nucleophilic substitution on the disubstituted CD skeleton failed as expected; subsequently, the CuAAC click reaction, developed for monosubstituted CD derivatives, was used in this preparation of disubstituted α-CD derivatives. The starting material $6^A,6^D$-diazido-α-CD (**7**) successfully reacted with quinine moiety (**18c**, Scheme 33), and the AD disubstituted product **27** was isolated in 76% yield.

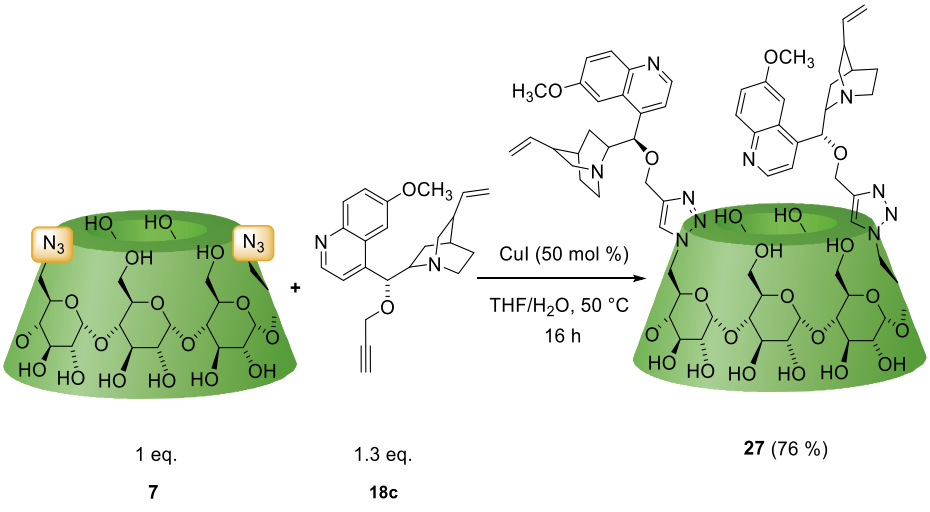

Scheme 33. Preparation of the AD disubstituted quinine-α-CD derivative (**27**).

Considering the possibility of the preparation of heterodisubstituted α-CD derivatives, the reaction was investigated in order to isolate first intermediate, quinine-azido-α-CD derivative (Scheme 34). However, a mixture of starting material **7**, monosubstituted Cinchona-azido-α-CD and disubstituted α-CD with two quinine moieties (**27**) was presented from the beginning of the reaction. Thus, the time-consuming isolation of this Cinchona-monosubstituted product yielded only traces of this product.

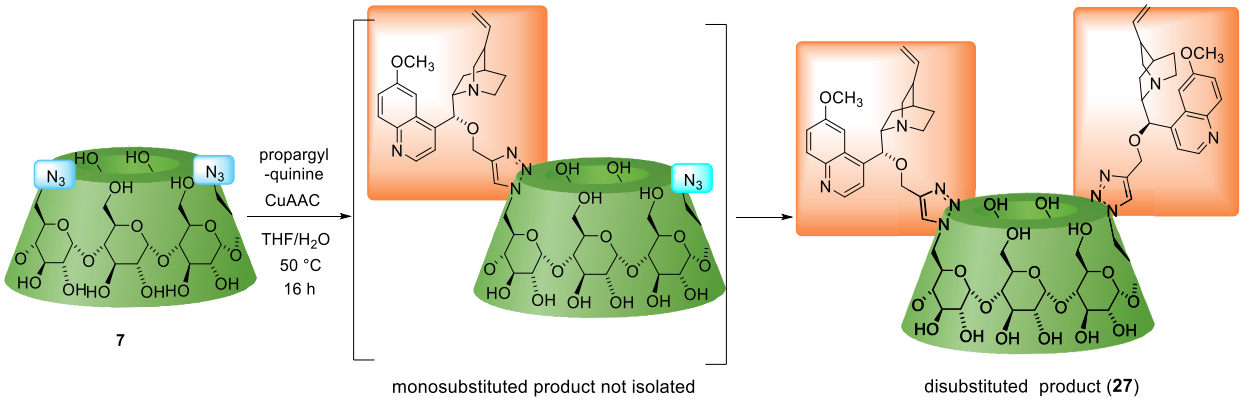

Scheme 34. Monosubstituted and disubstituted α-CD skeletons with quinine moieties

4.8. Evaluation of Cinchona-CD derivatives as organocatalysts

The prepared Cinchona-CD derivatives (monosubstituted and disubstituted) were evaluated in various asymmetric reactions. Initially, the CD derivatives were designed for reactions of aliphatic aldehydes, which were supposed to be included in the CD cavity; thus their inclusion may affect the enantioselectivity (Figure 24). In addition, Cinchona-CD derivatives were designed to be soluble in water or in mixtures of solvents with water. Hence, a series of permethylated and non-methylated CDs were prepared (**19a-19d**, **20a-20d**, **23a-23d**, **24a-24d**, **27**).

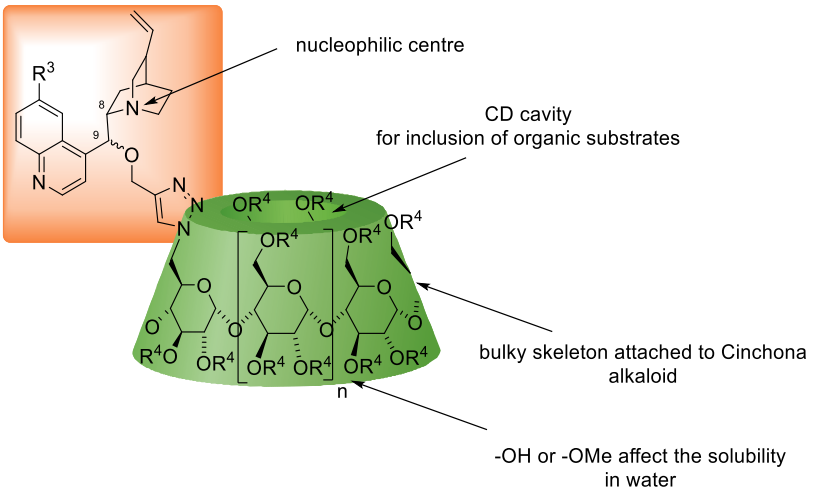

Figure 24. Active centers of Cinchona-CD derivatives possible affecting enantioselective reactions.

4.8.1. Evaluation of CD derivatives using the MBH reaction

The catalytic activity of CD derivatives was initially studied using the MBH reaction.[134] Therefore, the prepared CD derivatives were first evaluated using the classical substrates of the MBH reaction, benzaldehyde and methyl-acrylate (Scheme 35).

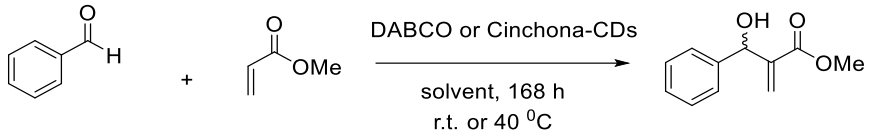

Scheme 35. MBH reaction for the evaluation of the catalytic activity of Cinchona-CD derivatives

Initially, the racemic version of this reaction was performed under standard conditions with 50% mol of the catalyst 1,4-diazabicyclo[2.2.2]octane (DABCO) in MeOH (Table 5, Entry 1). Then, different solvents (DMF, buffer/MeOH or MeOH), suitable for the prepared CD derivatives, were tested in this racemic MBH reaction. However, the conversion to the product drastically decreased (Entries 2-3); the rate of the reaction rate was much slower in DMF and in a mixture of phosphate buffer and with MeOH. The phosphate buffer was chosen to prevent a possible protonation of the quinuclidine moiety (as one of the possible centers for catalysis) and, thus, to maintain this moiety active for the reaction. Furthermore, the reaction with the prepared CD derivatives (**19b**, **20b**, **23c**, **24b**) yielded almost no products after one week at room temperature (Entries 4-8).

Table 5. Evaluation of prepared CD derivatives using the MBH reaction[a] from Scheme 35.

Entry	Catalyst	Time (h)	Conversion (%)[b]	Solvent	Yield[c] (%)
1	DABCO	72	90	MeOH	66
2	DABCO	72	< 10	DMF	-
3	DABCO	72	~30	Buffer[d]/MeOH	-
4	**19b**	168	< 10	Buffer[d]/MeOH	-
5	**19b**	168	< 10	DMF	-
6 [e]	**19b**	168	< 10	DMF	-
7	**20b**	168	< 10	Buffer[d]/MeOH	-
7	**23c**	168	< 10	Buffer[d]/MeOH	-
8	**24b**	168	< 10	MeOH	-

[a] Standard conditions: 1.3 eq. of methyl-acrylate, 1 eq. of catalysts (or 50 mol % of DABCO), solvent, 25 °C, 168 hours. [b] Determined *via* ^{1}H NMR. [c] Isolated yield. [d] Phosphate buffer (pH=7.1, 0.05 M). [e] Temperature 40 °C.

Aliphatic aldehydes and various esters were also tested in this MBH reaction with prepared CD derivatives (**19b**, **20b**, **23c**, **24b**, Scheme 36). Electron-withdrawing groups on aldehydes (nitro group) and electron donating groups on esters (commonly used[135] hexafluoroisopropyl-acrylate) were also tested. Similarly to the previous tests, all results were negative.

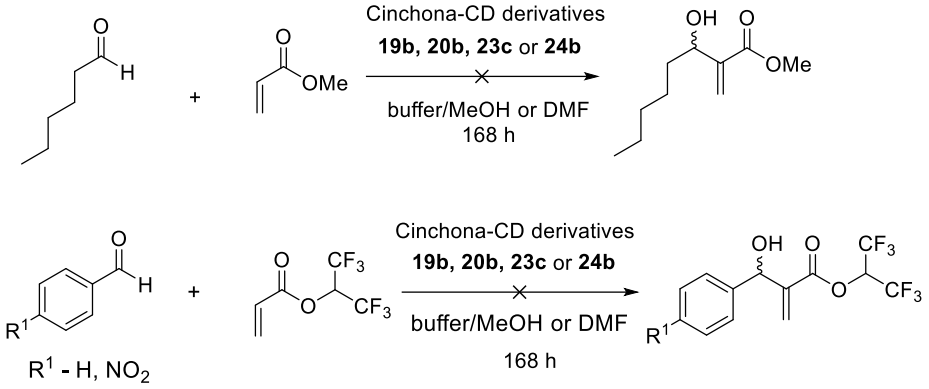

Scheme 36. MBH reaction with aliphatic aldehydes and esters for the evaluation of CD derivatives

4.8.2. Evaluation of CD derivatives using aldol-type reactions

Subsequently, Cinchona-CD derivatives were tested in aldol reactions considering the excellent results with native CDs (99% ee) in water[136] and considering the proline-CD derivatives (the section 3.2) were efficiently applied in aldol reactions.[89,88] Thus, *p*-NO_2-benzaldehyde and acetone were tested with Cinchona-CD derivatives **20c** and **23a** (Scheme 37). However, the products were isolated in low yields as the racemic mixtures.

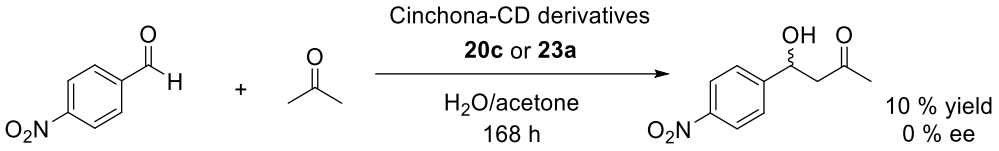

Scheme 37. Aldol reaction with acetone using the Cinchona-CD derivatives

Based on the previous results, the prepared CD derivatives unsuccessfully performed as catalysts in those reactions in water. Thus, new types of enantioselective reactions were further tested.

4.8.3. Evaluation of CD derivatives undergoing the Michael addition

We continued to screen these CD derivatives in other reactions. Michael addition was chosen to screen with our CD derivatives because previous studies have shown that Cinchona alkaloid catalyze this reaction with excellent yields and enantiomeric excess of up to 99% ee. Thus, the classical substrates for Michael addition (dimethyl-malonate and NO_2-styrene) were chosen for this

screening. In contrast to the previous reactions (MBH and aldol reactions), the product of Michael addition was isolated, albeit with no enantioselectivity (Scheme 38).

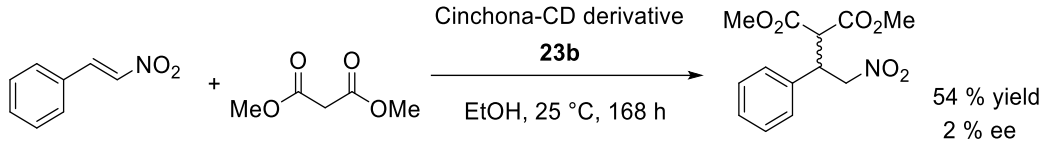

Scheme 38. Michael addition catalyzed with Cinchona-CD derivatives

4.8.4. Evaluation of permethylated CD derivatives using the AAA reaction

After unsuccessfully applying the Cinchona-CD derivatives in the MBH and aldol-type reactions and also in Michael addition, first, permethylated CD derivatives (**23a-23d**, **24a-24d**) were tested in the decarboxylative asymmetric allylic amination[137] (AAA) of MBH carbamate (**28**), as shown in Scheme 39. The previously published most efficient organocatalyst is the dimeric Cinchona alkaloid hydroquinidine(antraquinone-1,4-diyl)diether $(DHQD)_2AQN$, resulting in 98% isolated yield and 97% ee.[137]

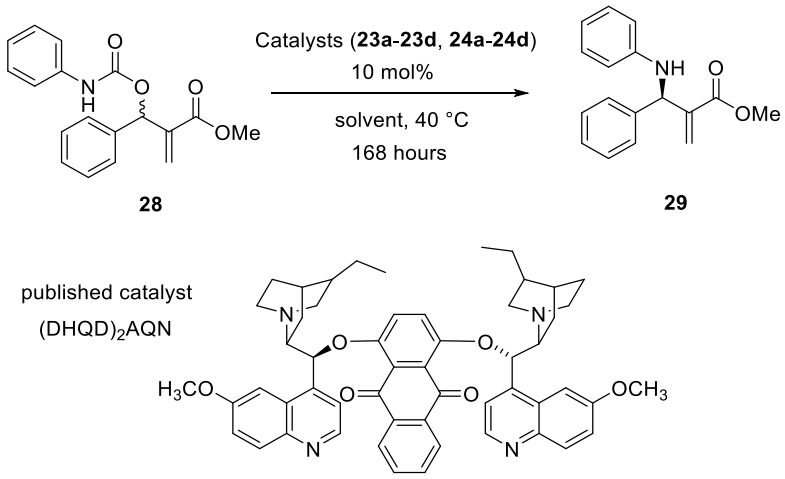

Scheme 39. Permethylated CD derivatives (**23a-23d**, **24a-24d**) tested as catalysts in the decarboxylative AAA.

Fortunately, the first tests showed that the prepared permethylated CD derivatives (**23a-23d**, **24a-24d**) catalyzed this AAA reaction with high isolated yields and with significantly high ee (Table 6).

Table 6. The catalyst and solvent screening in AAA reaction[a]

Entry	Catalyst	Solvent	Yield[b] (%)	ee (%)
1	DABCO	toluene	89	-
2	per-Me-α-CD	toluene	n.d.	-
3	per-Me-β-CD	toluene	n.d.	-
4	**23a**	toluene	42	74
5	**23b**	toluene	62	13
6	**23c**	toluene	76	25
7	**23d**	toluene	47	27
8	**24a**	toluene	55	69
9	**24b**	toluene	37	15
10	**24c**	toluene	12	15
11	**24d**	toluene	44	25
12	**24a**	$CHCl_3$	63	69
13	**24a**	MTBE	63	69
14	**24a**	MeOH	73	33
15[c]	**24a**	toluene	15	75

[a] Standard conditions: 10 mol % catalyst, 0.4 M solution, solvent 40 °C, 168 hours. [b] Isolated yield [c] Temperature 25 °C. "n.d." not detected, "-" not measured.

As outlined in Table 6, the racemic reaction of the MBH carbamate (**28**) was performed with DABCO (Entry 1) in toluene at 40 °C in one week. These reaction conditions were chosen based on a previous study[137] in which authors obtained 98% isolated yields and up to 97% ee with dimeric Cinchona alkaloid catalysts in aromatic solvents (Scheme 44). Thus, toluene was chosen as solvent for our permethylated Cinchona-CD derivatives.

Then, the permethylated α- and β-CDs without Cinchona alkaloid moieties were also tested as blank catalysts to confirm that the Cinchona alkaloid moiety is a necessary part of the catalyst (Entries 2 and 3). Subsequently, permethylated Cinchona-CD derivatives showed low to high ee (Entries 3-11). Surprisingly, significant differences were observed in pairwise comparisons between Cinchona alkaloid moieties, and cinchonidine-per-Me-CDs (**23b** and **24b**) showed the best ee (Entries 4 and 8), but other Cinchona alkaloids showed low ee ranging from 13 to 27 % (Entries 5-7 and 9-11). Based on

the comparison of CD cavity sizes between α- and β-CDs, it was concluded that the size of the cavity has no effect on the reaction because yield and ee results are similar (Entries 4-11). Quinine-per-Me-α-CD (**23c**) has the highest isolated yield (76%), but its ee was low (25%).

The advantage of the permethylated CD derivatives is their good solubility in organic solvents. The reactions in methyl(*tert*-butyl)ether (MTBE), in $CHCl_3$ and in toluene resulted in similar yields and ee (Entries 8, 12, 13). Although the yield of the reaction in MeOH was similar to toluene, ee was lower (Entry 14). Lastly, the reaction was performed at room temperature with 75% ee but unfortunately in 15% yield (Entry 15). Thus, the solvent strongly affects enantioselectivity and this problem will be further discussed in the section 4.9.2 in MD studies.

4.8.5. Evaluation of non-methylated CD derivatives using the AAA reaction

Non-methylated Cinchona-CD catalysts were also tested using the conditions found for Cinchona-per-Me-CDs. However, the solvent had to be changed because the prepared non-methylated CD derivatives (**19a-19d**, **20a-20d**) show low solubility in organic solvents (Scheme 45).

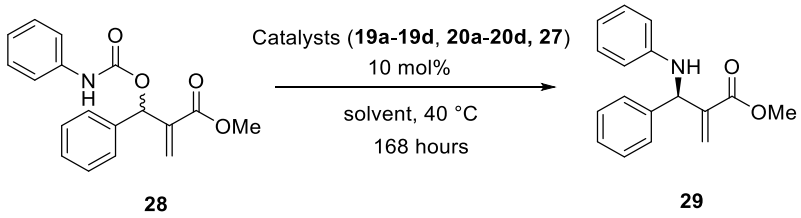

Scheme 45. Decarboxylative AAA reaction used prepared CD derivatives.

The results from the tests with non-methylated CD derivatives (**19a-19d**, **20a-20d**) and disubstituted CD derivative (**27**) are shown in Table 7. Native α- and β-CDs were also tested as blank catalysts (Entries 1-2). Although non-methylated monosubstituted CD derivatives (**19a–19d**) showed lower enantiomer excess (Entries 3–10), they achieved catalytic activity in a solvent mixture ACN/H_2O, which indicates the potential of these catalysts for future applications in water. DMF was also tested, albeit with no conversion into the product (Entries 12 and 13), and cinchonidine-α-CD (**19b**) was inactive (Entry 11). Similarly, cinchonidine-β-CD (**20b**) in DMF and DMSO showed low ee and low isolated yields (Entries 12 and 13). Lastly, the disubstituted CD derivative (**27**) was tested; unfortunately it also failed to show any activity (Entry 14). In addition, this derivative was unsuccessfully tested in this reaction with a cocatalyst, (1*S*)-10-camphorsulfonic acid (CSA) according to the original procedure,[137] in which this cocatalyst had enhanced the enantiomeric excess of dimeric Cinchona alkaloid $(DHQD)_2AQN$, as shown previously in Scheme 44.

Table 7. Catalyst and solvent screening[a] for Cinchona-non-methylated CDs

Entry	Catalyst	Solvent	Yield[b] (%)	ee (%)
1	α-CD	ACN/H_2O	n.d.	-
3	β-CD	ACN/H_2O	n.d.	-
3	**19a**	ACN/H_2O	5	0
4	**19b**	ACN/H_2O	10	3
5	**19c**	ACN/H_2O	12	0
6	**19d**	ACN/H_2O	18	21
7	**20a**	ACN/H_2O	19	19
8	**20b**	ACN/H_2O	26	5
9	**20c**	ACN/H_2O	5	0
10	**20d**	ACN/H_2O	21	13
11	**19a**	DMF	n.d.	-
12	**20a**	DMF	9	25
13	**20a**	DMSO	19	23
14	**27**	ACN/H_2O	n.d.	-
15[c]	**27**	ACN/H_2O	n.d.	-

[a] Standard conditions: 10 mol % catalyst, 0.4 M solution, solvent 40 °C, 168 hours. [b] Isolated yield. [c] With (1*S*)-CSA (5 mol %). "n.d." not detected, "-" not measured.

In conclusion, the Cinchona-CD derivatives were successfully applied in AAA with up to 76% isolated yield and up to 75% ee. Permethylated Cinchona-CD derivatives were more successful than non-methylated Cinchona-CD derivatives. Moreover, the size of the CD cavity in the case of permethylated derivatives had no effect on the reaction. In the case of non-methylated CDs, the enantiomeric excess was low but promising even in ACN/H_2O. Overall, these Cinchona-CD derivates can be used as catalysts for enantioselective reactions (even in water).

4.9. Molecular modeling of Cinchona-CD derivatives

Computational studies of CDs involved a wide range of simulation methods using various tools and algoritms.[113] Molecular docking and molecular dynamics simulations, most common used methods in molecular modeling of host-guest complexes, have been used to study inclusion complexes of CDs[113,138] and CD derivatives[112,113]. Researchers are able to specifically measure distances between hosts (CDs) and their ligands (guests). In addition, conformational changes of CD derivatives in different solvent environments can be also studied.[139] The MD studies provide detailed information on atomic positions, velocities and forces, thus allowing us to study the physics of the system.[117] Therefore, computer simulations enable description of driving forces responsible for complexation of guests-ligands into cavities of hosts-CDs in terms of the binding free energies.

More specifically, molecular modeling of CDs is mainly focused on the development of CD derivatives that could be potentially used as drug carriers. Importantly, drug encapsulation into the CD cavity remarkably enhances drug solubility and bioavailability in aqueous solutions.[140] In comparison to nuclear magnetic resonance (NMR)[141] or to differential thermal analysis (DTA)[142], *in silico* modeling of CD inclusion complexes provides crucial additional information and can substantially accelerate the development of sophisticated drug delivery systems.[143–145] For example, comprehensive studies on the complexation of steroids and cholesterol into the CD cavity have improved the treatment for Niemann-Pick disease.[146]

Specifically, Cinchona-CD derivatives are almost unexplored as regards molecular modeling. Only study, dealing with X-ray analysis of inclusion complexes, confirmed the encapsulation of quinine into the β-CD cavity.[147] Furthermore, just a simple QM geometry optimization (using density functional theory - DFT) of covalently attached Cinchona-CD derivatives, linked *via* thiourea and squaramide moieties, used as catalysts in Michael addition (discussed in section 3.4, Scheme 18) was studied by DFT calculations.[104] In contrast to the CD modeling, catalysis using Cinchona alkaloids has been mainly examined *in* (DFT) calculations.[148] However, according to our best knowledge, no MD study of Cinchona-CD catalysts and substrates has not been performed yet.

Therefore, in this thesis, spatial arrangements of CD derivatives and substrates were studied *in silico* by extensive MD simulations to shed some light on the catalytic (in)activity of prepared Cinchona-CD derivatives.

4.9.1. Inclusion of quinine into native β-CD

First, an MD protocol was developed to assess whether a ligand is able to penetrate spontaneously into the β-CD cavity. For this purpose, the simulated system consisting of quinine, native β-CD and water molecules was studied through series of 4000 nano-second MD simulations performed at different temperatures in the range of 300-400K using the AMBER software package.

The initial arrangement of β-CD and quinine is shown in Figure 25. The atoms that were chosen to track time-evolution of mutual distances between quinine and β-CD are numbered as follows: atoms C1 and C0 belong to the quinoline moiety, C19 and C10 to the quinuclidine part. Moreover, primary and secondary rims of CD are also indicated. Hydrogen atoms in MD snapshots are usually omitted to simplify the representations.

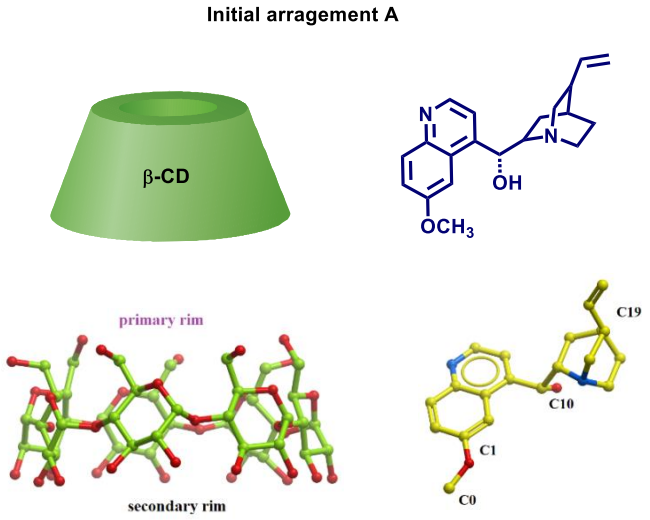

Figure 25. Initial arrangement (A) of native β-CD and quinine in MD studies.

Possible mutual orientations of quinine encapsulated into β-CD are schematically drawn in Figure 26. In principle, quinine can penetrate either the primary (orientation B or C) or the secondary (orientation F or G) rim of β-CD. In addition, either quinuclidine (orientation B or G) or quinoline (orientation C or F) can be involved in the encapsulation process. Furthermore, two intermediate complexes with fully buried quinine could also be formed in this process (orientation D or E).

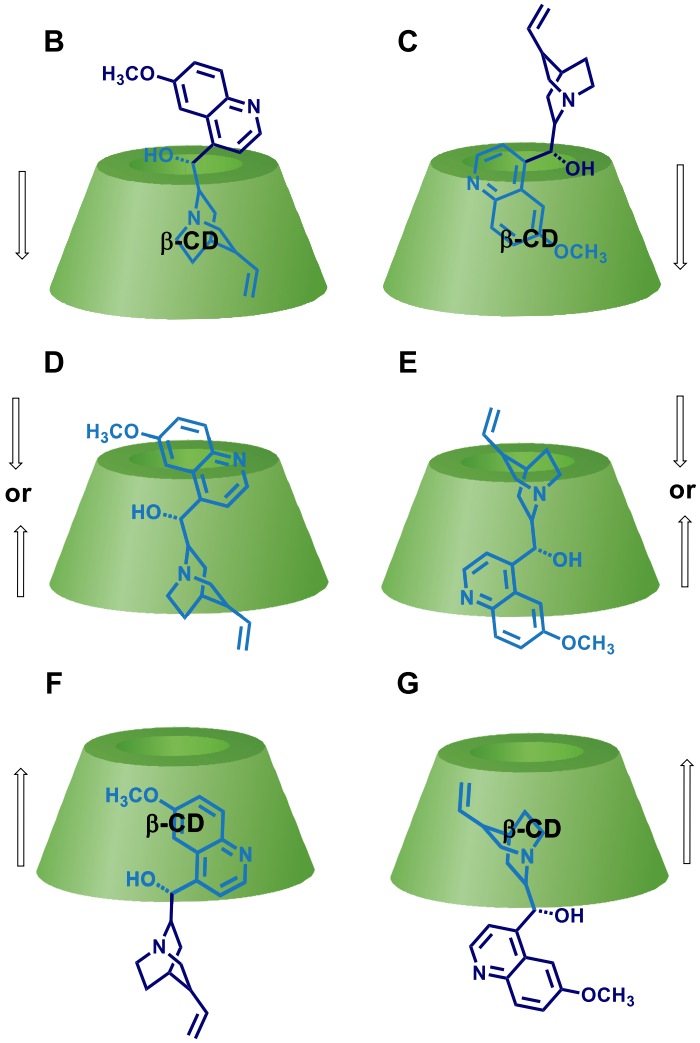

Figure 26. Possible orientations (B, C, D, E, F, G) of quinine encapsulation into the β-CD cavity.

Importantly, the time-evolution of distances between the centers of mass of quinine and β-CD unambiguously confirmed the formation of the inclusion complexes in our MD simulations (see Figure 27). The values of distances (y axis) were often lower 5Å in these MD simulations. At lower temperatures, the encapsulation times were slightly longer (almost 2000 ns at 300K), but the resulting complexes were more stable. In contrast, at higher temperatures, the complexes transiently formed, that is, CD repeatedly encapsulated and released quinine many times.

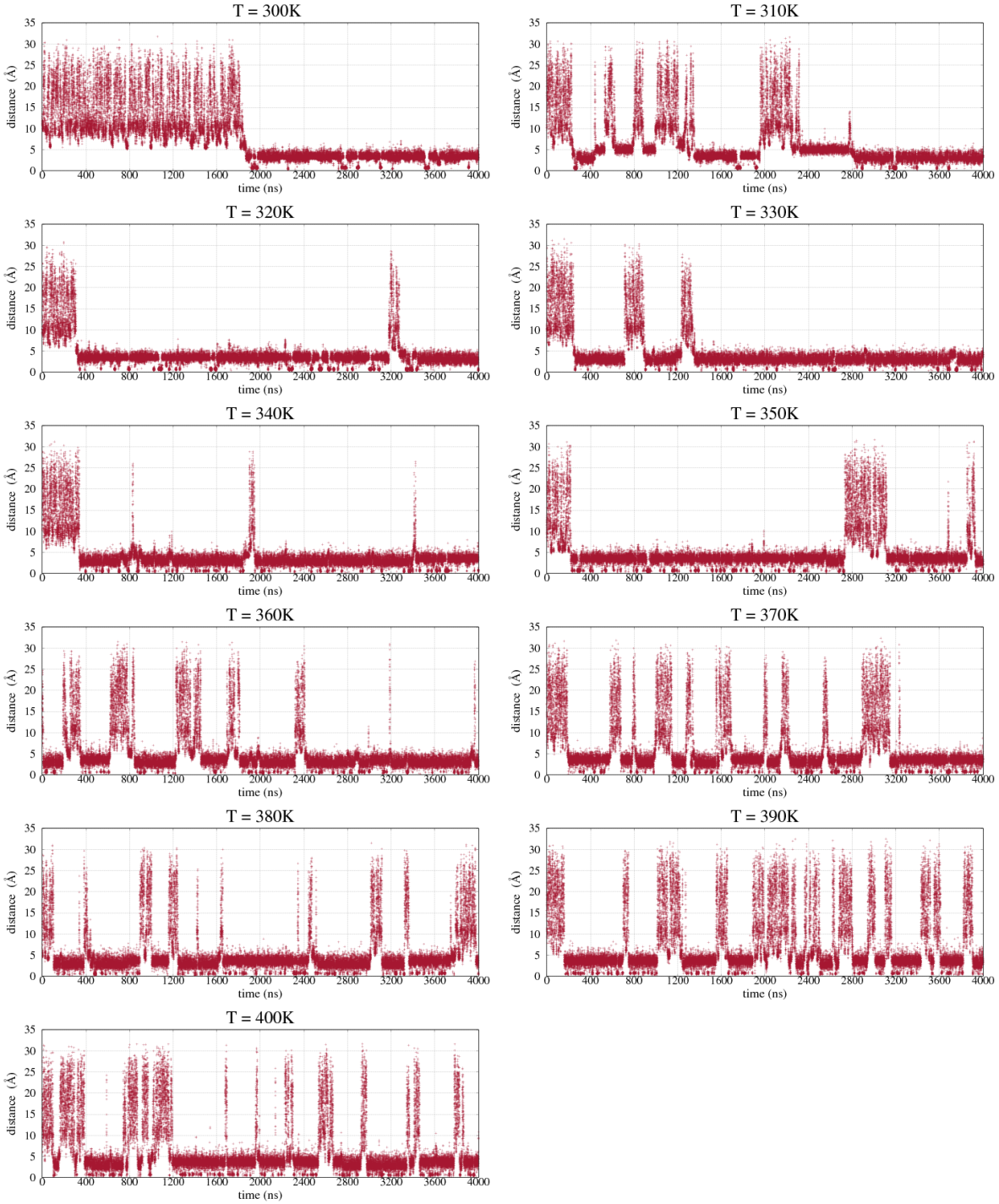

Figure 27. Time evolution of distances between the centers of mass of β-CD and quinine at 300-400 K MD runs.

Interestingly, even the whole-quinine inclusion into the β-CD cavity (i.e. the inclusion complexes D or E, as proposed in Figure 26) was confirmed by MD simulations (note the nearly zero y values shown in Figure 28).

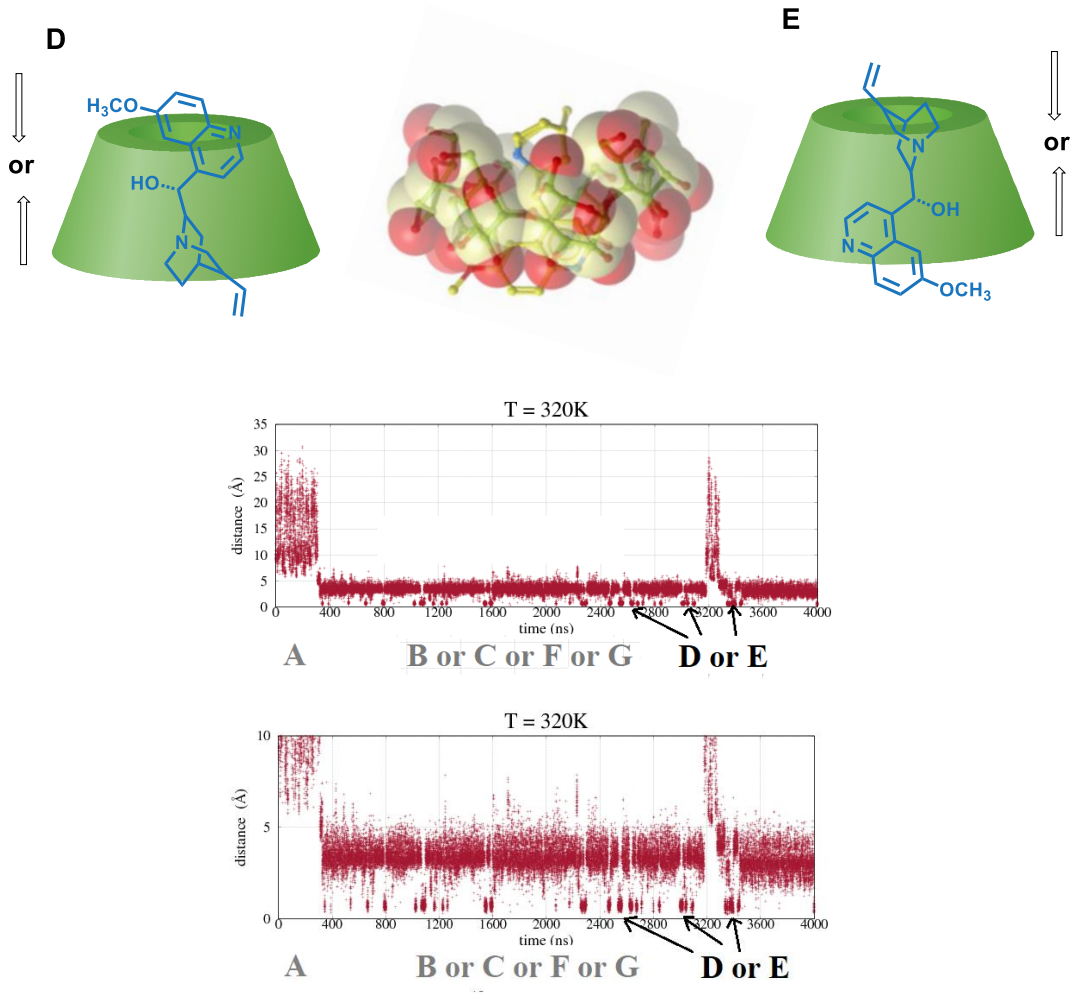

Figure 28. (*Top*) Schemes and snapshot from MD trajectories representing the D and E inclusion complexes.

(*Bottom*) Almost zero values for distances between the centers of mass of β-CD and quinine indicate complete inclusion of the whole quinine into the β-CD cavity.

Subsequently, the time evolution of the distances between selected atoms in quinine and in β-CD within MD runs were depicted to differentiate inclusion complexes B, C, F and G (see charts in Figures S1-S4). Accordingly, the results showed that quinine inclusion through the primary rim (i.e. B or C inclusion complexes – see Figure 29) was found as minor. The quinuclidine (B) and the quinoline moiety (C) were inserted into the β-CD cavity only for short intervals, for example, see the orange line in Figure 29 at the interval of 3600-4000 ns for B inclusion and the black line at the interval 3200-4000 ns interval for C inclusion.

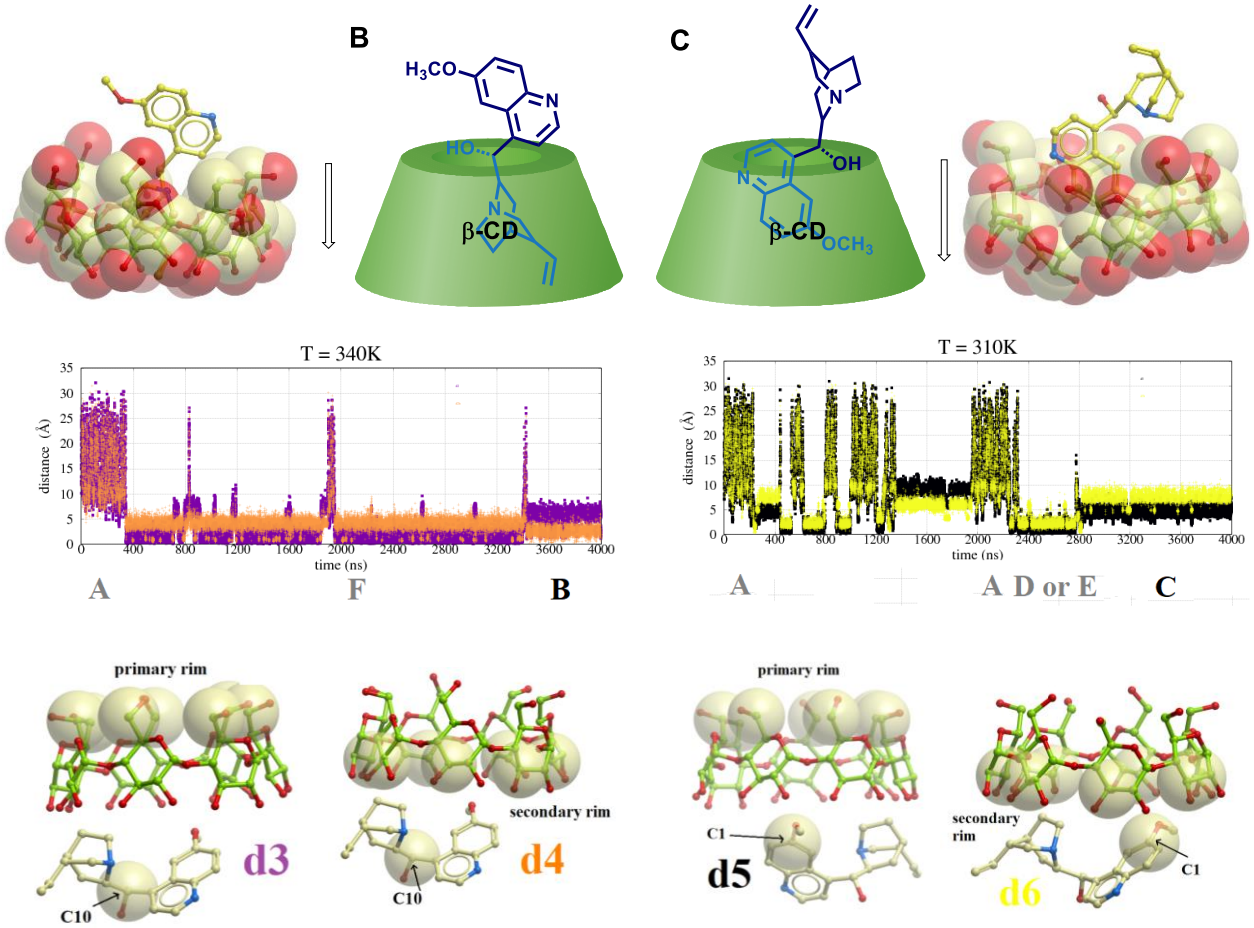

Figure 29. (*Top*) Schemes and snapshots of MD trajectories representing quinine inclusion into the β-CD cavity through primary rim leading to inclusion complexes B and C.

(*Middle - Left*) Time evolution of distance d3 (purple) between C10 of quinine (quinuclidine moiety) and the primary rim of β-CD. Time evolution of distance d4 (orange) between C10 of quinine and the secondary rim of β-CD.

(*Middle - Right*) Time evolution of distance d5 (black) between C1 of quinine (quinoline moiety) and the primary rim of β-CD. Time evolution of distance d6 (yellow) between C1 of quinine and the secondary rim of β-CD.

(*Bottom*) Atoms selected for tracking distances between Cinchona alkaloid substituents and CDs in MD are highlighted as yellow spheres. All hydrogen atoms are omitted to simplify and clarify this representation.

As suggested above, quinine inclusion through the secondary rim (Figure 30) is more favorable than through the primary rim. Shorter distances (10 Å) are observed during most of the simulation, more specifically, for 1400-4000 ns in quinoline (F) and for 400-3200 ns in quinuclidine (G) inclusion. Thus, quinuclidine inclusion is the most favored of all six possible orientations of quinine encapsulation into the β-CD cavity.

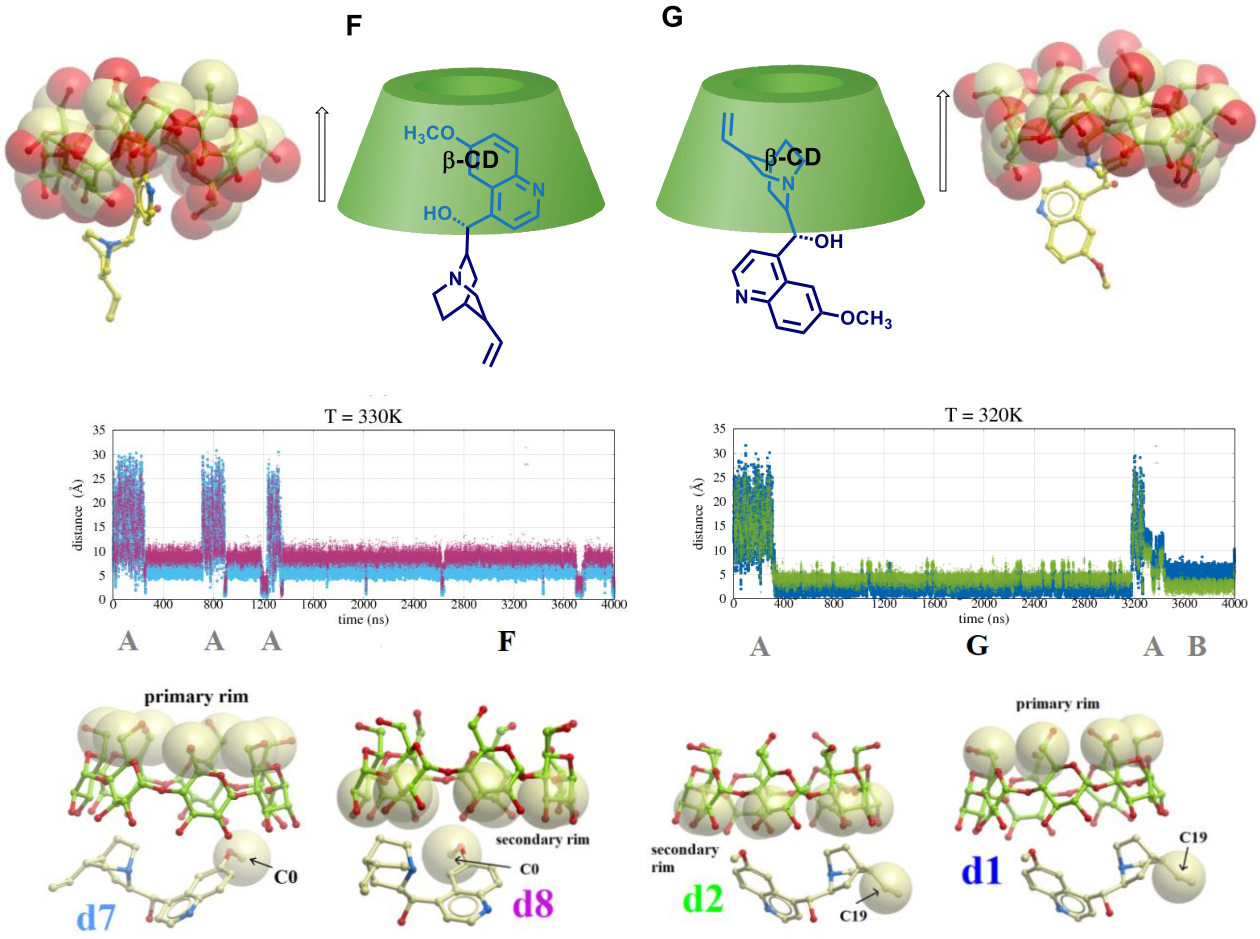

Figure 30. (*Top*) Schemes and snapshots of MD trajectories representing quinine inclusion into the β-CD cavity through the secondary rim, thereby forming inclusion complexes F and G. (*Middle - Left*) Time evolution of distance d7 (light-blue) between the C0 atom of the methoxy group of quinine (quinoline moiety) and the primary rim of β-CD. Time evolution of distance d8 (magenta) between the C0 atom of the methoxy group of quinine and the secondary rim of β-CD. (*Middle - Right*) Time evolution of distance d1 (dark-blue) between C19 of quinine (quinuclidine part) and the primary rim of β-CD. Time evolution of distance d2 (green) between C19 of quinine and the secondary rim β-CD. (*Bottom*) Atoms selected for tracking of distances between Cinchona alkaloid substituents and CDs in MD are highlighted as yellow spheres. All hydrogen atoms are omitted to simplify and clarify this representation.

Previously, quinine encapsulation into the β-CD cavity had been confirmed by X-ray analysis.[147] The authors showed that the quinuclidine moiety is preferably included in the CD cavity and that the quinoline moiety is surrounded by other native β-CDs that stabilize this aromatic moiety in higher-order crystal structures. The comparison between the inclusion complex experimentally solved by X-ray analysis[147] (X) and the most populated inclusion complex resulting from our MD simulations (G) shows that their structures are identical (Figure 31).

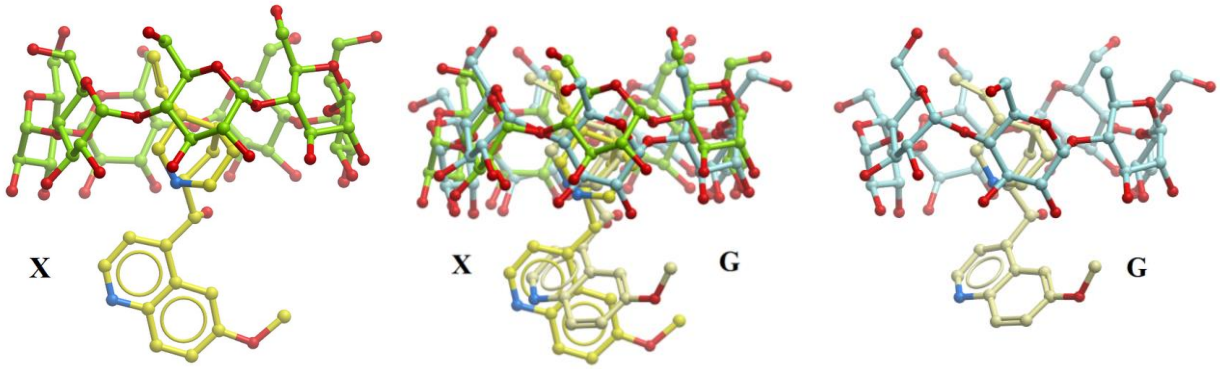

Figure 31. Comparison between structures of the inclusion complex solved by X-ray analysis[147] (X) and obtained by MD in this study (G).

In conclusion, our MD protocol, developed to study the formation of the inclusion complex between quinine and β-CD, enable us to find complexes with all possible mutual orientations of quinine encapsulation into the β-CD. The MD data on the most preferred complex, that is, the complex with quinuclidine included into the CD cavity, reproduces X-ray data, thus unambiguously confirming the appropriateness of our MD approach for further analysis of the spatial arrangements of new CDs and substrates in enantioselective reactions as described in detail below.

4.9.2. Molecular modeling of non-methylated Cinchona-CD derivatives

4.9.2.1. Geometry optimization

Subsequently, all prepared Cinchona-CD derivatives were studied in detail using MD simulations. First, non-methylated Cinchona-CD derivatives (**19a-19d** and **20a-20d,** Figure 32) in water were geometry optimized to the minimal potential energy and equilibrated in short MD runs produced using the NAMD software package.

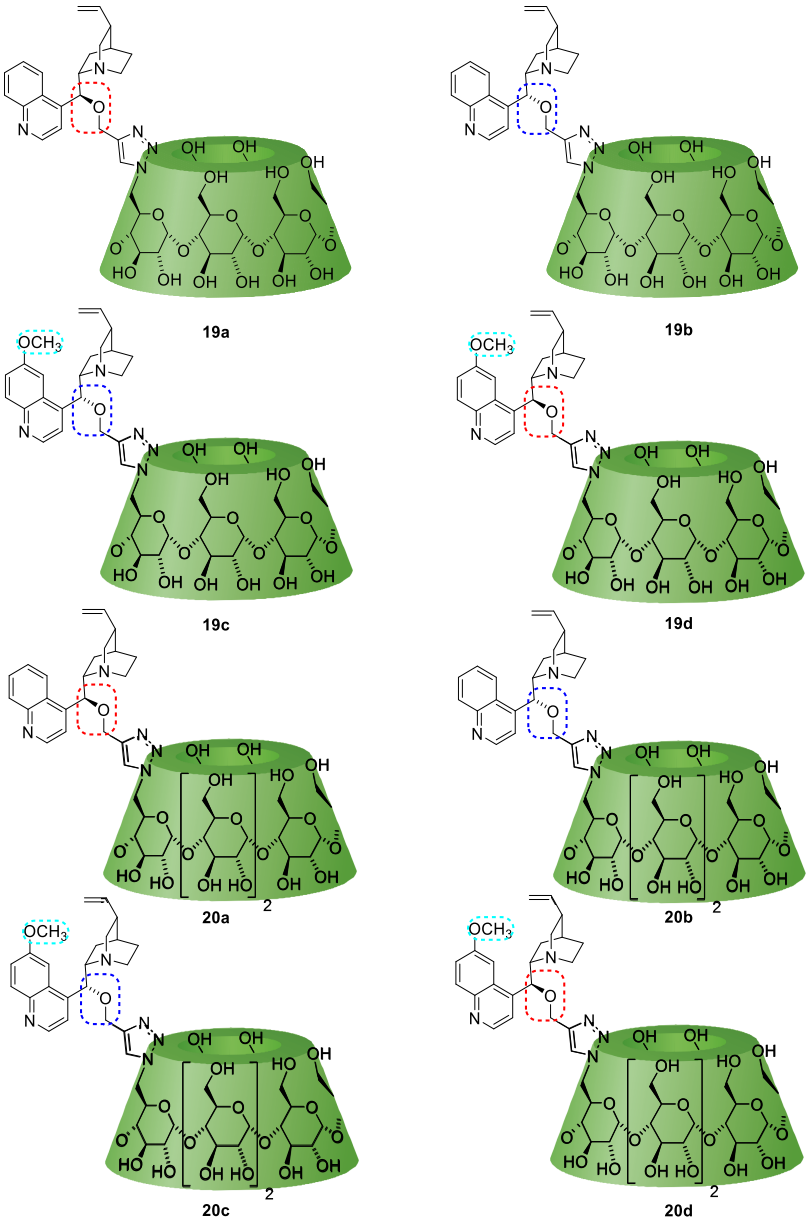

Figure 32. Schematic representations of non-methylated Cinchona-CD derivatives **19a-19d, 20a-20d**

The geometry-optimized and equilibrated conformations resulting from the short MD runs match a 6-monosubstituted, cone-shaped CD cavity. In contrast to the Cinchona-α-CD derivatives (**19a**-**19d**), whose triazole moiety is located outside the cavity and whose substituent is not included in the CD cavity, the triazole moiety of Cinchona-β-CD derivatives (**20a**-**20d**) is partly included in the cavity (Figure 33).

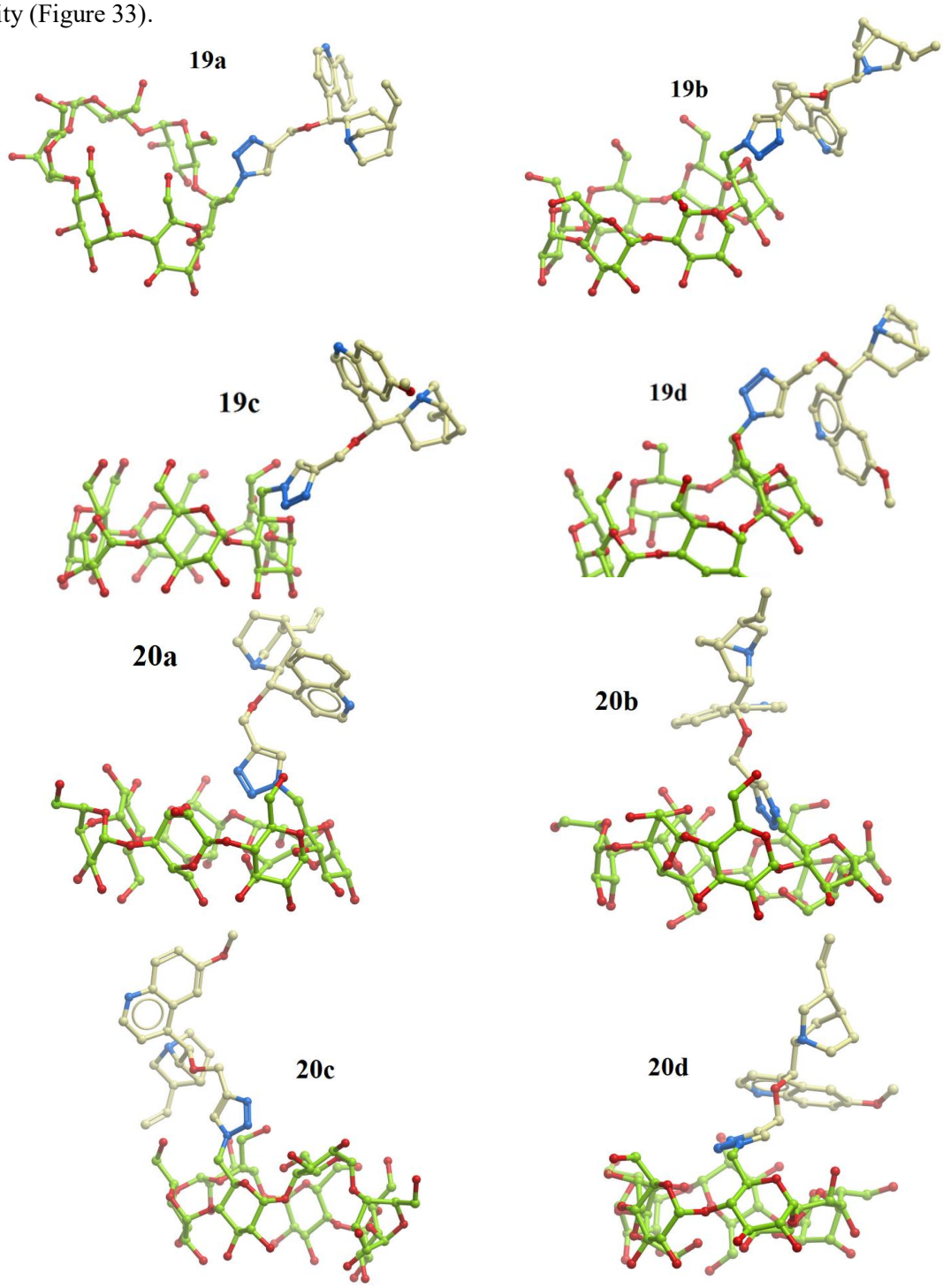

Figure 33. Optimized and equilibrated structures of non-methylated Cinchona-CD derivatives (**19a**-**19d** and **20a**-**20d**)

Water molecules and hydrogen atoms are omitted for the simplicity and clarity.

4.9.2.2. Substituent self-inclusion

The problem of self-inclusion of Cinchona-β-CD derivatives has already been discussed in section 4.4 (NMR elucidation of non-methylated Cinchona-CD derivatives). This NMR analysis revealed crosspeaks in 2D ROESY, thus confirming non-covalent interactions between H-3 protons inside the CD cavity and quinuclidine and quinoline hydrogen atoms of the Cinchona-alkaloid substituent.

Hence, the MD protocol developed for quinine-CD inclusion complexes, presented in previous section, was also applied here to non-methylated Cinchona-CD derivatives. The conformational preferences of solvated CD derivatives **20a**, **20b** and **20c** were investigated by 500 ns MD runs at different temperatures, more specifically, in the range of 300-400K. These MD simulations were produced using the AMBER software package.

Time evolution of distances between chosen atoms (i.e. hydrogen atom H76 of the vinyl group on the quinuclidine moiety, hydrogen atom H64 of the quinoline moiety and hydrogen atoms (H-3) of the CD cavity - see Figure 33) were tracked to confirm potential inclusion events of Cinchona alkaloid substituents into the CD cavity (see Figures S5-S7).

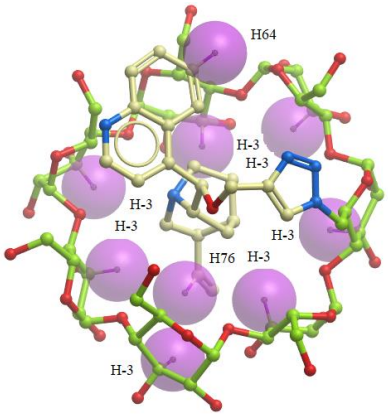

Figure 33. Atoms selected for tracking distances between Cinchona alkaloid substituents and CDs in MD simulations are highlighted as violet spheres (i.e., all H-3 atoms of β-CD derivatives**,** hydrogen atom H76 of the vinyl group on quinuclidine moiety and hydrogen atom H64 on the quinoline moiety). All other hydrogen atoms are omitted to simplify and clarify this representation.

Quinuclidine inclusion into the CD moiety of the first studied catalyst **20a** is represented in Figure 34. Importantly, the distances between H76 of the vinyl group of quinine and H-3 atoms of CD unambiguously confirmed quinuclidine inclusion as shown by the sharp and persistent decrease of y-values (blue line) at 340 K in the 320-500 ns interval. Similarly, the inclusion of the quinoline segment was also confirmed - note the decreasing y-values in the second chart (green line). The entire set of graphs for MD runs produced at 300-400 K are shown in Supplemental Information (Figure S5).

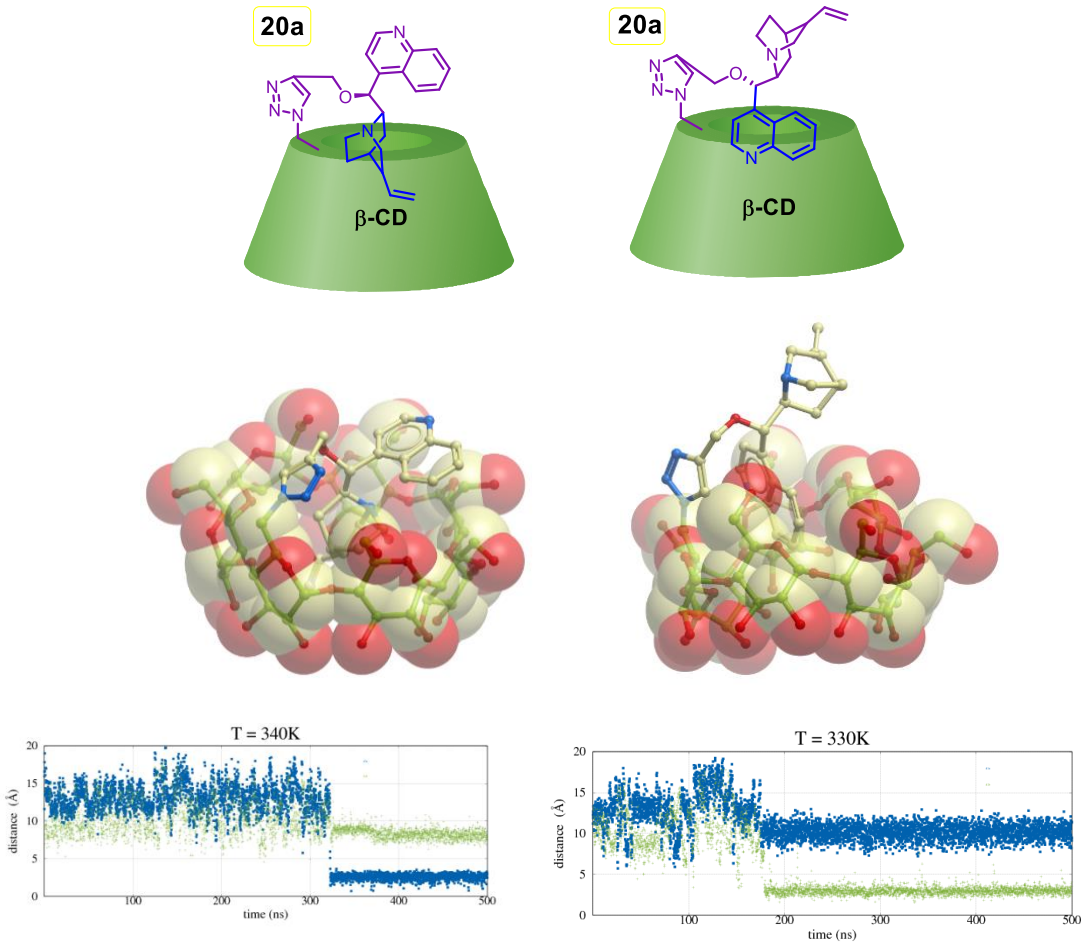

Figure 34. (*Top*) Schematic representations, (*middle*) MD snapshots and (*bottom*) time evolution of the inclusion of quinuclidine (blue line) or quinoline moieties (green line) into the non-methylated cinchonine-β-CD (**20a**).

MD study of the second catalyst **20b** showed Cinchona-alkaloid (in this case cinchonidine) moiety is not included into the β-CD cavity (Figure 35), in contrast to the previously investigated catalyst **20a**. In addition, the distances between H76 of the vinyl group (A) of quinine and H-3 atoms and between the quinoline moiety (B) and H-3 atoms were not constant during the whole simulation. The entire set of graphs of MD runs, produced at 300-400 K, is shown in Supplemental Information (Figure S6).

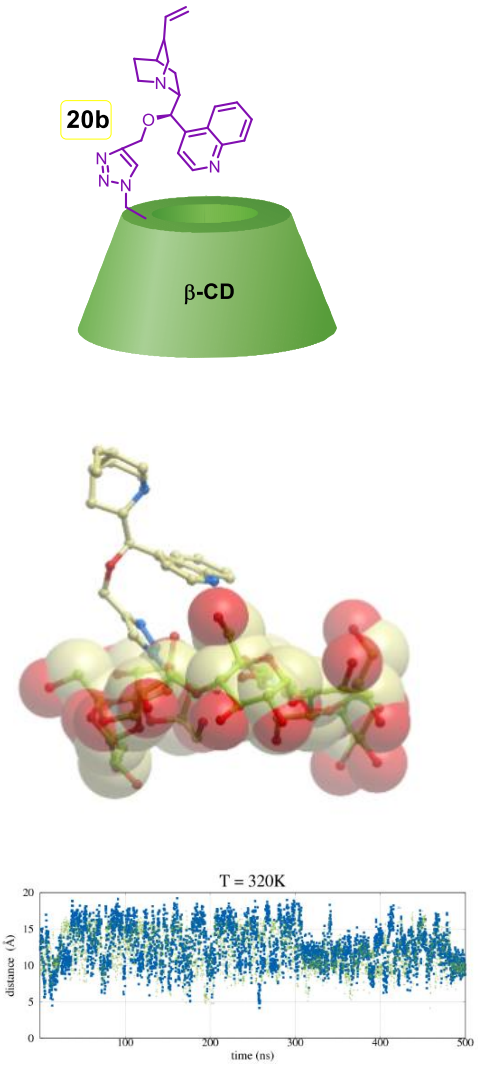

Figure 35. (*Top*) Schematic representations, (*middle*) MD snapshots and (*bottom*) time evolution of the inclusion of quinuclidine (blue line) or quinoline moieties (green line) into the non-methylated cinchonine-β-CD (**20b**).

Third MD studied catalyst **20c** confirmed the inclusion of both quinuclidine and quinoline moieties into the β-CD cavity (Figure 36). The distances between H76 of the vinyl group of quinine (blue line) and H-3 atoms of CDs and between the quinoline moiety (green line) and H-3 atoms decreased to low y-values after the inclusion. Moreover, quinuclidine inclusion is more pronounced than quinoline inclusion, most likely due to the methoxy functional group of this aromatic part. The entire set of graphs for MD runs produced at 300-400 K is shown in Supplemental Information (Figure S7).

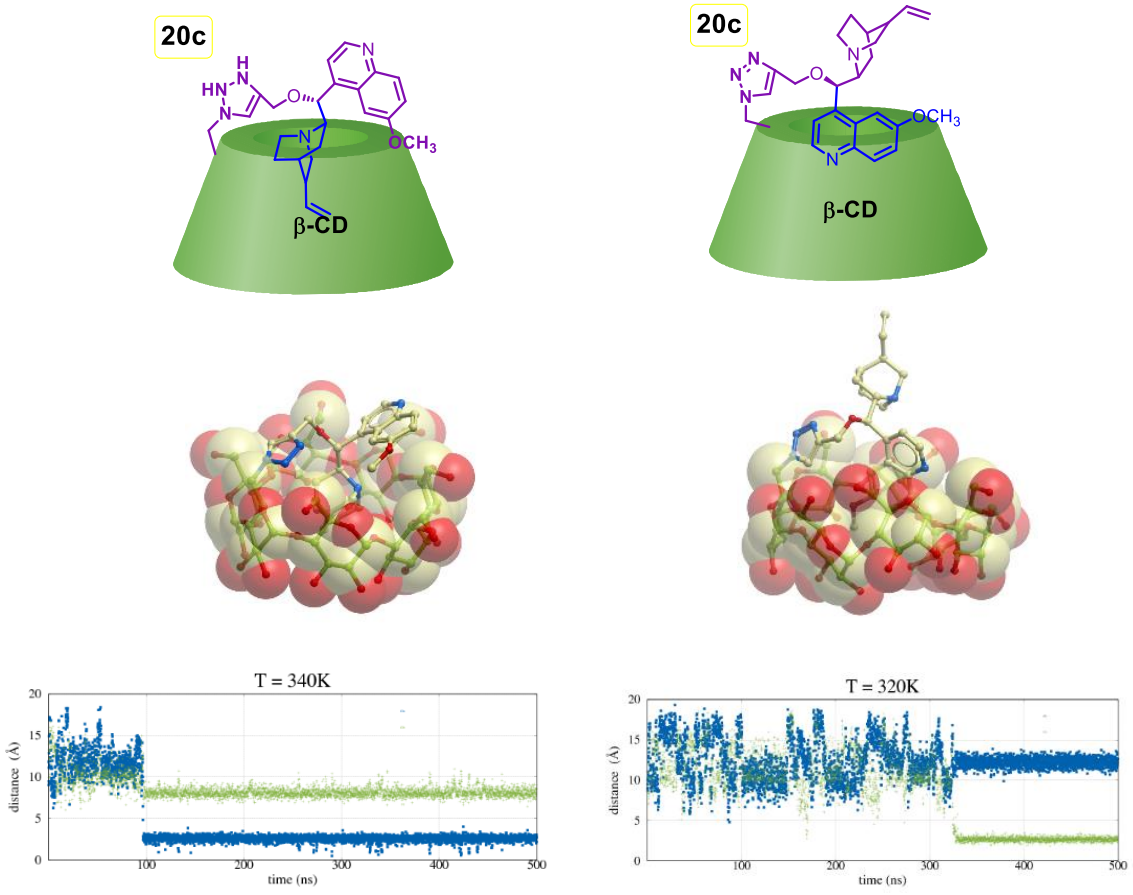

Figure 36. (*Top*) Schematic representations, (*middle*) MD snapshots and (*bottom*) time evolution of the inclusion of quinuclidine (blue line) or quinoline moieties (green line) into the non-methylated cinchonine-β-CD (**20c**).

4.9.3. Molecular modeling of permethylated Cinchona-CD derivatives

4.9.3.1. Geometry optimization

The structures of Cinchona alkaloid-permethylated CD derivatives (**23a-23d**, **24a-24d,** Figure 38) were optimized and equilibrated in MeOH.

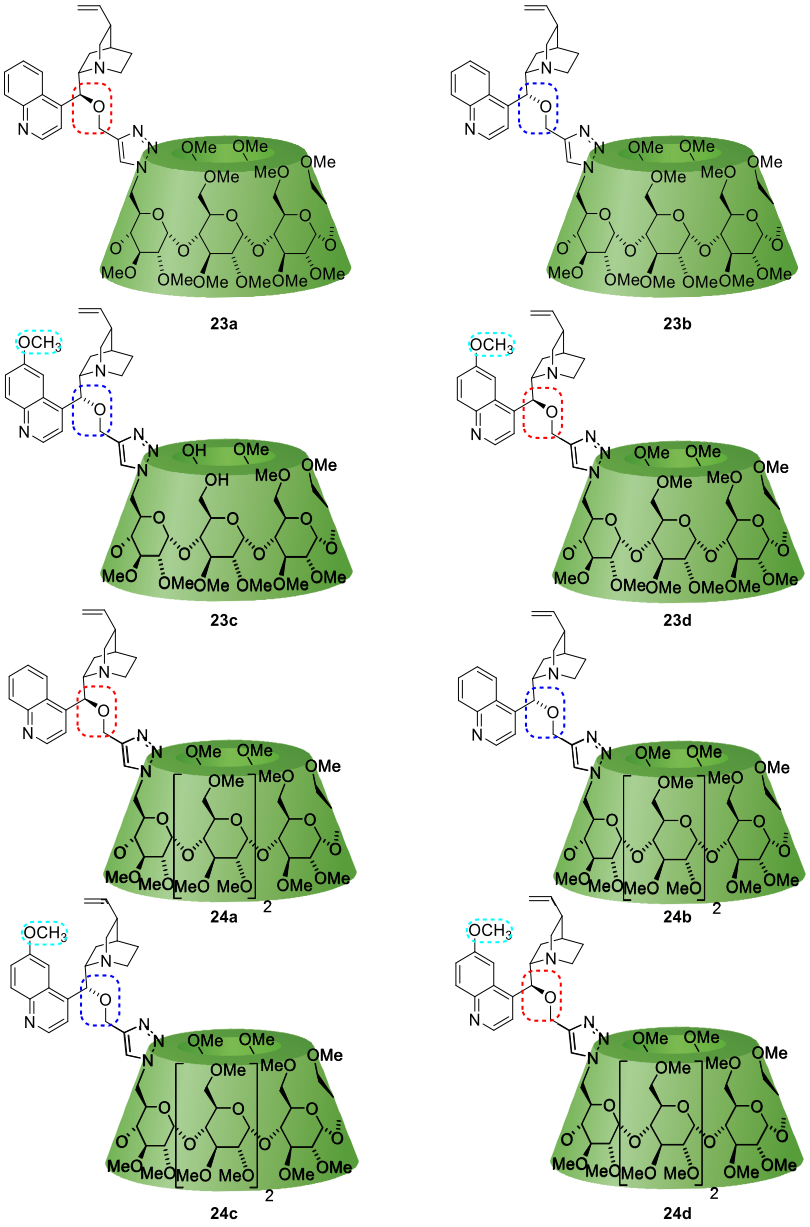

Figure 37. Schematic representations of permethylated Cinchona-CD derivatives **23a-23d**, **24a-24d**

The resulting conformers showed that the spatial arrangement of these permethylated Cinchona CD derivatives is completely different from that of non-methylated CD derivatives. The CD cavity lacks the typical cone shape, and the Cinchona alkaloid moieties are completely outside the CD skeleton (Figure 38). No inclusion was observed in either α- or β-CD derivatives.

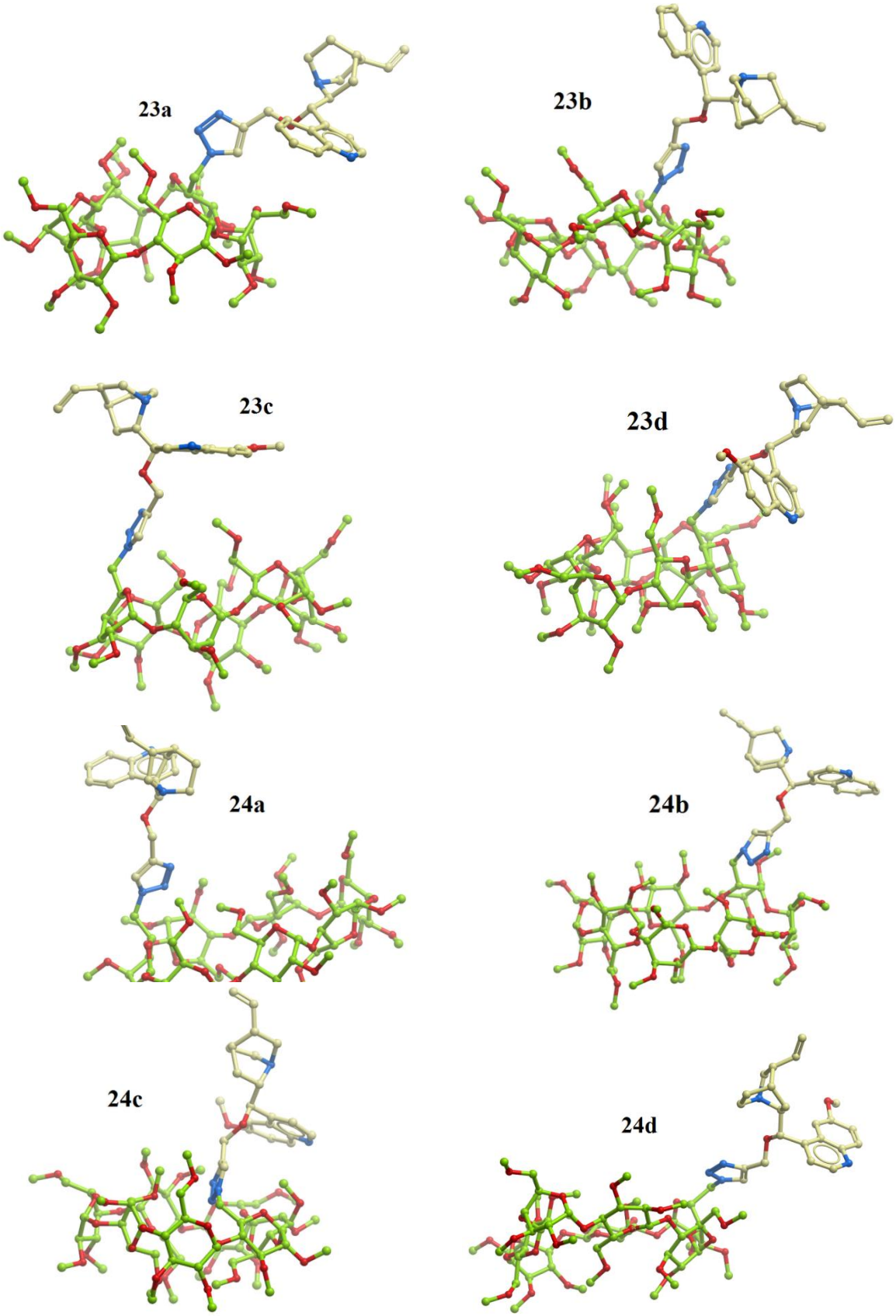

Figure 38. Optimized structures of permethylated Cinchona-CD derivatives (**23a**-**23d** and **24a**-**24d**) MeOH molecules and hydrogen atoms are omitted for the simplicity and clarity.

4.9.3.2. Substituent self-inclusion

To further investigate a potential self-inclusion of these permethylated Cinchona-CD derivatives, the most successful catalyst in enantioselective reactions – i.e., cinchonidine-per-Me-β-CD (**24b**) – was studied in 500 ns MD runs produced using the AMBER software package (Figure 39). Again, the atoms chosen to track this self-inclusion process were similar to those selected in non-methylated CD derivatives. The entire set of graphs of MD runs produced at 300 – 400 K is shown in Supplemental Information (Figure S8). The time evolution of distances between Cinchona H76 and inner H-3 atoms of the CD skeleton confirmed that no substituent inclusion into the CD cavity occurs in these complexes.

Based on these results, we concluded that neither self-inclusion of Cinchona moieties nor potential inclusion of substrates into the CD cavity are likely to occur because cone shape of the cavity collapses in permethylated catalysts. Accordingly, the enantioselective reaction catalyzed by the Cinchona alkaloid moiety should preferentially occur outside this permethylated CD cavity.

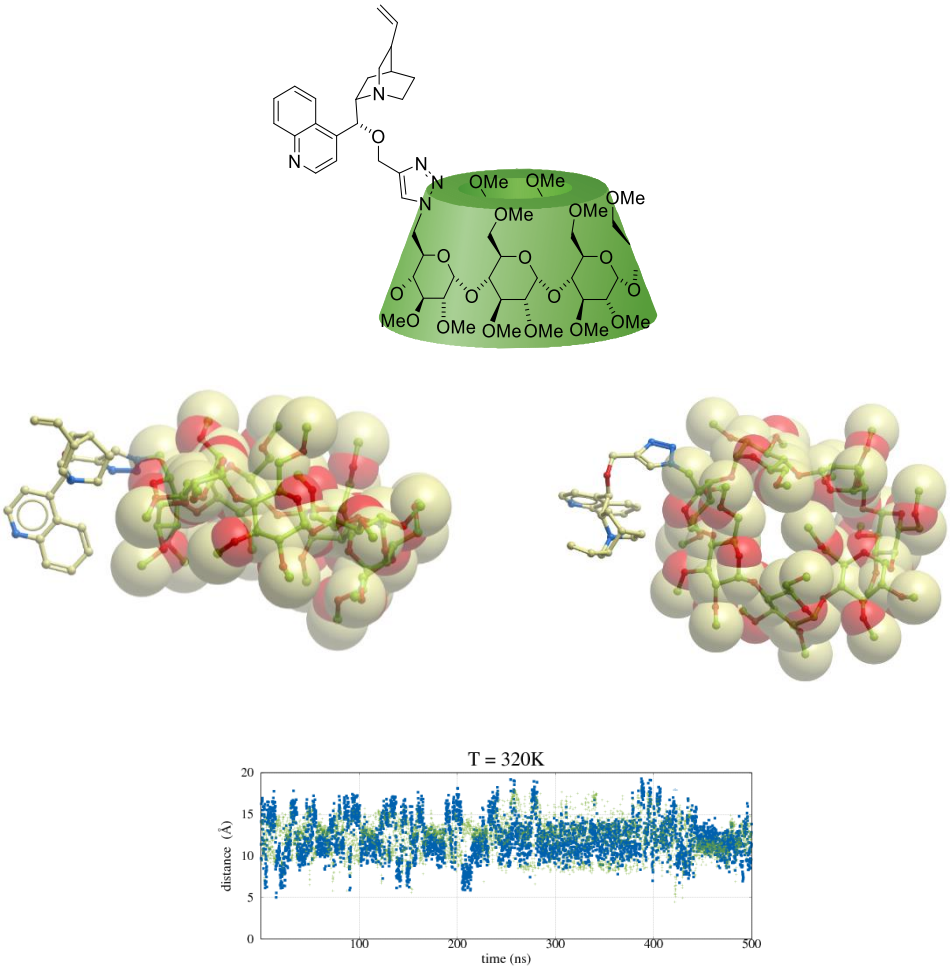

Figure 39. (*Top*) Schematic representations, (*middle*) MD snapshots and (*bottom*) time evolution of the inclusion of quinuclidine (blue line) or quinoline moieties (green line). The substituent clearly resides outside the CD cavity of the catalyst **24b**.

4.9.4. Complexes of permethylated Cinchona-CD catalysts and substrates

To further investigate the previously mentioned hypothesis about the occurrence of an enantioselective reaction outside our permethylated Cinchona-CD catalysts, the spatial arrangement of the most successful catalyst **24b** with MBH carbamate (**32**) as a substrate in AAA reaction was studied by MD simulations. The corresponding MD simulation revealed that the substrate **32** is positioned in a "outside pocket", as it was predicted (Figure 40).

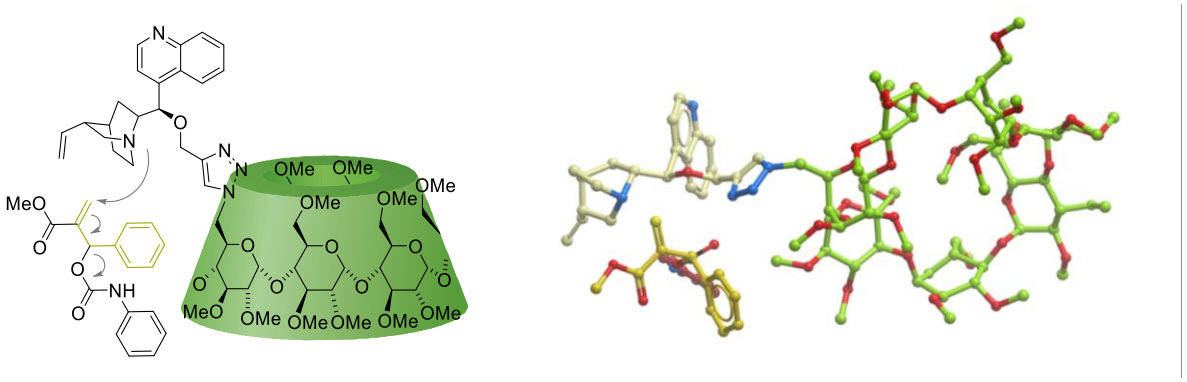

Figure 40. Representation and MD snapshots of cinchonidine-per-Me-β-CD (**24b**) in AAA reaction in toluene

Our spatial arrangement of CD catalyst and substrate were subsequently compared to the spatial arrangements of two previously mentioned, very recently published[104] CD catalysts, used in enantioselective Michael addition. First arrangement of Cinchona-CD catalysts with a thiourea linker (**XXXII**), β-nitrostyrene and 1,3-diketone compound (Figure 41) were visualized using VMD software. Hydrogen atoms are omitted for simplicity and clarity.

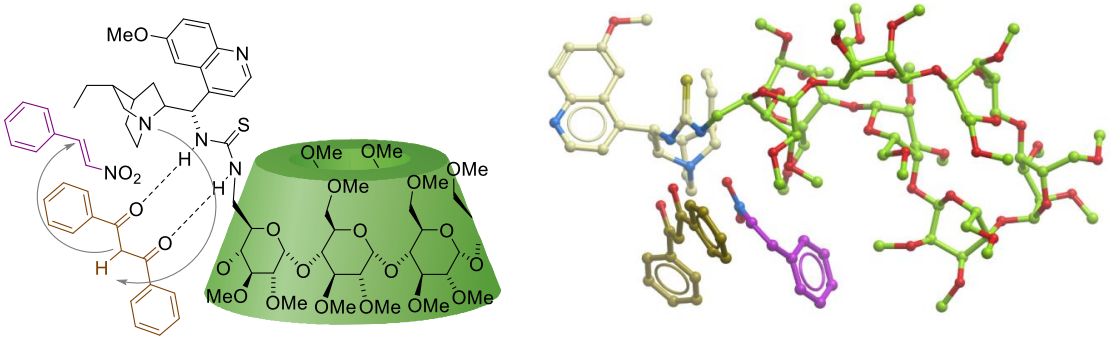

Figure 41. Representation and MD snapshots of previously published Cinchona alkaloid-per-Me-β-CD attached through a thiourea moiety in Michael addition.[104]

Spatial arrangement of the second previously published Cinchona-CD catalyst with a squaramide linker (**XXXI**), β-nitrostyrene and 1,3-diketone compound is shown in Figure 42.

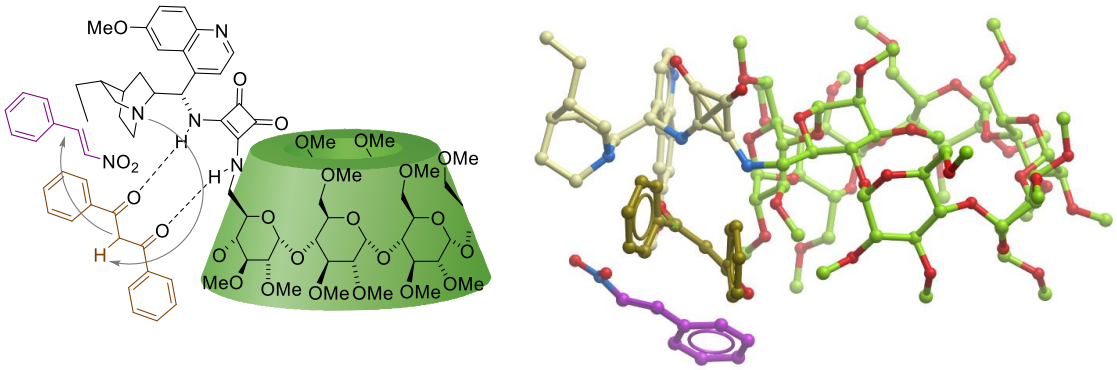

Figure 42. Representation and MD snapshots of previously published Cinchona alkaloid-per-Me-β-CD attached through a squaramide in Michael addition.

Both these published spatial arrangements (Figures 41 and 42) showed that the cone shape of the β-CD cavity collapsed, Cinchona-alkaloid moiety is positioned outside the cavity, resulting in the formation of "outer pocket", similarly to our findings by MD. Moreover, the hydrogen bonds between the substrates and the linkers fix the positions of these substrates and thus, affect the enantioselective formation of the products.

In conclusion, the collapsed cone-shape of the permethylated β-CD cavity and the Cinchona-alkaloid moiety positioned outside this CD cavity most likely created the "outer pocket" where the AAA reaction most likely occurs. Nevertheless, no hydrogen bonds can support the fixing of the substrate in this pocket resulting in lower enantiomeric excess (75% ee), compared to the previously published Cinchona-CD catalysts with squaramide and thiourea linkers (99% ee).

5. CONCLUSION

The research discussed in this thesis was divided into the following stages: (i) preparation of heterodisubstituted AC regioisomers on α-CD, (ii) synthesis of Cinchona-CD derivatives for enantioselective reactions and (iii) molecular modeling of the catalytic activity of Cinchona-CD derivatives.

In the first stage of this research, a method for the preparation of the heterodisubstituted α-CD derivatives was developed to prepare CD derivatives with two different moieties as pure regioisomer for enantioselective catalysis. The precursor for these catalysts, a CD derivative with azido and mesitylene sulfonyl group, was prepared and isolated as a pure AC regioisomer in gram scale from the mixture of AB, AC and AD regioisomers. In addition, the pseudoenantiomers of these heterodisubstituted AB and AC regioisomers were confirmed *via* HPLC-MS method at 10 °C. Furthermore, the regioisomer pattern of the most common disubstituted CD derivatives was investigated and used to investigate a regioisomer ratio of the mixture with this AC disubstituted regioisomer. Unfortunately, these heterodisubstituted regioisomers were not further studied to develop new CD-based organocatalysts because they have pseudoenantiomer pairs AB/BA and AC/CA, thereby preventing their application in enantioselective catalysis.

In the second stage, a method for attaching Cinchona alkaloids to CD skeletons was developed to prepare new CD-based organocatalysts for enantioselective reactions. First, four common Cinchona alkaloids (cinchonine, cinchonidine, quinine and quinidine) were attached to CD skeletons *via* a CuAAC reaction, subsequently preparing a series of new Cinchona-CD derivatives. Second, their permethylated analogs were synthesized to enhance their solubility in different organic solventsand in water. Third, their catalytic activity was evaluated in asymmetric reactions, specifically in the AAA reaction with high enantiomeric excess (up to 75% ee) and high isolated yields (up to 74%). Fourth, a disubstituted α-CD with two quinine moieties was prepared as a pure AD regioisomer and tested in this AAA reaction, albeit with no isolated product. Fifth, the supramolecular properties of Cinchona-β-CD derivatives were confirmed *via* 2D ROESY NMR interactions between protons of the substituent and inner protons of the β-CD cavity which showed the partial inclusion into the cavity.

In the third and final stage, the experimental findings about Cinchona-CD catalysts were further supported with computational studies based on MD calculations. Initially, the MD protocol, developed for this study, confirmed the quinine encapsulation into the native β-CD cavity in water. Subsequently, the spatial arrangements of non-methylated Cinchona-CD derivatives were studied, confirming the self-inclusion of the Cinchona alkaloid moiety into the non-methylated β-CD cavity. Moreover, permethylated Cinchona-CD derivatives were also tested for self-inclusion; however, this phenomenon was not observed. Conversely, permethylated CD derivatives create an “outer pocket” where substrates likely interact with the catalytic center of these catalysts, as confirmed in the AAA reaction by MD simulations.

6. EXPERIMENTAL SECTION

6.1. Synthesis - general information, instruments and materials

Organic solvents were distilled before use. Native CDs (α- and β-CDs) were purchased from Wacker Chemie (Germany). Other reagents were purchased from common commercial sources (Sigma, Penta Chemicals) and used without further purification. Concentrated (25%) aqueous solution of NH_3 was used.

Silica gel 60 (0.040–0.063 mm) was used for column chromatography, and TLC was performed on aluminium sheets with a layer of silica gel 60 F254, both purchased from Merck, Germany. The solvent ratio in elution mixtures is given as volume/volume. Argon was used as an inert gas. Spots on TLC plates were detected by using an UV lamp (λ = 254 nm for cinchonine and cinchonidine derivatives and λ = 365 nm for quinine and quinidine derivatives) and by dipping the TLC plates in sulfuric acid (50% aqueous solution) for CD derivatives or in basic $KMnO_4$ solution and by subsequent heating with a heat gun. Plates were developed in a saturated chamber; the mobile phases are given at each procedure in volume/volume ratio. CD starting materials and derivatives were dried to constant weight at oil bath at appropriate temperature using an oil pump or in a vacuum drying box in the presence of P_2O_5 and KOH. Quantitative analysis of TLC plates was performed with the software JustQuantify Free.

Preparative chromatographic separations of heterodisubtiuted AB-, AC- and AD-regioisomers were performed on a Büchi preparative chromatography system using SiliCycle SiliaCartridger – 40 mm Cartridge packed with Lichroprep RP-18 Phase (40-63 μm) reversed-phase silica gel as a stationary phase, ACN/water gradient elution and Büchi UV Photometer C-635 as a detector (detection wavelengths: 280 nm for mesitylene derivatives and 214 nm for azido derivatives). HPLC regiochemical measurements were carried out on an Agilent 1100 HPLC system equipped with UV-Vis and evaporative light scattering (ELS) detector. Reversed-phase separations were carried out on an Inertsil ODS-3 (4.6 × 150 mm, particle size 5 μm) analytical column using ACN/water as the mobile phase with gradient elution at a flow rate of 1.0 mL/min with UV (280 nm for mesitylene derivatives and 214 nm for azido derivatives). Inclusion assisted HPLC separations were obtained on a CD-Screen stationary phase (Bio-Sol-Dex Ltd, Hungary, 4.6 × 250 mm, particle size 5 μm) with the mobile phase of ACN/water with gradient elution at a flow rate of 0.5 mL/min with UV (280 nm for mesitylene and 214 nm for azido derivatives) detection.

The pseudoenantiomers HPLC-MS measurements were carried out on a Poroshell C-18 (4.6 × 150 mm, particle size 2.7 μm) analytical column using acetonitrile (+ 0.05% formic acid)/water (+ 0.05 % formic acid) as the mobile phase. Linear gradient elution was used as: 20% acetonitrile in 0 min, 30% acetonitrile at 15 min, 70% acetonitrile at 17.5 min and stop time was 25 min. Flow rate was 0.7 mL/min under the temperature 10 °C. UV detection was done at 280nm.

For IR measurements, samples were mixed with KBr powder and measured on a Thermo Nicolet AVATAR 370 FT-IR spectrometer using DRIFT method. Specific optical rotation was performed on Rudolph Research AUTOPOL III polarimeter at 589 nm (sodium D line) and the values of $[\alpha]^{25}_{D}$ are reported together with the concentration (*c*, g/100 mL) and solvent. Mass spectra (HRMS) were measured on an Agilent 6530Q-TOF MS spectrometer. Samples were dissolved in a mixture of ACN/H_2O.

^{1}H NMR spectra were acquired on Bruker AVANCE III spectrometer at 600 MHz, ^{13}C NMR spectra at 125 MHz, with DEPT and 2D NMR measurements (^{1}H, ^{1}H-COSY, HSQC, and HMBC). Samples were dissolved in DMSO-d_6, CD_3OD or D_2O with a drop of *tert*-butanol. Signals of tetramethylsilane (for ^{1}H NMR) and $CDCl_3$ (for ^{13}C NMR) served as internal standards. Chemical shifts are given in ppm; coupling constants *J* are given in Hz. For NMR, the atoms were numbered according to numbering system used in the literature on CD chemistry and on Cinchona alkaloids, thus alphabetical numbering was replaced with Greek numbering for the clarity (Figure 40).

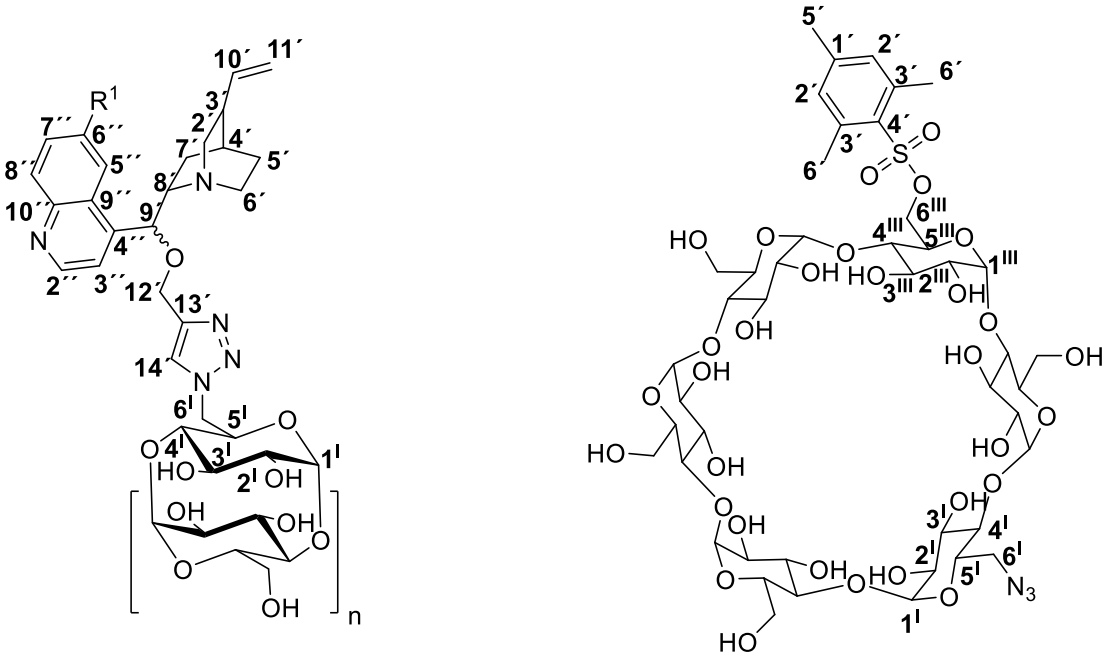

Figure 40. Numbering of CD skeletons in NMR spectra

6.2. Computational study – general information

The initial structures of α-CD, β-CD and quinine were retrieved from the Protein data bank (PDB identification: 5E6Y for α-CD[149], protein 5AB1 for β-CD[150] and protein 4UIN for quinine[151]). The initial structures for quinidine, cinchonine and cinchonidine were built from quinine using the Molefacture plugin[115] in the VMD 1.9.3 Their geometries were optimized at the semiempirical

quantum mechanics (SQM). The initial structures of Cinchona-CD derivatives were constructed using structures of CDs and Cinchona alkaloids, also in Molefacture plugin. Simple organic molecules such as MeOH, toluene and MBH carbamate were also obtained in Molefacture plugin. Non-methylated Cinchona α- and β-CD derivatives were surrounded by octahedral periodic boxes of 4875 water molecules represented by TIP3 potential[152]. Permethylated Cinchona-CD derivatives were surrounded by MeOH or by 1734 toluene molecules parameterized by CGenFF.[153]

The atom numbering in VMD simulations is presented in Figure 41. Labeled atoms C61, C62, C63, C64, C65, C66, C67 (violet) are the primary-rim (C-6) atoms, whereas C21, C22, C23, C24, C25, C26, C27 (black) are the secondary-rim (C-3) atoms.

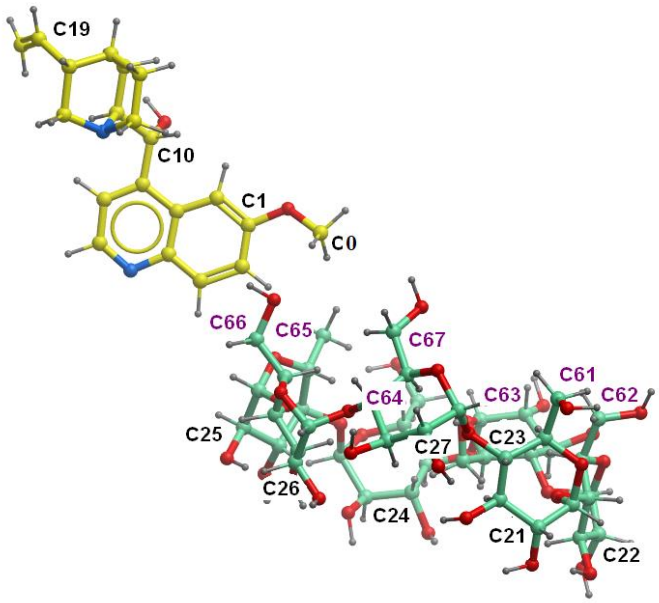

Figure 41. Atom numbering of Cinchona alkaloid-CD complexes and Cinchona-CD derivatives used in MD simulations

Preliminary MD trajectories were produced by NAMD software package.[109] Simulations were performed at 310 K. Langevin thermostat and Langevin-Hoover barostat were applied for the temperature and pressure control.[109] VdW interactions were computed using non-bonded cutoff 12 Å. The smooth-PME method was used for summation of long-range electrostatic interactions.[119] Long MD runs were obtained by AMBER software package.[118]

Analysis of MD trajectories

MD trajectories were analyzed by CPPTRAJ program.[154] Graphs were produced by Gnuplot 4.6 and figures were retrieved by ICM Molsoft and ChemBioOffice software packages.

6.3. Synthesis of starting materials – cyclodextrins

6^{A}-*O*-Toluenesulfonyl-α-CD (1a)

Compound **1a** was prepared according to a previously published procedure[19], with some modifications[20]. ^{1}H NMR and MS spectra are in accordance with this literature.

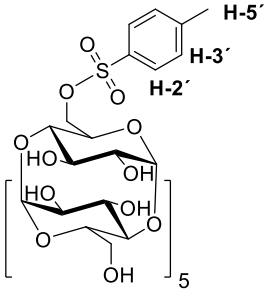

1a

^{1}H NMR (400 MHz, DMSO-*d6*): δ (ppm): 7.76 (d, *J* = 8.8 Hz, 2H, H-2'), 7.45 (d, *J* = 8.2 Hz, 2H, H-3'), 5.60-5.35 (m, 12H, 6 × OH-2, 6 × OH-3), 4.80 – 4.63 (6 × H-1), 4.54-4.42 (m, 5H, 5 × OH-6), 4.28 (m, 2H, 2 × H-6^{I}), 3.86-3.12 (m, 34H, 6 × H-2, 6 × H-3, 6 × H-4, 6 × H-5, 10 × H-6), 2.39 (s, 3H, H-5').

MS (ESI): found 1149.3. For $[M + Na]^{+}$ calculated 1149.3.

6^{A}-*O*-Toluenesulfonyl-β-CD (1b)

Compound **1b** was prepared according to a previously published procedure[19], with some modifications[20]. ^{1}H NMR and MS spectra are in accordance with these references.

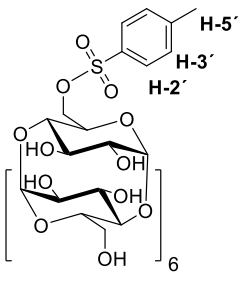

1b

^{1}H NMR (400 MHz, DMSO-*d6*): δ (ppm): 7.75 (d, *J* = 8.1 Hz, 1H, H-2'), 7.43 (d, *J* = 8.1 Hz, 1H, H-3'), 5.81-5.63 (m, 14H, 7 × OH-2, 7 × OH-3), 4.84-4.76 (m, 7H, 7 × H-1), 4.49-4.34 (m, 6H, 6 × OH-6), 4.43-3.20 (m, 42H, 7 × H-2, 7 × H-3, 7 × H-4, 7 × H-5, 14 × H-6), 2.43 (s, 3H, 3 × H-5').

MS (ESI): found 1311.3. For $[M + Na]^{+}$ calculated 1311.3.

6^{A}-Azido-6^{A}-deoxy-α-CD (2a)

Compound **2a** was prepared according to a previously published procedure[19], with some modifications of the purification process adapted from a different procedure[48]. ^{1}H NMR and MS spectra are in accordance with these references.

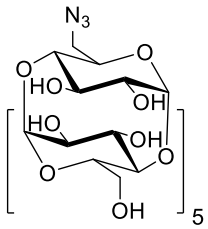

2a

^{1}H NMR (400 MHz, D_2O): δ (ppm): 5.13–5.04 (m, 6H, 6 × H-1), 4.06-3.80 (m, 24H, 12 × H-6, 6 × H-5, 6 × H-3), 3.74-3.51 (m, 12H, 6 × H-2, 6 × H-4).

MS (ESI): found 1020.8 For $[M + Na]^{+}$ calculated 1020.8.

6^{A}-Azido-6^{A}-deoxy-β-CD (2b)

Compound **2b** was prepared according to the a previously published procedure[19], with some modifications of the purification process, which was adapted from the literature[155]. ^{1}H NMR and MS spectra are in accordance with this literature.[156]

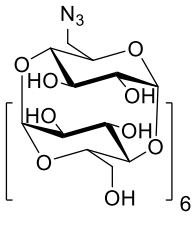

2b

^{1}H NMR (400 MHz, D_2O): δ (ppm): 5.13–5.04 (m, 7H, 7 × H-1), 4.25-3.80 (m, 28H, 14 × H-6, 7 × H-5, 7 × H-3), 3.74-3.44 (m, 14H, 7 × H-2, 7 × H-4).

MS (ESI): found 1182.9. For $[M + Na]^+$ calculated 1182.9

$2^{A-F},3^{A-F},6^{A-F}$-Octadeca-*O*-benzyl-α-CD (3)

Compound **3** was prepared according to a previously published procedure.[157] ^{1}H NMR and MS spectra are in accordance with the literature.[39]

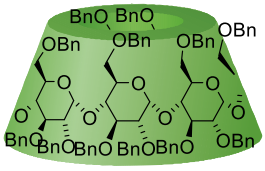

3

^{1}H NMR (400 MHz, $CDCl_3$): δ (ppm): 7.25-7.09 (m, 90H, H_{arom}), 5.20-5.15 (m, 6H, CH_2Ph), 5.10-5.06 (m, 6H, 6 × H-1), 4.88-4.84 (m, 6H, CH_2Ph), 4.51-4.36 (m, 18H, CH_2Ph), 4.34-4.28 (m, 6H, CH_2Ph), 4.16-4.09 (m, 6H, H-4), 4.06-4.96 (m, 12H, 6 × H-6, 6 × H-3), 3.92-3.86 (m, 6H, 6 × H-5), 3.50-3.42 (m, 12H, 6 × H-2, 6 × H-6).

MS (MALDI-TOF): found 2618.2. For $[M + Na]^+$ calculated 2618.1.

$2^{A-F},3^{A-F},6^{B-C},6^{E-F}$-Hexadeca-*O*-benzyl-α-CD (4)

Compound **4** was prepared according to a previously published procedure[38], which was subsequently modified.[54] ^{1}H NMR and MS spectra are in accordance with these references.[39]

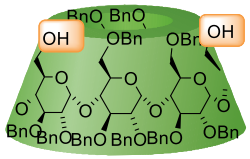

4

^{1}H NMR (400 MHz, $CDCl_3$): δ (ppm): 7.31-7.11 (m, 80H, H_{arom}), 5.73-5.70 (m, 2H, 2 × H-1), 5.47-5.40 (m, 2H, 1 × C*H*$_2$Ph), 5.20-5.14 (m, 2H, 1 × C*H*$_2$Ph), 4.92-3.53 (m, 64H, 4 × H-1, 2 × H-2, 6 × H-3, 6 × H-4, 6 × H-5, 12 × H-6, 14 × C*H*$_2$Ph), 3.45 – 3.37 (m, 4H, 4 × H-2), 3.25 (*br* s, 2H, 2 × OH-6).

MS (MALDI-TOF): found 2437.1. For $[M + Na]^+$ calculated 2437.8.

$2^{A-F},3^{A-F},6^{B-C},6^{E-F}$-Hexadeca-*O*-benzyl-$6^{A,D}$-dibromo-$6^{A,D}$-dideoxy-α-CD (5)

Compound **5** was prepared according to a previously published procedure.[23] ^{1}H NMR and MS spectra are in accordance with this literature.

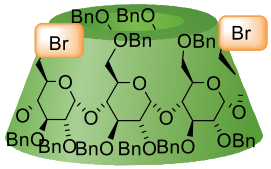

5

^{1}H NMR (400 MHz, $CDCl_3$): δ (ppm): 7.31-7.11 (m, 80H, H_{arom}), 5.25-3.35 (m, 74H, 6 × H-1, 6 × H-2, 6 × H-3, 6 × H-4, 6 × H-5, 12 × H-6, 16 × C*H*$_2$Ph).

MS (MALDI-TOF): found 2536.6. For $[M + H]^+$ calculated 2536.9.

$6^{A,D}$-Dibromo-$6^{A,D}$-dideoxy-α-CD (6)

Compound **6** was prepared according to a previously published procedure.[23] ^{1}H NMR and MS spectra are in accordance with this literature.

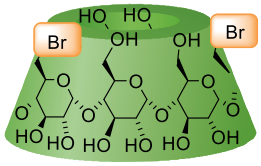

6

^{1}H NMR (400 MHz, DMSO-d6): δ (ppm): 5.72-5.38 (m, 12H, 6 × OH-2, 6 × OH-3), 4.89-4.79 (m, 6H, 6 × H-1), 4.61-4.54 (m, 4H, 4 × OH-6), 4.02-3.25 (m, 36H, 6 × H-2, 6 × H-3, 6 × H-4, 6 × H-5, 12 × H-6).

MS (ESI): found 1121.1, For $[M + Na]^+$ calculated 1121.6.

6^{A,D}-Diazido-6^{A,D}-dideoxy-α-CD (7d)

Compound **7d** was prepared according to a previously published procedure.[158] ^{1}H NMR and MS spectra are in accordance with the literature.[48]

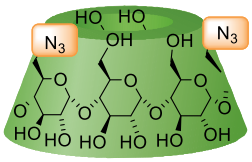

7d

^{1}H NMR (400 MHz, D_2O): δ (ppm): 5.07-4.98 (m, 6H, 6 × H-1), 4.02-3.82 (m, 24H, 6 × H-3, 6 × H-5, 12 × H-6), 3.71-3.57 (m, 12H, 6 × H-2, 6 × H-4).

MS (ESI): found 1045.3. For $[M + Na]^+$ calculated 1045.3.

2^{A-F},3^{A-F},6^{B-F}-Heptadeca-*O*-benzyl-α-CD (8)

Compound **8** was prepared as a byproduct of the preparation of compound **9** according to the original procedure.[38] ^{1}H NMR and MS spectra are in accordance with the literature.[43]

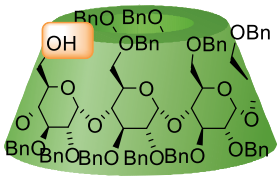

8

^{1}H NMR (400 MHz, $CDCl_3$): δ (ppm): 7.29-7.11 (m, 85H, H_{arom}), 5.73-5.70 (m, 2H, 2 × H-1), 5.47-5.40 (m, 2H, 1 × C$\underline{H_2}$Ph), 5.20-5.14 (m, 2H, 1 × C$\underline{H_2}$Ph), 4.92-3.53 (m, 64H, 4 × H-1, 2 × H-2, 6 × H-3, 6 × H-4, 6 × H-5, 12 × H-6, 15 × C$\underline{H_2}$Ph), 3.45-3.36 (m, 4H, 4 × H-2), 2.50 (*br* s, 1H, 1 × OH-6).

MS (MALDI-TOF): found 2526.5. For $[M + Na]^+$ calculated 2526.1.

6^{A}-*O*-Methanesulfonyl-2^{A-F},3^{A-F},6^{B-F}-Heptadeca-*O*-benzyl-α-CD (9)

Compound **9** was prepared according to a previously published procedure.[159] ^{1}H NMR and MS spectra are in accordance with this literature.

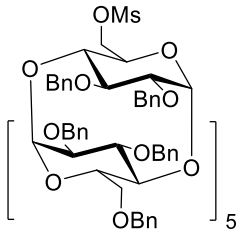

9

^{1}H NMR (400 MHz, $CDCl_3$): δ (ppm): 7.29-7.13 (m, 85H, H_{arom}), 5.31-4.83 (m, 12H, 6 × H-1, 3 × C$\underline{H_2}$Ph), 4.63-3.40 (m, 64H, 14 × C$\underline{H_2}$Ph, 6 × H-2, 6 × H-3, 6 × H-4, 6 × H-5, 12 × H-6), 2.61 (s, 3H, SO_2CH_3).

MS (MALDI-TOF): found 2604.3. For $[M + Na]^+$ calculated 2604.1.

6^{A}-Azido-6^{A}-deoxy-2^{A-F},3^{A-F},6^{B-F}-Heptadeca-*O*-benzyl-α-CD (10)

Compound **10** was prepared according to a previously published procedure.[159] ^{1}H NMR and MS spectra are in accordance with this literature.

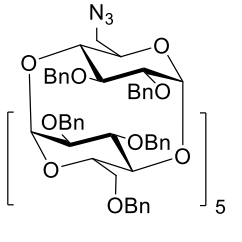

10

^{1}H NMR (400 MHz, $CDCl_3$): δ (ppm): 7.31-7.07 (m, 85H, H_{arom}), 5.24-4.77 (m, 12H, 6 × H-1, 3 × C$\underline{H}_2$Ph), 4.59-3.36 (m, 64H, 14 × C$\underline{H}_2$Ph, 6 × H-2, 6 × H-3, 6 × H-4, 6 × H-5, 12 × H-6).

MS (MALDI-TOF): found 2527.6. For $[M + H]^+$ calculated 2528.1.

6^A-Azido-6^A-deoxy-2^{A-F},3^{A-F},6^{B-F}-Heptadeca-*O*-methyl-α-CD (21)

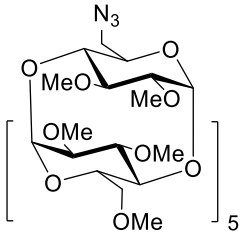

21

Compound **21** was prepared according a previously published procedure.[131] ^{1}H NMR and MS spectra are in accordance with this literature.

^{1}H NMR (400 MHz, $CDCl_3$): δ (ppm): 5.01-4.95 (m, 6H, 6 × H-1), 3.77-3.36 (m, 81H, 6 × H-3, 6 × H-4, 6 × H-5, 12 × H-6, 17 × OC$\underline{H}_3$), 3.22-3.15 (m, 6H, 6 × H-2).

MS (ESI): found 1259.1. For $[M + Na]^+$ calculated 1259.3.

6^A-Azido-6^A-deoxy-2^{A-G},3^{A-G},6^{B-G}-Heptadeca-*O*-methyl-β-CD (22)

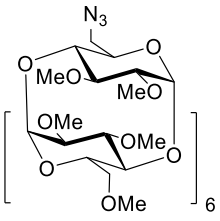

22

Compound **22** was prepared according to a previously published procedure.[155] ^{1}H NMR and MS spectra are in accordance with this literature.

^{1}H NMR (400 MHz, $CDCl_3$): δ (ppm): 5.14-5.05 (m, 7H, 7 × H-1), 4.00– 3.40 (m, 95H, 7 × H-3, 7 × H-4, 7 × H-5, 14 × H-6, 20 × OC$\underline{H}_3$), 3.19-3.10 (m, 7H, 7 × H-2).

MS (ESI): found 1463.2. For $[M + Na]^+$ calculated 1463.5.

6.4. Synthesis of starting materials – Cinchona alkaloid derivatives

(8*S*, 9*S*)-9-Amino-9-deoxy-*epi*-cinchonidine (17a)

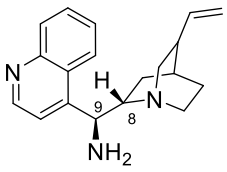

17a

Compound **17a** was prepared from (8*S*,9*R*)-cinchonidine *via* mesyl[127] and azido[160] functional groups. ^{1}H NMR and MS spectra correspond with this literature.[126]

^{1}H NMR (400 MHz, $CDCl_3$): δ (ppm): 8.89 (d, *J* = 4.4 Hz, 1H, H-2′), 8.35 (*br* s, 1H, H-5′), 8.14 (dd, *J* = 8.3 Hz, *J* = 1.2 Hz, 1H, H-8′), 7.70-7.65 (m, 1H, H-6′), 7.58-7.55 (m, 1H, H-7′), 7.53 (d, *J* = 4.4 Hz, 1H, H-3′), 5.78-5.75 (m, 1H, H-10), 5.02-4.94 (m, 2H, H-11), 4.70 (d, *J* = 9.6 Hz, 1H, H-9), 3.29-3.14 (m, 2H, H-2, H-6), 3.11-3.02 (m, 1H, H-8), 2.84-2.73 (m, 2H, H-2, H-6), 2.28 (*br* s, 3H, H-3, NH_2), 1.60-1.50 (m, 3H, H-4, H-5), 1.44-1.37 (m, 2H, H-7), 0.75-0.72 (m, 1H, H-7).

MS (ESI): found 294.1. For $[M + H]^+$ calculated 294.2

(8*R*,9*R*)-9-Amino-9-deoxy-*epi*-quinidine (17b)

Compound **17b** was prepared from (8*R*,9*S*)-quinidine in a sequence *via* mesyl[127] and azido[128] functional groups. ^{1}H NMR and MS spectra correspond with the literature.[161]

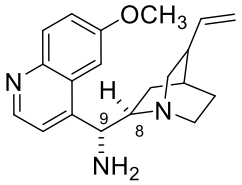

17b

^{1}H NMR (400 MHz, $CDCl_3$): δ (ppm): 8.74 (d, *J* = 4.4. Hz, 1H, H-2´), 8.03 (d, *J* = 9.2 Hz, 1H, H-5´), 7.65 (*br* s, 1H, H-5´), 7.46 (d, *J* = 4.4 Hz, 1H, H-3´), 7.38-7.35 (m, 1H, H-7´), 5.80-5.76 (m, 1H, H-10), 5.03-4.95 (m, 2H, H-11), 4.60 (d, *J* = 9.9 Hz, 1H, H-9), 3.95 (s, 3H, CH_3), 3.31-3.16 (m, 2H, H-2, H-6), 3.12-3.04 (m, 1H, H-8), 2.84-2.74 (m, 2H, H-2, H-6), 2.27 (*br* s, 1H, H-3), 2.18 (*br* s, 2H, NH_2), 1.63-1.52 (m, 3H, H-4, H-5), 1.46-1.38 (m, 1H, H-7), 0.75-0.72 (m, 1H, H-7).

MS (ESI): found 324.2. For $[M + H]^+$ calculated 324.4.

(8*R*, 9*S*)-9-*O*-Propargyl-cinchonine (18a)

Compound **18a** was prepared according to a previously published procedure.[162] ^{1}H NMR and MS spectra are in accordance with this literature.

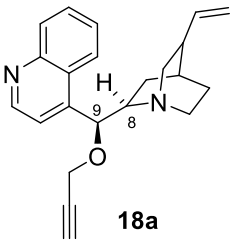

18a

^{1}H NMR (400 MHz, $CDCl_3$): δ (ppm): 8.91 (d, 1H, *J* = 4.3 Hz), 8.18-8.14 (m, 2H) 7.73-7.65 (m, 1H), 7.59-7.64 (m, 1H), 7.48 (d, 1H, *J* = 4.3 Hz), 6.10-6.02 (m, 1H), 5.14 (d, 1H, *J* = 11.1 Hz), 5.01 (d, 1H, *J* = 3.7 Hz), 4.25 (d, 1H, *J* = 2.4 Hz), 4.21 (d, 1H, *J* = 2.4 Hz), 3.95 (d, 1H, *J* = 1.8 Hz), 3.92 (d, 1H, *J* = 8.0 Hz), 3.11-3.06 (m, 1H), 2.72-2.97 (m, 3H), 2.46 (t, 1H, *J* = 2.3 Hz), 2.28 (q, 1H, *J* = 8.0 Hz), 2.11-2.02 (m, 2H), 1.52-1.40 (m, 2H), 1.24-1.21 (m, 1H).

MS (ESI): found 333.1. For $[M + H]^+$ calculated 333.2.

(8*S*, 9*R*)-9-*O*-Propargyl-cinchonidine (18b)

Compound **18b** was prepared according to a previously published procedure.[162,163] ^{1}H NMR and MS spectra are in accordance with this literature.

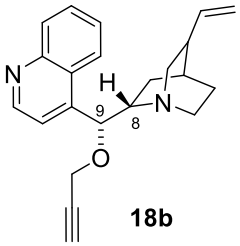

18b

^{1}H NMR (400 MHz, $CDCl_3$): δ (ppm): 8.89 (d, *J* = 4.5Hz, 1H), 8.20 – 8.10 (m, 2H), 7.78-7.65 (m, 1H), 7.62-7.53 (m, 1H), 7.46 (d, *J* = 4.5 Hz, 1H), 5.76-5.62 (m, 1H), 5.01-4.86 (m, 2H), 4.22 (dd, *J* = 15.8 Hz, *J* = 2.5Hz, 1H), 3.90 (dd, *J* = 15.8Hz, *J* = 2.5Hz, 1H), 3.17-3.04 (m, 2H), 2.69-2.54 (m, 2H), 2.44 (t, *J* = 2.5Hz, 1H), 2.28-2.18 (m, 1H), 1.88-1.45 (m, 6H).

MS (ESI): found 333.1. For $[M + H]^+$ calculated 333.2.

(8*S*, 9*R*)-9-*O*-Propargyl-quinine (18c)

Compound **18c** was prepared according to a previously published procedure.[164] ^{1}H NMR and MS spectra are in accordance with this literature.

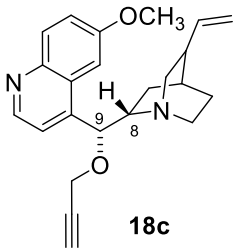

18c

^{1}H NMR (400 MHz, $CDCl_3$): δ (ppm): 8.77 (d, *J* = 4.5 Hz, 1H), 8.03 (d, *J* = 9.8 Hz, 1H), 7.33-7.45 (m, 3H), 6.02-6.17 (m, 1H), 5.36 (d, *J* = 4.0 Hz, 1H), 5.05-5.16 (m, 2H), 4.24 (dd, *J* = 16.0, *J* = 2.3 Hz, 1H), 3.93 (s, 3H), 3.95-3.87 (m, 1H), 3.21-3.35 (m, 1H), 3.16-3.04 (m, 1H), 2.97-2.70 (m, 3H), 2.46 (t, *J* = 2.4 Hz, 1H), 2.34-2.18 (m, 1H), 2.00 – 1.20 (m, 5H).

MS (ESI): found 263.2. For $[M + H]^+$ calculated 263.4.

(8*R*, 9*S*)-9-*O*-Propargyl-quinidine (18d)

Compound **18d** was prepared according to a previously published procedure.[164] ^{1}H NMR and MS spectra are in accordance with this literature.

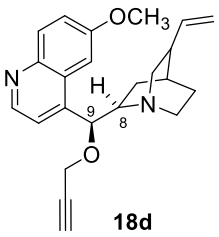

18d

^{1}H NMR (400 MHz, $CDCl_3$): δ (ppm): 8.77 (d, *J* = 4.5 Hz, 1H), 8.03 (d, *J* = 9.8 Hz, 1H), 7.33-7.45 (m, 3H), 6.02-6.17 (m, 1H), 5.36 (d, *J* = 4.0 Hz, 1H), 5.05-5.16 (m, 2H), 4.24 (dd, *J* = 16.0, *J* = 2.3 Hz, 1H), 3.93 (s, 3H), 3.95-3.87 (m, 1H), 3.21 – 3.35 (m, 1H), 3.16-3.04 (m, 1H), 2.97-2.70 (m, 3H), 2.46 (t, *J* = 2.4 Hz, 1H), 2.34-2.18 (m, 1H), 2.00-1.20 (m, 5H).

MS (ESI): found 263.2. For $[M + H]^+$ calculated 263.4.

6.5. Synthesis of new CD derivatives

6^A,6^B-Diazido-6^A,6^B-dideoxy-α-CD (7b) *via* 6^A, 6^B-capped-α-CD (12)

6^A,6^B-Capped α-CD (**2**) was prepared according by combining procedures first described for α-CD[32] and β-CD[28]. Dried α-CD (**1**, 5 g, 5.1 mmol) was dissolved in freshly distilled pyridine (115 mL). *m*-Benzene-1,3-disulfonyl chloride (1.41 g, 5.1 mmol) was dissolved in freshly distilled pyridine (40 mL), and the resulting pale, yellow solution was added dropwise to the α-CD solution under vigorous stirring at 8 °C within 1 hour. The mixture was stirred at 25 °C for another 4 hours. The white precipitate (part of unreacted α-CD), observed after fishing of stirring, was filtered off, and the mother liquid was evaporated under reduced pressure at 30 °C. The remaining gel-like, pale yellow residue was subsequently poured into 200 mL of MeOH resulting in the formation of a white precipitate. The solid was recovered by filtration, washed with MeOH (3 × 50 mL) and dried.

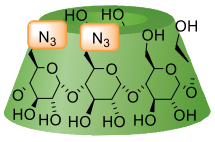

7b

This solid (0.87 g), containing unreacted α-CD (~90% based on TLC, R_F = 0.35, eluent: 1,4-dioxane/conc.aq.NH_3 10/7) and 6^A,6^B-capped α-CD (**7b**, ~10% based on TLC, R_F = 0.5, eluent: 1,4-dioxane/conc.aq.NH_3 10/7), was dissolved in DMF (20 mL). Then, sodium azide (0.14 g, 2.2

mmol) was added to the mixture, which was subsequently heated to 80 °C for 5 hours. DMF was removed under reduced pressure at 60 °C; the yellowish residue was poured into acetone (200 mL) under vigorous stirring. The white precipitate was recovered by filtration, washed with acetone (3 x 50 mL) and dried to constant weight (0.84 g). Direct-phase TLC (1,4-dioxane/conc.aq.NH_3 10/7) and reversed-phase HPLC (ACN/H_2O gradient elution) analysis revealed that the precipitate contained unreacted α-CD (R_F = 0.35), monoazido-α-CD (**2a**, R_F = 0.5) and diazido-α-CD (**7a**, R_F = 0.65). The diazido-α-CD fraction was isolated by direct column chromatography. The precipitate was dissolved in ACN/water/conc.aq.NH_3 10/7/1 (8.7 mL) and injected into the chromatographic column (44 g). The mobile phase was ACN/water/conc.aq.NH_3 10/5/1. After the chromatographic separation, the 6^A,6^B-diazido-α-CD (**7b**, 0.09 g, 2% yield) was obtained as a white solid. 6^A-Azido-α-CD (**2a**) was also obtained as a white solid (0.19 g, 4% yield) as the second eluted compound.

6^A,6^X-Diazido-6^A,6^X-dideoxy-α-CD (7) *via* 6^A,6^X-capped-α-CD (13)

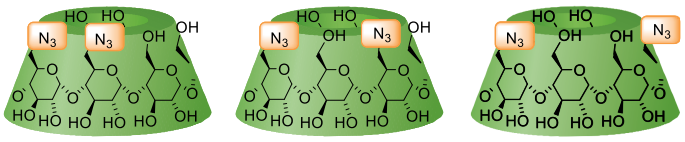

6^A,6^X-Capped α-CD (**13**) was prepared by modifying a procedure previously described for β-CD[29]. Dried α-CD (5 g, 5.1 mmol) was dissolved in freshly distilled pyridine (77 mL). The mixture was heated up to 50 °C and biphenyl-4,4′-disulfonyl chloride (1.4 g, 3.8 mmol) was added during one hour in four portions, every 15 minutes. The resulting yellow solution was stirred at 50 °C for another 1.5 h and then evaporated under reduced pressure at 25 °C. The remaining gel-like, pale yellow residue was subsequently poured into MeOH (200 mL) resulting in the formation of a white precipitate. The solid was recovered by filtration, washed with methanol (3 × 50 mL) and dried.

This white solid (3.27 g), containing unreacted α-CD (~85% based on TLC, R_F = 0.35, eluent: 1,4-dioxane/conc.aq.NH_3 10/7) and 6^A,6^X-capped α-CD (**13**, ~15% based on TLC, R_F = 0.55, eluent: 1,4-dioxane/conc.aq.NH_3 10/7), was dissolved in DMF (30 mL). Sodium azide (0.34 g, 5.2 mmol) was added, and the reaction mixture was heated to 80 °C for 5 h. Unreacted NaN_3 was filtered off, and the reaction mixture was concentrated under reduced pressure at 50 °C; the yellowish residue was poured into acetone (220 mL) under vigorous stirring. The white precipitate was recovered by filtration, washed with acetone (3 × 50 mL) and dried to constant weight (2.45 g) in a vacuum drying box in the presence of P_2O_5 and KOH. Direct-phase TLC (1,4-dioxane/conc.aq.NH_3 10/7) and reversed-phase HPLC (ACN/H_2O gradient elution) analysis revealed that the precipitate contained unreacted α-CD (R_F = 0.35), monoazido-α-CD (**7**, R_F = 0.5) and diazido-α-CD (**7**, R_F = 0.65). The diazido-α-CD fraction was isolated by direct column chromatography. The precipitate was dissolved in ACN/water/conc.aq.NH_3 10/7/1 (24 mL) and injected into the chromatographic column (134 g). The mobile phase was ACN/water/conc.aq.NH_3 10/5/1. After the chromatographic separation, the

$6^A,6^X$-diazido-α-CD (**7**, 0.25 g, 5% yield) was obtained as a white solid material. 6^A-Azido-α-CD (**2a**) was also obtained as a white solid (0.34 g, 7% yield) as the second eluted compound.

$6^A,6^X$-Diazido-$6^A,6^X$-dideoxy-α-CD (7) *via* $6^A,6^X$-dibromo-α-CD (14)

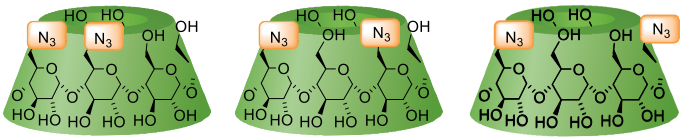

$6^A,6^X$-Brominated α-CD (**14**) was prepared following a modified procedure previously described for $6^A,6^X,6^Y$-tribromo-α-CD.[165] Triphenylphosphine (36.4 g, 138 mmol) was dissolved in 125 mL of freshly distilled DMF under Ar atmosphere. The solution was cooled down to 8 °C, and NBS was slowly added to the solution which became dark violet. Dried α-CD (**1**, 25 g, 25.7 mmol) was dissolved in 100 mL of DMF and added to the dark violet reaction mixture in one portion for 20 minutes. The mixture was heated up to 50 °C, and the conversion to dibromo-α-CD was monitored by direct phase TLC (1,4-dioxane/conc.aq.NH_3/1-propanol 10/7/3). After 7.5 h the reaction was stopped by adding 100 mL of MeOH. After 10 minutes of vigorous stirring, the red-violet reaction mixture was cooled down and poured into 1.3 L of MeOH (pH = 3). The addition of a sodium methoxide solution (100 mL) resulted in slow precipitation (pH = 12). The yellowish precipitate was recovered by filtration, washed with MeOH (3 × 300 mL) and dried.

The white solid (15.27 g), containing unreacted α-CD (~35% based on TLC, R_F = 0.15, eluent: 1,4-dioxane/conc.aq.NH_3/1-propanol 10/7/3), monobromo α-CD (~35 % based on TLC, R_F = 0.25, eluent: 1,4-dioxane/conc.aq.NH_3/1-propanol 10/7/3), dibromo-α-CD (**14**, ~20% based on TLC, R_F = 0.35, eluent: 1,4-dioxane/conc.aq.NH_3/1-propanol 10/7/3) and oversubstituted products (less than 10% based on TLC, R_F = 0.5, eluent: 1,4-dioxane/conc.aq.NH_3/1-propanol 10/7/3) was dissolved in DMF (300 mL), sodium azide (2.72 g, 42.0 mmol) was added, and the mixture was heated to 80 °C for 5 h. DMF was removed under reduced pressure at 60 °C; the yellowish residue was poured into acetone (1.3 L) under vigorous stirring. The white precipitate was recovered by filtration, washed with acetone (3 × 100 mL) and dried to constant weight (17.9 g). Direct-phase TLC (eluent: 1,4-dioxane/conc.aq.NH_3/1-propanol 10/7/3) and reversed-phase HPLC (ACN/H_2O gradient elution) analysis revealed that the precipitate contained unreacted α-CD (R_F = 0.15), monoazido-α-CD (**7**, R_F = 0.35) and diazido-α-CD (**7**, R_F = 0.45). The diazido-α-CD fraction was isolated by direct column chromatography. The one-third of precipitate was dissolved in ACN/water/conc.aq.NH_3 10/7/1 (40 mL) and injected to the chromatographic column (310 g). After chromatographic separation of all three parts of crude mixture using mobile phase ACN/water/conc.aq.NH_3 10/5/1, the $6^A,6^X$-diazido-α-CD (**7**, 1.26 g, 5% yield) was obtained as a white solid material. 6^A-Azido-α-CD (**2a**) was also obtained as a white solid (3.69 g, 15% yield) as the second eluted compound.

$6^A,6^X$-Diazido-$6^A,6^X$-dideoxy-α-CD (7) *via* $6^A,6^X$-*O*-ditosyl-α-CD (15)

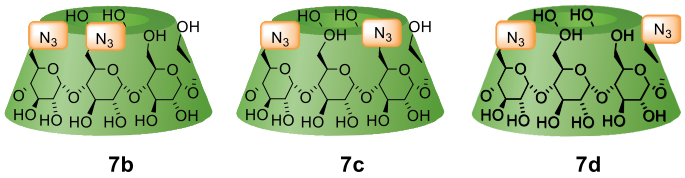

$6^A,6^X$-Ditosyl-α-CD (**15**) was prepared according a modified procedure previously published for monotosyl-α-CD.[19] Dried α-CD (**1**, 5 g, 5 mmol) was dissolved in freshly distilled pyridine (150 mL), cooled down to 0 °C, and *p*-toluenesulfonyl chloride (3.49 g, 18 mmol) was added gradually spoon by spoon. After adding of *p*-toluenesulfonyl chloride, the reaction mixture was stirred at room temperature for 6 h, and then pyridine was evaporated under reduced pressure at 30 °C. After solvent evaporation, the remaining gel-like, light yellow residue was then dissolved in MeOH (30 mL) and subsequently poured into acetone (350 mL), resulting in the immediate formation of a white precipitate. The solid was recovered by filtration, washed with acetone (3 × 50 mL) and dried.

The white material (6.3 g), containing unreacted α-CD (~35% based on TLC, R_F = 0.15, eluent: 1,4-dioxane/conc.aq.NH_3/1-propanol 10/7/3), 6^A-tosyl-α-CD (~30% based on TLC, R_F = 0.3, eluent: 1,4-dioxane/conc.aq.NH_3/1-propanol 10/7/3), $6^A,6^X$-ditosyl-α-CD (**15**, ~30% based on TLC, R_F = 0.45, eluent: 1,4-dioxane/conc.aq.NH_3/1-propanol 10/7/3) and the overtosylated $6^A,6^X,6^Y$-tritosyl-α-CD (~20% based on TLC, R_F = 0.55, eluent: 1,4-dioxane/conc.aq.NH_3/1-propanol 10/7/3) was dissolved in DMF (120 mL), sodium azide (0.76 g, 17 mmol) was added and the reaction mixture was heated to 80 °C for 5 hours. DMF was removed under reduced pressure at 60 °C; the yellowish residue was poured into acetone (300 mL) under vigorous stirring. The white precipitate was recovered by filtration, washed with acetone (3 × 50 mL) and dried to constant weight (5.74 g). Direct-phase TLC (1,4-dioxane/conc.aq.NH_3/1-propanol 10/7/3) and reversed-phase HPLC (ACN/H_2O gradient elution) analysis revealed that the precipitate contained unreacted α-CD (R_F = 0.15), monoazido-α-CD (**2a**, R_F = 0.35) and diazido-α-CD (**7**, R_F = 0.45) and triazido-α-CD (R_F = 0.5). The diazido-α-CD fraction was isolated by direct column chromatography (394 g). The precipitate was dissolved in ACN/water/conc.aq.NH_3 10/7/1 (50 mL) and injected to the chromatographic column. After chromatographic separation in the mobile phase ACN/water/conc.aq.NH_3 10/5/1, the $6^A,6^X$-diazido-α-CD (**7**, 0.69 g, 16% yield) was obtained as a white solid material. 6^A-Azido-α-CD (**2a**) was also obtained as a white solid (**7**, 0.46 g, 11% yield) as the second eluted compound.

$6^A,6^X$-Diazido-$6^A,6^X$-dideoxy-α-CD (7) *via* 6^A-azido-6^X-*O*-mesitylenesulfonyl-α-CD (16)

6^A-Azido-6^X-mesitylenesulfonyl-α-CD (**16**, 0.3 g, 0.2 mmol) was dissolved in freshly distilled DMF (5 mL), sodium azide (0.044 g, 1.9 mmol) was added, and the reaction mixture was heated to 80 °C for 5 h. DMF was removed under reduced pressure at 60 °C; the yellowish residue was poured into acetone

(300 mL) under vigorous stirring. The white precipitate was recovered by filtration, washed with acetone (3 x 50 mL) and dried to constant weight (0.2 g). Direct-phase TLC (eluent: 1,4-dioxane/conc.aq.NH_3/1-propanol 10/7/3) and reversed-phase HPLC (ACN/H_2O gradient elution) analysis revealed that the precipitate contained 6^A-azido-α-CD (**2a**, ~60% based on TLC, R_F = 0.35) and 6^A,6^X-diazido-α-CD (**7**, ~35% based on TLC, R_F = 0.45) and more substituted 6^A,6^X,6^Y-triazido-α-CD (~5% based on TLC, R_F = 0.5). The 6^A,6^X-diazido-α-CD fraction was not isolated by direct column chromatography but instead used directly as a mixture of the starting material, diazido-α-CD and triazido-α-CD in HPLC separations.

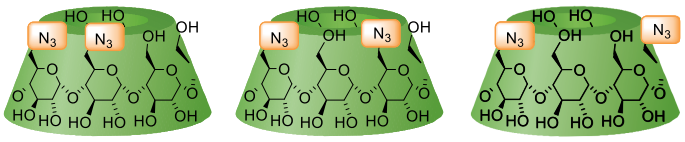

7b **7c** **7d**

^{1}H NMR, ^{13}C NMR spectra for diazido-α-CDs (**7**) were measured (i) as a mixture of three regioisomers (ii) as a single AD isomer and are in accordance with literature.[48]

^{1}H NMR (600 MHz, D_2O): δ (ppm): 5.07 (m, H-1, 6H), 4.02 –3.82 (m, 24H, H-3, H-5, H-6), 3.71 – 3.57 (m, 12H, H-2, H-4).

^{13}C NMR (150 MHz, D_2O): δ (ppm): 103.99, 103.81, 84.73, 83.90, 75.87, 75.65, 74.71, 74.51, 74.17, 74.10, 73.29, 63.00, 53.80.

HRMS data are identical for all homobifunctionalized 6^A,6^X-diazido-α-CDs (**7**).

HRMS: $[M + Na]^+$ found 1045.3094. For $C_{36}H_{58}N_6O_{28}$ $[M + Na]^+$ calculated 1045.3191.

IR (KBr) ν = 3354, 3321, 2104, 1416, 1332, 1293, 1655, 1207, 1033 cm^{-1}.

(i) $[\alpha]_D^{25}$ = + 90.3^0 (c = 0.30, H_2O) (ii) $[\alpha]_D^{25}$ = + 133.3^0 (*c* = 0.31, H_2O)

6^A-Azido-6^A-deoxy-6^X-*O*-mesitylenesulfonyl-α-CD (16)

Dried 6^A-azido-α-CD (**7**, 1.23 g, 1.2 mmol) was dissolved in pyridine (12 mL) and cool down to 0 °C. 2-Mesitylenesulfonyl chloride (0.52 g, 2.4 mmol) was gradually added spoon by spoon. The reaction mixture was stirred at room temperature for 2 hours; the yellowish residue was poured into acetone (300 mL) under vigorous stirring. The white precipitate was recovered by filtration, washed with acetone (3 x 50 mL) and dried to constant weight (1.60 g). Direct-phase TLC (eluent: 1,4-dioxane/conc.aq.NH_3/1-propanol 10/7/3) and reversed-phase HPLC (H_2O/ACN gradient elution) analysis revealed that the precipitate contained unreacted 6^A-azido-α-CD (**2a**, ~60% based on TLC, R_F = 0.35, eluent: 1,4-dioxane/conc.aq.NH_3/1-propanol 10/7/3), 6^A-azido-6^X-mesitylenesulfonyl-α-CD (**16**, ~35% based on TLC, R_F = 0.5, eluent: 1,4-dioxane/conc.aq.NH_3/1-propanol 10/7/3) and 6^A-azido-6^X,6^Y-dimesitylenesulfonyl-α-CD (~5% based on TLC, R_F = 0.6, eluent: 1,4-dioxane/conc.aq.NH_3/1-propanol 10/7/3). The 6^A-azido-6^X-mesitylenesulfonyl-α-CD fraction was isolated by reversed-phased column chromatography (H_2O/ACN gradient elution). The first eluted

(95:5), starting material, 6^A-azido-α-CD (520 mg) was recovered. Then, 6^A-azido-6^X-mesitylenesulfonyl-α-CD was eluted (70:30): AD regioisomer in 10.0 min, AC regioisomer (mixture of AC/CA pseudoenantiomers) in 13.5 min and AB regioisomer (mixture of AB/BA pseudoenantiomers) in 19.5 min. The isolated yield of regioisomers was 26.4 mg (3%) for AD (**16d**), 37.5 mg (4%) for AC (**16c**) and 38.2 mg (4%) for AB (**16b**), obtained from 960 mg precipitate of reaction mixture.

6^A-Azido-6^A-deoxy-6^D-*O*-mesitylenesulfonyl-α-CD (16d)

Compound **16d** was prepared according to above described procedure. From the mixture of 6^A-azido-6^X-mesitylenesulfonyl-α-CD, 26 mg of product was obtained in the form of a white solid (3% yield calculated from the starting 6^A-azido-α-CD).

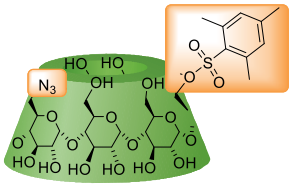

16d

^{1}H NMR (600 MHz, D_2O): δ (ppm): 7.19 (2H, s, C-2′), 5.24 (1H, m, H-1-I), 5.08 (4H, m, H-1), 4.95 (1H, m, H-1-IV), 4.39 (2H, s, H-6-IV), 4.04 (1H, m, H-5-IV), 3.95-3.41 (34H, m, H-5, H-6, H-3, H-4, H-2), 2.60 (6H, s, C*H*$_3$-6′), 2.34 (3H, s, C*H*$_3$-5′).

^{13}C NMR (150 MHz, D_2O): δ (ppm): 144.74 (C-1′), 140.07 (2 × C-3′), 131.67 (2 × C-2′), 128.73 (C-4′), 101.51 (5 × C-1), 99.36 (1× C-1-I), 81.11 (6 × C-4), 73.14 (6 × C-3), 72.10 (4 × C-5, 5 × C-2), 70.50 (1 × C-2^I), 69.97 (1 × C-5^{IV}), 68.82 (1 × C-6^{IV}), 60.18 (4 × C-6), 58.37 (1 × C-5-I), 51.36 (1 × C-6-I), 21.93 (2 × *C*H$_3$-6′), 20.32 (*C*H$_3$-5′).

HRMS: $[M+Na]^+$, found: 1202.3444. For $C_{45}H_{69}N_3O_{31}S$ $[M+Na]^+$ calculated 1202.3528.

IR (KBr) ν = 3294, 2929, 2101, 1461, 1347, 1287, 1156, 1018 cm^{-1}.

$[\alpha]_D^{25}$ = + 124.6 ^{0} (*c* = 0.25, DMSO).

6^A-Azido-6^A-deoxy-6^C-*O*-mesitylenesulfonyl-α-CD (16c)

Compound **16c** was prepared according to above described procedure. From the mixture of 6^A-azido-6^X-mesitylenesulfonyl-α-CD, 38 mg of product the (mixture of AC/CA pseudoenantiomers) was obtained in the form of a white solid (4% yield calculated from the starting 6^A-azido-α-CD).

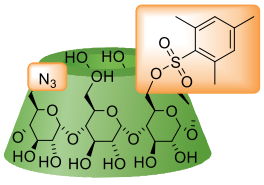

16c

^{1}H NMR (600 MHz, D_2O): δ (ppm): 7.19 (2H, s, C-2′), 5.08 (4H, m, H-1), 4.98 (1H, m, H-1^I), 4.95 (1H, m, H-1^{III}), 4.40 (2H, m, H-6^{III}), 4.03-3.72 (20H, m, H-2, H-5, H-6, H-3), 3.73-3.44 (14H, m, H-6^I, H-4), 2.59 (6H, s, C*H*$_3$-6′), 2.30 (3H, s, C*H*$_3$-5′).

^{13}C NMR (150 MHz, D_2O): δ (ppm): 144.74 (C-1′), 140.07 (2 × C-3′), 131.67 (2 × C-2′), 128.73 (C-4′), 101.51 (5 × C-1), 100.08 (1 × C-1^I), 81.59 (6 × C-4), 73.34 (6 × C-3), 71.90 (4 × C-5, 5 × C-2),

70.83 (1 × C-2^{I}), 69.59 (1 × C-5^{III}), 68.60 (1 × C-6^{III}), 60.23 (4 × C-6), 51.33 (1 × C-6^{I}), 21.93 (2 × $\underline{C}H_3$-6′), 20.32 ($\underline{C}H_3$-5′).

HRMS: $[M + Na]^+$ found: 1202.3435. For $C_{45}H_{69}N_3O_{31}S$ $[M + Na]^+$ calculated 1202.3528.

IR (KBr) ν = 3294, 2929, 2101, 1721, 1335, 1237, 1153, 1078 cm^{-1}.

$[\alpha]_D^{25}$ = + 107.9^0 (*c* = 0.26, DMSO).

6^{A}-Azido-6^{A}-deoxy-6^{B}-*O*-mesitylenesulfonyl-α-CD (16b)

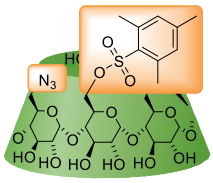

16b

Compound **16b** was prepared according to above described procedure. From the mixture of 6^{A}-azido-6^{X}-mesitylenesulfonyl-α-CD, 38 mg of product (the mixture of AB/BA pseudoenantiomers) was obtained in the form of a white solid (4% yield calculated from the starting 6^{A}-azido-α-CD).

^{1}H NMR (600 MHz, D_2O): δ (ppm): 7.19 (2H, s, H-2′), 5.07 (4H, m, H-1), 4.98 (1H, m, H-1^{I}), 4.95 (1H, s, H-1^{II}), 4.40 (2H, m, H-6^{II}), 4.03-3.72 (20H, m, H-2, H-5, H-6, H-3), 3.66-3.45 (14H, m, H-6^{I}, H-4), 2.60-2.59 (6H, s, C$\underline{H_3}$-6′), 2.34 (3H, s, C$\underline{H_3}$-5′).

^{13}C NMR (150 MHz, D_2O): δ (ppm): 144.74 (C-1′), 140.07 (2 × C-3′), 131.67 (2 × C-2′), 128.73 (C-4′) 101.51 (6 × C-1), 81.05 (6 × C-4), 73.14 (6 × C-3), 72.10 (4 × C-2, 5 × C-2), 70.65 (1 × C-2^{I}), 68.60 (1 × C-5^{II}), 60.18 (4 × C-6), 51.10 (1 × C-6^{I}), 21.95-21.89 (2 × CH_3-6′), 20.32 (CH_3-5′).

HRMS: $[M + Na]^+$, found: 1202.3432. For $C_{45}H_{69}N_3O_{31}S$ $[M + Na]^+$ calculated 1202.3528.

IR (KBr) ν = 3294, 2929, 2104, 1419, 1350, 1242, 1150, 1030 cm^{-1}.

$[\alpha]_D^{25}$ = + 95.0^0 (*c* = 0.25, DMSO).

General procedure for the preparation of monosubstituted non-methylated Cinchona-CD derivatives (GP1)

For α-CD derivatives: The first starting material, 9-*O*-propargyl Cinchona alkaloids (**18a–18d**, 0.13 mmol) was dissolved in 0.5 mL of distilled THF (sonicated for 10 minutes under Ar atmosphere). Then, 6^I-azido-6^I-deoxy-α-CD[19] (**2a**, 0.10 mmol) was dissolved in 0.4 mL of distilled H_2O (sonicated for 10 minutes under Ar atmosphere) and added to the stirring solution of the Cinchona alkaloid. Lastly, copper iodide (0.02 mmol), suspended in H_2O (0.1 mL), was added to the reaction mixture and stirred at 50 °C for 2-3 hours.

For β-CD derivatives: The first starting material, 9-*O*-propargyl Cinchona alkaloid (**18a–18d,** 0.11 mmol) was dissolved in 0.5 mL of distilled DMF (sonicated for 10 minutes under Ar atmosphere). The second starting material, 6^I-azido-6^I-deoxy-β-CD[19] (**2b**, 0.09 mmol), was dissolved in 0.5 mL of distilled DMF (sonicated for 10 minutes under Ar atmosphere) and added to the solution of the Cinchona alkaloid under stirring. Copper iodide (0.02 mmol), suspended in 0.1 mL of distilled DMF (sonicated for 10 minutes under Ar atmosphere), was added to the reaction mixture and stirred at 60 °C for 2-3 hours.

Conversion into the product was monitored by TLC in eluent ACN/H_2O/conc.aq.NH_3 (10/5/1). After full conversion into the product, the reaction mixture was slowly added to acetone (75 mL) under stirring, resulting in a white-yellow precipitate. This solid was recovered by filtration, washed with acetone (3 × 20 mL) and dried to constant weight. Crude product was purified on column chromatography (50 g of silica gel) with mobile phase ACN/H_2O/conc.aq.NH_3 12/5/1. When full conversion into the product was not achieved, the CD starting material was regenerated (eluted as the second compound). A blue precipitate formed at the top of the column creates as copper cations interacted with ammonia. The purified product was dried at 50 °C under reduced pressure.

6^{I}-Deoxy-6^{I}-(4-(((*S*)-quinolin-4-yl(5-vinylquinuclidin-2-yl)methoxy) methyl)-1*H*-1,2,3-triazol-1-yl)-α-CD (19a)

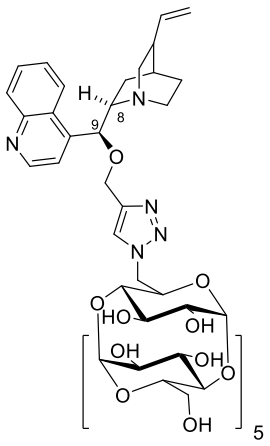

19a

Compound **19a** was prepared according to the general procedure (**GP1**). From 6^{I}-azido-6^{I}-deoxy-α-CD **2a** (164 mg, 0.16 mmol), 9-*O*-propargyl-cinchonine **18a** (71 mg, 0.2 mmol) and copper-iodide (6 mg, 0.03 mmol), 168 mg of product was obtained in the form of a white-yellow solid (77% yield). TLC (ACN/H_2O/conc.aq.NH_3 10/5/1): R_F = 0.45.

^{1}H NMR (600 MHz, DMSO-d_6): δ (ppm): 8.96-8.94 (m, 1H, H-2′′), 8.39-8.37 (m, 1H, H-8′′), 8.14-8.13 (s, 1H, H-14′), 8.10-8.08 (m, 1H, H-5′′), 7.82-7.80 (m, 1H, H-6′′), 7.70-7.68 (m, 1H, H-7′′), 7.64-7.63 (m, 1H, H-3′′), 5.89-5.87 (m, 1H, H-10′), 5.65-5.35 (m, 12H, OH-2, OH-3), 5.06-5.04 (m, 1H, H-1^{I}), 5.05-5.03 (m, 2H, H-11′), 4.86-4.72 (m, 5H, H-1), 4.84-4.83 (m, 2H, H-6^{I}), 4.58-4.50 (m, 5H, OH-6), 4.52-4.50 (m, 2H, H-12′), 4.02-4.00 (m, 1H, H-5^{I}), 3.84-3.18 (m, 33H, H-2, H-3, H-4, H-5, H-6), 3.40-3.38 (m, 1H, H-8′), 3.14-3.12 (m, 2H, H-2′), 3.08-3.06 (m, 1H, H-6a′), 2.95-2.94 (m, 1H, H-6b′), 2.48-2.45 (m, 1H, H-3′), 1.81-1.79 (m, 1H, H-4′), 1.65-1.63 (m, 2H, H-5′), 1.29-1.27 (m, 2H, H-7′).

H-9′and C-9′signals are not seen.

^{13}C NMR (150 MHz, DMSO-d_6): δ (ppm): 150.24 (C-2′′), 147.97 (C-10′′*), 143.71 (C-4′′*), 142.67 (C-13′), 138.56 (C-10′), 129.81 (C-5′′), 129.34 (C-6′′), 126.98 (C-7′′), 126.14 (C-14′), 125.80 (C-9′′), 123.75 (C-8′′), 119.07 (C-3′′), 115.79 (C-11′), 101.59 (6 × C-1), 82.42 (6 × C-4), 72.62 (5 × C-5, 6 × C-3, 6 × C-2), 69.58 (C-5^{I}), 61.93 (C-12′), 60.02 (5 × C-6), 59.36 (C-8′), 49.96 (C-6^{I}), 48.62 (C-6′), 47.48 (C-2′), 37.25 (C-3′), 26.98 (C-4′), 23.80 (C-7′), 23.57 (C-5′).

Signals tagged with * can be mutually interchanged.

HRMS (ESI): found 1330.5064. For $C_{58}H_{83}N_5O_{30}$ $[M+H]^+$ calculated 1330.5196.

IR (KBr) 3291, 3105, 2938, 1640, 1413, 1240, 1150, 1076, 1039 cm^{-1}.

$[\alpha]_D^{25}$ = +61.7° (*c* = 0.30, DMSO).

6^I-Deoxy-6^I-(4-(((*R*)-quinolin-4-yl(5-vinylquinuclidin-2-yl)methoxy) methyl)-1*H*-1,2,3-triazol-1-yl)-α-CD (19b)

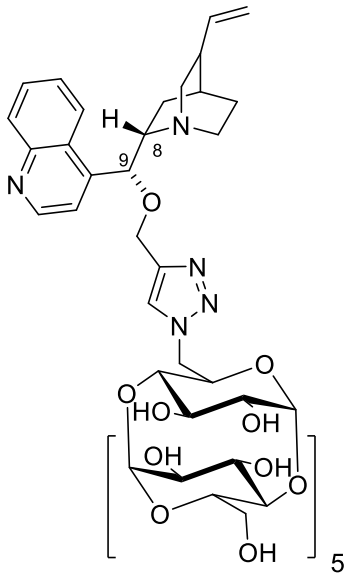

19b

Compound **19b** was prepared according to the general procedure (**GP1**). From 6^I-azido-6^I-deoxy-α-CD **2a** (100 mg, 0.10 mmol), 9-*O*-propargyl-cinchonidine **18b** (43 mg, 0.13 mmol) and copper-iodide (4 mg, 0.02 mmol), 115 mg od product **19b** was obtained in the form of a white-yellow solid (86% yield). TLC (ACN/H_2O/conc.aq.NH_3 10/5/1): R_F = 0.45.

^{1}H NMR (600 MHz, DMSO-d_6): δ (ppm): 8.96-8.94 (m, 1H, H-2′′), 8.43-8.40 (m, 1H, H-8′′), 8.27-8.24 (s, 2H, H-14′), 8.12-8.09 (m, 1H, H-5′′), 7.85-7.81 (m, 1H, H-6′′), 7.73-7.69 (m, 1H, H-7′′), 7.69 -7.64 (m, 1H, H-3′′), 5.80-5.76 (m, 1H, H-10′), 5.67-5.34 (m, 12H, OH-2, OH-3), 5.04-5.00 (m, 1H, H-11a′), 5.01-4.99 (m, 1H, H-1^I), 4.95-4.93 (m, 1H, H-1b′), 4.84-4.73 (m, 5H, H-1), 4.81-4.79 (m, 1H, H-$6a^I$), 4.61-4.59 (m, 1H, H-$6b^I$), 4.58-4.50 (m, 5H, OH-6), 4.55-4.52 (m, 1H, H-12a′), 4.50-4.47 (m, 1H, H-12b′), 4.10-4.08 (m, 1H, H-5^I), 3.88-3.16 (m, 33H, H-2, H-3, H-4, H-5, H-6), 3.59-3.56 (m, 2H, H-6′), 3.51-3.48 (m, 1H, H-8′), 3.32-3.29 (m, 1H, H-2a′), 2.92-2.89 (m, 1H, H-2b′), 2.51-2.49 (m, 1H, H-3′), 1.89-1.85 (m, 1H, H-4′), 1.27-1.23 (m, 2H, H-5′), 1.24-1.21 (m, 2H, H-7′).

H-9′and C-9′signals are not seen.

^{13}C NMR (150 MHz, DMSO-d_6): δ (ppm): 150.19 (C-2′′), 147.99 (C-10′′*), 143.56 (C-4′′*), 142.85 (C-13′), 139.69 (C-10′), 129.77 (C-5′′), 129.39 (C-6′′), 127.14 (C-7′′), 125.94 (C-14′), 125.75 (C-9′′), 123.87 (C-8′′), 119.11 (C-3′′), 115.70 (C-11′), 101.30 (6 × C-1), 82.57 (6 × C-4), 72.35 (6 × C-2, 6 × C-3, 5 × C-5), 69.41 (C-5^I), 62.03 (C-12′), 60.14 (5 × C-6), 59.32 (C-8′), 53.92 (C-2′), 50.25 (C-6^I), 42.69 (C-6′), 37.45 (C-3′), 30.64 (C-7′), 26.62 (C-4′), 22.59 (C-5′).

Signals tagged with * can be mutually interchanged.

HRMS (ESI): found 1330.5151. For $C_{58}H_{83}N_5O_{30}$ $[M+H]^+$ calculated 1330.5196.

IR (KBr) 3288, 3166, 3105, 2926, 2361, 1156, 1120, 1075, 1036 cm^{-1}.

$[\alpha]_D^{25}$ = +25.8° (*c* = 0.33, DMSO).

6^{I}-Deoxy-6^{I}-((4-(((*S*)-(6-methoxyquinolin-4-yl)(5-vinylquinuclidin-2-yl)methoxy)methyl)-1*H*-1,2,3-triazol-1-yl)-α-CD (19c)

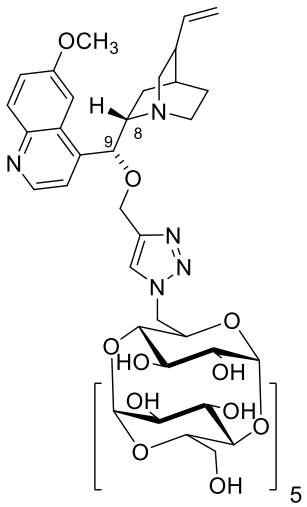

19c

Compound **19c** was prepared according to the general procedure (**GP1**). From 6^{I}-azido-6^{I}-deoxy-α-CD **2a** (316 mg, 0.3 mmol), 9-*O*-propargyl-quinine **18c** (149 mg, 0.4 mmol) and copper-iodide (12 mg, 0.06 mmol), 306 mg of product **19c** was obtained in the form of a white-yellow solid (72% yield). TLC (ACN/H_2O/conc.aq.NH_3 10/5/1): R_F = 0.45.

^{1}H NMR (600 MHz, DMSO-d_6): δ (ppm): 8.76-8.75 (m, 1H, H-2´´), 8.21 (s, 1H, H-14´), 7.98-7.96 (m, 1H, H-8´´), 7.87-7.86 (m, 1H, H-3´´), 7.56-7.55 (m, 1H, H-5´´), 7.44-7.42 (m, 1H, H-7´´), 5.82-5.76 (m, 1H, H-10´), 5.65-5.36 (m, 12H, OH-2, OH-3), 5.01-4.99 (m, 1H, H-11a´), 4.94-4.92 (m, 1H, H-11b´), 4.82-4.73 (m, 5H, H-1), 4.80-4.79 (m, 2H, H-6^{I}), 4.58-4.44 (m, 5H, OH-6), 4.52-4.50 (m, 1H, H-12a´), 4.47-4.45 (m, 1H, H-12b´), 4.05-4.04 (m, 1H, H-5^{I}), 3.95 (s, 3H, OC*H*$_3$-6´´), 3.84-3.13 (m, 33H, H-2, H-3, H-4, H-5, H-6), 3.33-3.31 (m, 1H, 8´´), 3.24-3.22 (m, 1H, H-5^{I}), 3.13-3.12 (m, 2H, H-2´), 2.75-2.73 (m, 2H, H-6´), 2.38-2.36 (m, 1H, H-3´), 1.80-1.78 (m, 1H, H-4´), 1.69-1.65 (m, 1H, H-5a´), 1.55-1.52 (m, 1H, H-5b´), 1.53-1.51 (m, 2H, H-7´).

H-9´and C-9´signals are not seen.

^{13}C NMR (152 MHz, DMSO-d_6): δ (ppm): 157.41 (C-6´´), 147.50 (C-2´´), 147.20 (C-4´´*), 144.01 (C-10´´*), 143.12 (C-13´), 140.79 (C-10´), 131.26 (C-8´´), 127.09 (C-9´´), 126.07 (C-14´), 121.53 (C-7´´), 119.07 (C-3´´), 114.96 (C-11´), 102.33 (C-5´´), 101.90 (6 × C-1), 83.16 (C-4^{I}), 82.66 (5 × C-4), 72.22 (6 × C-2, 6 × C-3, 5 × C-5), 69.52 (C-5^{I}), 61.93 (C-12´), 60.18 (5 × C-6), 59.38 (C-8´), 55.97 (O*C*H$_3$-6´´), 54.59 (C-2´), 50.12 (C-6^{I}), 42.39 (C-6´), 38.18 (C-3´), 26.79 (C-4´), 25.74 (C-5´), 23.18 (C-7´).

Signals tagged with * can be mutually interchanged.

HRMS (ESI): found 1360.5155. For $C_{59}H_{85}N_5O_{31}$ calculated $[M+H]^+$ 1360.5301.

IR (KBr) 3282, 2920, 1625, 1512, 1431, 1242, 1153, 1078, 1039 cm^{-1}.

$[\alpha]_D^{25}$ = +57.4° (*c* = 0.31, DMSO).

6^{I}-Deoxy-6^{I}-((4-(((*R*)-(6-methoxyquinolin-4-yl)(5-vinylquinuclidin-2-yl)methoxy)methyl)-1*H*-1,2,3-triazol-1-yl)-α-CD (19d)

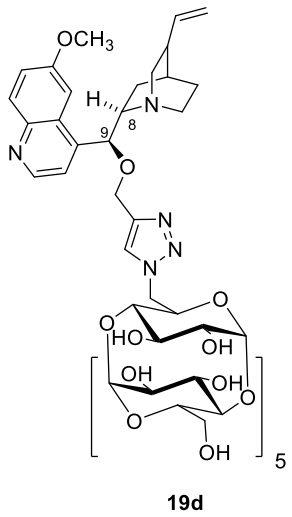

19d

Compound **19d** was prepared according to the general procedure (**GP1**). From 6^{I}-azido-6^{I}-deoxy-α-CD **2a** (174 mg, 0.17 mmol), 9-*O*-propargyl-quinidine **18d** (82 mg, 0.23 mmol) and copper-iodide (6 mg, 0.03 mmol), 176 mg of product **19d** was obtained in the form of a white-yellow solid (74% yield). TLC (ACN/H_2O/conc.aq.NH_3 10/5/1): R_F = 0.45.

^{1}H NMR (600 MHz, DMSO-d_6): δ (ppm): 8.80-8.79 (m, 1H, H-2′′), 8.16-8.14 (m, 1H, H-14′), 8.00-7.99 (m, 1H, H-8′′), 7.60-7.56 (m, 1H, H-3′′), 7.57-7.55 (m, 1H, H-5′′), 7.48-7.45 (m, 1H, H-7′′), 5.88-5.81 (m, 1H, H-10′), 5.67-5.42 (m, 12H, OH-2, OH-3), 5.07-5.01 (m, 1H, H-1^{I}), 5.05-5.03 (m, 1H, H-11a′), 5.02-5.00 (m, 1H, H-11b′), 4.97-4.74 (m, 5H, H-1), 4.82-4.80 (m, 1H, H-6a^{I}), 4.76-4.74 (m, 1H, H-6b^{I}), 4.64-4.50 (m, 5H, OH-6), 4.55-4.53 (m, 2H, H-12′), 3.99 (s, 3H, OC*H*$_3$-6′′), 3.98-3.95 (m, 1H, H-5^{I}), 3.86-3.18 (m, 33H, H-2, H-3, H-4, H-5, H-6), 3.69-3.67 (m, 1H, H-2a′), 3.49-3.47 (m, 1H, H-8′), 3.44-3.42 (m, 1H, H-9′), 3.28-3.26 (m, 1H, H-2b′), 3.23-3.21 (m, 1H, H-6a′), 3.07-3.05 (m, 1H, H-6b′), 2.53-2.51 (m, 1H, H-3′), 1.85-1.82 (m, 1H, H-4′), 1.71-1.69 (m, 2H, H-7′), 1.23-1.21 (m, 2H, H-5′).

^{13}C NMR (150 MHz, DMSO-d_6): δ (ppm): 157.73 (C-6′′), 147.57 (C-2′′), 144.05 (C-10′′*), 142.69 (C-13′), 141.43 (C-4′′*), 138.06 (C-10′), 131.34 (C-8′′), 126.64 (C-9′′), 126.13 (C-14′), 121.88 (C-7′′), 118.80 (C-3′′), 116.02 (C-11′), 101.89 (6 × C-1), 101.20 (C-5′′), 82.21 (6 × C-4), 73.10 (C-9′), 72.06 (6 × C-2, 6 × C-3, 5 × C-5), 69.66 (C-5^{I}), 62.02 (C-12′), 60.20 (5 × C-6), 58.81 (C-8′), 56.28 (O*C*H$_3$-6′′), 49.98 (C-6^{I}), 48.43 (C-6′), 47.25 (C-2′), 36.75 (C-3′), 28.98 (C-5′), 26.87 (C-4′), 23.12 (C-7′).

Signals tagged with * can be mutually interchanged.

HRMS (ESI): found 1360.5182. For $C_{59}H_{85}N_5O_{31}$ calculated $[M+H]^+$ 1360.5301.

IR (KBr) 3381, 3330, 2995, 1625, 1515, 1365, 1245, 1156, 1054 cm^{-1}.

$[\alpha]_D^{25}$ = +60.0° (*c* = 0.30, DMSO).

6^{I}-Deoxy-6^{I}-((4-(((*S*)-quinolin-4-yl(5-vinylquinuclidin-2-yl)methoxy)methyl)-1*H*-1,2,3-triazol-1-yl)-β-CD (20a)

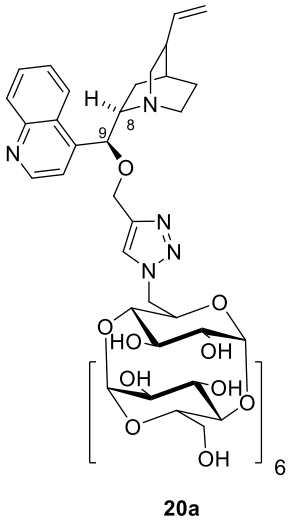

20a

Compound **20a** was prepared according to the general procedure (**GP1**). From 6^{I}-azido-6^{I}-deoxy-β-CD **2b** (100 mg, 0.09 mmol) and 9-*O*-propargyl-cinchonine **18a** (37 mg, 0.11 mmol) and copper-iodide (3 mg, 0.02 mmol), 114 mg of product **20a** was obtained in the form of a white-yellow solid (89% yield). TLC (ACN/H_2O/conc.aq.NH_3 10/5/1): R_F = 0.39.

^{1}H NMR (600 MHz, DMSO-d$_6$): δ (ppm): 8.93-8.90 (m, 1H, H-2′′), 8.34-8.31 (m, 1H, H-8′′), 8.08-8.07 (m, 1H, H-5′′), 8.03-8.01 (m, 1H, H-14′), 7.82-7.76 (m, 1H, H-6′′), 7. 67-7.65 (m, 1H, H-7′′), 7.60-7.58 (m, 1H, H-3′′), 5.96-5.93 (m, 1H, H-10′), 5.85-5.64 (m, 14H, OH-2, OH-3), 5.05-4.91 (m, 7H, H-1), 5.03-5.01 (m, 2H, H-11′), 4.85-4.83 (m, 1H, H-6a^{I}), 4.64-4.62 (m, 1H, H-6b^{I}), 4.63-4.51 (m, 6H, OH-6), 4.46-4.44 (m, 1H, H-12a′), 4.38-4.36 (m, 1H, H-12b′), 3.98-3.96 (m, 1H, H-5^{I}), 3.79-3.24 (m, 39H, H-2, H-3, H-4, H-5, H-6), 3.17-3.15 (m, 1H, H-8′), 3.10-3.08 (m, 1H, H-2a′), 2.74-2.72 (m, 1H, H-2b′), 2.60-2.58 (m, 1H, H-6a′), 2.24-2.22 (m, 1H, H-3′), 1.83-1.81 (m, 1H, H-7a′), 1.69-1.67 (m, 1H, H-4′), 1.49-1.47 (m, 2H, H-5′), 1.48-1.46 (m, 1H, H-6b′), 1.43-1.41 (m, 1H, H-7b′).

H-9′signal is not seen.

^{13}C NMR (DMSO-d$_6$): δ (ppm): 150.13 (C-2′′), 147.93 (C-10′′*), 146.21 (C-4′′*), 143.20 (C-13′), 140.29 (C-10′), 129.75 (C-5′′), 129.50 (C-9′′), 129.06 (C-6′′), 126.54 (C-7′′), 125.40 (C-14′), 123.94 (C-8′′), 119.70 (C-3′′), 114.84 (C-11′), 101.94 (7 × C-1), 81.60 (7 × C-4), 80.60 (C-9′), 72.22 (7 × C-2, 7 × C-3, 6 × C-5), 69.83 (C-5^{I}), 61.71 (C-12′), 60.10 (6 × C-6), 60.05 (C-8′), 50.11 (C-6^{I}), 47.85 (C-2′), 39.50 (C-3′), 27.39 (C-4′), 25.41 (C-5′), 48.89 (C-6′), 25.41 (C-7′).

Signals tagged with * can be mutually interchanged.

HRMS (ESI): found 1492.5610. For $C_{64}H_{93}N_5O_{35}$ calculated $[M+H]^+$ 1492.5724.

IR (KBr) 3348, 3105, 2929, 1646, 1422, 1156, 1105, 1081, 1033 cm^{-1}.

$[\alpha]_D^{25}$ = + 75.0° (*c* = 0.30, DMSO).

6^I-Deoxy-6^I-((4-(((*R*)-quinolin-4-yl(5-vinylquinuclidin-2-yl)methoxy)methyl)-1*H*-1,2,3-triazol-1-yl)-β-CD (20b)

Compound **20b** was prepared according to the general procedure (**GP1**). From 6^I-azido-6^I-deoxy-β-CD **2b** (100 mg, 0.09 mmol), 9-*O*-propargyl-cinchonidine **18b** (37 mg, 0.11 mmol) and copper-iodide (3 mg, 0.02 mmol), 90 mg of product was obtained in the form of a white-yellow solid (70% yield). TLC (ACN/H_2O/conc.aq.NH_3 10/5/1): R_F = 0.39.

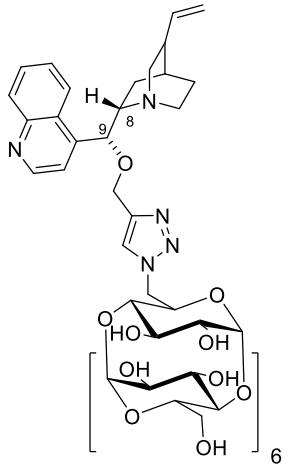

20b

^{1}H NMR (600 MHz, DMSO-d_6): δ (ppm): 8.93-8.91 (m, 1H, H-2′′), 8.39-8.37 (m, 1H, H-8′′), 8.09-8.07 (m, 1H, H-5′′), 8.08-8.07 (m, 1H, H-14′), 7.80-7.78 (m, 1H, H-6′′), 7.66-7.64 (m, 1H, H-7′′), 7.61-7.59 (m, 1H, H-3′′), 5.81-5.79 (m, 1H, H-10′), 5.79-5.64 (m, 14H, OH-2, OH-3), 5.08-5.07 (m, 1H, H-1^I), 5.00-4.98 (m, 1H, H-11a′), 4.93-4.91 (m, 1H, H-11b′), 4.87-4.85 (m, 1H, H-$6a^I$), 4.85-4.81 (m, 6H, H-1), 4.63-4.49 (m, 6H, OH-6), 4.61-4.58 (m, 1H, H-$6b^I$), 4.45-4.43 (m, 2H, H-12′), 3.99-3.97 (m, 1H, H-5^I), 3.78-3.26 (m, 39H, H-2, H-3, H-4, H-5, H-6), 3.31-3.29 (m, 1H, H-6a′), 3.27-3.25 (m, 1H, H-8′), 3.00-2.98 (m, 1H, H-2a′), 2.61-2.59 (m, 1H, H-6b′), 2.60-2.58 (m, 1H, H-2b′), 2.32-2.30 (m, 1H, H-3′), 1.77-1.75 (m, 1H, H-4′), 1.69-1.67 (m, 1H, H-5a′), 1.51-1.49 (m, 1H, H-5b′), 1.64-1.61 (m, 2H, H-7′).

H-9′and C-9′ signals are not seen.

^{13}C NMR (150 MHz, DMSO-d_6): δ (ppm): 150.13 (C-2′′), 147.97 (C-10′′), 145.50 (C-4′′), 143.14 (C-13′), 141.24 (C-10′), 129.75 (C-5′′), 129.17 (C-6′), 126.73 (C-7′′), 126.24 (C-9′′), 125.40 (C-14′), 123.94 (C-8′′), 119.46 (C-3′′), 114.76 (C-11′), 101.83 (7 × C-1), 81.75 (7 × C-4), 72.46 (7 × C-2, 7 × C-3, 6 × C-5), 69.81 (C-5^I), 61.86 (C-12′), 60.10 (6 × C-6), 59.05 (C-8′), 55.14 (C-2′), 50.20 (C-6^I), 42.13 (C-6′), 38.61 (C-3′), 26.20 (C-5′), 26.97 (C-4′), 22.96 (C-7′).

Signals tagged with * can be mutually interchanged.

HRMS (ESI): found 1492.5604. For $C_{64}H_{93}N_5O_{35}$ calculated $[M+H]^+$ 1492.5724.

IR (KBr) 3297, 2932, 1661, 1637, 1509, 1461, 1362, 1335, 1030 cm^{-1}.

$[\alpha]_D^{25}$ = +48.3° (*c* = 0.30, DMSO).

6^{I}-Deoxy-6^{I}-((4-(((*S*)-(6-methoxyquinolin-4-yl)(5-vinylquinuclidin-2-yl)methoxy)methyl)-1*H*-1,2,3-triazol-1-yl)-β-CD (20c)

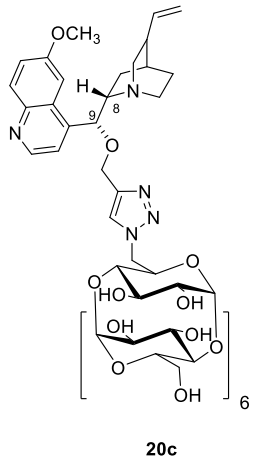

20c

Compound **20c** was prepared according to the general procedure (**GP1**). From 6^{I}-azido-6^{I}-deoxy-β-CD **2b** (100 mg, 0.09 mmol), 9-*O*-propargyl-quinine **18c** (41 mg, 0.11 mmol) and copper-iodide (3 mg, 0.02 mmol), 105 mg of product was obtained in the form of a white-yellow solid (80% yield). TLC (ACN/H_2O/conc.aq.NH_3 10/5/1): R_F = 0.43.

^{1}H NMR (600 MHz, DMSO-d_6): δ (ppm): 8.78-8.76 (m, 1H, H-2′′), 8.21-8.19 (m, 1H, H-14′), 7.99-7.97 (m, 1H, H-8′′), 7.66-7.64 (m, 1H, H-5′′), 7.59-7.57 (m, 1H, H-3′′), 7.46-7.44 (m, 1H, H-7′′), 5.84-5.71 (m, 14H, OH-2, OH-3), 5.82-5.80 (m, 1H, H-10′), 5.07-5.05 (m, 1H, H-11a′), 5.04-4.95 (m, 7H, H-1), 4.94-4.92 (m, 1H, H-11b′), 4.95-4.93 (m, 1H, H-6a^{I}), 4.64-4.50 (m, 6H, OH-6), 4.59-4.57 (m, 1H, H-6b^{I}), 4.50-4.48 (m, 2H, H-12′), 4.10-4.08 (m, 1H, H-5^{I}), 3.97 (s, 3H, OC*H*$_3$-6′′), 3.78-3.16 (m, 39H, H-2, H-3, H-4, H-5, H-6), 3.07-3.05 (m, 1H, H-8′), 3.75-3.73 (m, 2H, H-2′), 2.54-2.52 (m, 2H, H-6′), 2.42-2.40 (m, 1H, H-3′), 1.85-1.83 (m, 1H, H-4′), 1.77-1.75 (m, 1H, H-5a′), 1.59-1.57 (m, 1H, H-5b′), 1.30-1.28 (m, 2H, H-7′).

H-9′and C-9′ signals are not seen.

^{13}C NMR (150 MHz, DMSO-d_6): δ (ppm): 157.58 (C-6′′), 147.44 (C-2′′), 144.01 (C-10′′*), 144.01 (C-4′′*), 143.11 (C-13′), 140.31 (C-10′), 131.17 (C-8′′), 127.09 (C-9′′), 125.34 (C-14′), 121.67 (C-7′′), 118.93 (C-3′′), 115.17 (C-11′), 102.16 (C-5′′), 101.50 (7 × C-1), 83.56 (C-4^{I}), 81.70 (6 × C-4), 73.12 (7 × C-2, 7 × C-3, 6 × C-5), 61.95 (C-12′), 69.76 (C-5^{I}), 60.05 (6 × C-6), 59.30 (C-8′), 56.07 (O*C*H$_3$-6′′), 54.39 (C-2′), 50.38 (C-6^{I}), 42.53 (C-6′), 38.15 (C-3′), 26.85 (C-4′), 25.52 (C-5′), 25.15 (C-7′).

Signals tagged with * can be mutually interchanged.

HRMS (ESI): found 1522.5741. For $C_{65}H_{95}N_5O_{36}$ calculated $[M+H]^+$ 1522.5831.

IR (KBr) 3396, 3330, 3073, 2935, 1655, 1622, 1419, 1237, 1030 cm^{-1}.

$[\alpha]_D^{25}$ = + 46.7° (*c* = 0.30, DMSO).

6^{I}-Deoxy-6^{I}-((4-(((*R*)-(6-methoxyquinolin-4-yl)(5-vinylquinuclidin-2-yl)methoxy)methyl)-1*H*-1,2,3-triazol-1-yl)-β-CD (20d)

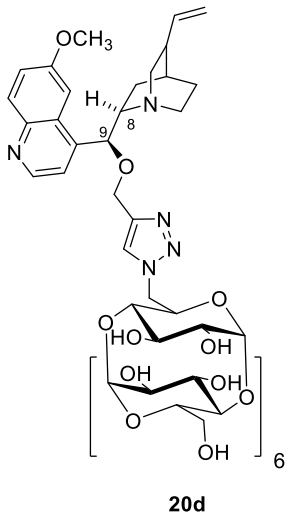

20d

Compound **20d** was prepared according to the general procedure (**GP1**). From 6^{I}-azido-6^{I}-deoxy-β-CD **2b** (100 mg, 0.09 mmol), 9-*O*-propargyl-quinidine **18d** (41 mg, 0.11 mmol) and copper-iodide (3 mg, 0.02 mmol), 124 mg of product was obtained in the form of a white-yellow solid (95% yield). TLC (ACN/H_2O/conc.aq.NH_3 10/5/1): R_F = 0.43.

^{1}H NMR (600 MHz, DMSO-d_6): δ (ppm): 8.78-8.76 (m, 1H, H-2′′), 8.09-8.05 (m, 1H, H-14′), 8.00-7.98 (m, 1H, H-8′′), 7.58-7.56 (m, 1H, H-5′′), 7.59-7.57 (m, 1H, H-3′′), 7.46-7.44 (m, 1H, H-7′′), 5.93-5.88 (m, 1H, H-10′), 5.86-5.70 (m, 14H, OH-2, OH-3), 5.05-4.75 (m, 7H, H-1), 5.02-5.00 (m, 2H, H-11′), 4.85-4.83 (m, 1H, H-6a^{I}), 4.64-4.50 (m, 6H, OH-6), 4.63-4.60 (m, 1H, H-6b^{I}), 4.49-4.46 (m, 1H, H-12a′), 4.40-4.38 (m, 1H, H-12b′), 3.98-3.95 (m, 1H, H-5^{I}), 3.96 (s, 3H, OC*H*$_3$-6′′), 3.78-3.16 (m, 39H, H-2, H-3, H-4, H-5, H-6), 3.07-3.05 (m, 1H, H-8′), 3.75-3.73 (m, 2H, H-2′), 2.54-2.52 (m, 2H, H-6′), 2.30-2.28 (m, 1H, H-3′), 1.73-1.71 (m, 1H, H-4′), 1.65-1.62 (m, 2H, H-5′), 1.30-1.28 (m, 2H, H-7′).

H-9′and C-9′signals are not seen.

^{13}C NMR (150 MHz, DMSO-d_6): δ (ppm): 157.20 (C-6′′), 147.58 (C-2′′), 144.0 (C-10′′*), 144.00 (C-4′′*), 143.17 (C-13′), 140.29 (C-10′), 131.24 (C-8′′), 127.31 (C-9′′), 125.41 (C-14′), 121.46 (C-7′′), 119.31 (C-3′′), 115.10 (C-11′), 101.50 (7 × C-1), 100.16 (C-5′′), 83.26 (C-4^{I}), 81.70 (6 × C-4), 73.12 (7 × C-2, 7 × C-3, 6 × C-5), 69.77 (C-5^{I}), 61.66 (C-12′), 60.05 (6 × C-6), 59.30 (C-8′), 55.75 (O*C*H$_3$-6′′), 50.17 (C-6^{I}), 48.76 (C-6′), 47.74 (C-2′), 38.15 (C-3′), 27.25 (C-4′), 25.52 (C-5′), 25.15 (C-7′).

Signals tagged with * can be mutually interchanged.

HRMS (ESI): found 1522.5646. For $C_{65}H_{95}N_5O_{36}$ calculated $[M+H]^+$ 1522.5831.

IR (KBr) 3321, 2923, 2881, 1658, 1622, 1350, 1299, 1156, 1030 cm^{-1}.

$[\alpha]_D^{25}$ = +76.7° (*c* = 0.30, DMSO).

General procedure for the preparation of monosubstituted permethylated CD derivatives (GP2)

The first starting material, 9-*O*-propargyl Cinchona alkaloids (**18a–18d**, 0.10 mmol), was dissolved in 0.5 mL of distilled DMF (sonicated for 10 minutes under Ar atmosphere). Second starting material, 6^{I}-azido-6^{I}-deoxy-permethyl-α-CD[131] (**21**, 0.08 mmol) or 6^{I}-azido-6^{I}-deoxy-permethyl-β-CD[132] (**22**, 0.06 mmol), was dissolved in 0.4 mL distilled DMF (sonicated for 10 minutes under Ar atmosphere) and added to the Cinchona alkaloid solution. Copper iodide (0.02 mmol), suspended in 0.1 mL of distilled DMF (sonicated for 10 minutes under Ar atmosphere), was added to the reaction mixture and stirred at 50 °C for 16 hours. The conversion into product was monitored by TLC in eluent $CHCl_3$/MeOH/conc.aq.NH_3 20/1/0.1. After the spot of the starting material **21** or **22** disappeared on TLC, DMF was evaporated on a rotary evaporator at 50 °C and the crude product was purified by column chromatography (50 g of silica gel) with the mobile phase $CHCl_3$/MeOH/conc.aq.NH_3 (25/1/0.1 → 20/1/0.1). When full conversion to the product was not achieved, the starting material was regenerated (eluted as the first compound). A blue precipitate formed at the top of the column as copper cations interacted with ammonia. The purified product was dried at 50 °C under reduced pressure.

6^{I}-Deoxy-6^{I}-(4-(((*S*)-quinolin-4-yl(5-vinylquinuclidin-2-yl)methoxy) methyl)-1*H*-1,2,3-triazol-1-yl)-permethyl-α-CD (23a)

Compound **23a** was prepared according to the general procedure (**GP2**). From 6^{I}-azido-6^{I}-deoxy-permethyl-α-CD **21** (100 mg, 0.08 mmol), 9-*O*-propargyl-cinchonine **18a** (35 mg, 0.10 mmol) and copper-iodide (3 mg, 0.02 mmol), 75 mg of product was obtained in the form of a white-yellow solid (59% yield). TLC ($CHCl_3$/MeOH/conc.aq.NH_3 20/1/0.1): R_F = 0.40.

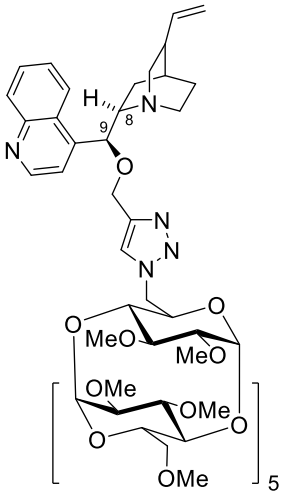

23a

^{1}H NMR (600 MHz, CD_3OD): δ (ppm): 8.88-8.87 (m, 1H, H-2′′), 8.29-8.27 (m, 1H, H-8′′), 8.11-8.09 (m, 1H, H-5′′), 7.94 (s, 1H, H-14′), 7.83-7.80 (m, 1H, H-6′′), 7.72-7.69 (m, 1H, H-3′′), 7.71-7.68 (m, 1H, H-7′′), 6.03-5.97 (m, 1H, H-10′), 5.33-5.32 (m, 1H, H-1^{I}), 5.07-5.01 (m, 5H, H-1), 5.04-5.00 (m, 2H, H-11′), 4.93-4.90 (m, 2H, H-6^{I}), 4.58 (*b*s, 2H, H-12′), 4.21-4.18 (m, 1H, H-5^{I}), 4.12-3.89 (m, 5H, H-5), 3.91-3.79 (m, 10H, H-6), 3.66-3.62 (m, 18H, OC<u>*H*</u>$_3$-3), 3.57-3.55 (m, 1H, H-9′), 3.55-3.49 (m, 18H, OC<u>*H*</u>$_3$-2), 3.61-3.49 (m, 12H, H-3, H-4), 3.37-3.35 (m, 1H, H-2a′), 3.32-3.25 (m, 15H, OC<u>*H*</u>$_3$-6), 3.21-3.23 (m, 1H, H-8′), 3.19-3.10 (m, 6H, H-2), 2.89-2.86 (m, 1H, H-6a′), 2.88-2.82 (m, 1H, H-2b′), 2.77-2.73 (m, 1H, H-6b′), 2.32-2.29 (m, 1H, H-3′), 2.09-2.06 (m, 1H, H-7a′), 1.73-1.72 (m, 1H, H-4′), 1.60-1.51 (m, 2H, H-5′), 1.32-1.28 (m, 1H, H-7b′).

^{13}C NMR (150 MHz, CD_3OD): δ (ppm): 150.98 (C-2′′), 149.19 (C-10′′*), 147.89 (C-4′′*), 144.95 (C-13′), 141.46 (C-10′), 130.98 (C-6′′), 130.31 (C-5′′), 128.43 (C-7′′), 127.89 (C-9′′), 127.48 (C-14′), 124.59 (C-8′′), 120.73 (C-3′′), 115.52 (C-11′), 100.19 (6 × C-1), 83.07 (6 × C-2, 6 × C-3, 6 × C-4), 81.03 (C-9′), 72.83 (5 × C-5, 5 × C-6), 71.66 (C-5^{I}), 63.50 (C-12′), 62.05 (6 × O$\underline{C}H_3$-3), 61.35 (C-8′), 59.39 (5 × O$\underline{C}H_3$-6), 58.64 (6 × O$\underline{C}H_3$-2), 52.41 (C-6^{I}), 50.81 (C-6′), 50.09 (C-2′), 40.94 (C-3′), 29.43 (C-4′), 26.95 (C-5′), 23.11 (C-7′).

Signals tagged with * can be mutually interchanged.

HRMS (ESI): found 1568.7713. For $C_{75}H_{117}N_5O_{30}$ $[M+H]^+$ calculated 1568.7856.

IR (KBr) 2926, 2830, 1715, 1512, 1461, 1365, 1196, 1168, 1036 cm^{-1}.

$[\alpha]_D^{25}$ = +139.0° (*c* = 0.30, MeOH).

6^{I}-Deoxy-6^{I}-(4-(((*R*)-quinolin-4-yl(5-vinylquinuclidin-2-yl)methoxy) methyl)-1*H*-1,2,3-triazol-1-yl)-permethyl-α-CD (23b)

Compound **23b** was prepared according to the general procedure (**GP2**). From 6^{I}-azido-6^{I}-deoxy-permethyl-α-CD **21** (100 mg, 0.08 mmol), 9-*O*-propargyl-cinchonidine **18b** (35 mg, 0.10 mmol) and copper-iodide (3 mg, 0.02 mmol), 61 mg of product was obtained in the form of a white-yellow solid (48% yield). TLC ($CHCl_3$/MeOH/conc.aq.NH_3 20/1/0.1): R_F = 0.40.

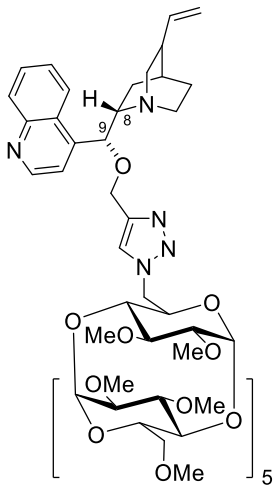

23b

^{1}H NMR (600 MHz, CD_3OD): δ (ppm): 8.87-8.85 (m, 1H, H-2′′), 8.33-8.29 (m, 1H, H-8′′), 8.11-8.08 (m, 1H, H-5′′), 7.97 (s, 1H, H-14′), 7.82-7.80 (m, 1H, H-6′′), 7.73-7.70 (m, 1H, H-3′′), 7.70-7.68 (m, 1H, H-7′′), 5.80-5.75 (m, 1H, H-10′), 5.32-5.31 (m, 1H, H-1^{I}), 5.07-4.97 (m, 5H, H-1), 4.97-4.95 (m, 1H, H-6a^{I}), 4.93-4.90 (m, 2H, H-11′), 4.89-4.86 (m, 1H, H-6b^{I}), 4.58 (*b*s, 2H, H-12′), 4.18-4.16 (m, 1H, H-5^{I}), 4.02-3.96 (m, 5H, H-5), 3.98-3.85 (m, 10H, H-6), 3.65-3.59 (m, 18H, OC$\underline{H}_3$-3), 3.60-3.56 (m, 12H, H-3, H-4), 3.58-3.47 (m, 18H, OC$\underline{H}_3$-2), 3.41-3.40 (m, 1H, H-6a′), 3.36-3.27 (m, 15H, OC$\underline{H}_3$-6), 3.22-3.19 (m, 1H, H-8′), 3.07-3.05 (m, 1H, H-2a′), 3.10-2.99 (m, 6H, H-2), 2.66-2.64 (m, 1H, H-6b′), 2.59-2.56 (m, 1H, H-2b′), 2.35-2.33 (m, 1H, H-3′), 1.79-1.76 (m, 1H, H-4′), 1.67-1.62 (m, 1H, H-5a′), 1.60-1.54 (m, 1H, H-5b′), 1.37-1.33 (m, 1H, H-7a′), 1.28-1.24 (m, 1H, H-7b′).

H-9′signal is not seen.

^{13}C NMR (150 MHz, CD_3OD): δ (ppm): 151.00 (C-2′′), 149.21 (C-10′′*), 148.07 (C-4′′*), 145.07 (C-13′), 142.53 (C-10′), 131.00 (C-6′′), 130.33 (C-5′′), 128.46 (C-7′′), 127.93 (C-9′′), 127.43 (C-14′), 124.65 (C-8′′), 120.54 (C-3′′), 115.11 (C-11′), 100.27 (6 × C-1), 83.04 (6 × C-4, 6 × C-3, 6 × C-2), 81.30 (C-9′), 72.50 (5 × C-5, 5 × C-6), 71.69 (C-5^{I}), 63.50 (C-12′), 62.03 (6 × O$\underline{C}H_3$-3), 59.57 (5 ×

O<u>C</u>H$_3$-6), 58.90(6 × O<u>C</u>H$_3$-2), 61.73 (C-8′), 57.46 (C-2′), 52.45 (C-6^I), 43.88 (C-6′), 40.81 (C-3′), 29.02 (C-4′), 28.25 (C-5′), 23.48 (C-7′).

Signals tagged with * can be mutually interchanged.

HRMS (ESI): found 1568.7708. For $C_{75}H_{117}N_5O_{30}$ calculated $[M+H]^+$ 1568.7856.

IR (KBr) 2920, 2839, 1595, 1455, 1359, 1165, 1111, 1069, 1039 cm^{-1}.

$[\alpha]_D^{25}$ = +75.0° (*c* = 0.30, MeOH).

6^I-Deoxy-6^I-(4-(((*R*)-1-(6-methoxyquinolin-4-yl(5-vinylquinuclidin-2-yl)methoxy) methyl)-1*H*-1,2,3-triazol-1-yl)-permethyl-α-CD (23c)

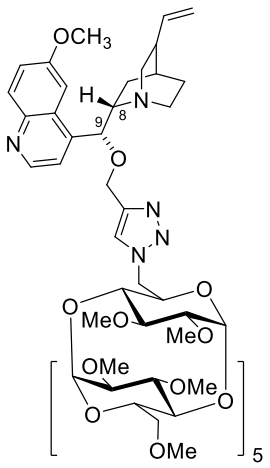

23c

Compound **23c** was prepared according to the general procedure (**GP2**). From 6^I-azido-6^I-deoxy-permethyl-α-CD **21** (100 mg, 0.08 mmol), 9-*O*-propargyl-quinine **18c** (38 mg, 0.10 mmol) and copper-iodide (4 mg, 0.02 mmol), 63 mg of product was obtained in the form of a white-yellow solid (49% yield). TLC ($CHCl_3$/MeOH/conc.aq.NH_3 20/1/0.1): R_F = 0.40.

^{1}H NMR (600 MHz, CD_3OD): δ (ppm): 8.71-8.70 (m, 1H, H-2′′), 7.99-7.98 (m, 1H, H-8′′), 7.98 (s, 1H, H-14′), 7.69-7.67 (m, 1H, H-3′′), 7.53-7.50 (m, 1H, H-5′′), 7.48-7.45 (m, 1H, H-7′′), 5.81-5.74 (m, 1H, H-10′), 5.34-5.28 (m, 1H, H-1^I), 5.00-4.88 (m, 5H, H-1), 4.97-4.92 (m, 2H, H-11′), 4.93-4.91 (m, 2H, H-6^I), 4.59 (s, 2H, H-12′), 4.19-4.16 (m, 1H, H-5^I), 3.99 (s, 3H, OC<u>*H*$_3$</u>-6′′), 3.92-3.81 (m, 5H, H-5) 3.82-3.25 (m, 10H, H-6), 3.67-3.60 (m, 18H, OC<u>*H*$_3$</u>-3), 3.63-3.61 (m, 1H, H-8′), 3.55-3.53 (m, 1H, H-9′), 3.52-3.45 (m, 18H, OC<u>*H*$_3$</u>-2), 3.61-3.41 (m, 12H, H-3, H-4), 3.37-3.25 (m, 15H, OC<u>*H*$_3$</u>-6), 3.21-3.12 (m, 6H, H-2), 3.08-3.05 (m, 1H, H-2a′), 2.69-2.66 (m, 2H, H-6′), 2.61-2.59 (m, 1H, H-2b′), 2.38-2.33 (m, 1H, H-3′), 1.80-1.79 (m, 1H, H-4′), 1.77-1.75 (m, 1H, H-5a′), 1.58-1.56 (m, 1H, H-5b′), 1.33-1.28 (m, 2H, H-7′).

^{13}C NMR (150 MHz, CD_3OD): δ (ppm): 159.90 (C-6′′), 148.22 (C-2′′), 146.39 (C-10′′*), 145.18 (C-4′′*), 145.12 (C-13′), 142.60 (C-10′), 131.65 (C-8′′), 128.98 (C-9′′), 127.42 (C-14′), 123.63 (C-7′′), 120.40 (C-3′′), 102.55 (C-5′′), 100.26 (6 × C-1), 83.10 (6 × C-2, 6 × C-3, 6 × C-4), 79.47 (C-9′), 72.42 (6 × C-5, 6 × C-6), 63.40 (C-12′), 62.07 (6 × O<u>C</u>H$_3$-3), 61.16 (C-8′), 59.29 (6 × O<u>C</u>H$_3$-2), 58.99 (5 × O<u>C</u>H$_3$-6), 57.50 (C-2′), 56.56 (O<u>C</u>H$_3$-6′′), 52.44 (C-6^I), 44.08 (C-6′), 40.84 (C-3′), 29.07 (C-4′), 28.32 (C-5′), 22.51 (C-7′).

Signals tagged with * can be mutually interchanged.

HRMS (ESI): found 1568.7849. For $C_{76}H_{119}N_5O_{31}$ $[M+H]^+$ calculated 1598.7962.

IR (KBr) 2926, 2836, 1622, 1506, 1476, 1365, 1228, 1141, 1036 cm^{-1}.

$[\alpha]_D^{25}$ = +92.4° (*c* = 0.21, MeOH).

6^I-Deoxy-6^I-(4-(((*S*)-1-(6-methoxyquinolin-4-yl(5-vinylquinuclidin-2-yl)methoxy) methyl)-1*H*-1,2,3-triazol-1-yl)-permethyl-α-CD (23d)

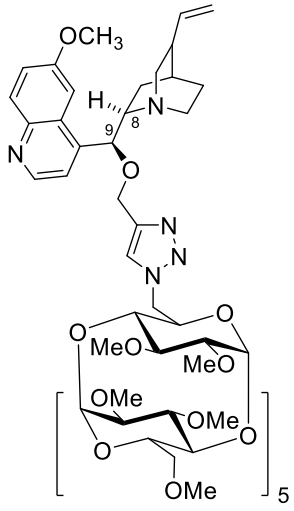

23d

Compound **23d** was prepared according to the general procedure (**GP2**). From 6^I-azido-6^I-deoxy-permethyl-α-CD **21** (100 mg, 0.08 mmol), 9-*O*-propargyl-quinidine **18d** (38 mg, 0.10 mmol) and copper-iodide (4 mg, 0.02 mmol), 54 mg of product was obtained in the form of a white-yellow solid (42% yield). TLC ($CHCl_3$/MeOH/conc.aq.NH_3 20/1/0.1): R_F = 0.40.

^{1}H NMR (600 MHz, CD_3OD): δ (ppm): 8.71-8.70 (m, 1H, H-2′′), 7.99-7.98 (m, 1H, H-8′′), 7.96 (s, 1H, H-14′), 7.66-7.65 (m, 1H, H-3′′), 7.51-7.50 (m, 1H, H-5′′), 7.46-7.44 (m, 1H, H-7′′), 6.00-5.97 (m, 1H, H-10′), 5.33-5.32 (m, 1H, H-1^I), 5.08-5.00 (m, 5H, H-1), 5.05-5.03 (m, 2H, H-11′), 4.92-4.91 (m, 2H, H-6^I), 4.60-4.58 (m, 1H, H-9′), 4.55 (s, 2H, H-12′), 4.20-4.16 (m, 1H, H-5^I), 3.99 (s, 3H, OC$\underline{H}_3$-6′′), 3.91-3.81 (m, 4H, H-5), 3.91-3.61 (m, 10H, H-6), 3.69-3.63 (m, 18H, OC$\underline{H}_3$-3), 3.65-3.21 (m, 12H, H-3, H-4), 3.49-3.41 (m, 18H, OC$\underline{H}_3$-2), 3.34-3.32 (m, 1H, H-2a′), 3.25-3.31 (m, 15H, OC$\underline{H}_3$-6), 3.12-3.10 (m, 1H, H-8′), 3.21-3.05 (m, 6H, H-2), 2.88-2.85 (m, 1H, H-2b′), 2.87-2.85 (m, 1H, H-6a′), 2.79-2.74 (m, 1H, H-6b′), 2.31-2.28 (m, 1H, H-3′), 2.11-2.08 (m, 1H, H-7a′), 1.72-1.70 (m, 1H, H-4′), 1.60-1.53 (m, 2H, H-5′), 1.32-1.24 (m, 1H, H-7b′).

^{13}C NMR (150 MHz, CD_3OD): δ (ppm): 159.82 (C-6′′), 148.22 (C-2′′), 146.37 (C-10′′*), 145.15 (C-4′′*), 145.05 (C-13′), 141.64 (C-10′), 131.60 (C-8′′), 128.92 (C-9′′), 127.46 (C-14′), 123.59 (C-7′′), 120.54 (C-3′′), 115.42 (C-11′), 102.59 (C-5′′), 100.27 (6 × C-1), 83.08 (6 × C-2, 6 × C-3, 6 × C-4), 81.33 (C-9′), 72.33 (5 × C-5, 5 × C-6), 71.67 (C-5^I), 63.44 (C-12′), 61.11 (6 × O$\underline{C}$H$_3$-3), 60.88 (C-8′), 59.80 (6 × O$\underline{C}$H$_3$-2), 58.52 (5 × O$\underline{C}$H$_3$-6), 56.45 (O$\underline{C}$H$_3$-6′′), 52.41 (C-6^I), 50.85 (C-6′), 50.24 (C-2′), 41.06 (C-3′), 29.50 (C-4′), 27.07 (C-5′), 22.66 (C-7′).

Signals tagged with * can be mutually interchanged.

HRMS (ESI): found 1598.7962. For $C_{76}H_{119}N_5O_{31}$ $[M+H]^+$ calculated 1598.7859.

IR (KBr) 2929, 2839, 1622, 1512, 1456, 1368, 1257, 1144, 1039 cm^{-1}.

$[\alpha]_D^{25}$ = +154.8° (*c* = 0.20, MeOH).

6^{I}-Deoxy-6^{I}-(4-(((*S*)-quinolin-4-yl(5-vinylquinuclidin-2-yl)methoxy) methyl)-1*H*-1,2,3-triazol-1-yl)-permethyl-β-CD (24a)

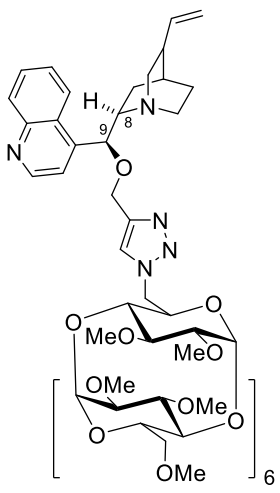

24a

Compound **24a** was prepared according to the general procedure (**GP2**). From 6^{I}-azido-6^{I}-deoxy-permethyl-β-CD **22** (100 mg, 0.07 mmol), 9-*O*-propargylcinchonine **18a** (29 mg, 0.09 mmol) and copper-iodide (3 mg, 0.01 mmol), 38 mg of product was obtained in the form of a white-yellow solid (64% yield). TLC ($CHCl_3$/MeOH/conc.aq.NH_3 20/1/0.1): R_F = 0.38.

^{1}H NMR (600 MHz, CD_3OD): δ (ppm): 8.90-8.89 (m, 1H, H-2′′), 8.32-8.29 (m, 1H, H-8′′), 8.12-8.10 (m, 1H, H-5′′), 7.94 (s, 1H, H-14′), 7.84-7.81 (m, 1H, H-6′′), 7.72-7.69 (m, 1H, H-3′′), 7.71-7.68 (m, 1H, H-7′′), 6.05-5.99 (m, 1H, H-10′), 5.55-5.21 (m, 7H, H-1), 5.04-5.01 (m, 1H, H-6a^{I}), 5.04-5.03 (m, 2H, H-11′), 4.80-4.79 (m, 1H, H-6b^{I}), 4.57 (s, 2H, H-12′), 4.09-4.07 (m, 1H, H-5^{I}), 3.88-3.50 (m, 18H, H-5, H-6), 3.65-3.41 (m, 14H, H-3, H-4), 3.65-3.59 (m, 21H, OC$\underline{H}_3$-3), 3.52-3.43 (m, 21H, OC$\underline{H}_3$-2), 3.36-3.25 (m, 18H, OC$\underline{H}_3$-6), 3.28-3.26 (m, 1H, H-2a′), 3.18-3.16 (m, 1H, H-8′), 3.19-3.10 (m, 7H, H-2), 2.86-2.84 (m, 1H, H-2b′), 2.84-2.81 (m, 1H, H-6a′), 2.74-2.73 (m, 1H, H-6b′), 2.33-2.29 (m, 1H, H-3′), 2.10-2.07 (m, 1H, H-7a′), 1.73-1.72 (m, 1H, H-4′), 1.58-1.54 (m, 2H, H-5′), 1.31-1.28 (m, 1H, H-7b′).

H-9′signal is not seen.

^{13}C NMR (150 MHz, CD_3OD): δ (ppm): 150.99 (C-2′′), 149.18 (C-10′′*), 148.04 (C-4′′*), 144.98 (C-13′), 141.59 (C-10′), 130.96 (C-6′′), 130.29 (C-5′′), 128.41 (C-7′′), 127.91 (C-9′′), 127.46 (C-14′), 124.62 (C-8′′), 120.81 (C-3′′), 115.45 (C-11′), 99.67 (7 × C-1), 83.65 (7 × C-4, 7 × C-2), 81.67 (C-9′), 81.03 (7 × C-3), 72.87 (6 × C-5, 6 × C-6), 71.81 (C-5^{I}), 63.45 (C-12′), 62.14 (7 × O$\underline{C}$H$_3$-3), 61.38 (C-8′), 59.72 (6 × O$\underline{C}$H$_3$-6, 7 × O$\underline{C}$H$_3$-2), 52.33 (C-6^{I}), 50.81 (C-6′), 50.10 (C-2′), 41.07 (C-3′), 29.45 (C-4′), 27.07 (C-5′), 23.34 (C-7′).

Signals tagged with * can be mutually interchanged.

HRMS (ESI): found 1772.8706. For $C_{84}H_{133}N_5O_{35}$ $[M+H]^+$ calculated 1772.8716.

IR (KBr) 2923, 2833, 1679, 1458, 1368, 1195, 1162, 1108, 1033 cm^{-1}.

$[\alpha]_D^{25}$= +152.9° (*c* = 0.43, MeOH).

6^{I}-Deoxy-6^{I}-(4-(((*R*)-quinolin-4-yl(5-vinylquinuclidin-2-yl)methoxy) methyl)-1*H*-1,2,3-triazol-1-yl)-permethyl-β-CD (24b)

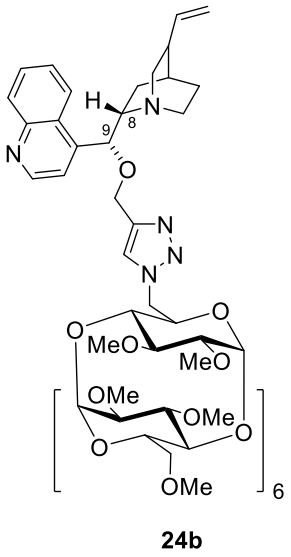

24b

Compound **24b** was prepared according to the general procedure (**GP2**). From 6^{I}-azido-6^{I}-deoxy-permethyl-β-CD **22** (100 mg, 0.07 mmol), 9-*O*-propargylcinchonidine **18b** (29 mg, 0.09 mmol) and copper-iodide (3 mg, 0.01 mmol), 85 mg of product was obtained in the form of a white-yellow solid (69% yield). TLC ($CHCl_3$/MeOH/conc.aq.NH_3 20/1/0.1): R_F = 0.38.

^{1}H NMR (600 MHz, CD_3OD): δ (ppm): 8.88-8.86 (m, 1H, H-2′′), 8.33-8.31 (m, 1H, H-8′′), 8.12-8.10 (m, 1H, H-5′′), 7.97 (s, 1H, H-14′), 7.83-7.80 (m, 1H, H-6′′), 7.73-7.71 (m, 1H, H-3′′), 7.71-7.69 (m, 1H, H-7′′), 5.80-5.75 (m, 1H, H-10′), 5.37-5.36 (m, 1H, H-1^{I}), 5.27-5.13 (m, 6H, H-1), 5.12-5.10 (m, 1H, H-6a^{I}), 4.98-4.96 (m, 1H, H-11a′), 4.93-4.91 (m, 1H, H-11b′), 4.78-4.74 (m, 1H, H-6b^{I}), 4.58 (s, 2H, H-12′), 4.09-4.06 (m, 1H, H-5^{I}), 3.90-3.72 (m, 18H, H-5, H-6), 3.68-3.60 (m, 21H, OC$\underline{H}_3$-3), 3.59-3.40 (m, 13H, H-3, H-4), 3.52-3.45 (m, 21H, OC$\underline{H}_3$-2), 3.44-3.42 (m, 1H, H-6b′), 3.39-3.36 (m, 1H, H-4^{I}), 3.39-3.24 (m, 18H, OC$\underline{H}_3$-6), 3.22-3.20 (m, 1H, H-8′), 3.20-3.07 (m, 7H, H-2), 3.07-3.05 (m, 1H, H-2a′), 2.71-2.67 (m, 1H, H-6a′), 2.61-2.58 (m, 1H, H-2b′), 2.36-2.33 (m, 1H, H-3′), 1.82-1.77 (m, 1H, H-4′), 1.80-1.77 (m, 1H, H-5a′), 1.60-1.59 (m, 1H, H-5b′), 1.32-1.29 (m, 2H, H-7′).

H-9′ and C-9′ signals are not seen.

^{13}C NMR (150 MHz, CD_3OD): δ (ppm): 151.00 (C-2′′), 149.22 (C-10′′*), 147.92 (C-4′′*), 145.08 (C-13′), 142.43 (C-10′), 131.00 (C-6′′), 130.35 (C-5′′), 128.48 (C-7′′), 127.90 (C-9′′), 127.38 (C-14′), 124.63 (C-8′′), 120.67 (C-3′′), 115.19 (C-11′), 99.38 (7 × C-1), 83.21 (7 × C-2, 7 × C-4), 80.37 (7 × C-3), 72.57 (6 × C-5, 6 × C-6), 71.85 (C-5^{I}), 63.52 (C-12′), 61.88 (7 × O$\underline{C}$H$_3$-3), 61.71 (C-8′), 59.25 (6 × O$\underline{C}$H$_3$-6, 7 × O$\underline{C}$H$_3$-2), 57.43 (C-2′), 52.38 (C-6^{I}), 43.91 (C-6′), 40.81 (C-3′), 29.02 (C-4′), 28.22 (C-5′), 23.46 (C-7′).

Signals tagged with * can be mutually interchanged.

HRMS (ESI): found 1772.8671. For $C_{84}H_{133}N_5O_{35}$ $[M+H]^+$ calculated 1772.8716.

IR (KBr) 2944, 2836, 1679, 1455, 1329, 1201, 1159, 1105, 1033 cm^{-1}.

$[\alpha]_D^{25}$= +96.9° (*c* = 0.18, MeOH).

6^I-Deoxy-6^I-(4-(((*R*)-1-(6-methoxyquinolin-4-yl(5-vinylquinuclidin-2-yl)methoxy) methyl)-1*H*-1,2,3-triazol-1-yl)-permethyl-β-CD (24c)

Compound **24c** was prepared according to the general procedure (**GP2**). From 6^I-azido-6^I-deoxy-permethyl-β-CD **22** (100 mg, 0.07 mmol), 9-*O*-propargyl-quinine **18c** (32 mg, 0.09 mmol) and copper-iodide (3 mg, 0.01 mmol), 60 mg of product was obtained in the form of a white-yellow solid (48% yield). TLC ($CHCl_3$/MeOH/conc.aq.NH_3 20/1/0.1): R_F = 0.38.

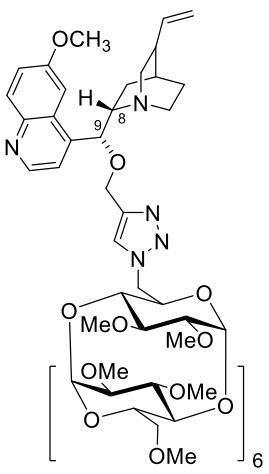

24c

^{1}H NMR (600 MHz, CD_3OD): δ (ppm): 8.72-8.71 (m, 1H, H-2′′), 8.01 (s, 1H, H-14′), 8.00-7.99 (m, 1H, H-8′′), 7.70-7.68 (m, 1H, H-3′′), 7.56-7.54 (m, 1H, H-5′′), 7.48-7.46 (m, 1H, H-7′′), 5.82-5.78 (m, 1H, H-10′), 5.38-5.36 (m, 1H, H-1^I), 5.28-5.10 (m, 6H, H-1), 5.12-5.10 (m, 1H, H-$6a^I$), 5.00-4.99 (m, 1H, H-11a′), 4.97-4.94 (m, 1H, H-11b′), 4.84-4.80 (m, 1H, H-$6b^I$), 4.65-4.60 (m, 2H, H-12′), 4.10-4.07 (m, 1H, H-5^I), 4.02 (s, 3H, OC$\underline{H}_3$-6′′), 4.01-3.21 (m, 18H, H-5, H-6), 3.65-3.58 (m, 21H, OC$\underline{H}_3$-3), 3.55-3.45 (m, 21H, OC$\underline{H}_3$-2), 3.35-3.25 (m, 18H, OC$\underline{H}_3$-6), 3.64-3.62 (m, 1H, H-8′), 3.18-3.16 (m, 1H, H-2a′), 3.65-3.25 (m, 14H, H-3, H-4), 3.25-3.07 (m, 7H, H-2), 2.82-2.80 (m, 2H, H-6′), 2.73-2.70 (m, 1H, H-2b′), 2.43-2.40 (m, 1H, H-3′), 1.86-1.85 (m, 1H, H-4′), 1.83-1.80 (m, 1H, H-5a′), 1.67-1.60 (m, 1H, H-5b′), 1.39-1.24 (m, 2H, H-7′).

H-9′signal is not seen.

^{13}C NMR (150 MHz, CD_3OD): δ (ppm): 160.00 (C-6′′), 148.23 (C-2′′), 145.86 (C-10′′*), 145.20 (C-4′′*), 144.98 (C-13′), 142.08 (C-10′), 131.66 (C-8′′), 128.89 (C-9′′), 127.45 (C-14′), 123.75 (C-7′′), 120.30 (C-3′′), 115.40 (C-11′), 102.52 (C-5′′), 99.38 (7 × C-1), 83.69 (7 × C-2, 7 × C-3, 7 × C-4), 80.05 (C-9′), 72.62 (6 × C-5, 6 × C-6), 71.89 (C-5^I), 63.37 (C-12′), 61.84 (7 × O$\underline{C}$H$_3$-3), 61.14 (C-8′), 59.10 (7 × O$\underline{C}$H$_3$-2, 7 × O$\underline{C}$H$_3$-6), 57.20 (C-2′), 56.77 (O$\underline{C}$H$_3$-6′′), 52.38 (C-6^I), 44.31 (C-6′), 40.49 (C-3′), 28.97 (C-4′), 27.90 (C-5′), 23.11 (C-7′).

Signals tagged with * can be mutually interchanged.

HRMS (ESI): found 1802.8819. For $C_{85}H_{135}N_5O_{36}$ calculated $[M+H]^+$ 1802.8960.

IR (KBr) 2932, 2830, 1715, 1626, 1512, 1467, 1365, 1144, 1036 cm^{-1}.

$[\alpha]_D$= +105.9° (*c* = 0.25, MeOH).

6^I-Deoxy-6^I-(4-(((*S*)-1-(6-methoxyquinolin-4-yl(5-vinylquinuclidin-2-yl)methoxy) methyl)-1*H*-1,2,3-triazol-1-yl)-permethyl-β-CD (24d)

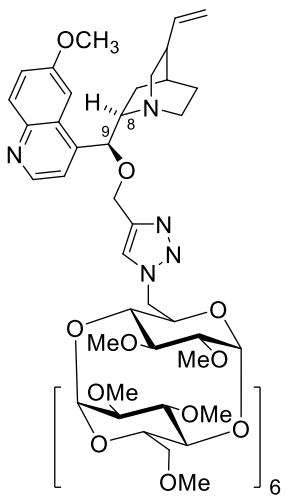

24d

Compound **24d** was prepared according to the general procedure (**GP2**). From 6^I-azido-6^I-deoxy-permethyl-β-CD **22** (100 mg, 0.07 mmol), 9-*O*-propargylquinidine **18d** (32 mg, 0.09 mmol) and copper-iodide (3 mg, 0.01 mmol), 78 mg of product was obtained in the form of a white-yellow solid (63% yield). TLC $CHCl_3$/MeOH/conc.aq.NH_3 20/1/0.1): R_F = 0.38.

^{1}H NMR (600 MHz, CD_3OD): δ (ppm): 8.74-8.72 (m, 1H, H-2′′), 8.00-7.99 (m, 1H, H-8′′), 7.97 (s, 1H, H-14′), 7.69-7.66 (m, 1H, H-3′′), 7.54-7.50 (m, 1H, H-5′′), 7.49-7.46 (m, 1H, H-7′′), 6.03-5.97 (m, 1H, H-10′), 5.39-5.37 (m, 1H, H-1^I), 5.25-5.10 (m, 6H, H-1), 5.06-5.04 (m, 1H, H-$6a^I$), 5.03-5.01 (m, 2H, H-11′), 4.85-4.83 (m, 1H, H-$6b^I$), 4.59 (s, 2H, H-12′), 4.15-4.11 (m, 1H, H-5^I), 3.99 (s, 3H, OC*H*$_3$-6′′), 3.90-3.35 (m, 18H, H-5, H-6), 3.67-3.53 (m, 21H, OC*H*$_3$-3), 3.58-3.48 (m, 21H, OC*H*$_3$-2), 3.62-3.45 (m, 14H, H-3, H-4), 3.45-3.27 (m, 18H, OC*H*$_3$-6), 3.23-3.05 (m, 7H, H-2), 3.13-3.11 (m, 1H, H-8′), 2.89-2.87 (m, 2H, H-6′), 2.86-2.84 (m, 1H, H-2a′), 2.77-2.75 (m, 1H, H-2b′), 2.34-2.31 (m, 1H, H-3′), 2.16-2.12 (m, 1H, H-7a′), 1.74-1.72 (m, 1H, H-4′), 1.62-1.54 (m, 2H, H-5′), 1.35-1.27 (m, 1H, H-7b′).

H-9′signal is not seen.

^{13}C NMR (150 MHz, CD_3OD): δ (ppm): 159.82 (C-6′′), 148.44 (C-2′′), 146.45 (C-10′′*), 145.14 (C-4′′*), 145.06 (C-13′), 141.69 (C-10′), 131.59 (C-8′′), 128.94 (C-9′′), 127.42 (C-14′), 123.61 (C-7′′), 120.66 (C-3′′), 115.39 (C-11′), 102.56 (C-5′′), 99.39 (7 × C-1), 81.52 (C-9′), 83. 47 (7 × C-2, 7 × C-3, 7 × C-4), 72.51 (6 × C-5, 6 × C-6), 71.80 (C-5^I), 63.41 (C-12′), 61.91 (7 × O*C*H$_3$-3), 60.89 (C-8′), 59.25 (7 × O*C*H$_3$-2, 6 × O*C*H$_3$-6), 56.46 (O*C*H$_3$-6′′), 52.33 (C-6^I), 50.85 (C-2′), 50.26 (C-6′), 41.12 (C-3′), 29.50 (C-4′), 27.12 (C-5′), 23.67 (C-7′).

Signals tagged with * can be mutually interchanged.

HRMS (ESI): found 1802.8839. For $C_{85}H_{135}N_5O_{36}$ $[M+H]^+$ calculated 1802.8960.

IR (KBr) 2929, 2836, 1619, 1461, 1365, 1228, 1135, 1072, 1042 cm^{-1}.

$[\alpha]_D^{25}$= +146.9° (*c* = 0.48, MeOH).

$6^A,6^D$-Dideoxy-$6^A,6^D$-Bis((4-(((*S*)-(6-methoxyquinolin-4-yl)(5-vinylquinuclidin-2-yl)methoxy)methyl)-1*H*-1,2,3-triazol-1-yl)-α-CD (27)

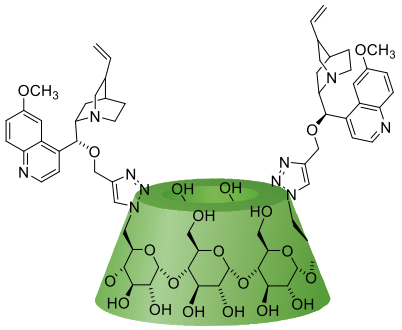

27

The starting material $6^{A,D}$-diazido-$6^{A,D}$-dideoxy-α-CD (25 mg, 0.025 mmol, **7**), prepared according to a combination of previously published procedures[38,43,23], was dissolved in 0.2 mL of distilled H_2O (sonicated for 10 minutes under Ar atmosphere). 9-*O*-propargyl-quinine **18c** (12 mg, 0.03 mmol) was dissolved in 0.2 mL of distilled THF (sonicated for 10 minutes under Ar atmosphere) and added to the CD derivative. Copper iodide (0.013 mmol), suspended in 0.1 mL of distilled H_2O (sonicated for 10 minutes under Ar atmosphere), was added to the reaction mixture and stirred at 50 °C for 16 hours. Conversion into the product was monitored by TLC in ACN/H_2O/conc.aq.NH_3 (10/5/1). After full conversion into the product, the reaction mixture was slowly added to acetone (75 mL) under stirring, resulting in a white-yellow precipitate. This solid was recovered by filtration, washed with acetone (3 × 20 mL) and dried to constant weight in a vacuum drying box in the presence of P_2O_5 and KOH. The crude product was purified by column chromatography (50 g of silica gel) with the mobile phase ACN/H_2O/NH_3 12/5/1. A blue precipitate formed at the top of the column as copper cations interacted with ammonia ions. The purified product was dried at 50 °C under reduced pressure. It was isolated 33 mg of a white-yellow product **27** (76% yield). TLC (ACN/H_2O/conc.aq.NH_3 (10/5/1): R_F = 0.60.

^{1}H NMR (600 MHz, DMSO-d_6): δ (ppm): 8.75-8.73 (m, 2H, H-2′′), 8.22 (s, 2H, H-14′), 7.94-7.95 (m, 2H, H-8′′), 7.83-7.81 (m, 2H, H-3′′), 7.65-7.63 (m, 2H, H-5′′), 7.43-7.41 (m, 2H, H-7′′), 5.78-5.76 (m, 2H, H-10′), 5.62-5.36 (m, 12H, OH-2, OH-3), 5.01-4.99 (m, 2H, H-11a′), 4.94-4.92 (m, 2H, H-11b′), 4.87-4.85 (m, 2H, H-$6a^{I,IV}$), 4.80-4.72 (m, 6H, H-1), 4.78-4.76 (m, 2H, H-$6b^{I,IV}$), 4.58-4.44 (m, 4H, OH-6), 4.52-4.50 (m, 2H, H-12a′), 4.40-4.38 (m, 2H, H-12b′), 4.00-3.98 (m, 2H, H-$5^{I,IV}$), 3.95 (s, 6H, OC$\underline{H}_3$-6′′), 3.88-3.21 (m, 33H, H-2, H-3, H-4, H-5, H-6), 3.38-3.39 (m, 2H, 8′′), 2.44-2.42 (m, 2H, H-3′), 1.80-1.78 (m, 2H, H-4′).

H-2′, H-6′, H-5′, H-7′, H-9′, C-5′, C-7′, C-9′signals are not fully seen.

^{13}C NMR (150 MHz, DMSO-d_6): δ (ppm): 157.56 (2 × C-6′′), 147.44 (2 × C-2′′), 144.20 (2 × C-4′′*), 144.02 (2 × C-10′′*), 142.94 (2 × C-13′), 140.35 (2 × C-10′), 131.21 (2 × C-8′′), 126.95 (2 × C-9′′), 125.50 (2 × C-14′), 121.76 (2 × C-7′′), 118.77 (2 × C-3′′), 115.22 (2 × C-11′), 102.18 (2 × C-5′′), 101.90 (6 × C-1), 83.06 (6 × C-4), 71.52 (6 × C-2, 6 × C-3, 4 × C-5), 69.07 (2 × C-$5^{I,IV}$), 61.93 (2 × C-12′), 61.58 (4 × C-6), 59.02 (2 × C-8′), 56.18 (2 × O$\underline{C}$H$_3$-6′′), 54.10 (2 × C-2′), 50.46 (2 × C-$6^{I,IV}$), 42.65 (2 × C-6′), 37.79 (2 × C-3′), 26.73 (2 × C-4′).

Signals tagged with * can be mutually interchanged.

HRMS (ESI): found 874.3652. For $C_{82}H_{110}N_{10}O_{32}$ calculated $[M+2H]^{2+}$ 874.3717.

IR (KBr) 3183, 3120, 2935, 1710, 1650, 1401, 1258, 1111, 1048 cm^{-1}.

$[\alpha]_D^{25}$= +40.7° (c = 0.17, DMSO).

6.6. Synthesis of substrates for the organocatalytic reactions

Methyl 2-(hydroxy(phenyl)methyl)acrylate (28)

Compound **28** was prepared according to a previously published procedure.[166] ^1H NMR and MS spectra are in accordance with the literature.

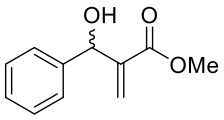

28

^1H NMR (400 MHz, $CDCl_3$): δ (ppm): 7.40-7.30 (m, 5H), 6.35 (t, *J* = 1.6 Hz, 1H), 5.88 (t, *J* = 2.4 Hz, 1H), 5.56 (s, 1H), 3.71 (s, 3H), 3.36 (*b*s, 1H).

MS (ESI): found 192.1. For $C_{11}H_{12}O_3$ calculated $[M+Na]^+$ 192.1.

Methyl 2-(hydroxy(4-nitrophenyl)methyl)acrylate (29)

Compound **29** was prepared according to a previously published procedure.[166] ^1H NMR and MS spectra are in accordance with the literature.

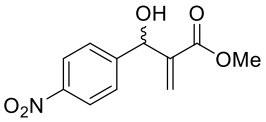

29

^1H NMR (400 MHz, $CDCl_3$): δ (ppm): 8.18-8.16 (m, 2H), 7.56-7.54 (m, 2H), 6.38 (s, 1H), 5.88 (d, *J* = 0.8 Hz, 1H), 5.62 (s, 1H), 3.73 (s, 3H), 3.33 (*b*s, 1H).

MS (ESI): found 237.1. For $C_{11}H_{11}NO_5$ calculated $[M+Na]^+$ 237.1.

4-Hydroxy-4-(4-nitrophenyl)butan-2-one (30)

Compound **30** was prepared according to a previously published procedure.[167] ^1H NMR and MS spectra are in accordance with the literature.[168,169]

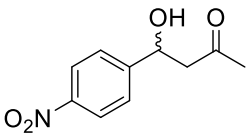

30

^1H NMR (400 MHz, $CDCl_3$): δ (ppm): 8.17-8.15 (m, 2H), 7.53-7.51 (m, 2H), 5.27 (t, *J* = 6.0 Hz, 1H), 3.69 (*b*s, 1H), 2.87 (d, *J* = 6.0 Hz, 1H), 2.23 (s, 3H).

MS (ESI): found 209.1. For $C_{10}H_{11}NO_4$ calculated $[M+Na]^+$ 209.1.

Dimethyl 2-(2-nitro-1-phenylethyl)malonate (31)

Compound **31** was prepared according to a previously published procedure.[170] ^1H NMR and MS spectra are in accordance with this literature.

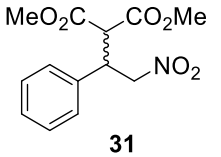

31

^1H NMR (400 MHz, $CDCl_3$): δ (ppm): 7.30-7.25 (m, 5H), 4.90-4.87 (m, 2H), 4.23-

4.21 (m, H), 3.86 (d, *J* = 6.9 Hz, 1H), 3.73 (s, 3H), 3.53 (s, 3H).

MS (ESI): found 281.2. For $C_{13}H_{15}NO_6$ calculated $[M+Na]^+$ 281.2.

Methyl 2-(phenyl((phenylcarbamoyl)oxy)methyl)acrylate (32)

Compound **32** was prepared according to a previously published procedure.[137] ^{1}H NMR and MS spectra are in accordance with this literature.

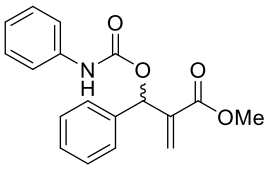

32

^{1}H NMR (400 MHz, $CDCl_3$): δ (ppm): 7.46 – 7.24 (m, 9H), 7.06 (t, J = 7.4 Hz, 1H), 6.80 (s, 1H), 6.71 (s, 1H), 6.44 (s, 1H), 5.91 (s, 1H), 3.72 (s, 3H).

MS (ESI): found: 334.1. For $C_{18}H_{17}NO_4$ calculated $[M+Na]^+$ 334.1.

Methyl (*R*)-2-(phenyl(phenylamino)methyl)acrylate (33)

Compound **32** was prepared according to a previously published procedure from MBH carbamate **32**.[137] ^{1}H NMR and MS spectra are in accordance with this reference.[171]

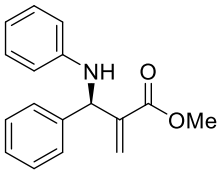

33

^{1}H NMR (400 MHz, $CDCl_3$): δ (ppm): 7.41 – 7.27 (m, 5H), 7.22 – 7.10 (m, 2H), 6.77 (t, *J* = 7.3 Hz, H), 6.64 (d, *J* = 7.8 Hz, 2H), 6.41 (s, 1H), 6.03 (s, 1H), 5.43 (s, 1H), 4.17 (*b*s, 1H) 3.71 (s, 3H).

MS (ESI): found 290.1. For $C_{17}H_{17}NO_2$ calculated $[M+Na]^+$ 290.1.

6.7. General procedures for organocatalytic reactions

General procedure for the MBH reaction

The starting material, aromatic or aliphatic aldehydes were dissolved in DMF, MeOH or buffer/MeOH (phosphate buffer (pH=7.1, 0.05M or pH=8.0, 0.05M). Corresponding acrylates (methyl-acrylate or hexafluoroisopropyl-acrylate) and Cinchona-CD derivatives (**19b, 20b**, **23c** or **24b**) were added to the mixture and stirred at 25 °C for 168 hours. Conversion into the product was monitored by TLC in hexane/EtOAc (6:1) and by ^{1}H NMR.

General procedure for the aldol reaction

The starting material, *p*-NO_2-benzaldehyde were dissolved in acetone (5 eq.) and Cinchona-CD derivatives (1 eq., **20c** or **23a**) were dissolved in H_2O/acetone (5 eq.) and added to the mixture and stirred at 25 °C for 168 hours. Conversion into the product was monitored by TLC in hexane/EtOAc (5:1). The reaction mixture was evaporated and crude product was purified by column chromatography (hexane/EtOAc 5:4). NMR and MS spectra of racemic products are in accordance

with the literature.[167] The enantiomeric excess was measured on IA column (heptane/propan-2-ol 90:10, λ = 235 nm, flow = 0.5 mL/min, t = 25 °C). Retention times of the products: t_R = 30.0-31.0 min.

General procedure for the Michael addition

The starting materials, *trans*-NO_2-styrene and dimethyl-malonate were dissolved in EtOH. Cinchona-CD derivative (**23b**) were added to the mixture and stirred at 25 °C for 168 hours. Conversion into the product was monitored by TLC in hexane/EtOAc (1:1). The reaction mixture was evaporated and crude product was purified by column chromatography (hexane/EtOAc 3:1). NMR and MS spectra of the racemic product are in accordance with the literature.[170] The enantiomeric excess was measured on OD-H column (heptane/propan-2-ol 70:30, λ = 230 nm, flow = 0.9 mL/min, t = 25 °C). Retention times of the products: t_R = 11.6 min (major enantiomer), t_R = 13.7 min (minor enantiomer).

General procedure for the AAA reaction

The starting material, MBH carbamate **32** was dissolved in ACN/H_2O (for CD catalysts **19a–19d, 20a–20d** and **27**) or toluene (for CD catalysts **23a–23d, 24a–24d**) to achieve 0.4 M solution. Cinchona-CD derivatives (**19a–19d, 20a–20d**, **27, 23a–23d, 24a–24d**) were added to the mixture and stirred at 40 °C for 168 hours. Conversion into the product was monitored by TLC in hexane/EtOAc (6:1). The reaction mixture was evaporated and crude product was purified by column chromatography (hexane/EtOAc 10:1). NMR and MS spectra of product **33** are in accordance with the literature[137]. The enantiomeric excess was measured on IB column (heptane/propan-2-ol 99:1, λ = 205 nm, flow = 1.0 mL/min, t = 25 °C). Retention times of the products: t_R = 9.0 – 10.5 min (major enantiomer), t_R = 9.5 – 11.2 min (minor enantiomer).

7. REFERENCES

(1) Crini, G. *Chem. Rev.* **2014**, *114* (21), 10940–10975.
(2) Hapiot, F.; Menuel, S.; Ferreira, M.; Léger, B.; Bricout, H.; Tilloy, S.; Monflier, E. *ACS Sustain. Chem. Eng.* **2017**, *5* (5), 3598–3606.
(3) Bogliotti, N.; Dalko, P. I. Shape- and Site-Selective Asymmetric Reactions. In *Enantioselective organocatalysis: reactions and experimental procedures*; Dalko, P. I., Ed.; Wiley-VCH: Weinheim, 2007.
(4) Hapiot, F.; Tilloy, S.; Monflier, E. *Chem. Rev.* **2006**, *106* (3), 767–781.
(5) Szejtli, J. *Chem. Rev.* **1998**, *98* (5), 1743–1754.
(6) Horikoshi, K.; Nakamura, N.; Matsuzawa, N.; Yamamoto, M. Industrial Production of Cyclodextrins. In *Proceedings of the First International Symposium on Cyclodextrins*; Szejtli, J., Ed.; Springer Netherlands: Dordrecht, 1982; pp 25–39.
(7) Biwer, A.; Antranikian, G.; Heinzle, E. *Appl. Microbiol. Biotechnol.* **2002**, *59* (6), 609–617.
(8) Gould, S.; Scott, R. C. *Food Chem. Toxicol.* **2005**, *43* (10), 1451–1459.
(9) Hedges, A. R. *Chem. Rev.* **1998**, *98* (5), 2035–2044.
(10) Loftsson, T.; Duchene, D. *Int. J. Pharm.* **2007**, *329* (1–2), 1–11.
(11) Keating, G. M. *Drugs* **2016**, *76* (10), 1041–1052.
(12) Schneider, H.-J.; Hacket, F.; Rüdiger, V.; Ikeda, H. *Chem. Rev.* **1998**, *98* (5), 1755–1786.
(13) Kfoury, M.; Landy, D.; Fourmentin, S. *Molecules* **2018**, *23* (5), 1204.
(14) Tomimasu, N.; Kanaya, A.; Takashima, Y.; Yamaguchi, H.; Harada, A. *J. Am. Chem. Soc.* **2009**, *131* (34), 12339–12343.
(15) Řezanka, M. *Eur. J. Org. Chem.* **2016**, *2016* (32), 5322–5334.
(16) Davis, M. E.; Brewster, M. E. *Nat. Rev. Drug Discov.* **2004**, *3*, 1023.
(17) Khan, A. R.; Forgo, P.; Stine, K. J.; D'Souza, V. T. *Chem Rev* **1998**, *98* (5), 1977–1996.
(18) Jindřich; Tišlerová, I. *J. Org. Chem.* **2005**, *70* (22), 9054–9055.
(19) Tang, W.; Ng, S.-C. *Nat. Protoc.* **2008**, *3* (4), 691–697.
(20) Popr, M.; Hybelbauerová, S.; Jindřich, J. *Beilstein J. Org. Chem.* **2014**, *10*, 1390–1396.
(21) Faugeras, P.-A.; Boëns, B.; Elchinger, P.-H.; Brouillette, F.; Montplaisir, D.; Zerrouki, R.; Lucas, R. *Eur. J. Org. Chem.* **2012**, *2012* (22), 4087–4105.
(22) Meldal, M.; Tornøe, C. W. *Chem. Rev.* **2008**, *108* (8), 2952–3015.
(23) Kumprecht, L.; Buděšínský, M.; Vondrášek, J.; Vyměťal, J.; Černý, J.; Císařová, I.; Brynda, J.; Herzig, V.; Koutník, P.; Závada, J.; Kraus, T. *J. Org. Chem.* **2009**, *74* (3), 1082–1092.
(24) Wenz, G. *Angew. Chem. Int. Ed. Engl.* **1994**, *33* (8), 803–822.
(25) Sollogoub, M. *Eur. J. Org. Chem.* **2009**, *2009* (9), 1295–1303.
(26) Engeldinger, E.; Armspach, D.; Matt, D. *Chem. Rev.* **2003**, *103* (11), 4147–4174.
(27) Yuan, D.-Q.; Kitagawa, Y.; Fukudome, M.; Fujita, K. *Org. Lett.* **2007**, *9* (22), 4591–4594.
(28) Tabushi, I.; Nabeshima, T.; Fujita, K.; Matsunaga, A.; Imoto, T. *J. Org. Chem.* **1985**, *50* (15), 2638–2643.
(29) Tabushi, I.; Yamamura, K.; Nabeshima, T. *J. Am. Chem. Soc.* **1984**, *106* (18), 5267–5270.
(30) La Mendola, D.; Mineo, P.; Rizzarelli, E.; Scamporrino, E.; Vecchio, G.; Vitalini, D. *J. Supramol. Chem.* **2001**, *1* (3), 147–151.
(31) Ding, Y.; Vara Prasad, C. V. N. S.; Ding, C.; Wang, B. *Carbohydr. Polym.* **2018**, *181*, 957–963.
(32) Breslow, R.; Doherty, J. B.; Guillot, G.; Lipsey, C. *J. Am. Chem. Soc.* **1978**, *100* (10), 3227–3229.
(33) Breslow, R.; Canary, J. W.; Varney, M.; Waddell, S. T.; Yang, D. *J. Am. Chem. Soc.* **1990**, *112* (13), 5212–5219.
(34) Koga, K.; Yuan, D.-Q.; Fujita, K. *Tetrahedron Lett.* **2000**, *41* (35), 6855–6857.
(35) Tabushi, I.; Shimokawa, K.; Fujita, K. *Tetrahedron Lett.* **1977**, *18* (18), 1527–1530.
(36) Armspach, D.; Matt, D. *Carbohydr. Res.* **1998**, *310* (1–2), 129–133.
(37) Jouffroy, M.; Armspach, D.; Louati, A.; Matt, D.; Toupet, L. *Chem. - Eur. J.* **2014**, *20* (9), 2565–
(38) Pearce, A. J.; Sinaÿ, P. *Angew. Chem.* **2000**, *39* (20), 3610–3612.
(39) Lecourt, T.; Herault, A.; Pearce, A. J.; Sollogoub, M.; Sinaÿ, P. *Chem. - Eur. J.* **2004**, *10* (12), 2960–2971.

(40) Bistri, O.; Sinaÿ, P.; Sollogoub, M.. *Tetrahedron Lett.* **2005**, *46* (45), 7757–7760.
(41) Bistri, O.; Sinaÿ, P.; Sollogoub, M. **2006**, *47* (25), 4137–4139. (42) Bistri, O.; Sinaÿ, P.; Jiménez Barbero, J.; Sollogoub, M. *Chem. - Eur. J.* **2007**, *13* (35), 9757–9774. (43) Guieu, S.; Sollogoub, M. *J. Org. Chem.* **2008**, *73* (7), 2819–2828.
(44) Guieu, S.; Sollogoub, M. *Angew. Chem. Int. Ed.* **2008**, *47* (37), 7060–7063.
(45) Zaborova, E.; Guitet, M.; Prencipe, G.; Blériot, Y.; Ménand, M.; Sollogoub, M. *Angew. Chem. Int. Ed.* **2013**, *52* (2), 639–644.
(46) Ménand, M.; Sollogoub, M.; Boitrel, B.; Le Gac, S. *Chem. - Eur. J.* **2018**, *24* (22), 5804–5812.
(47) Zhu, X.; Xiao, S.; Zhou, D.; Sollogoub, M.; Zhang, Y. *Eur. J. Med. Chem.* **2018**, *146*, 194–205.
(48) Fredy, J. W.; Scelle, J.; Guenet, A.; Morel, E.; Adam de Beaumais, S.; Ménand, M.; Marvaud, V.; Bonnet, C. S.; Tóth, E.; Sollogoub, M.; et al. *Chem. - Eur. J.* **2014**, *20* (35), 10915–10920.
(49) Cutrone, G.; Benkovics, G.; Malanga, M.; Casas-Solvas, J. M.; Fenyvesi, É.; Sortino, S.; García-Fuentes, L.; Vargas-Berenguel, A. *Carbohydr. Polym.* **2018**, *199*, 649–660.
(50) Wang, B.; Zaborova, E.; Guieu, S.; Petrillo, M.; Guitet, M.; Blériot, Y.; Ménand, M.; Zhang, Y.; Sollogoub, M. *Nat. Commun.* **2014**, *5* (1).
(51) Rawal, G. K.; Rani, S.; Ling, C.-C. *Tetrahedron Lett.* **2009**, *50* (32), 4633–4636.
(52) Rawal, G. K.; Rani, S.; Ward, S.; Ling, C.-C. *Org Biomol Chem* **2010**, *8* (1), 171–180. https://doi.org/10.1039/B915450G.
(53) Krejčí, L.; Buděšínský, M.; Císařová, I.; Kraus, T. *Chem. Commun.* **2009**, No. 24, 3557.
(54) Kumprecht, L.; Buděšínský, M.; Bouř, P.; Kraus, T. *New J. Chem.* **2010**, *34* (10), 2254.
(55) Grishina, A.; Stanchev, S.; Kumprecht, L.; Buděšínský, M.; Pojarová, M.; Dušek, M.; Rumlová, M.; Křížová, I.; Rulíšek, L.; Kraus, T. *Chem. - Eur. J.* **2012**, *18* (39), 12292–12304.
(56) Volkov, S.; Kumprecht, L.; Buděšínský, M.; Lepšík, M.; Dušek, M.; Kraus, T. *Org. Biomol. Chem.* **2015**, *13* (10), 2980–2985.
(57) Petrillo, M.; Marinescu, L.; Rousseau, C.; Bols, M. *Org. Lett.* **2009**, *11* (9), 1983–1985. https://doi.org/10.1021/ol900413s.
(58) Petrillo, M.; Marinescu, L.; Bols, M. *J. Incl. Phenom. Macrocycl. Chem.* **2011**, *69* (3–4), 425–431.
(59) McNaught, A. D. *Pure Appl. Chem.* **1996**, *68* (10), 1919–2008.
(60) Guieu, S.; Sollogoub, M. Advances in Cyclodextrin Chemistry. In *Modern Synthetic Methods in Carbohydrate Chemistry*; Werz, D., Vidal, S., Eds.; Wiley-VCH: Weinheim, Germany, 2014; pp 241–283.
(61) NOMENCLATURE OF CARBOHYDRATES. *Pure Appl. Chem.* **1996**, *68*.
(62) Tichá, I.; Benkovics, G.; Malanga, M.; Jindřich, J. *Beilstein J. Org. Chem.* **2018**, *14*, 2829–2837.
(63) Guieu, S.; Zaborova, E.; Blériot, Y.; Poli, G.; Jutand, A.; Madec, D.; Prestat, G.; Sollogoub, M. *Angew. Chem. Int. Ed.* **2010**, *49* (13), 2314–2318.
(64) Matsuura, Y.; Kusunoki, M.; Harada, W.; Kakudo, *J. Biochem. (Tokyo)* **1984**, *95* (3), 697–702.
(65) Fujita, K.; Matsunaga, A.; Imoto, T. *J. Am. Chem. Soc.* **1984**, *106* (19), 5740–5741..
(66) Fujita, K.; Yamamura, H.; Matsunaga, A.; Imoto, T.; Mihashi, K.; Fujioka, T. *J. Am. Chem. Soc.* **1986**, *108* (15), 4509–4513.
(67) Yoshikiyo, K.; Matsui, Y.; Yamamoto, T. *Beilstein J. Org. Chem.* **2015**, *11*, 1530–1540.
(68) Takahashi, K. *Chem. Rev.* **1998**, *98* (5), 2013–2034.
(69) Breslow, R.; Graff, A. *J. Am. Chem. Soc.* **1993**, *115* (23), 10988–10989.
(70) Breslow, R.; Yang, J.; Yan, J. *Tetrahedron* **2002**, *58* (4), 653–659.
(71) Yang, J.; Gabriele, B.; Belvedere, S.; Huang, Y.; Breslow, R. *J. Org. Chem.* **2002**, *67* (15), 5057–5067.
(72) Breslow, R. *Acc. Chem. Res.* **1995**, *28* (3), 146–153.
(73) Breslow, R.; Dong, S. D. *Chem. Rev.* **1998**, *98* (5), 1997–2012.
(74) Marchetti, L.; Levine, M. *ACS Catal.* **2011**, *1* (9), 1090–1118..
(75) Menuel, S.; Rousseau, J.; Rousseau, C.; Vaičiūnaite, E.; Dodonova, J.; Tumkevičius, S.; Monflier, E. *Eur. J. Org. Chem.* **2014**, *2014* (20), 4356–4361.
(76) Zhang, G.; Luan, Y.; Han, X.; Wang, Y.; Wen, X.; Ding, C.; Gao, J. *Green Chem.* **2013**, *15* (8), 2081.
(77) Tayade, Y. A.; Padvi, S. A.; Wagh, Y. B.; Dalal, D. S. *Tetrahedron Lett.* **2015**, *56* (19), 2441–2447.

(78) Marinescu, L.; Bols, M. *Curr. Org. Chem.* **2010**, *14* (13), 1380–1398.
(79) Rousseau, C.; Christensen, B.; Petersen, T. E.; Bols, M. *Org. Biomol. Chem.* **2004**, *2* (23), 3476.
(80) Rousseau, C.; Christensen, B.; Bols, M. *Eur. J. Org. Chem.* **2005**, *2005* (13), 2734–2739.
(81) Fenger, T. H.; Marinescu, L. G.; Bols, M. *Org. Biomol. Chem.* **2009**, *7* (5), 933.
(82) Marinescu, L. G.; Doyagüez, E. G.; Petrillo, M.; Fernández-Mayoralas, A.; Bols, M. *Eur. J. Org. Chem.* **2010**, *2010* (1), 157–167.
(83) Chan, W.-K.; Yu, W.-Y.; Che, C.-M.; Wong, M.-K. *J. Org. Chem.* **2003**, *68* (17), 6576–6582.
(84) Venema, A.; Henderiks, H.; v. Geest, R. *J. High Resolut. Chromatogr.* **1991**, *14* (10), 676–680.
(85) Macaev, F.; Boldescu, V. *Symmetry* **2015**, *7* (4), 1699–1720.
(86) Bai, C.; Tian, B.; Zhao, T.; Huang, Q.; Wang, Z. *Molecules* **2017**, *22* (9), 1475.
(87) Shen, Z.; Ma, J.; Liu, Y.; Jiao, C.; Li, M.; Zhang, Y. *Chirality* **2005**, *17* (9), 556–558.
(88) Liu, K.; Zhang, G. *Tetrahedron Lett.* **2015**, *56* (1), 243–246.
(89) Doyagüez, E. G.; Fernández-Mayoralas, *Tetrahedron* **2012**, *68* (36), 7345–7354.
(90) Kanagaraj, K.; Suresh, P.; Pitchumani, K. *Org. Lett.* **2010**, *12* (18), 4070–4073.
(91) Mojr, V.; Herzig, V.; Buděšínský, M.; Cibulka, R.; Kraus, T. *Chem. Commun.* **2010**, *46* (40), 7599.
(92) Hartman, T.; Herzig, V.; Buděšínský, M.; Jindřich, J.; Cibulka, R.; Kraus, T. *Tetrahedron Asymmetry* **2012**, *23* (22–23), 1571–1583.
(93) Mojr, V.; Buděšínský, M.; Cibulka, R.; Kraus, T. *Org. Biomol. Chem.* **2011**, *9* (21), 7318.
(94) Appelt, H. R.; Limberger, J. B.; Weber, M.; Rodrigues, O. E. D.; Oliveira, J. S.; Lüdtke, D. S.; Braga, A. L. *Tetrahedron Lett.* **2008**, *49* (33), 4956–4957.
(95) Mikami, K.; Tanaka, S.; Tonoi, T.; Matsumoto, S. *Tetrahedron Lett.* **2004**, *45* (32), 6133–6135.
(96) Hu, S.; Li, J.; Xiang, J.; Pan, J.; Luo, S.; Cheng, J.-P. *J. Am. Chem. Soc.* **2010**, *132* (20), 7216–7228.
(97) Kacprzak, K. M. Chemistry and Biology of Cinchona Alkaloids. In *Natural Products*; Ramawat, K. G., Mérillon, J.-M., Eds.; Springer Berlin Heidelberg: Berlin, Heidelberg, 2013; pp 605–641.
(98) *Cinchona Alkaloids in Synthesis and Catalysis: Ligands, Immobilization and Organocatalysis*; Song, C. E., Ed.; Wiley-VCH: Weinheim, 2009.
(99) Ma, B.; Parkinson, J. L.; Castle, S. L. *Tetrahedron Lett.* **2007**, *48* (12), 2083–2086. (100) Liu, Y.; Li, L.; Zhang, H.-Y.; Fan, Z.; Guan, X.-D. *Bioorganic Chem.* **2003**, *31* (1), 11–23.
(101) Liu, Y.; Chen, G.-S.; Chen, Y.; Ding, F.; Chen, J. *Org. Biomol. Chem.* **2005**, *3* (14), 2519.
(102) Armstrong, D.; Ward, T.; Armstrong, R.; Beesley, T. *Science* **1986**, *232* (4754), 1132–1135.
(103) Aski, S. N.; Kowalewski, J. *Magn. Reson. Chem.* **2008**, *46* (3), 261–267.
(104) Kisszekelyi, P.; Alammar, A.; Kupai, J.; Huszthy, P.; Barabas, J.; Holtzl, T.; Szente, L.; Bawn, C.; Adams, R.; Szekely, G. *J. Catal.* **2019**, *371*, 255–261.
(105) *Reviews in Computational Chemistry Volume 28: Parrill/Reviews in Computational Chemistry Volume 28*; Parrill, A. L., Lipkowitz, K. B., Eds.; Reviews in Computational Chemistry; John Wiley & Sons, Inc: Hoboken, NJ, USA, 2015.
(106) Brunold, T. C. Computational Studies: B $_{12}$ Cofactors and Their Interaction with Enzyme Active Sites. In *Encyclopedia of Inorganic and Bioinorganic Chemistry*; Scott, R. A., Ed.; John Wiley & Sons, Ltd: Chichester, UK, 2011.
(107) Radivojac, P.; Clark, W. T.; Oron, T. R.; Schnoes, A. M.; Wittkop, T.; Sokolov, A.; Graim, K.; Funk, C.; Verspoor, K.; Ben-Hur, A.; et al. *Nat. Methods* **2013**, *10* (3), 221–227.
(108) Lengauer, T.; Rarey, M. *Curr. Opin. Struct. Biol.* **1996**, *6* (3), 402–406.
(109) Phillips, J. C.; Braun, R.; Wang, W.; Gumbart, J.; Tajkhorshid, E.; Villa, E.; Chipot, C.; Skeel, R. D.; Kalé, L.; Schulten, K. *J. Comput. Chem.* **2005**, *26* (16), 1781–1802.
(110) Salmaso, V.; Moro, S. *Front. Pharmacol.* **2018**, *9*.
(111) Maurer, M.; de Beer, S.; Oostenbrink, C. *Molecules* **2016**, *21* (4), 499.
(112) Lipkowitz, K. B. *Chem. Rev.* **1998**, *98* (5), 1829–1874.
(113) Quevedo, M. A.; Zoppi, A. *J. Incl. Phenom. Macrocycl. Chem.* **2018**, *90* (1–2), 1–14.
(114) Leach, A. R. Ligand-Based Approaches: Core Molecular Modeling. In *Comprehensive Medicinal Chemistry II*; Elsevier, 2007; pp 87–118.
(115) Humphrey, W.; Dalke, A.; Schulten, K. *J. Mol. Graph.* **1996**, *14* (1), 33–38.
(116) Petrenko, R.; Meller, J. Molecular Dynamics. In *Encyclopedia of Life Sciences*; John Wiley & Sons, Ltd, Ed.; John Wiley & Sons, Ltd: Chichester, UK, 2010.

(117) González, M. A. *Éc. Thématique Société Fr. Neutron.* **2011**, *12*, 169–200.
(118) Pearlman, D. A.; Case, D. A.; Caldwell, J. W.; Ross, W. S.; Cheatham, T. E.; DeBolt, S.; Ferguson, D.; Seibel, G.; Kollman, P. *Comput. Phys. Commun.* **1995**, *91* (1–3), 1–41.
(119) Cheatham, T. E. I.; Miller, J. L.; Fox, T.; Darden, T. A.; Kollman, P. *J. Am. Chem. Soc.* **1995**, *117* (14), 4193–4194.
(120) Zhang, H.; Tan, T.; Hetényi, C.; Lv, Y.; van der Spoel, D. *J. Phys. Chem. C* **2014**, *118* (13), 7163–7173.
(121) Mieda, S.; Ikeda, A.; Shigeri, Y.; Shinoda, W. *J. Phys. Chem. C* **2014**, *118* (23), 12555–12561.
(122) He, J.; Chipot, C.; Shao, X.; Cai, W. *J. Phys. Chem. C* **2014**, *118* (41), 24173–24180.
(123) Yuan, D.-Q.; Yang, C.; Fukuda, T.; Fujita, K. *Tetrahedron Lett.* **2003**, *44* (3), 565–568.
(124) Dai, Y.; Wang, S.; Wu, J.; Tang, J.; Tang, W. *RSC Adv.* **2012**, *2* (33), 12652.
(125) Fujita, K.; Matsunaga, A.; Imoto, T.. *Tetrahedron Lett.* **1984**, *25* (48), 5533–5536.
(126) Oliva, C. G.; Silva, A. M. S.; Resende, D. I. S. P.; Paz, F. A. A.; Cavaleiro, J. A. S. *Eur. J. Org. Chem.* **2010**, *2010* (18), 3449–3458.
(127) Zielińska-Błajet, M.; Kucharska, M.; Skarżewski, J. *Synthesis* **2006**, No. 7, 1176–1182.
(128) Kacprzak, K.; Gierczyk, B. *Tetrahedron Asymmetry* **2010**, *21* (21–22), 2740–2745.
(129) Popr, M.; Hybelbauerová, S.; Jindřich, J. *Beilstein J. Org. Chem.* **2014**, *10*, 1390–1396.
(130) Menuel, S.; Azaroual, N.; Landy, D.; Six, N.; Hapiot, F.; Monflier, E. *Chem. - Eur. J.* **2011**, *17* (14), 3949–3955.
(131) Bauer, M.; Fajolles, C.; Charitat, T.; Wacklin, H.; Daillant, J. *J. Phys. Chem. B* **2011**, *115* (51), 15263–15270.
(132) Al Temimi, A. H. K.; Boltje, T. J.; Zollinger, D.; Rutjes, F. P. J. T.; Feiters, M. C. *Bioconjug. Chem.* **2017**, *28* (8), 2160–2166.
(133) Saokham, P.; Muankaew, C.; Jansook, P.; Loftsson, T. *Molecules* **2018**, *23* (5), 1161.
(134) Pellissier, H. *Tetrahedron* **2017**, *73* (20), 2831–2861.
(135) Iwabuchi, Y.; Nakatani, M.; Yokoyama, N.; Hatakeyama, S. *J. Am. Chem. Soc.* **1999**, *121* (43), 10219–10220.
(136) Huang, J.; Zhang, X.; Armstrong, D. W. *Angew. Chem. Int. Ed.* **2007**, *46* (47), 9073–9077.
(137) Dočekal, V.; Šimek, M.; Dračínský, M.; Veselý, J. *Chem. - Eur. J.* **2018**, *24* (51), 13441–13445.
(138) Ivanov, P. M.; Salvatierra, D.; Jaime, C. *J. Org. Chem.* **1996**, *61* (20), 7012–7017.
(139) Koehler, J. E. H.; Saenger, W.; van Gunsteren, W. F. *J. Mol. Biol.* **1988**, *203* (1), 241–250.
(140) Loftsson, T.; Másson, M.; Brewster, M. E. *J. Pharm. Sci.* **2004**, *93* (5), 1091–1099.
(141) Ross, B. Hyperpolarized Magnetic Resonance Imaging and Spectroscopy of the Brain. In *Magnetic Resonance Spectroscopy*; Elsevier, 2014; pp 331–349.
(142) Hădărugă, N. G.; Bandur, G. N.; Hădărugă, D. I. Thermal Analyses of Cyclodextrin Complexes. In *Cyclodextrin Fundamentals, Reactivity and Analysis*; Fourmentin, S., Crini, G., Lichtfouse, E., Eds.; Springer International Publishing: Cham, 2018; Vol. 16, pp 155–221.
(143) Cai, W.; Sun, T.; Liu, P.; Chipot, C.; Shao, X. *J. Phys. Chem. B* **2009**, *113* (22), 7836–7843.
(144) Zhang, H.; Chen, M.; He, Z.; Wang, Z.; Zhang, M.; He, Z.; Wan, Q.; Liang, D.; Repka, M. A.; Wu, C. *AAPS PharmSciTech* **2013**, *14* (1), 10–18.
(145) Fifere, A.; Marangoci, N.; Maier, S.; Coroaba, A.; Maftei, D.; Pinteala, M. *Beilstein J. Org. Chem.* **2012**, *8*, 2191–2201.
(146) Yu, Y.; Chipot, C.; Cai, W.; Shao, X. *J. Phys. Chem. B* **2006**, *110* (12), 6372–6378.
(147) Fan, Z.; Diao, C.-H.; Song, H.-B.; Jing, Z.-L.; Yu, M.; Chen, X.; Guo, M.-J. *J. Org. Chem.* **2006**, *71* (3), 1244–1246.
(148) Tanriver, G.; Dedeoglu, B.; Catak, S.; Aviyente, V. *Acc. Chem. Res.* **2016**, *49* (6), 1250–1262.
(149) Feng, L.; Fawaz, R.; Hovde, S.; Sheng, F.; Nosrati, M.; Geiger, J. H. *Acta Crystallogr. Sect. Struct. Biol.* **2016**, *72* (5), 641–647.
(150) Alvarez Dorta, D.; Sivignon, A.; Chalopin, T.; Dumych, T. I.; Roos, G.; Bilyy, R. O.; Deniaud, D.; Krammer, E.-M.; de Ruyck, J.; Lensink, M. F.; Bouckaert, j.; Barnich, N.; Gouin, S. *ChemBioChem* **2016**, *17* (10), 936–952.
(151) Zhu, J.; Zhu, J.; Bougie, D. W.; Aster, R. H.; Springer, T. A. *Blood* **2015**, *126* (18), 2138–2145.

(152) Jorgensen, W. L.; Chandrasekhar, J.; Madura, J. D.; Impey, R. W.; Klein, M. L. *J. Chem. Phys.* **1983**, *79* (2), 926–935.
(153) Vanommeslaeghe, K.; MacKerell, A. D. *Biochim. Biophys. Acta BBA - Gen. Subj.* **2015**, *1850* (5), 861–871.
(154) Roe, D. R.; Cheatham, T. E. *J. Chem. Theory Comput.* **2013**, *9* (7), 3084–3095.
(155) Boffa, L.; Gaudino, E. C.; Martina, K.; Jicsinszky, L.; Cravotto, G. *New J. Chem.* **2010**, *34* (9), 2013.
(156) Bonnet, V.; Duval, R.; Tran, V.; Rabiller, C. *Eur. J. Org. Chem.* **2003**, *2003* (24), 4810–4818.
(157) Sato, T.; Nakamura, H.; Ohno, Y.; Endo, T. *Carbohydr. Res.* **1990**, *199* (1), 31–35.
(158) Ruiz García, Y.; Zelenka, J.; Pabon, Y. V.; Iyer, A.; Buděšínský, M.; Kraus, T.; Edvard Smith, C. I.; Madder, A. *Org. Biomol. Chem.* **2015**, *13* (18), 5273–5278.
(159) Rawal, G. K.; Zhang, P.; Ling, C.-C. *Org. Lett.* **2010**, *12* (13), 3096–3099.
(160) Barrulas, P.; Benaglia, M.; Burke, A. J. *Tetrahedron Asymmetry* **2014**, *25* (12), 923–935.
(161) Brunner, H.; Bügler, J.; Nuber, B. *Tetrahedron Asymmetry* **1995**, *6* (7), 1699–1702.
(162) Celewicz, L.; Kacprzak, K.; Ruszkowski, P. Application of Cinchona Alkaloid Derivatives as Cytotoxic Compounds. CA 2891633, March 26, 2015.
(163) Cornilleau, T.; Audrain, H.; Guillemet, A.; Hermange, P.; Fouquet, E. *Org. Lett.* **2015**, *17* (2), 354–357.
(164) Ishii, Y.; Fujimoto, R.; Mikami, M.; Murakami, S.; Miki, Y.; Furukawa, Y. *Org. Process Res. Dev.* **2007**, *11* (3), 609–615.
(165) Heck, R.; Jicsinszky, L.; Marsura, A. *Tetrahedron Lett.* **2003**, *44* (29), 5411–5413.
(166) van Steenis, D. J. V. C.; Marcelli, T.; Lutz, M.; Spek, A. L.; van Maarseveen, J. H.; Hiemstra, H. *Adv. Synth. Catal.* **2007**, *349* (3), 281–286.
(167) Georgiou, I.; Whiting, A. *Org. Biomol. Chem.* **2012**, *10* (12), 2422.
(168) Peng, Y.-Y.; Peng, S.-J.; Ding, Q.-P.; Wang, Q.; Cheng, J.-P. *Chin. J. Chem.* **2007**, *25* (3), 356–363.
(169) Guillena, G.; Hita, M. del C.; Nájera, C.; Viózquez, S. F. *J. Org. Chem.* **2008**, *73* (15), 5933–5943.
(170) Ashokkumar, V.; Siva, A. *Org. Biomol. Chem.* **2015**, *13* (40), 10216–10225.
(171) Liu, J.; Han, Z.; Wang, X.; Wang, Z.; Ding, K. *J. Am. Chem. Soc.* **2015**, *137* (49), 15346–15349.

8. CONTRIBUTIONS OF OTHER RESEARCHERS TO THIS THESIS

HPLC and HPLC-MS spectra of AB-, AC- and AD-regioisomers of heterodisubstituted α-CD derivatives were measured by Ing. Gábor Benkovics, Ph.D., in Analytical Laboratory of CycloLab, Cyclodextrin Research and Development, Ltd., Illatos út 7, H-1525, Budapest, Hungary.

2D NMR spectra acquired on 600 MHz Bruker AVANCE III and NMR elucidation of Cinchona-CD derivatives were performed by RNDr. Simona Hybelbauerová, Ph.D., Department of Teaching and Didactics of Chemistry, Faculty of Science, Charles University, Hlavova 8, 128 40, Prague 2, Czech Republic.

MD simulations were performed by the author of this thesis under tutoring of RNDr. Ivan Barvík, Ph.D., Institute of Physics, Faculty of Matematics and Physics, Ke Karlovu 5, 121 16, Prague 2, Czech Republic).

9. AUTHOR'S PUBLICATIONS

Used in this thesis

1. Tichá, I.; Benkovics, G.; Malanga, M.; Jindřich, J. Enhanced Single-Isomer Separation and Pseudoenantiomer Resolution of New Primary Rim Heterobifunctionalized α-Cyclodextrin Derivatives. *Beilstein J. Org. Chem.* **2018**, *14*, 2829–2837. https://doi.org/10.3762/bjoc.14.261

2. Tichá, I.; Hybelbauerová, S; Jindřich, J. New α- and β-cyclodextrin derivatives with Cinchona alkaloids used in asymmetric organocatalytic reactions. *Beilstein J. Org. Chem.* **2019**, accepted.

3. Chena Tichá, I.; Barvík, I.; Jindřich, J. Molecular-dynamics studies of Cinchona alkaloids with cyclodextrins. *Manuscript in preparation.*

Other publications

4. Putaj, P.; Tichá, I.; Císařová, I.; Veselý, J. One-pot Preparation of Chiral Carbycycles from Morita-Baylis-Hillman Carbonates by an Asymmetric Allylic Alkylation/Metathesis Sequence. *Eur. J. of Org. Chem.* **2014**, *30*, 6615–6620. https://doi.org/10.1002/ejoc.201402899

10. SUPPLEMENTAL INFORMATION

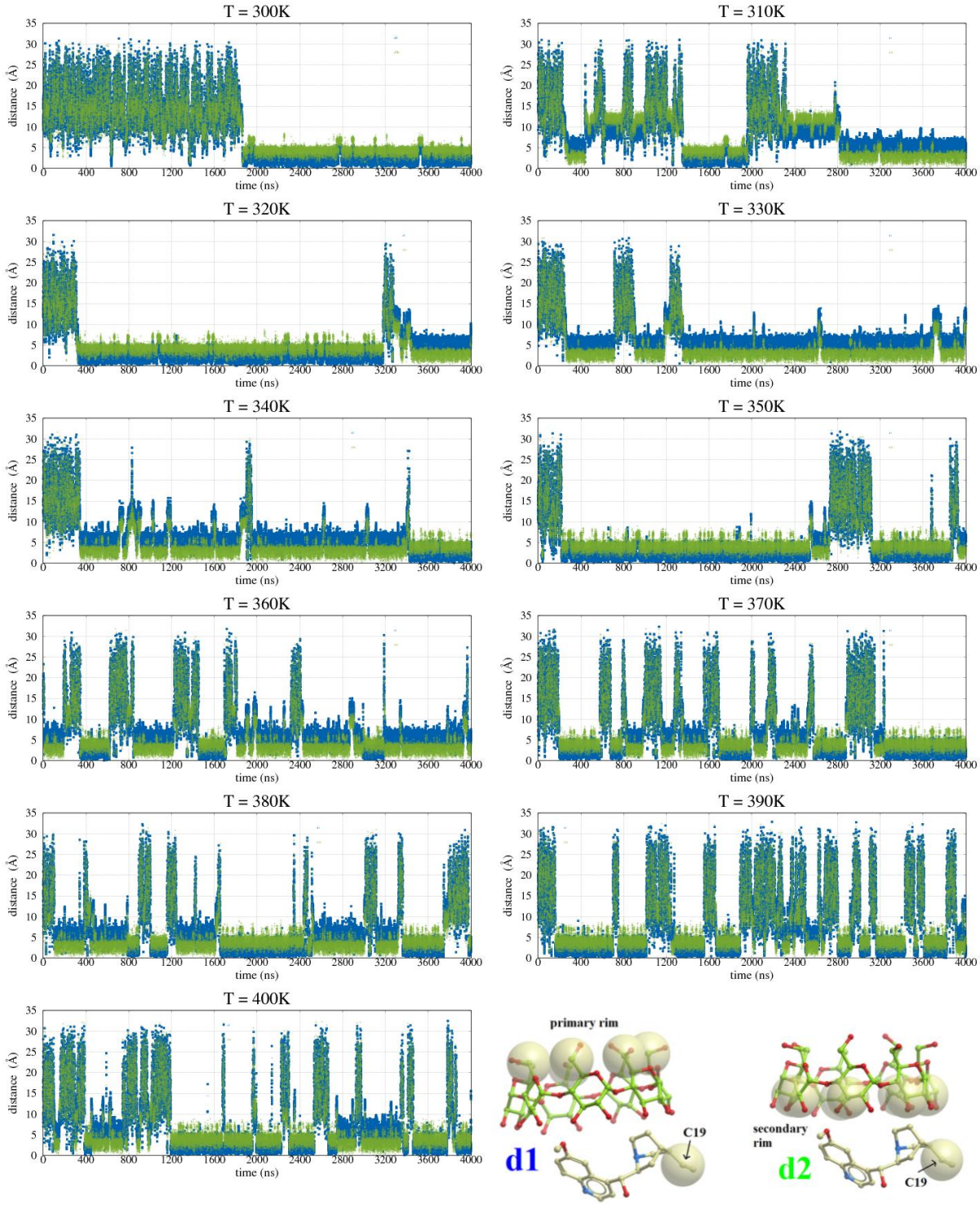

Figure S1. Distances d1 (blue) between C19 of quinine (quinuclidine part) and the primary rim of β-CD, and d2 (green) between C19 of quinine and the secondary rim β-CD, presented the inclusion complex of β-CD and quinine.

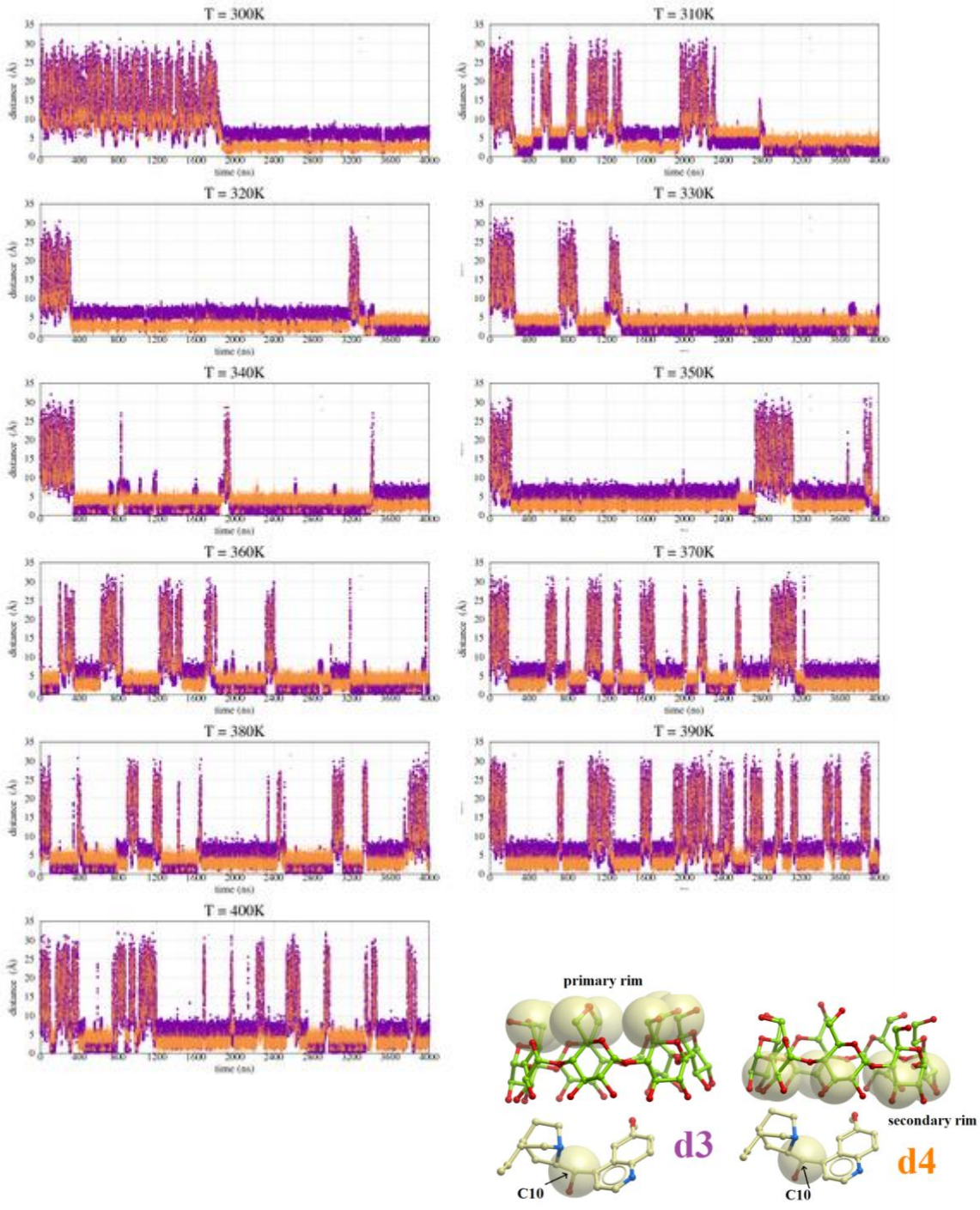

Figure S2. Distances d3 (purple) between C10 of quinine (quinuclidine part) and the primary rim of β-CD, and d4 (orange) between C10 of quinine and the secondary rim of β-CD and quinine, presented the inclusion complex of β-CD and quinine.

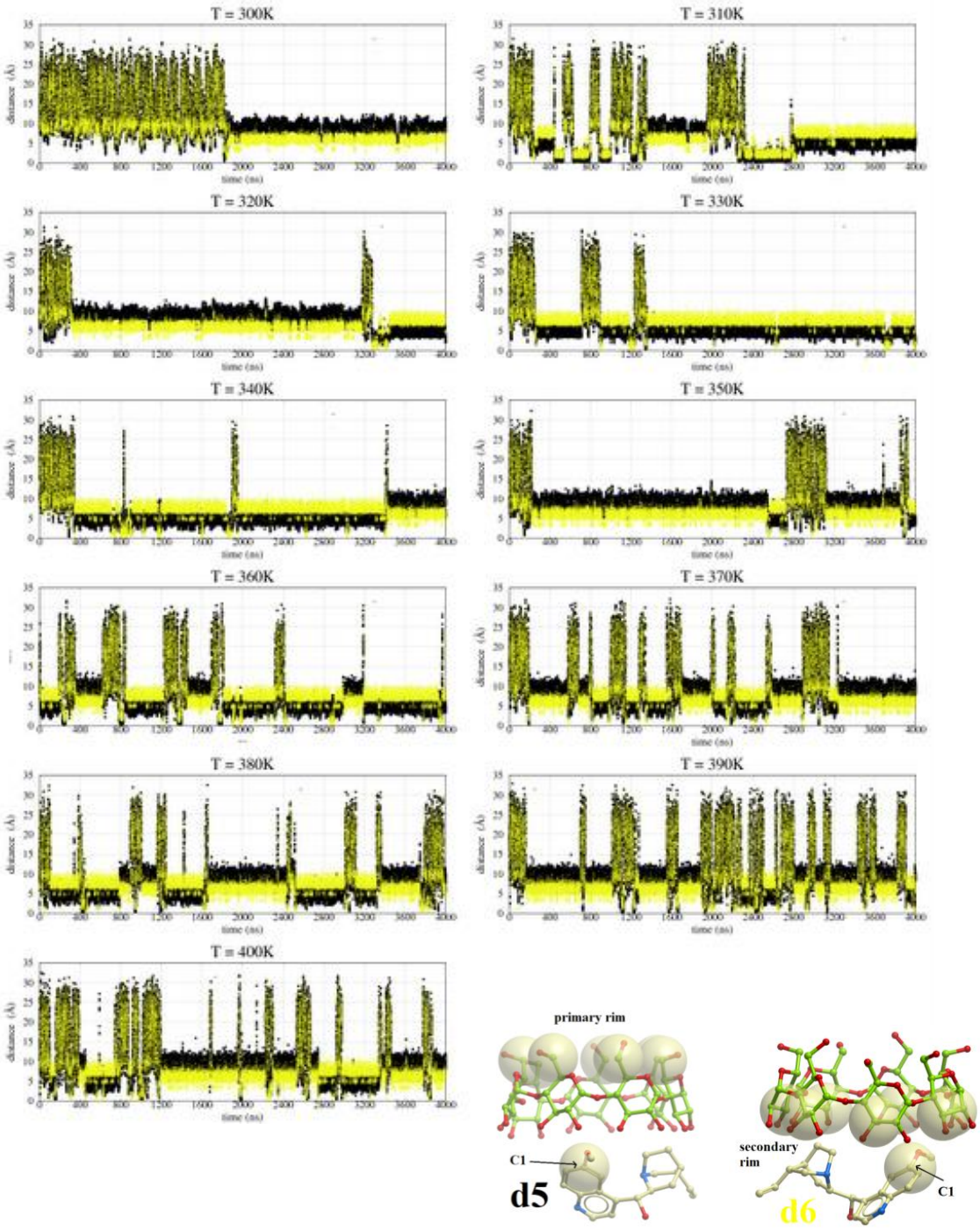

Figure S3. Distances d5 (black) between C1 of quinine (quinoline part) and the primary rim of β-CD, and d6 (yellow) between C1 of quinine and secondary rim of β-CD and quinine, presented the inclusion of β-CD and quinine.

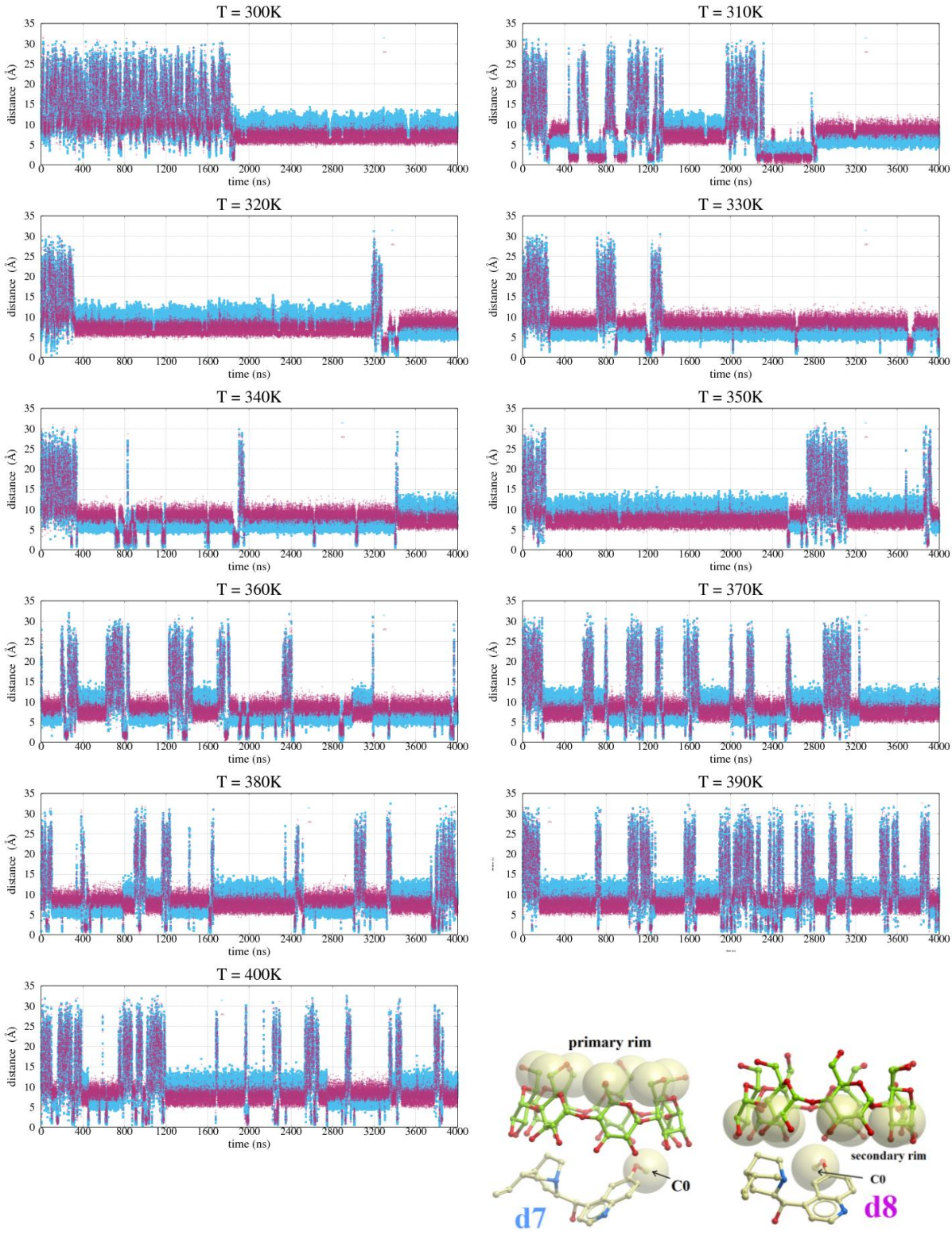

Figure S4. Distances d7 (light-blue) between C0 atom of methoxy group of quinine (quinoline part) and the primary rim of β-CD, and d8 (magenta) between C0 atom of methoxy group of quinine, presented the inclusion of β-CD and quinine.

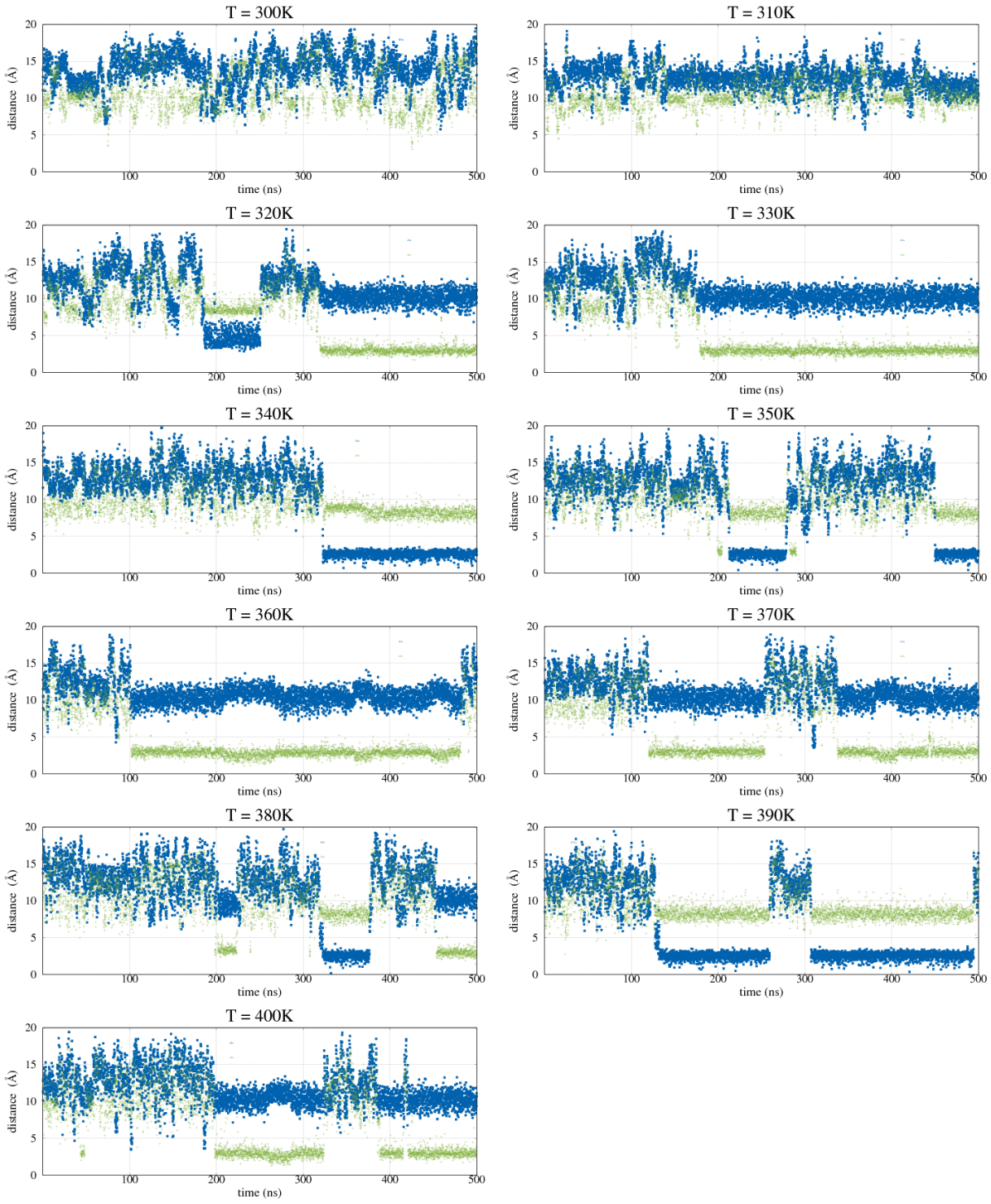

Figure S5. Distances d1 (blue) between H76 of vinyl group of quinuclidine moiety and H-3 atoms of the cavity, and d2 (green) between H64 of quinoline moiety and H-3 atoms of the CD cavity, confirming the self-inclusion of catalyst **20a**.

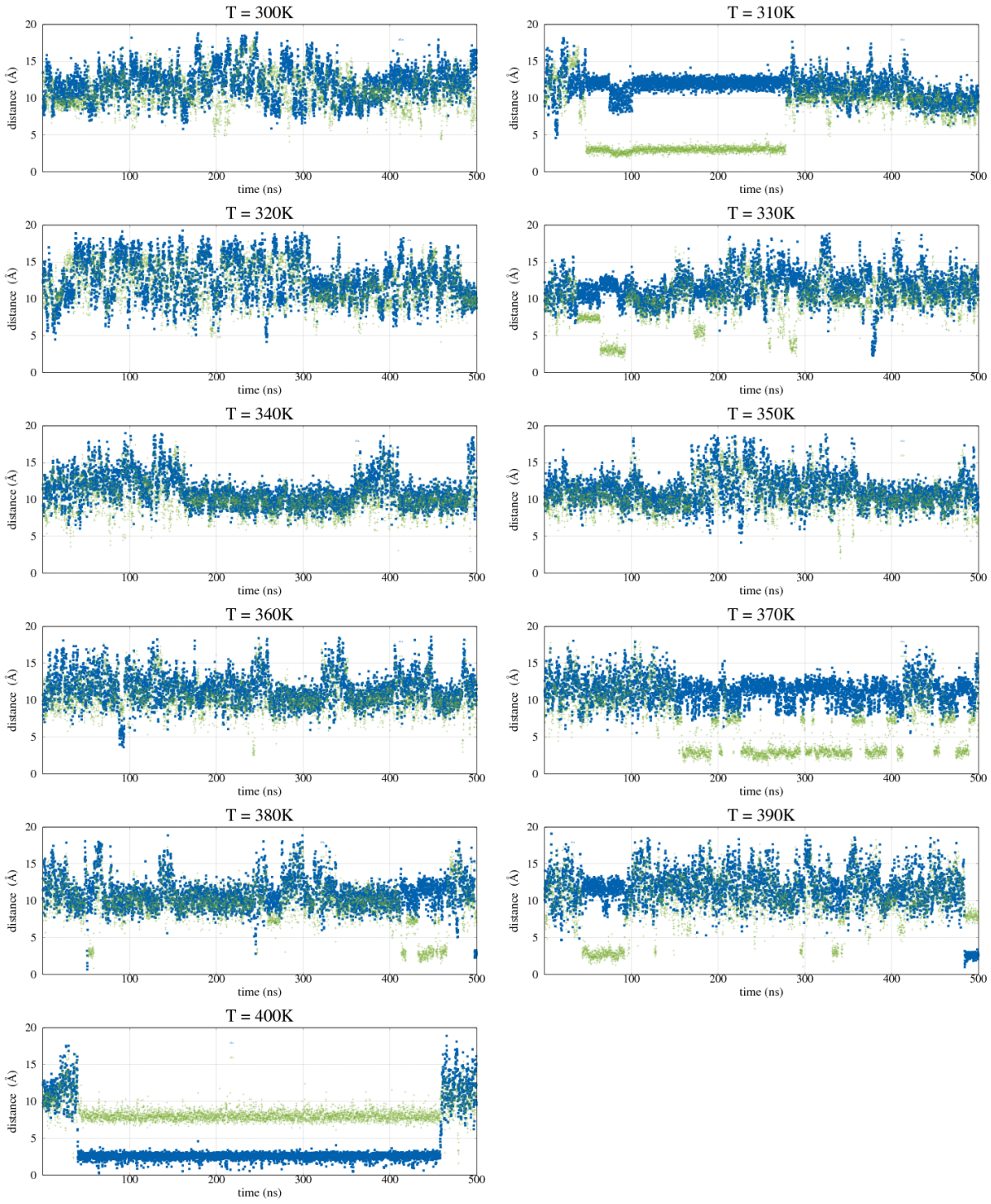

Figure S6. Distances d1 (blue) between H76 of vinyl group of quinuclidine moiety and H-3 atoms of the cavity, and d2 (green) between H64 of quinoline moiety and H-3 atoms of the CD cavity, confirming the self-inclusion of catalyst **20b**.

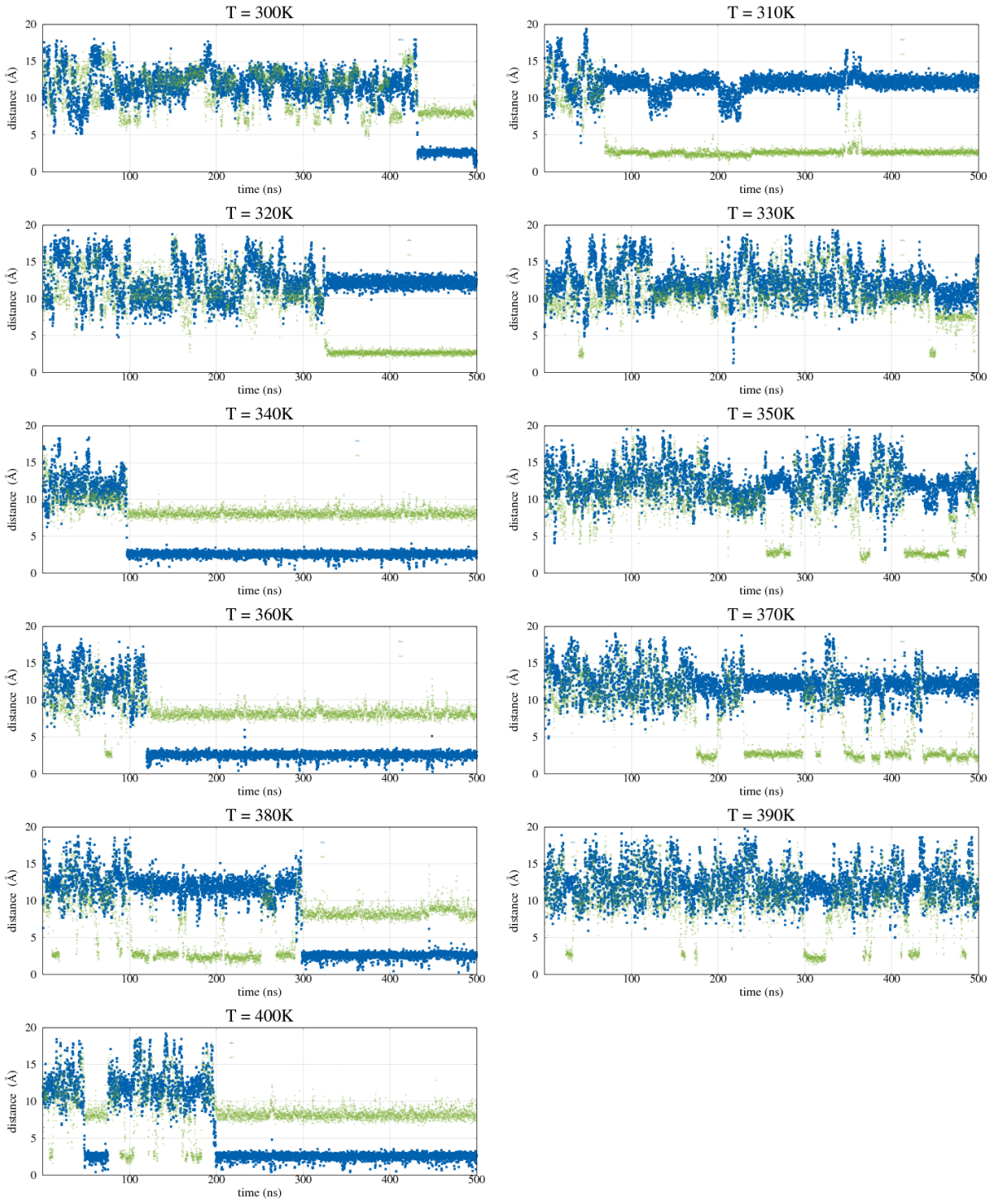

Figure S7. Distances d1 (blue) between H76 of vinyl group of quinuclidine moiety and H-3 atoms of the cavity, and d2 (green) between H64 of quinoline moiety and H-3 atoms of the CD cavity, confirming the self-inclusion of catalyst **20c**.

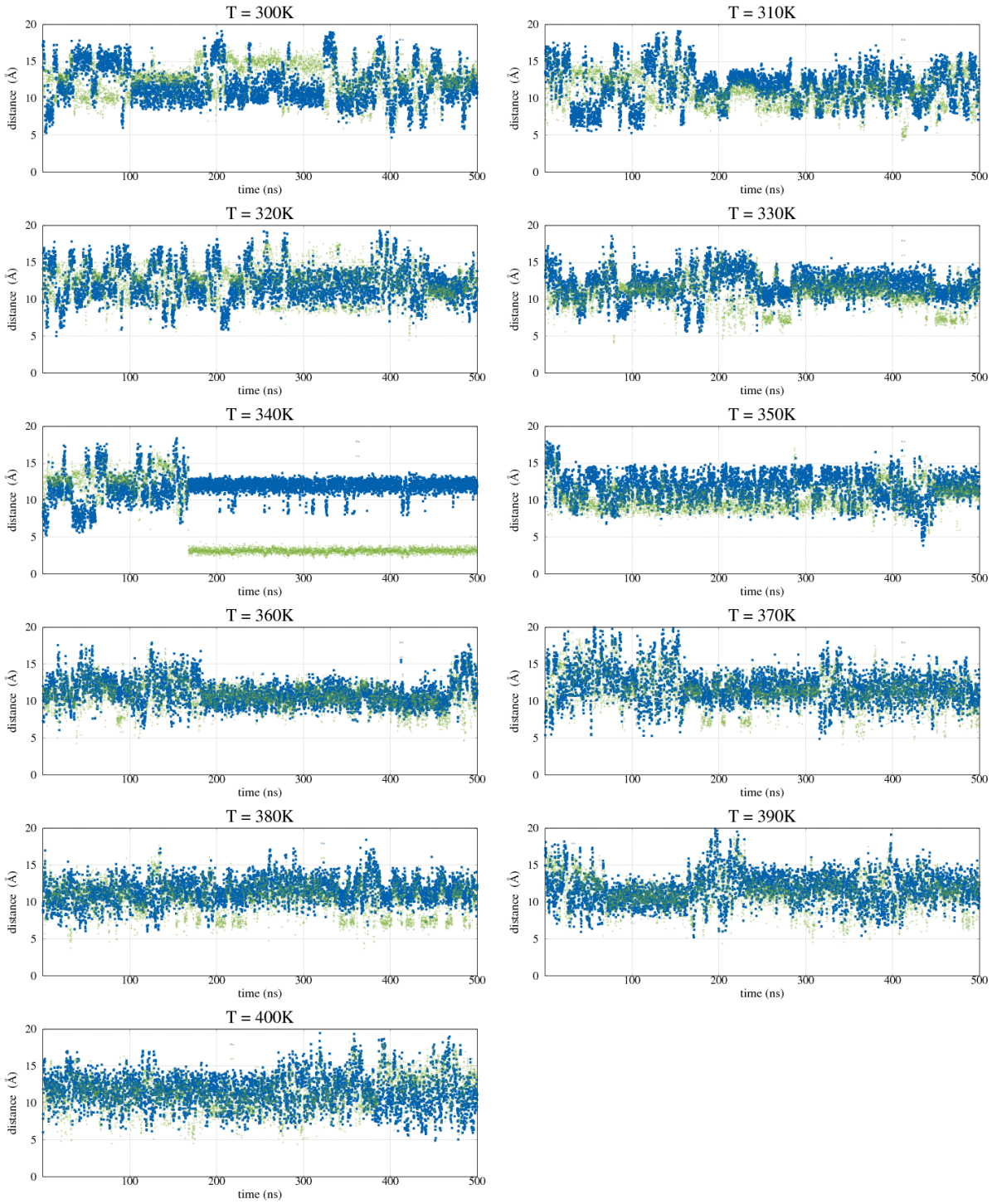

Figure S8. Distances d1 (blue) and d2 (green) for the inclusion of the substituent inclusion into the CD cavity in catalyst **24b**.